# Relationship between the lack of VDR and PTEN and their implication in glucose and lipid metabolism

Maria Crespo Masip

Universitat de Lleida

# TESI DOCTORAL

# Relationship between the lack of VDR and PTEN and their implication in glucose and lipid metabolism

Maria Crespo Masip

Memòria presentada per optar al grau de Doctora per la Universitat de Lleida

Programa de Doctorat en Salut

Director i Tutor

Jose Manuel Valdivielso Revilla

Lleida, 2019

Universitat de Lleida

IRBLleida
Institut de Recerca Biomèdica

Jose Manuel Valdivielso Revilla, PhD, Investigador principal i director del grup de recerca *Vascular and Renal Translational Research Group* de l'Institut de Recerca Biomèdica de Lleida i professor del departament de Medicina de la Universitat de Lleida.

Com a supervisor de la present tesi doctoral titulada: "**Relationship between the lack of VDR and PTEN and their implication in glucose and lipid metabolism**", presentada per **Maria Crespo Masip**, Graduada en Ciències Biomèdiques i Màster en Investigació Biomèdica per la Universitat de Lleida.

Per la present declaro que aquest treball compleix les condicions adequades per a poder ser defensat davant del tribunal de tesis i, si correspon, obtenir el títol de Doctora per la Universitat de Lleida.

Signat,

Dr. Jose Manuel Valdivielso Revilla

Lleida, 30 d'agost de 2019

Als meus pares,
als meus padrins,
i al Pau.

"No s'ha de tenir por a la vida, només s'ha de comprendre.
Ara és hora d'entendre més, per a témer menys."

"Nothing in life is to be feared, it is only to be understood.
Now is the time to understand more, so that we may fear less."

**Marie Curie**
(1867-1934)

# Acknowledgements

Sembla impossible que ja hagin passat set anys des de que vaig arribar com a alumna de pràctiques del grau en ciències biomèdiques a l'IRBLleida, i sis des de que vaig començar al grup de Nefro com a estudiant de màster. Però el temps vola i els dies, els mesos i els anys passen molt ràpid. Durant tot aquest temps hi ha hagut moltes persones que m'han donat suport, ensenyat i guiat. I per aquest motiu, voldria agrair i dedicar aquesta tesi doctoral a totes elles i tots ells.

En primer lloc, vull agrair-li al Jose i a l'Elvira l'oportunitat que em van brindar a l'obrir-me les portes del seu grup d'investigació, Vascular and Renal Translational Research Group, i així poder realitzar el meu treball de final de màster i seguidament, la present tesi doctoral. En especial, al Jose, que ha estat el meu tutor i director de tesis. Gràcies per tots els coneixements i ajuda que m'has transmès durant aquests anys, així com també, per la llibertat de prendre decisions en les investigacions. A més, sempre m'has incentivat a aprendre tècniques noves i a no tenir por de fer-ho, i sens dubte, ha estat un dels aprenentatges més importants que m'emporto i dels que més he gaudit.

Agrair el suport i ajuda constant de totes les companyes i companys del laboratori de Nefro, les que hi havia quan vaig arribar, les que ja han marxat i les que han anat arribant: Milica, Maite, Alicia, Aurora, Sandra, Núria, Ana, Rajesh, Marcelí, Serafí, Montse, Adriana, Petya, Vicky i Noèlia. Així com a totes les alumnes de pràctiques que he tingut el plaer de guiar durant aquest temps, com la Sandra, la Francesca o la Marina.

A part de companyes de laboratori, també m'emporto un grup d'amigues per sempre que han fet que durant aquests últims anys els dies al laboratori, i fora d'ell, siguin molt més divertits. Aurora, Alicia, Sandra i Núria heu estat un gran suport i unes grans amigues, us estimo i us trobaré a faltar! Cada una de vosaltres em té el cor robat: Aurora, saps que des del primer dia ets la nena dels meus ulls, m'has ajudat sempre incondicionalment i m'has demostrat ser una gran amiga i científica, espero haver-te ensenyat moltes coses, almenys he intentat fer-ho amb tot l'amor, t'estimo; Alicia, moltíssimes gràcies per tota l'ajuda tècnica d'aquests anys, però sobretot gràcies per tantes rialles d'aquestes contagioses que ens agafen amb només una mirada i que no se'ns acabin mai; Sandra, eres una de las mejores científicas y personas que conozco, fuerte y valiente, ojalá algún día me parezca aunque sea un poquito a ti; i Núria, vas arribar al lab revolucionant-ho tot amb aquesta energia que et caracteritza per donar vida i omplir-nos de felicitat i rialles el laboratori, els sopars, les festes, els beures i tot, no canviïs mai, ets única! També al Lluís, Marc, Maxi i Jose.

També vull donar les gràcies a la Maite, amb qui he compartit laboratori des de quasi el primer dia, tot el suport, les llargues xarrades, els viatges a congressos amb moments únics com trobar-nos a la reialesa danesa amb carruatge per sorpresa o les nits de festa per Burgos. Ha estat un plaer compartir aquests sis anys amb tu, et desitjo molta sort i que ens seguim trobant per Lleida o per Tàrrega de fira, a la Cava o de carnaval. Gràcies per aquests anys i que en siguin molts més!

Thanks to Milica for her help from the beginning of my days in the lab. I have learned a lot of technics and skills from you that I really appreciate.

I would like to do a special mention to Dr. Volker Vallon who was my stay's supervisor in the University of California San Diego. He was a really inspiring mentor for me from whom I have learned a lot. In addition, I'm really glad to be part of a scientific paper that we have published this year showing the results of the gene

expression studies I performed during my stay in his lab. Moreover, I also want to thank to all the Division of Nephrology & Hypertension laboratory's members to make me feel like home even I was 6000 miles from Lleida: Winnie, Rohit, Brent and Josselin. I hope we meet again somewhere in the world!

Agradecer al Dr. Ramiro Jover, Carla Guzmán y Petar Petrov, del grupo de Hepatología Experimental del Instituto de Investigación Sanitaria de la Fe de Valencia, toda su ayuda, conocimiento y soporte en la parte del metabolismo lipídico así como la posibilidad de ir a hacer una pequeña estancia en su laboratorio para realizar algunos experimentos.

A més a més, també voldria agrair a diversos professors de l'IRBLleida que m'han estat ajudant i aconsellant al llarg dels anys com al Dr. Xavi Dolcet, amb el que vaig aprendre des de zero a treballar al laboratori i a l'estabulari durant el meu treball de final de grau i del que vaig aprendre moltes coses treballant dia a dia al seu costat; al Dr. Xavier Matías Guiu, que em va acollir al seu grup durant el treball final de grau; al Dr. Mario Encinas, sempre disposat a ajudar-me i donar-me consells; al Dr. Eloi Garí, que amb el seu bon humor de sempre em va ajudar molt amb la part dels experiments amb radioactivitat; al Dr. Jose Serrano, qui em va estar aconsellant des del començament amb els estudis de glucosa; a la Dra. Conchi Mora, per ensenyar-me a extreure illots pancreàtics; i a la Dra. Anna Casanoves, que m'ha estat ajudant moltíssim amb un altre projecte en el que he estat treballant aquests anys. Així com també al Dr. Jose Ramon Bayascas de la Universitat Autònoma de Barcelona per la seva ajuda amb els estudis de glicogen hepàtic.

M'agradaria expressar el meu agraïment als treballadors de l'estabulari de la Universitat de Lleida, la Núria, el Marc, la Leti i la Jessica, que han estat tenint cura dels nostres animals d'experimentació durant tots aquests anys.

Donar les gràcies a les diferents institucions que han fet possible la realització d'aquesta tesi doctoral i les estades a altres centres de recerca: Secretaria d'Universitats i Recerca del Departament d'Economia i Coneixement de la Generalitat de Catalunya – Fons Social Europeu (EU); Universitat de Lleida; IRBLleida i Diputació de Lleida i Gerència Territorial de l'Institut Català de la Salut a Lleida, Alt Pirineu i Aran, i Gestió de Serveis Sanitaris.

Els anys al laboratori no haguessin estat el mateix sense la pinya d'amics que vam fer des del començament i que m'emporto com un tresor. Heu estat l'alegria i la desconnexió de cada dia a l'hora de dinar, però també de les mil i una excursions, caps de setmana, celebracions d'aniversaris, sopars, festes, carnavals, el nostre comiat de solters i boda, piscines, estanys... Gràcies per ser uns grans amics, us estimo molt a tots i espero que tots aquests moments viscuts els guardem per sempre! Gràcies Tania i Isidre (units des de "las vacas no son transgénicas" i espero que per sempre), Esther i Dani (amb vosaltres he trobat uns grans companys de vida amb qui m'encanta compartir el temps), David i Marta (grans persones i millors científics ara per Suècia, us trobo a faltar!), Nati, Marc, Laura, Jaume, Roger, Fernando, Alba, Coral, Jessica, Eva i Marta.

Una menció especial a les meves nenes de biomed. Quina sort haver-nos trobat, i quina sort seguir tenint-nos cada dia. Sou les millors Anabel, Carmen, Jana, Celia, Marta, Laura i Paula, us estimo molt! Ani, gracias por ser mi amiga des del día 0 en la universidad, porque sin ti la vida sería mucho más aburrida, porque con tus telenovelas me alegras los días! Tenerte lejos en estos momentos me pone triste, pero a la vez no sabes lo

orgullosa que estoy de ti y de que estés creciendo como científica en Columbia. Eres una súper investigadora! Te quiero y te echo de menos! Carmen, mi pollito, mi alma gemela, mi amiga. Qué suerte tengo de tenerte! Porque por mucho tiempo que pasemos sin vemos, cuando nos juntamos es como si el tiempo no pasara. Os quiero mucho Carmen y Francesco, nos vemos pronto por Italia amigos! Jana, ets llum i l'alegria en persona, que la Júlia us porti, a tu i al Javi, tota la felicitat del món i a nosaltres també!

I ara, deixant de banda totes les amigues, amics, companyes i companys que m'emporto de deu anys en el món universitari i científic. Toca passar als que porten al meu costat tota una vida, i que sense ells res hagués estat possible.

Gràcies als amics dels Torms per ser d'aquells que van arribar de petits i que s'han quedat per sempre, perquè el moments amb vosaltres sempre formen part dels més feliços de la meva vida. Sou llum, energia i els millors amics del món mundial! Només desitjo que ens fem vellets tots junts colla eeesss!! Us estimo molt Olga, Sandra, Eduard, Sergi, Arnau, Jaume, Sade, Carla i Josep Antoni. També gràcies a la Marina i l'Àlex per ser-hi des de sempre! Olga, gràcies per una vida juntes d'amistat, ets una dona meravellosa i un pilar molt important en la meva vida, i tot i que ara ja no ens passem les 24h juntes com d'adolescents, seguim tenint-nos sempre, t'estimo molt!

Gràcies també al Gerard i a la Silvia, perquè vosaltres sempre heu estat amics, professors de música i com a germans grans per mi. Encara no em puc creure que no vegis a la teva "bio" doctorar-se, Gerard. No m'ho crec, no m'ho vull creure... Allà on estiguis aquesta tesi també és teva. Et trobo a faltar.

Gràcies a tota la meva família, que sempre ha estat aquí per recolzar-me, perquè tinc la sort de tenir una família molt gran a la que m'estimo amb totes les meves forces! Ja sabeu que m'encanta passar el temps amb tots i cada un de vosaltres. Estius, nadals, aniversaris... tots són moments especials! També gràcies als que ja no hi són o que no he arribat a conèixer però que sempre els he tingut presents i que em falten cada dia! Gràcies a tots: Família de la Granadella: padrí Víctor, padrina Lore, tieta Mari, tiet Jordi, Roger, Isa, Clàudia, Èric, tiet Ramón, tieta Elena, Ferran, Júlia, tieta Glòria, Maribel (padrineta), Manuel, Elena, Alba, Eloi, Bego, Aina i Pau. Família dels Torms: padrí Macià, padrina Salut, Joan (padrinet), tieta Montse, Àngels i Joana. I Família de Sudanell: Josepet, Enriqueta, Josep, Rosa, Josep, Dolors, Josep, Maria, Pere, Sagrari, Núria, Enric, Amparo i Óscar. Família de Durango: Jose, Mica, Arelí, Beto, Elena, Anel, Mac, Alina i Armando.

Mare, pare, ja sabeu que quatre ratlles no poden expressar tota la gratitud que sento per vosaltres, perquè si d'algú és aquesta tesi, ÉS VOSTRA. Perquè des dels meus primers aprenentatges heu estat vosaltres els que m'heu guiat, ensenyat, educat, transmès valors i donat suport incondicional amb totes les meves decisions. Us heu trencat sempre les banyes perquè jo pogués tenir la millor educació i us ho agraeixo de tot cor. Us admiro i estimo fins a l'infinit! XAVIER i MERCÈ sou els millors pares del món!

I per últim, gràcies Pau. Gràcies per ser el meu millor amic, company de classe, de ciència, de vida, parella i ara, també marit. Perquè són quasi deu anys durant els quals ens hem fet grans junts, hem anat superant totes les fites que ens hem proposat i ara, com diu un cantant que ens agrada molt: "*El cor em diu que tot anirà bé, i ara el món em diu que tot anirà bé*". I jo afegeixo, n'estic segura, si és amb TU. T'ESTIMO MOLT PAU!

# Index

# Abstract

# Abstract

Phosphatase and tensin homolog gene (PTEN) is the main negative regulator of the PI3K/Akt pathway; a route involved in glucose and lipid metabolism after its activation downstream the insulin receptor. Moreover, vitamin D receptor (VDR) is implicated in insulin secretion and lipid accumulation. During the last years, insulin-signaling pathway has become a major focus of study to find new diabetes therapeutic targets. Furthermore, there are some studies associating PTEN and VDR with lipid metabolism, although it is a rather unknown field of study. Thus, we were interested in the generation of a double KO PTEN-VDR to study interactions between PI3K/Akt pathway and vitamin D, in glucose and lipid metabolism.

The first obtained result was the premature death of DKO mice. However, we discarded cancer, as the cause of their mortality, because mice autopsies did not show tumor differences. Furthermore, DKO mice did not survive short fasting periods, showing rapid signs of lethargy and nonresposiveness.

Regarding glucose metabolism, we reported that PTEN deficiency induces severe hypoglycemia, both in postprandial and starving state, and hypoinsulinemia due to hyperstimulation of the insulin receptor in PTEN-KO and DKO mice. However, glucose supplementation did not prevent DKO increased death rate. In addition, PTEN ablation promoted defects on insulin secretion that were increased with the lost of VDR in DKO mice. DKO mice had increased insulin-independent glucose uptake in all their tissues. Later on, we analyzed different tissues related to glucose metabolism in PTEN and VDR single or double KO mice. We observed that PTEN-KO mice had a deregulation of renal glucose transporters expression, *in vitro* and *in vivo*. This defect could explain the mild increase in glycosuria, which was exacerbated when VDR was also deleted in DKO mice. In liver, PTEN deletion induced a pre-steatotic state, which was attenuated by VDR ablation in DKO mice. Moreover, we detected delayed hepatic gluconeogenesis activation in PTEN-KO and DKO mice. Therefore, we assumed that almost all the alterations found in DKO mice were due to the loss of PTEN. Hence, we focused on lipid metabolism because it is essential to survive during fasting state.

There are previous results that linked insulin, PI3K/Akt pathway and lipogenesis in liver. Furthermore, previous studies in our laboratory also reported a hepatic relationship between VDR and lipid metabolism. We found that, although PTEN-KO and DKO mice ate more, they used ketone bodies even when they were not food-restricted. In addition, when we treated DKO mice with high fat diet, we observed an increase in survival supporting the theory that lipid metabolism played an important role in the increased death rate of DKO mice. Moreover, we performed a complete analysis of genes involved in lipid metabolism, from which we concluded that PTEN deletion delayed β-oxidation and decreased lipogenesis. This phenotype was aggravated when VDR was also absent, additionally affecting fatty acid transport in DKO mice.

In conclusion, lack of PTEN highly affects glucose and lipid metabolism and VDR deletion exacerbates the phenotype. Consequently, if we extrapolate our DKO mice results to humans, we propose that vitamin D levels should be clinically monitored in type 1 diabetes mellitus subjects that have lean phenotype and recurrent severe hypoglycemia. Furthermore, diet supplementation with vitamin D and fats could reduce the risk of fatal consequences, like coma or death.

# Resum

El gen homòleg de fosfatasa i tensina (PTEN) és el principal regulador negatiu de la via PI3K/Akt, una ruta involucrada en el metabolisme glucídic i lipídic després d'activar-se pel receptor d'insulina. Endemés, el receptor de la vitamina D (VDR) està implicat en la secreció d'insulina i l'acumulació de lípids. En els darrers anys, la via de senyalització de la insulina ha esdevingut un gran focus d'estudi per trobar noves dianes terapèutiques en la diabetis. A més a més, hi ha estudis que associen PTEN i VDR amb el metabolisme lipídic, tot i que és un camp d'estudi encara bastant desconegut. Per tant, ens vam interessar en la generació d'un doble KO PTEN-VDR per estudiar interaccions entre la via PI3K/Akt i la vitamina D en el metabolisme glucídic i lipídic.

El primer resultat obtingut va ser la mort prematura dels ratolins DKO, en els quals vam descartar que l'elevada causa de mortalitat fos el càncer ja que les autòpsies dels ratolins no demostraven diferencies en tumors. A més, els ratolins DKO no sobrevivien a períodes curts de dejú que es manifestava amb signes ràpids de letargia i no resposta.

Pel que fa al metabolisme de la glucosa, vam demostrar que la deficiència de PTEN induïa hipoglucèmia severa, tan en estat postprandial com en dejú, i hipoinsulinèmia deguda a la hiperestimulació del receptor d'insulina en els ratolins PTEN-KO i DKO. Tot i així, la suplementació amb glucosa no disminuïa l'alta taxa de mortalitat dels ratolins DKO. Endemés, l'ablació de PTEN promovia defectes en la secreció d'insulina que encara es veien incrementats amb la pèrdua del VDR en els ratolins DKO. Els ratolins DKO tenien incrementada la captació de glucosa en tots els teixits de manera independent a la insulina. Després, vam analitzar diferents teixits relacionats amb el metabolisme de la glucosa en els ratolins amb manca de PTEN, VDR o ambdós. Vam observar que els ratolins PTEN-KO tenien una desregulació de l'expressió dels transportadors de glucosa, tan *in vitro* com *in vivo*. Aquest defecte podia explicar el lleuger increment de la glucosúria, que es veia exacerbat quan el VDR també s'eliminava en els ratolins DKO. En el fetge, la deleció de PTEN induïa un estat pre-esteatòtic, que estava atenuat quan hi havia ablació del VDR en els ratolins DKO.

Endemés, vam detectar que la pèrdua de PTEN retardava l'activació de la gluconeogènesis en el fetge en els ratolins PTEN-KO i DKO. Per tant, vam assumir que quasi totes les alteracions trobades en els ratolins DKO eren degudes a la pèrdua de PTEN. Per això ens vam focalitzar en el metabolisme lipídic, ja que és essencial per la supervivència durant el dejú.

Resultats previs relacionen la insulina, la via PI3K/Akt i la lipogènesis en el fetge. Addicionalment, estudis anteriors en el nostre laboratori van demostrar una relació hepàtica entre el VDR i el metabolisme lipídic. Vam trobar que, encara que els ratolins PTEN-KO i DKO menjaven més, utilitzaven cossos cetònics inclús quan no tenien restricció de menjar. A més a més, quan vam tractar els ratolins DKO amb dieta alta en greix, vam observar un increment en la supervivència, cosa que donava suport a la teoria de que el metabolisme lipídic jugava un paper molt important en l'alta taxa de mortalitat dels ratolins DKO. Endemés, vam dur a terme un anàlisis complet de gens involucrats en el metabolisme lipídic del que vam concloure que la deleció de PTEN retardava la β-oxidació i disminuïa la lipogènesis. Aquest fenotip s'agreujava quan el VDR estava absent, afectant també al transport d'àcids grassos en els ratolins DKO.

En conclusió, la falta de PTEN afecta el metabolisme glucídic i lipídic i la deleció de VDR exacerba el fenotip. Conseqüentment, si extrapolem els resultats dels ratolins DKO als humans, proposem que els nivells de vitamina D haurien d'estar degudament monitoritzats en pacients amb diabetis tipus 1 que tenen poc greix corporal i hipoglucèmies recurrents. Així com també, la suplementació de la dieta amb vitamina D i greixos els podria ajudar a reduir el risc de sofrir conseqüències fatals, com el coma o la mort.

# Resumen

El gen homólogo de fosfatasa y tensina (PTEN) es el principal regulador negativo de la vía PI3K/Akt, una ruta involucrada en el metabolismo glucídico y lipídico tras activarse por el receptor de insulina. Además, el receptor de vitamina D (VDR) está implicado en la secreción de insulina y la acumulación de lípidos. En los últimos años, la vía de señalización, de la insulina se ha convertido en un gran foco de estudio para encontrar nuevas dianas terapéuticas en la diabetes. Asimismo, hay estudios que asocian PTEN y VDR con el metabolismo lipídico, aunque se trata de un campo de estudio todavía bastante desconocido. Por lo tanto, nos interesamos en la generación de un doble KO PTEN-VDR para estudiar interacciones entre la vía PI3K/Akt y la vitamina D en el metabolismo glucídico y lipídico.

El primer resultado obtenido fue la muerte prematura de los ratones DKO, en los que descartamos que la causa de la elevada mortalidad fuera el cáncer ya que las autopsias de los ratones no mostraban diferencias en tumores. Además, los ratones DKO no sobrevivían a periodos cortos de ayuno que se manifestaba con signos rápidos de letargia y no respuesta.

Con respecto al metabolismo de la glucosa, demostramos que la deficiencia de PTEN inducía hipoglucemia severa, tanto en estado postprandial como en ayunas, y hipoinsulinemia debida a la hiperestimulación del receptor de insulina en los ratones PTEN-KO y DKO. No obstante, la suplementación con glucosa no disminuía la alta tasa de mortalidad de los ratones DKO. Asimismo, la ablación de PTEN promovía defectos en la secreción de insulina que aun se veían más aumentados con la pérdida del VDR en los ratones DKO. Los ratones DKO tenían incrementada la captación de glucosa en todos los tejidos de manera independiente a insulina. Después, analizamos diferentes tejidos relacionados con el metabolismo de la glucosa en los ratones con falta de PTEN, VDR o ambos. Observamos que los ratones PTEN-KO tenían una desregulación de la expresión de los transportadores de glucosa, tanto *in vitro* como *in vivo*. Este defecto podía explicar el ligero incremento de la glucosuria, que se veía exacerbada cuando el VDR también se eliminaba en los ratones DKO. En el hígado, la depleción de PTEN

inducía un estado pre-esteatótico, que estaba atenuado cuando había ablación del VDR en los ratones DKO. Además, detectamos que la pérdida de PTEN retardaba la activación de la gluconeogénesis en el hígado en los ratones PTEN-KO y DKO. Por lo tanto, asumimos que casi todas las alteraciones encontradas en los ratones DKO se debían a la pérdida de PTEN. Por esto, nos focalizamos en el metabolismo lipídico, ya que es esencial para la supervivencia durante el ayuno.

Resultados previos relacionan la insulina, la vía PI3K/Akt y la lipogénesis en el hígado. Adicionalmente, estudios anteriores en nuestro laboratorio demostraron una relación hepática entre el VDR y el metabolismo lipídico. Encontramos que, aunque los ratones PTEN-KO y DKO comían más, utilizaban cuerpos cetónicos hasta cuando no tenían restricción de comida. Además, cuando tratamos los ratones DKO con dieta alta en grasa, observamos un incremento de la supervivencia, lo cual daba soporte a la teoría de que el metabolismo lipídico jugaba un papel muy importante en la alta tasa de mortalidad de los ratones DKO. También realizamos un análisis completo de genes involucrados en el metabolismo lipídico del que concluimos que la depleción de PTEN retardaba la β-oxidación y disminuía la lipogénesis. Este fenotipo se agudizaba cuando el VDR estaba ausente, afectando también al transporte de ácidos grasos en los ratones DKO.

En conclusión, la falta de PTEN afecta el metabolismo glucídico y lipídico y la eliminación de VDR exacerba el fenotipo. Consecuentemente, si extrapolamos los resultados de los ratones DKO a los humanos, proponemos que los niveles de vitamina D deberían estar debidamente monitorizados en pacientes con diabetes tipo 1 que tienen poca grasa corporal e hipoglucemias recurrentes. Así como también, la suplementación de la dieta con vitamina D y grasas podría ayudar a reducir el riesgo de padecer consecuencias fatales, como el coma o la muerte.

# Abbreviations

# 1-9

$1,25(OH)_2D_3$: 1α,25-dihydroxyvitamin $D_3$

1-α-hydroxylase or CYP27B1: 25-hydroxyvitamin$D_3$-1-α-hydroxylase

$25(OH)D_3$: 25-hydroxyvitamin $D_3$

# A

AB: Alcian blue

ACC: Acetyl-CoA carboxylase

Acetyl-CoA: Acetyl coenzyme A

ACOX1: Acyl-CoA oxidase 1

ADP: Adenosine diphosphate

AF-2: Activation function 2

Akt or PKB: Protein kinase B

ANGPTL8: Angiopoietin-like protein 8

ATP: Adenosine triphosphate

# B

BAAT: Bile acid CoA:amino acid *N*-acyltransferase

Bcl-2: β-cell lymphoma 2

BSA: Bovine serum albumin

BUN: Blood urea nitrogen

# C

$Ca^{+2}$: Calcium

CaSR: Calcium sensor receptor

cAMP: Cyclic adenosine monophosphate

cDNA: Complementary deoxyribonucleic acid

CEBPa: CCAAT/enhancer-binding protein alpha

CKD: Chronic kidney disease

CNT: Control

$CO_2$: Carbon dioxide

CPM: Counts per minute

CPT1: Carnitine palmitoyl transferase 1

CREB: cAMP-response element binding protein

Ct: Cycle threshold

CYP27A1: 25-hydroxylase or P450 cytochrome

CYP27B1 or 1-α-hydroxylase: 25-hydroxyvitamin$D_3$-1-α-hydroxylase

## D

DBD: DNA binding domain

DBP: Vitamin D binding protein

DM: Diabetes mellitus

DMEM: Dulbecco's modified eagle medium

DNA: Deoxyribonucleic acid

DNS: 3,5-Dinitrosalicylic acid

DPX: Dibutylphthalate polystyrene xylene

DRIP205: VDR-interacting protein 205

## E

EDTA: Ethylenediaminetetraacetic acid

EGFR: Epidermal growth factor receptor

ELISA: Enzyme-linked immunosorbent assay

ENTPD5: Ectonucleoside triphosphate diphosphohydrolase 5

ER: Estrogen receptor

ERK: Extracellular signal-regulated kinase

ERRα: Estrogen-related receptor α

*E. Coli*: *Escherichia coli*

ETC: Electron transport chain

## F

$FAD^+$: Flavin adenine dinucleotide oxidized

$FADH_2$: Flavin adenine dinucleotide reduced

Fasn: Fatty acid synthase

FBS: Fetal bovine serum

FGF21: Fibroblast growth factor 21

FGF23: Fibroblast growth factor 23

FOXA2: Forkhead box A2

FOXO1: Forkhead box O1

FOXO3: Forkhead box O3

## G

G6P: Glucose-6-phosphate

G6PC: Glucose-6-phosphatase catalytic subunit

GAPDH: Glyceraldehyde-3-phosphate dehydrogenase

GF: Growth factor

GFP: Green fluorescence protein

GFR: Glomerular filtration rate

GLUT1: Glucose transporter 1

GLUT2: Glucose transporter 2

GLUT4: Glucose transporter 4

GPCR: G-protein coupled receptor

GSK3: Glycogen synthase kinase 3

GTP: Guanosine triphosphate

GTT: Glucose tolerance test

## H

H&E: Hematoxylin-eosin

HAT: Histone acetyltransferase

HDAC: Histone deacetylase

HFD: High fat diet

HIF1α: Hypoxia inducible factor 1α

HK-2 cells: Human kidney-2 cells

HMGC2: Hydroxymethylglutaryl-CoA synthase 2

HCl: Hydrochloric acid

## I

Ig: Immunoglobulin

IGF1: Insulin-like growth factor 1

IGFR1: Insulin growth factor 1 receptor

IL-2: Interleukin-2

IR: Insulin receptor

IRS1: Insulin receptor substrate 1

IRS2: Insulin receptor substrate 2

## J

JNK: C-Jun-N terminal kinase

## K

$K^+$: Potassium

KI: Knock in

KO: Knock out

## L

LB: Lysogeny broth

LB5x: Loading buffer 5x

LBD: Ligand binding domain

LPL: Lipoprotein lipase

## M

Maf1: Maf1 homolog, negative regulator of RNA polymerase III

MAPK: Mitogen-activated protein kinase

mTORC1: Mammalian target of rapamycin complex 1

mTORC2: Mammalian target of rapamycin complex 2

## N

$Na^+$: Sodium

$NAD^+$: Nicotinamide adenine dinucleotide oxidized

NADH: Nicotinamide adenine dinucleotide reduced

NAFLD: Non-alcoholic fatty liver disease

NaOH: Sodium hydroxide

NF-κB: Nuclear factor kappa-light-chain-enhancer of activated B cells

NRF1: Nuclear respiratory factor 1

nVDRE: Negative vitamin D response elements

## P

P: Phosphorus

pAkt: Phosphorilated Akt

PAS: Periodic acid Schiff

PFA 4%: Paraformaldehyde 4%

PBD: PIP2 binding domain

PBS1x: Phosphate-buffered saline 1x

PCR: Polymerase chain reaction

PDK1: Phosphoinositide dependent protein kinase 1

PDH: Pyruvate dehydrogenase

PDZ-BD: PDZ binding domain

PEI: Polyethylenimine

PEPCK: Phosphoenolpyruvate carboxykinase

PEST: Proline-glutamic acid-serine-threonine

PFK-2/FBPase-2: Phosphofructokinase-2/fructose bisphosphatase-2

PGC1a: Proliferator-activated receptor gamma coactivator 1 alpha

PH: Pleckstrin homology

PI3K: Phosphatidylinositol 3-kinase

$PIP_2$: Phosphatidylinositol (4,5)-bisphosphate

$PIP_3$: Phosphatidylinositol (3,4,5)-trisphosphate

PKA: Protein kinase A

PKB or Akt: Protein kinase B

PKC: Protein kinase C

PLCγ: Phospholipase Cγ

PP1: Protein phosphatase 1

PP2: Protein phosphatase 2

PPARA: Peroxisome proliferator-activated receptor A

PPARγ: Peroxisome proliferator-activated receptor γ

PPia: Peptidylprolyl isomerase A

PTEN: Phosphatase and tensin homolog

PTH: Parathyroid gland hormone

PTT: Pyruvate tolerance test

PVDF: Polyinvinyldene diflororide

## Q

qRT-PCR: Quantitative reverse transcription polymerase chain reaction

## R

RNA: Ribonucleic acid

RNA Pol II: RNA polymerase II

RTK: Tyrosine kinase receptor

RXR: Retinoid X receptor

## S

SGLT1: Sodium-glucose cotransporter 1

SGLT2: Sodium-glucose cotransporter 2

SH2: Src homology 2

SOC: Store-operated channel

SRC: Steroid receptor coactivator

SREBP: Sterol-regulatory element-binding protein

STZ: Streptozotocin

## T

T1DM: Type 1 diabetes mellitus

T2DM: Type 2 diabetes mellitus

TAE: Tris-acetate-EDTA

TBP: TATA-box binding protein

TCA: Tricarboxylic acid

TRPV5: Transient receptor potential cation channel subfamily V member 5

TRPV6: Transient receptor potential cation channel subfamily V member 6

## U

UCP2: Uncoupling protein 2

UV: Ultraviolet light

## V

VEGF: Vascular endothelial growth factor

VD: Vitamin D

VDIR: VDR-interacting repressor

VDR: Vitamin D receptor

VDRE: Vitamin D response elements

## W

WT: Wild Type

# Introduction

# 1. Metabolism

Metabolism is the sum of all the chemical reactions that occur in our bodies to generate energy to maintain life. This energy comes from the nutrients that our body extracts from food, such as carbohydrates, fats and proteins. It is divided in two types: catabolism, a process whereby cells break down complex substances into smaller ones; and anabolism, which is just the opposite, cells convert simple substances into more complex compounds. The enzymes are catalytic proteins responsible for bringing about a specific biochemical reaction, for instance, speed up chemical reactions in metabolic pathways. The key energy players in the metabolic activities are some compounds like ATP, which is the main energy molecule used by cells, NADH and $FADH_2$ *(Figure 1)*. [1]

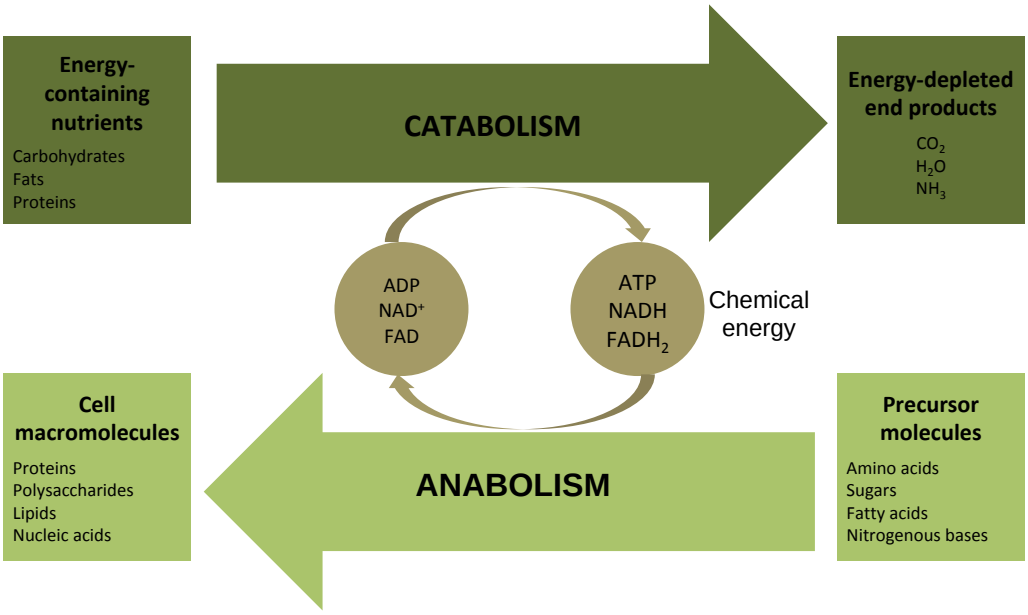


**Figure 1: Catabolic and anabolic processes.** *The catabolic routes transfer energy in form of energetic molecules (ATP, NADH, NADPH and $FADH_2$) to anabolic pathways that will transform precursor molecules into macromolecules. Adapted from Principles of biochemistry. Lehninger.* ***Figure abbreviations:*** *ADP, adenosine diphosphate; ATP, adenosine triphosphate; $CO_2$, carbon dioxide; FAD, flavin adenine dinucleotide oxidized; $FADH_2$, flavin adenine dinucleotide reduced; $H_2O$, water; $NAD^+$, nicotinamide adenine dinucleotide oxidized; NADH, nicotinamide adenine dinucleotide reduced; $NH_3$, ammonia.*

# 2. Carbohydrate Metabolism

Carbohydrates are the main molecules intended for energy supply due to its easy metabolism. Glucose is a really important molecule in the metabolism of many organisms because of its ability to make a vast amount of energy from its oxidation. The central role of glucose in metabolism arose early in evolution. Some tissues, such as brain, erythrocytes or renal medulla depend almost completely on glucose for their metabolism. The organism has the ability of store glucose as a high molecular weight polymer such as glycogen. There are some metabolic pathways to extract usable energy from glucose in cells: glycolysis, the conversion of pyruvate to acetyl-CoA, Krebs cycle, electron transport chain (ETC) and hepatic glucose production (glycogenolysis and gluconeogenesis). [1,2]

## 2.1 Glycolysis

Glycolysis is the metabolic route responsible for the oxidation of glucose in the cytosol of the cell; a molecule of 6 carbons (glucose) yields two molecules of 3 carbons (pyruvate). ATP and NADH are the result of the free energy released in this anaerobic process.

Ten steps are necessary to obtain the breakdown of the glucose into pyruvate. On the first phase, ATP is invested to obtain glyceraldehyde 3-phosphate as a product. After the second phase, the final yield is two molecules of ATP and two molecules of NADH per molecule of glucose. [1,2]

Three chemical transformations are remarkable in the glycolysis pathway: degradation of the carbon skeleton of glucose to pyruvate, phosphorylation of ADP to ATP and transfer of a hydride ion to $NAD^+$ forming NADH. The overall equation of glycolysis is:

$$Glucose + 2NAD^+ + 2ADP + 2P_i \rightarrow 2\ Pyruvate + 2NADH + 2H^+ + 2ATP + 2H_2O$$

## 2.2 Pyruvate to acetyl-CoA

Pyruvate, before entering to the Krebs cycle, needs to be degraded to acetyl-CoA, the form in which the cycle accepts most of its fuel input. Pyruvate dehydrogenase (PDH)

complex catalyzes the irreversible oxidative decarboxylation reaction from pyruvate to acetyl-CoA with an aerobic process in the mitochondria. The end products of this pathway are acetyl-CoA, $CO_2$ and NADH.

## 2.3 Krebs cycle

The Krebs cycle (citric acid cycle or tricarboxylic acid cycle) is a circular metabolic pathway formed by a set of reactions in the mitochondrial matrix that has the main function of release stored energy through acetyl-CoA oxidation. Acetyl-CoA comes from the conversion of the glycolysis outcome, pyruvate. The main products of this cycle are GTP derived from carbohydrates, fats and proteins, and $CO_2$. For each acetyl-CoA oxidized by the Krebs cycle, three NADH, one $FADH_2$ and one ATP or GTP are gained.[1]

## 2.4 Electron transport chain

ETC is form by a series of complexes found in the inner mitochondrial membrane that produce ATP as long as oxygen is available (aerobic conditions). Krebs cycle and ETC are located in the mitochondria, a fact that facilitates the transfer of electrons from one reaction to the other. NADH (mainly) and $FADH_2$ deliver pairs of high-energy electrons to the beginning of the chain. A sum of linked reactions, called oxidative phosphorylation, occurs in the inner mitochondrial membrane where electrons are passed between the ETC complexes, releasing energy along the way to power up the final production of ATP.

The electron pairs carried by NADH from glycolysis, which take place in the cytosol of the cells, transfer its high-energy electrons to some molecules capable of pumping them through the outer mitochondrial membrane. Once inside, the electron pair may be used for the formation of NADH or $FADH_2$. The complete oxidation of one molecule of glucose yields 30 to 32 ATP. [1,2]

## 2.5 Hepatic glucose production

Hepatic glucose may derive from glycogenolysis or gluconeogenesis. In short fasting periods, glycogenolysis is the main glucose source. Nevertheless, in long fasting,

glycogen reserves can get exhausted, and gluconeogenesis becomes the glucose source for the body. [3]

### *2.5.1 Glycogenolysis*

After a meal, glucose is stored in the liver as glycogen. In contrast, in fasting periods, glycogenolysis releases glucose from glycogen to be used by other tissues. [3]

Glycogenolysis is the breakdown of glycogen chains into glucose molecules. In the liver, when the body detects low glycemia, glycogenolysis is activated releasing glucose to the bloodstream. In the muscle, glycogenolysis is used to produce energy (ATP) by glycolysis of the glucose obtained.[2]

### *2.5.2 Gluconeogenesis*

Gluconeogenesis is a really clever strategy that the body has created in order to make glucose from precursors that are not carbohydrates (pyruvate, fructose, lactate, alanine and glycerol) when there is not enough sugar in our blood (fasting state or intensive exercise). Liver is the main organ responsible of gluconeogenesis (90%), whereas the kidneys make the rest (10%).

The body can make glucose by gluconeogenesis from several sources: pyruvate; lactate, the production of which is increased during exercise; glycogenic amino acids (alanine), that are capable to be transformed into glucose, and glycerol, which enters the pathway through conversion to dihydroxyacetone phosphate.

There are two main enzymes involved in gluconeogenesis: glucose-6-phosphatase catalytic subunit (G6PC) that catalyzes the hydrolysis of glucose-6-phosphate to glucose in the endoplasmic reticulum and phosphoenolpyruvate carboxykinase (PEPCK) that catalyzes the conversion of oxaloacetate to phosphoenolpyruvate.[1] Moreover, the mechanism used to extract glucose from hepatocytes is the glucose transporter 2 (GLUT2).

Liver contains the protein kinase A (PKA), which is a kinase that depends on cyclic adenosine monophosphate (cAMP) concentration and it has an important role in the regulation of glucose and lipid metabolism, activating glycogenolysis, gluconeogenesis

and lipolysis. CCAAT/enhancer-binding protein alpha (CEBPa) is a key protein that stimulate cAMP production and, in consequence, PKA activation and G6PC and PEPCK transcription. [4] CEBPa$^{-/-}$ mice born without glycogen reserves and lipids and, as a result, they die due to hypoglycemia, some hours after being born. [5]

## 2.6 Insulin and glucagon as glycolysis and gluconeogenesis regulators

Two essential hormones in glucose metabolism, insulin and glucagon, regulate the key steps in glycolysis and gluconeogenesis.

On the one hand, insulin is increased after a meal and stimulates the expression of phosphofructokinase, pyruvate kinase and Phosphofructokinase-2/fructose bisphosphatase-2 (PFK-2/FBPase-2) bifunctional enzyme that are enzymes involved in glycolysis pathway. On the other hand, after fasting, glucagon inhibits these enzymes and activates PEPCK and fructose-1,6-bisphosphatase expression, which are enzymes implicated in gluconeogenesis.

### *2.6.1 Insulin*

Insulin is a small endocrine peptidic hormone produced by β-cells from Islets of Langerhans in the pancreas. It has two polypeptide chains joined by two disulphide bonds. It is synthesized as a larger precursor called preproinsulin. After the removal of the signal sequence (an amino-terminal sequence) and formation of 3 disulfide bonds, it produces proinsulin, which is stored in secretory granules in β-cells. Finally, when glucose levels are high, a second proteolytic cleavage will convert proinsulin to mature insulin by removing C-peptide.

Insulin is released from pancreatic β-cells into the bloodstream in response to high glucose levels. When glycemia is elevated, β-cells raise intracellular ATP, resulting in the closure of $K^+$ channels and depolarizing the plasma membrane. As a consequence, the change in membrane potential will open calcium ($Ca^{+2}$) channels leading to the entering of $Ca^{+2}$ in the β-cell and activating insulin exocytosis from insulin granules *(Figure 2)*. [1,2]

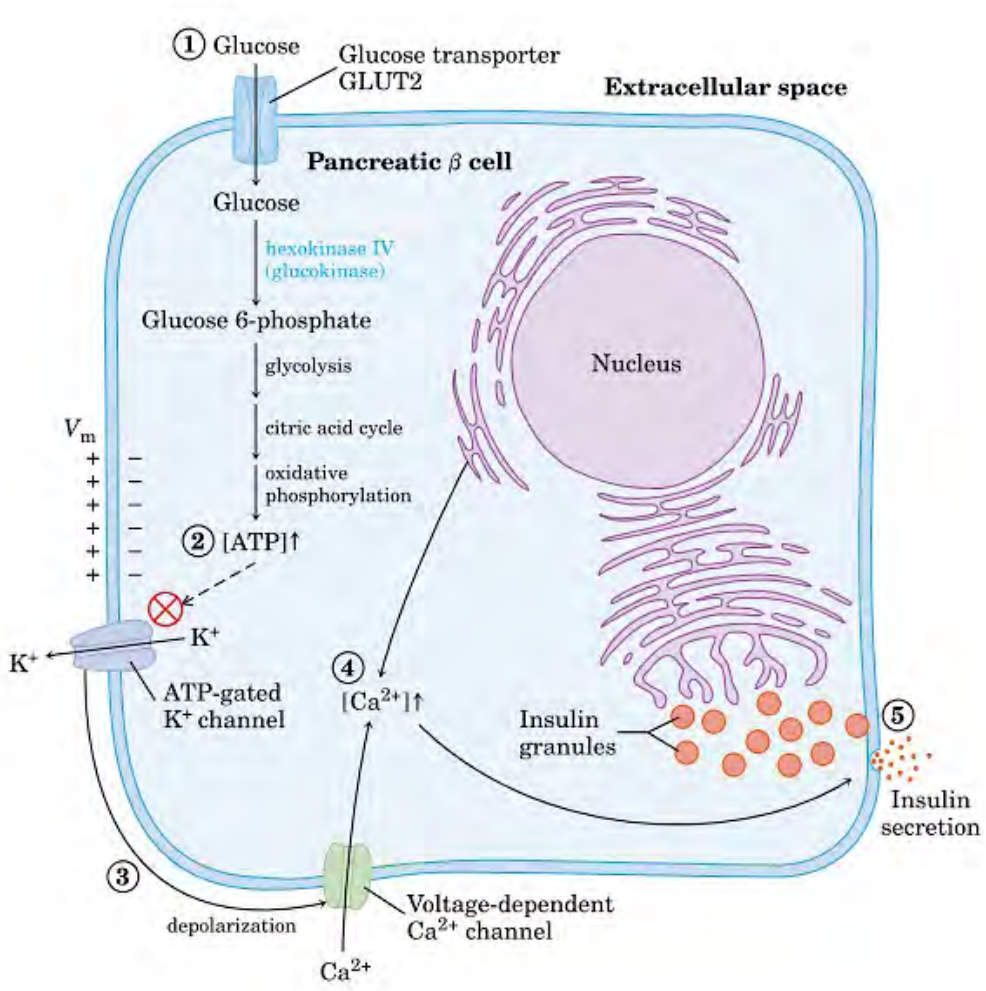


**Figure 2: Insulin secretion from pancreatic β-cell.** ***(1)*** *When there is high glycemia, glucose enters into the β-cell through GLUT2 channel.* ***(2)*** *After glucose metabolization, ATP increases and $K^+$ channels are closed in the plasma membrane, with its subsequent depolarization.* ***(3)*** *Voltage-dependent $Ca^{+2}$ channels in the plasma membrane are opened due to the previous membrane potential changes.* ***(4)*** *$Ca^{+2}$ concentration is incremented into the β-cell cytosol.* ***(5)*** *The $Ca^{+2}$ increase activates insulin granules release by exocytosis and the insulin secretion to the bloodstream. Extracted from Principles on biochemistry. Lehninger. Figure abbreviations: ATP, adenosine triphosphate; $Ca^{+2}$, calcium; GLUT2, glucose transporter 2; $K^+$, potassium; $V_m$, membrane potential.*

After a meal, amino acids, glucose and fatty acids will go to the liver and will trigger insulin response, stimulating glucose uptake by the tissues. In the liver, the excess of glucose will be transformed into acetyl-CoA to synthesize fatty acids in form of triacylglycerols, which will be exported to fat and muscle *(Figure 3)*.

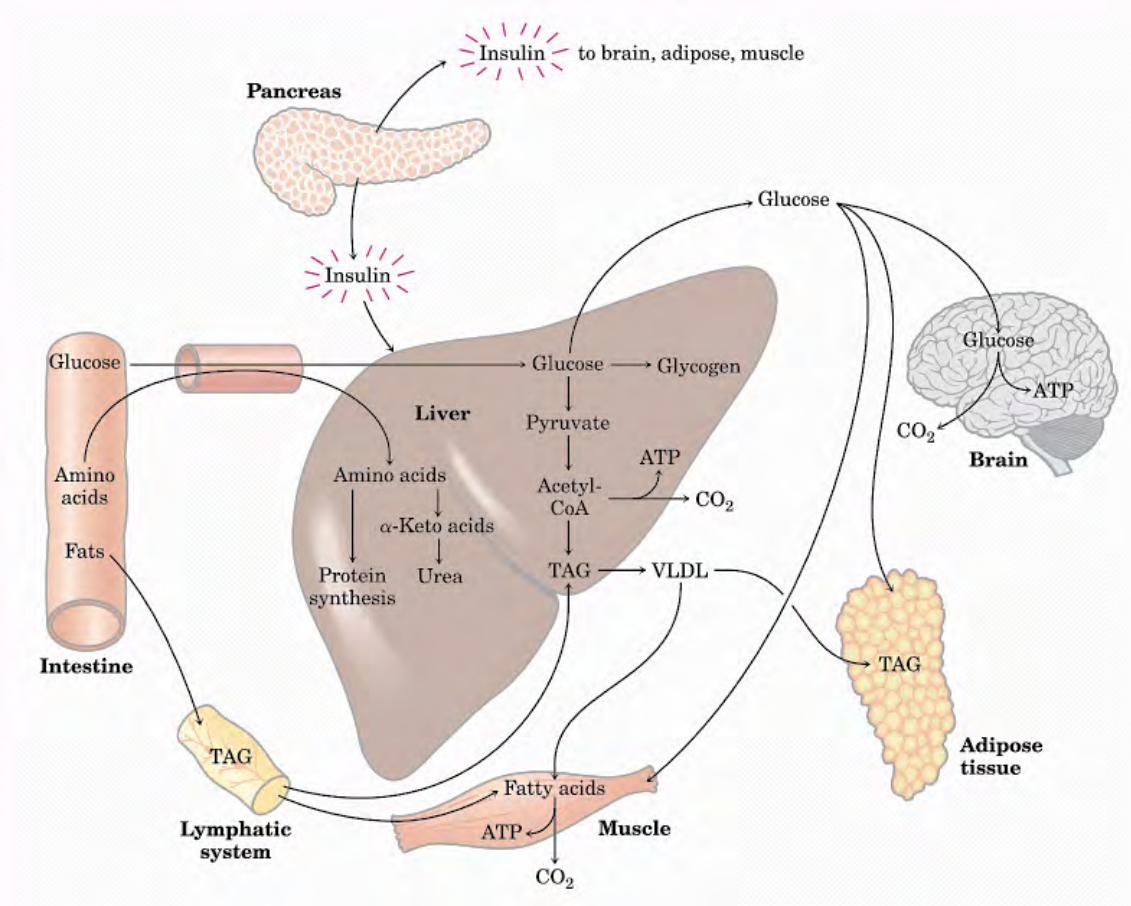


**Figure 3: Liver responses after a meal.** *When a high calorie meal is ingested, glucose, fatty acids and amino acids are introduced into the liver. After insulin action, glucose enters into the liver and its excess is oxidized to acetyl-CoA, which is used to synthesize fatty acids for export as TAGs to muscle and adipose tissue. Extracted from Principles on biochemistry. Lehninger. Figure abbreviations: Acetyl-CoA, acetyl coenzyme A; ATP, Adenosine triphosphate; $CO_2$, carbon dioxide; TAG, triacylglycerols; VLDL, very low-density lipoprotein.*

Insulin controls metabolism and gene expression by activating the insulin receptor, which is a tyrosine-kinase receptor. The receptor is formed by two α chains (located in the outer surface of the plasma membrane) and two β chains (transmembrane subunits with a carboxyl domain in the cytosol).

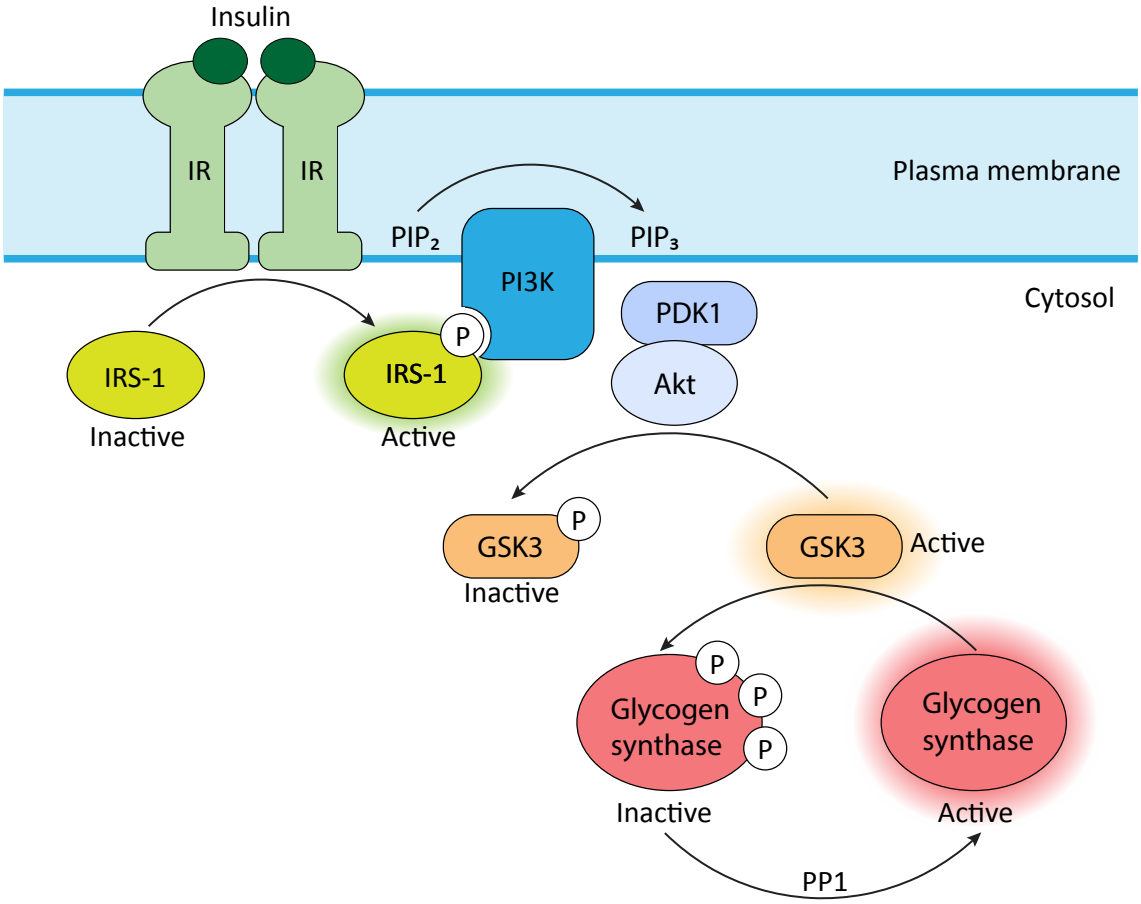


**Figure 4:** ***Insulin triggers glycogen synthesis.*** *When insulin is bound to IR, IRS-1 is phosphorylated and activates the PI3K-Akt pathway, which phosphorylates and inactivates GSK3. The inactivation of GSK3 allows the glycogen synthesis. Adapted from Principles on biochemistry. Lehninger. Figure abbreviations: Akt, protein kinase B; GSK3, glycogen synthase kinase 3; IR, insulin receptor, IRS-1, insulin receptor substrate 1; PDK1, phosphoinositide dependent protein kinase 1; PI3K, phosphatidylinositol 3-kinase; $PIP_2$, phosphatidylinositol (4,5)-bisphosphate; $PIP_3$, phosphatidylinositol (3,4,5)-trisphosphate; PP1, protein phosphatase 1.*

When insulin is bound to insulin receptor (IR), its tyrosin kinase activity catalyzes the phosphorilation of tyrosin residues on proteins such as insulin receptor substrate 1 (IRS-1). Phosphorilated IRS-1 will join PI3K, which converts phosphatidylinositol (4,5)-bisphosphate ($PIP_2$) to phosphatidylinositol (3,4,5)-trisphosphate ($PIP_3$) in the inner plasma membrane. Then, PDK1 will be recruited and triggered and then, Akt will be in charge inactivate glycogen synthase kinase 3 (GSK3) by phosphorilation. GSK3 inactivation allows phosphoprotein phosphatase 1 (PP1) to activate glycogen synthase by dephosphorylation. Hence, insulin stimulates glycogen synthesis pathway to help storing glucose as glycogen in hepatocytes, decreasing blood glucose levels *(Figure 4)*.[1,2]

In the liver, fatty acid oxidation suppression inhibits gluconeogenesis by decreasing the production of acetyl-CoA, which is the pyruvate carboxylase activator. Pyruvate carboxylase is in charge of transforming pyruvate into oxaloacetate, so the accumulation of acetyl-CoA stimulates gluconeogenesis. Insulin can inhibit lipolysis decreasing fatty acid availability and its plasmatic concentration, hence suppressing gluconeogenesis. [6,7]

### *2.6.2 Glucagon*

Glucagon is an endocrine peptide hormone produced by α-cells from islets of Langerhans in the pancreas.

It is secreted from pancreatic α-cells during fasting to promote glucose release from liver. Hepatic glycogen reserves will be broken down into glucose-6-phosphate (G6P) and then, into free glucose to be released into the bloodstream. Gluconeogenesis will be enhanced by glycerol from triacylglycerol breakdown and amino acids from proteins *(Figure 5)*.

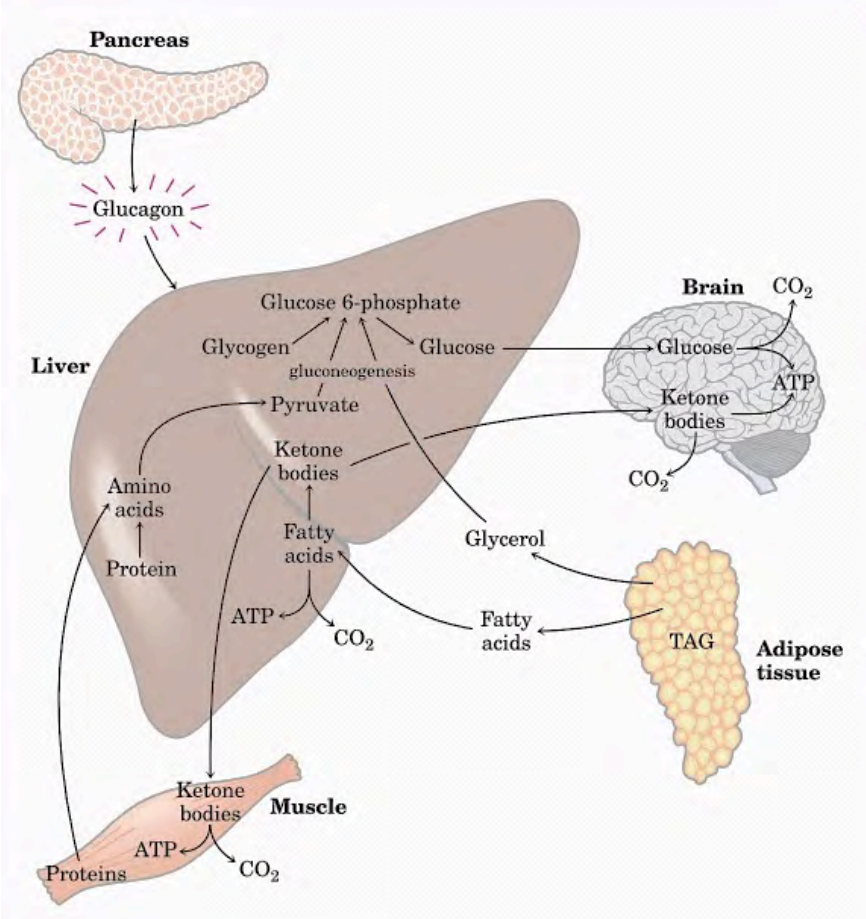

**Figure 5: Glucagon effects during the fasting state.** *When there is a long time of food starvation, glucagon activates in the liver the glycogenolysis to obtain free glucose, which is released into the bloodstream. Moreover, gluconeogenesis is also activated to generate enough glucose to maintain the brain with energy fuel. Extracted from Principles on biochemistry. Lehninger. Figure abbreviations: ATP, adenosine triphosphate; $CO_2$, carbon dioxide; TAG, triacylglycerols.*

Glucagon activates PKA through increasing cAMP leading to the activation of glycogen phosphorylase. It inactivates glycogen synthesis by phosphorylating glycogen synthase, and it also reduces glycolysis by phosphorylating both PFK-2/FBPase-2 and pyruvate kinase. [1,2]

Another gene that can modulate gluconeogenesis is peroxisome proliferator-activated receptor gamma coactivator 1 alpha (PGC1a), which is an important regulator of mitochondrial biogenesis and energy expenditure.[8] In the liver, under glucagon stimuli, PGC1a expression is increased during fasting periods. Glucagon will activate cAMP, and bound to PKA, will trigger CREB and will transcribe PGC1a. PGC1a is the coactivator of Forkhead box O1 (FOXO1) to regulate on a transcriptional level the activation of PEPCK and G6PC.[9,10,11,12] PKA pathway is not the only one involved in the regulation of PGC1a, as there are some more such as the PI3K/Akt signalling pathway. [11]

A summary of insulin and glucagon actions during high and low blood glucose levels is schematized in *Figure 6*.

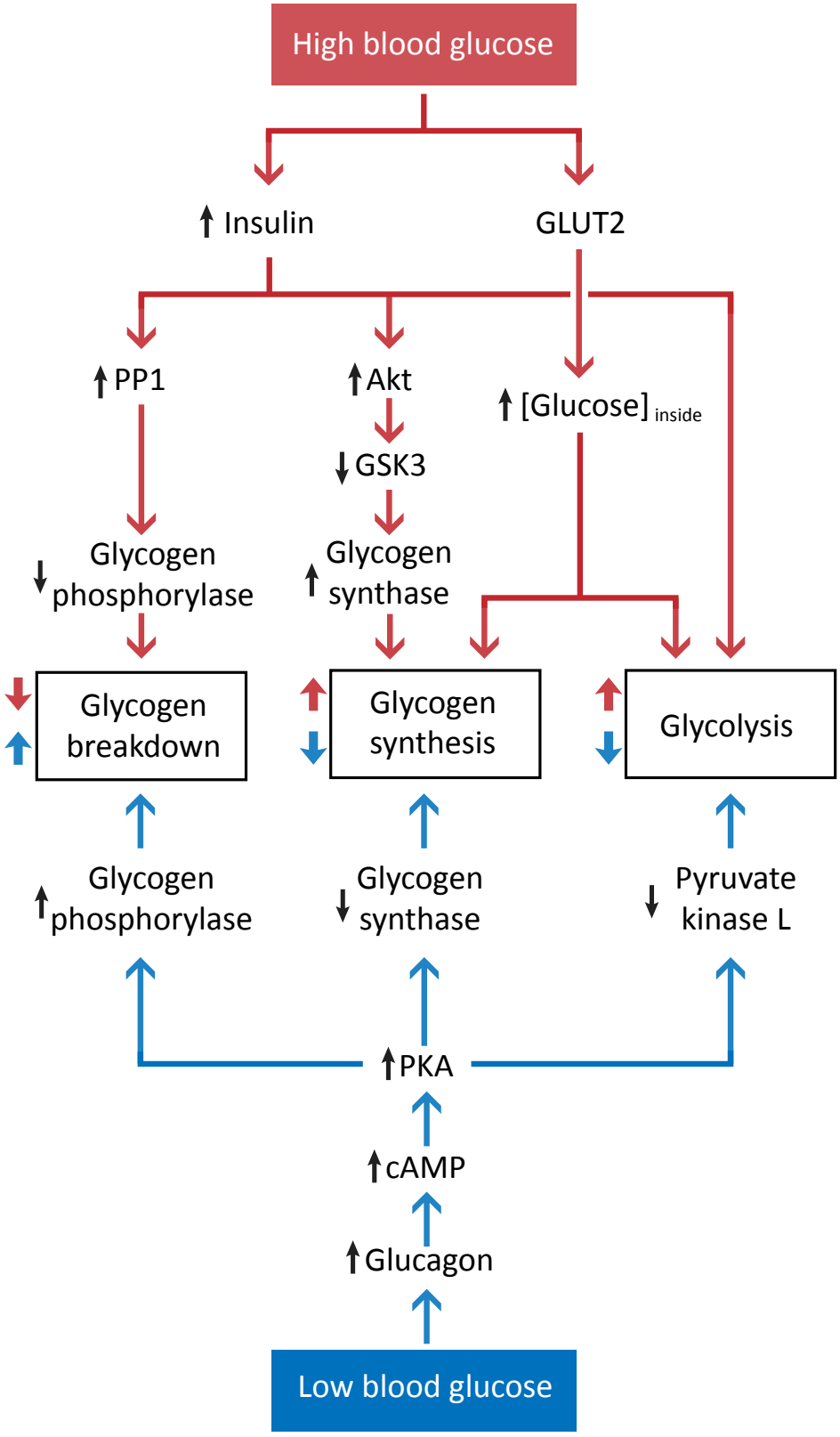


**Figure 6: Summary of high and low blood glucose reactions in liver.** *↑A →↓B means that an increase in A induces a decrease in B. Red arrows are related to high blood glucose and blue arrows to low blood glucose. Adapted from Principles on biochemistry. Lehninger. Figure abbreviations: Akt, protein kinase B; cAMP cyclic adenosine monophosphate; GLUT2, glucose transporter 2; GSK3, glycogen synthase kinase 3; PKA, protein kinase A; PP1, protein phosphatase 1*

## 2.7 Kidney glucose transport

The kidneys play an important role in glucose homeostasis controlling glucose reabsorption, gluconeogenesis and glucose uptake. Human glycemia should stay between 70-100 mg/dl before meals and under 140mg/dl after meals. Glucose is a key molecule in the body, so kidneys try to reabsorb all the glucose that is filtered in the glomerulus. Healthy kidneys can filter from 160 to 180g of glucose per day, but urine contains less than 1% of it. [13]

The reabsorption of glucose in the kidney takes place in the proximal tubule, where different glucose transporters and cotransporters play a key role *(Figure 7)*. Glucose is reabsorbed into the proximal tubule epithelial cells though the sodium-glucose cotransporters 1 (SGLT1) and 2 (SGLT2) located in the apical membrane. This process is guided by an electrochemical gradient in the membrane. The glucose accumulated leaves the cell though the basolateral membrane by the glucose transporters 1 (GLUT1) and 2 (GLUT2). Either the active (SGLTs) or the facilitated (GLUTs) glucose transporters have different distribution profiles along the proximal tubule. In consequence, the majority of filtered glucose (more than 90%) is reabsorbed in the segment 1 in the early portion of the proximal tubule by SGLT2 and GLUT2, while the other 10% is reabsorbed in the distal portion, segment 3, by SGLT1 and GLUT1. However, if SGLT2 is inefficient, SGLT1 can assume up to a 35% of the reabsorption *(Figure 8)*.[13,14,15,16,17,18]

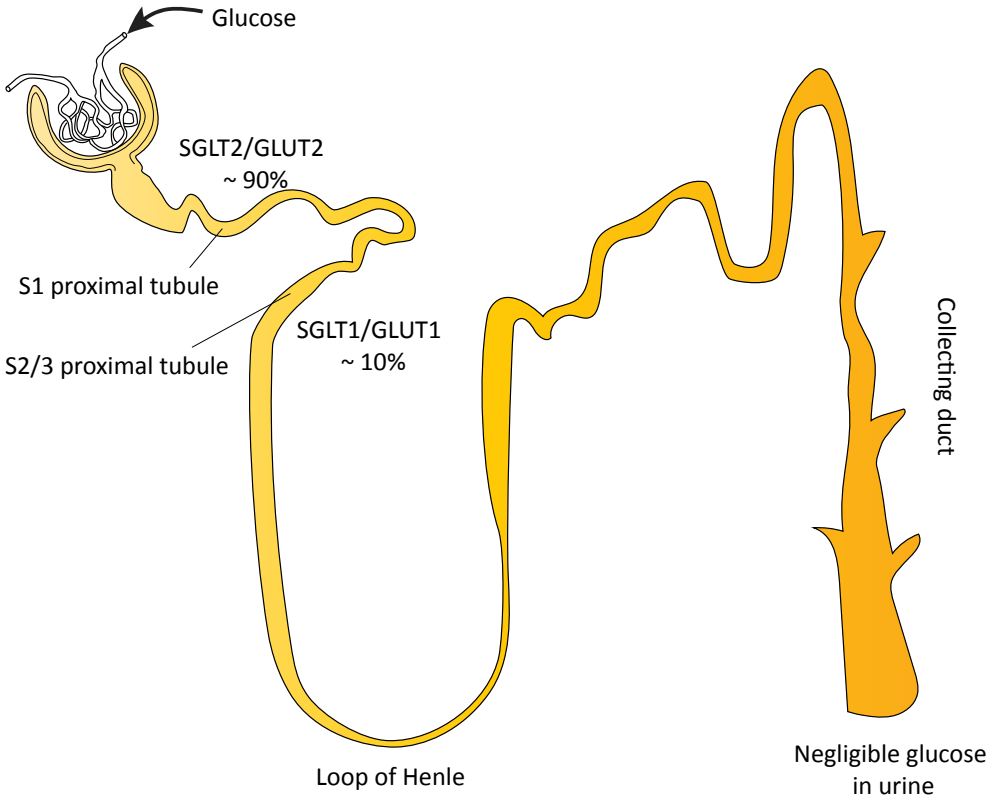


**Figure 7: Glucose reabsorption in kidney proximal tubules.** *Glucose is reabsorbed from the glomerular filtrate to bloodstream by glucose transporters situated in renal proximal tubules. Up to 90% of glucose reabsorption occurs in the S1 by SGLT2 and GLUT2. The remaining 10% is reabsorbed through SGLT1 and GLUT1, which are located in the S3 of proximal tubule. If all the reabsorption is successful, negligible glucose in urine has to be found. Adapted from Bailey, C. J. et al. (2011). Figure abbreviations: GLUT1, glucose transporter 1; GLUT2, glucose transporter 2; S1, segment 1; S2/3, segment 2/3; SGLT1, sodium-glucose transporter 1; SGLT2, sodium-glucose transporter 2.*

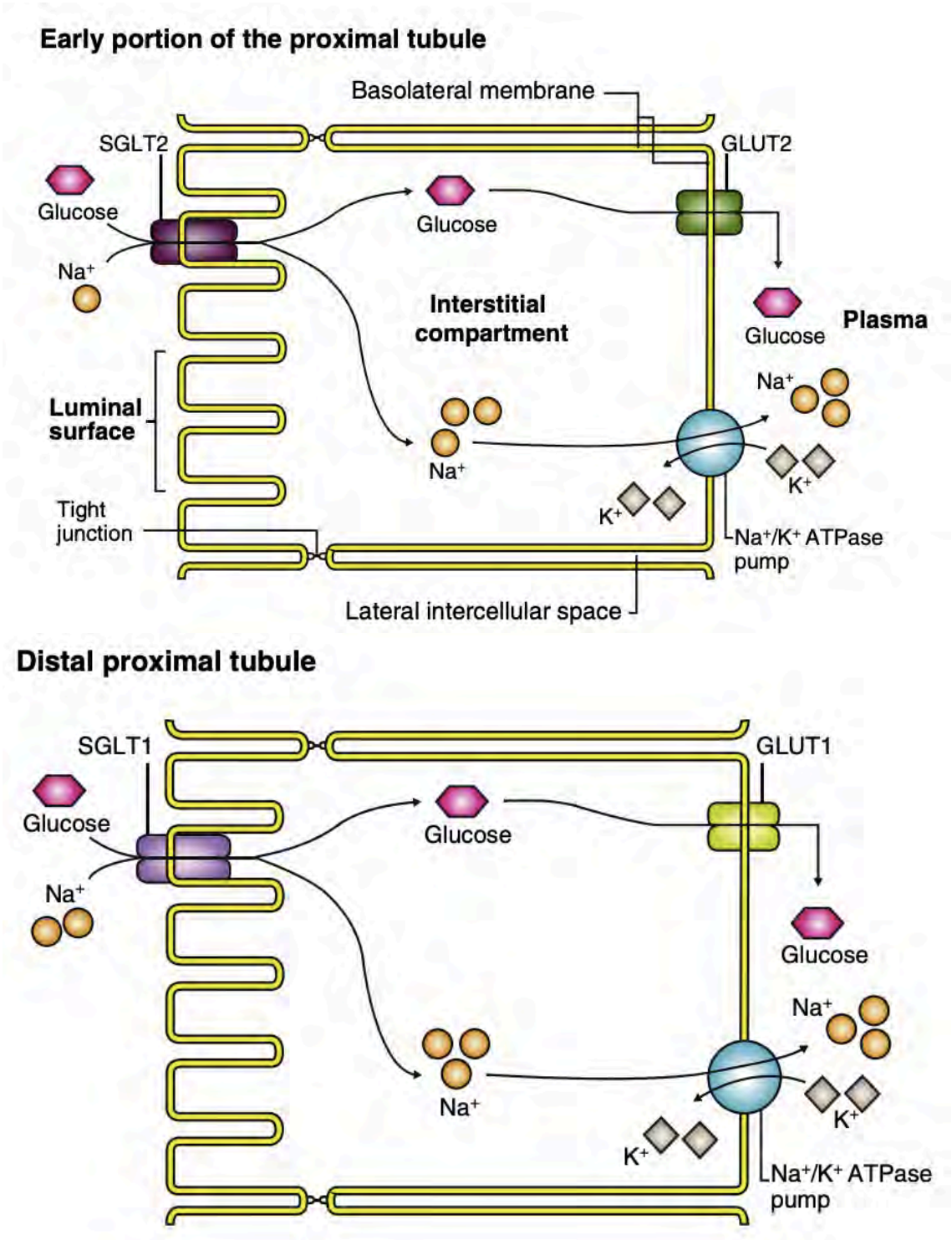


**Figure 8: Detailed glucose reabsorption in kidney proximal tubule cells. (*Early portion of the proximal tubule)*** *Glucose is reabsorbed in the S1 of the proximal tubule cells by SGLT2 by coupling glucose with ingoing diffusion of $Na^+$. As $Na^+$ concentration in the cytosol is increased, a $Na^+/K^+$/ATPase pump maintains the ion equilibrium extracting $Na^+$ ions across the basolateral membrane of the cell in exchange for $K^+$ ions in 3:2 stoichiometry. Glucose is extracted from the cells to the interstitial compartment by the facilitative glucose transporter GLUT2.* ***(Distal proximal tubule)*** *The same mechanism occurs in the S3 of the proximal tubule with SGLT1 and GLUT1 glucose transporters. Extracted from Wilding, J. et al. (2014) Figure abbreviations: ATPase pump, adenosine triphosphatase pump; GLUT1, glucose transporter 1; GLUT2, glucose transporter 2; $K^+$, potassium; $Na^+$, sodium; SGLT1, sodium-glucose transporter 1; SGLT2, sodium-glucose transporter 2.*

# 3. Lipid Metabolism

Human cells can obtain energy also from fats ingested in the diet, mobilizing fats stored in adipocytes and converting dietary carbohydrates, in the liver, into fats to export them to other tissues.

Epithelial cells in the small intestine absorb triacylglycerols ingested from the diet, but before, they must be emulsified by bile acids (derived from cholesterol) and hydrolyzed by intestinal lipases. Bile acid amidation requires two different enzymes, bile acid CoA ligase and bile acid CoA:amino acid *N*-acyltransferase (BAAT), which mediates the conjugation of an amino acid with a CoA-activated bile acid.[19] Finally, triacylglycerols will be broken down by lipoprotein lipase (LPL) in chylomicrons, which are in charge of delivery to tissues.

Triacylglycerol lipolysis in adipose tissue will release fatty acids into the bloodstream during starvation, to be used as energy source. Their excess together with glycerol 3-phosphate will be used for its resynthesis in the liver.[1] Angiopoietin-like protein 8 (ANGPTL8) increases serum triacylglycerol levels by inhibiting LPL in liver. High levels of ANGPTL8 are related to T2DM, obesity and insulin resistance.[20,21]

When fatty acids are inside the cells, they will be oxidized in mitochondria into acetyl-CoA that will enter into the Krebs cycle. Finally, the electrons generated are used to form ATP through the ETC. [1,2,22]

## 3.1 β-oxidation

β-oxidation is the metabolic process by which fatty acids are broken down to obtain acetyl-CoA. The overall reaction for every single cycle of β-oxidation is:

$C_n$-acyl-CoA + $FAD^+$ + $NAD^+$ + $H_2O$ + CoA → $C_{n-2}$-acyl-CoA + $FADH_2$ + NADH + $H^+$ + acetyl-CoA

This catabolic process is tightly regulated because it consumes a lot of precious energy and, thus, it is only activated when required. β-oxidation is not necessary when the amount of circulating glucose is enough. Then, insulin will trigger the dephosphorylation of acetyl-CoA carboxylase (ACC), which catalyzes the malonyl-CoA production that is involved in fatty acid synthesis, preventing fatty acid entry into the mitochondrial matrix. In contrast, in order to obtain energy from fatty acids, β-oxidation will be activated when glycemia drops and glucagon rises. Then PKA will be activated, which phosphorylates and inactivates acetyl-CoA carboxylase decreasing malonyl-CoA concentration allowing the entry of fatty acids into the mitochondria *(Figure 9)*. [1,2]

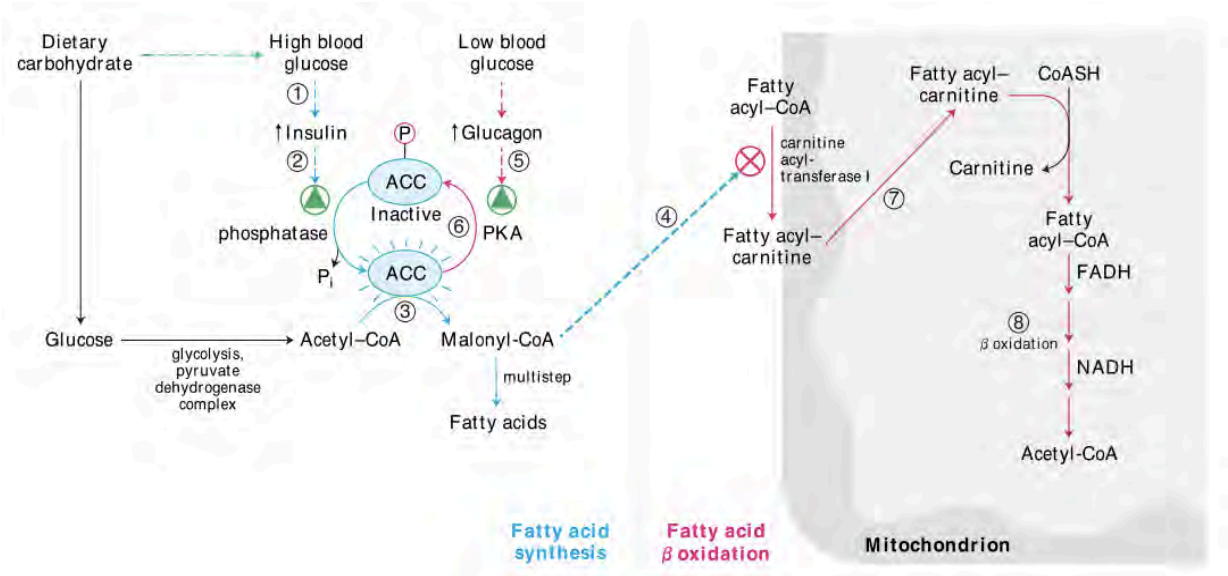


**Figure 9: Fatty acid synthesis** ***(1)*** *High blood glucose triggers insulin.* ***(2)*** *Insulin activates ACC* ***(3)****, which starts the fatty acid synthesis converting Acetyl-CoA to Malonyl-CoA.* ***(4)*** *Malonyl-CoA inhibits carnitine acyl-trasnferase 1 preventing fatty acid entry into the mitochondrial matrix.* **Fatty acid β-oxidation** ***(5)*** *Low blood glucose stimulates glucagon,* ***(6)*** *which inactivates ACC.* ***(7)*** *Fatty acids enter into the mitochondrial matrix.* ***(8)*** *β-oxidation takes place in order to become the main source of fuel. Extracted from Principles on biochemistry. Lehninger. Figure abbreviations: ACC, acetyl-CoA carboxylase; FADH, flavin adenine dinucleotide reduced; NADH, Nicotinamide adenine dinucleotide reduced; PKA, protein kinase A.*

## 3.2 Ketogenesis

If the carbon skeleton of an amino acid can form acetyl-CoA instead of glucose, it is called a ketogenic amino acid. Hence, ketogenesis is the process where the liver transforms acetyl-CoA to ketone bodies. It mainly occurs when fatty acid oxidation produces an abundance of acetyl-CoA and the levels of oxaloacetate are too low (for instance, in a fasting state or in type 1 diabetes mellitus (T1DM)). During starvation, ketone bodies are the suppliers of energy to all the tissues, especially to the central nervous system. If the brain cannot use glucose as fuel, the only sources of energy remaining are ketone bodies. They provide nearly half of the body's total energy and up to 70% of the energy required by the brain.[23] Once in the tissue, ketone bodies are transformed back to acetyl-CoA to produce ATP by Krebs cycle and ETC. Three types of ketone bodies (acetoacetate, β-hydroxybutyrate and acetone) can be made from pyruvate, fatty acids, glycerol and glycogenic amino acids, which are precursors of acetyl-CoA. A key ketogenic enzyme is hydroxymethylglutaryl-CoA synthase 2 (HMGCS2) that catalyzes the first ketogenesis reaction.[24]

However, if there is an excess of ketone bodies accumulated in the bloodstream (ketosis) the blood acidity quickly raises leading on ketoacidosis, a really dangerous disease that can induce coma and eventually death if untreated. Ketosis is likely to occur in uncontrolled T1DM, being one of the main causes of death in those patients.[1,24]

Forkhead Box A2 (FOXA2) also regulates ketone body formation and lipid metabolism. When FOXA2 is phosphorylated, it is maintained in the cytoplasm by insulin signaling via PI3K/Akt pathway.[25] However, when insulinemia goes down during fasting, FOXA2 is dephosphorylated and translocated into the nucleus enhancing the transcription of genes related to ketogenesis and β-oxidation.[26]

The nuclear receptor peroxisome proliferator-activated receptor-A (PPARA) is a regulator of hepatic metabolism activated by fatty acids in response to fasting. PPARA bound to retinoid X receptor (RXR) is suggested to promote the transcription of genes related to ketogenesis, β-oxidation and fatty acid transport. Some of them, which are directly regulated by PPARA, are those encoding acyl-CoA oxidase (ACOX1) (involved in

peroxisomal β-oxidation); carnitine palmitoyl transferase 1 (CPT1) (which transports fatty acids across the mitochondrial membrane); and HMGCS2. Furthermore it also activates, fibroblast growth factor 21 (FGF21), which is a crucial intermediate between hepatic lipid metabolism, diet and PPARA in ketonic state. In summary, increasing the supply of free fatty acids to the liver will stimulate ketogenesis and CPT1 and HMGCS2 are required for ketone body production. [27,28,29,30]

# 4. Diabetes Mellitus

## 4.1 Physiopathology and mechanisms of DM

DM is a metabolic chronic disease characterized by high blood sugar, which might be triggered either by insulin resistance (the use of insulin by the body is not effective) or to the malfunction of β-cells in pancreas leading to altered insulin production. DM leads to serious health complications in heart, blood vessels, nerves, kidneys or eyes.

DM is a huge problem worldwide and one of the major causes of morbidity and mortality affecting the youth and middle-aged population. According to the last *International Diabetes Federation* publication in 2017, around 425 million adults (20-79 years) suffer DM and it is estimated that by 2045 this will raise to 629 million. [31,32]

There are two main types of diabetes: T1DM and T2DM, characterized by hyperglycemia due to different reasons.

## 4.2 Type 1 Diabetes Mellitus

T1DM is a chronic autoimmune disease characterised by degeneration of β-cells from Langerhans pancreatic islets, which are in charge of insulin secretion. It affects mainly to young people, under 20, with normal weight. Immune cells, T lymphocytes or T cells ($CD4^+$ and $CD8^+$) and infiltrated macrophages, are the major effectors of this guided autoimmune response, reacting to proteins from β-cells. Like all the autoimmune diseases, it is a result of multiple factors, either genetic (in the major histocompatibility region) or environmental (temperature, infections, diet…). The autoantibodies, such as insulin and glutamic acid decarboxylase autoantibodies, can be detectable before the symptoms appear.

In T1DM the cells do not receive glucose from blood because insulin is not working properly, and blood sugar is maintained at high concentrations; in consequence, cells will not have enough energy to develop their normal functions. As a result, these patients need pharmacological insulin to control their glycemia. However, sometimes their drug-regulated euglycemia gets out of control, either because almost all insulin

preparations are pharmacokinetically imperfect or due to errors in the insulin's dosage. All this could result in severe hypoglycemia, triggering deprivation of glucose in the brain and leading to confusion, loss of consciousness, coma or even death. Furthermore, if the DM patients do not handle accurately the insulin treatment, they will suffer maintained hyperglycemia, which may lead to ketoacidosis that can induce coma or even death. [23,31,33]

The *American Diabetes Association* describes hypoglycemia in people with DM as "all episodes of abnormally low plasma glucose concentration that expose the individual to potential harm", and it goes from concentrations of less than or equal to 70 mg/dl or 3.9 mmol/l. In fact, they also suggest a classification of five different types of hypoglycemia *(Figure 10)*: [34]

- *Severe hypoglycemia*: an event requiring assistance of another person to raise glucose levels and promote neurologic recovery.
- *Documented symptomatic hypoglycemia*: documented symptomatic hypoglycemia (symptoms plus low glucose).
- *Asymptomatic hypoglycemia*: asymptomatic hypoglycemia (low glucose without symptoms)
- *Probable symptomatic hypoglycemia*: symptoms without a glucose estimate.
- *Relative hypoglycemia*: symptoms with glucose levels that are not low but are approaching that level.

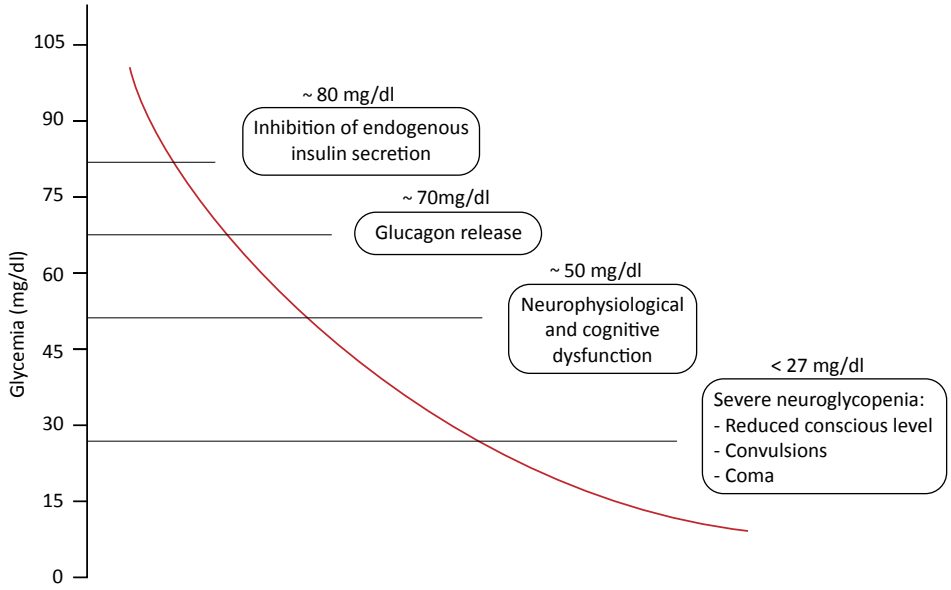

**Figure 10: Hypoglycemia effects depending on the glucose concentration in non-diabetic humans.** *Behavior of glucose-related hormones and physiopathology associated with different types of hypoglycemia.*

There are many different risk factors to suffer hypoglycemia in T1DM, such as, inappropriate insulin doses, decreased insulin clearance with renal failure, decreased exogenous glucose in fasting or inappropriate absorption of glucose (celiac disease), increased insulin sensitivity, increased glucose use during exercise or decreased endogenous production after alcohol consumption, among others.

People with T1DM suffer untold numbers of episodes of asymptomatic hypoglycemia. It is estimated that they suffer hypoglycemia during a 6.3% of the time in a day (around 1.5 hours). Most episodes are asymptomatic, but they lead to physiological consequences as they impair physiologic and behavioural defences against subsequent hypoglycemia. These patients experience an average of two episodes of symptomatic hypoglycemia per week and one episode of severe hypoglycemia per year. In consequence, between 6-10% of deaths in T1DM are caused by hypoglycemia. [35]

Hypoglycemia triggers a decrease in insulin release and an increase in glucagon and epinephrine secretion. In addition, it leads to neurogenic symptoms like sweating, hunger, paraesthesia, anxiety, palpitations and tremor, due to adrenergic and cholinergic stimulation. However, all this functional brain failures are corrected after the restoration of euglycemia. In summary, many of the physiological defenses against falling glycemia are compromised due to DM (mainly in T1DM, but also in advanced T2DM) *(Figure 11)*.

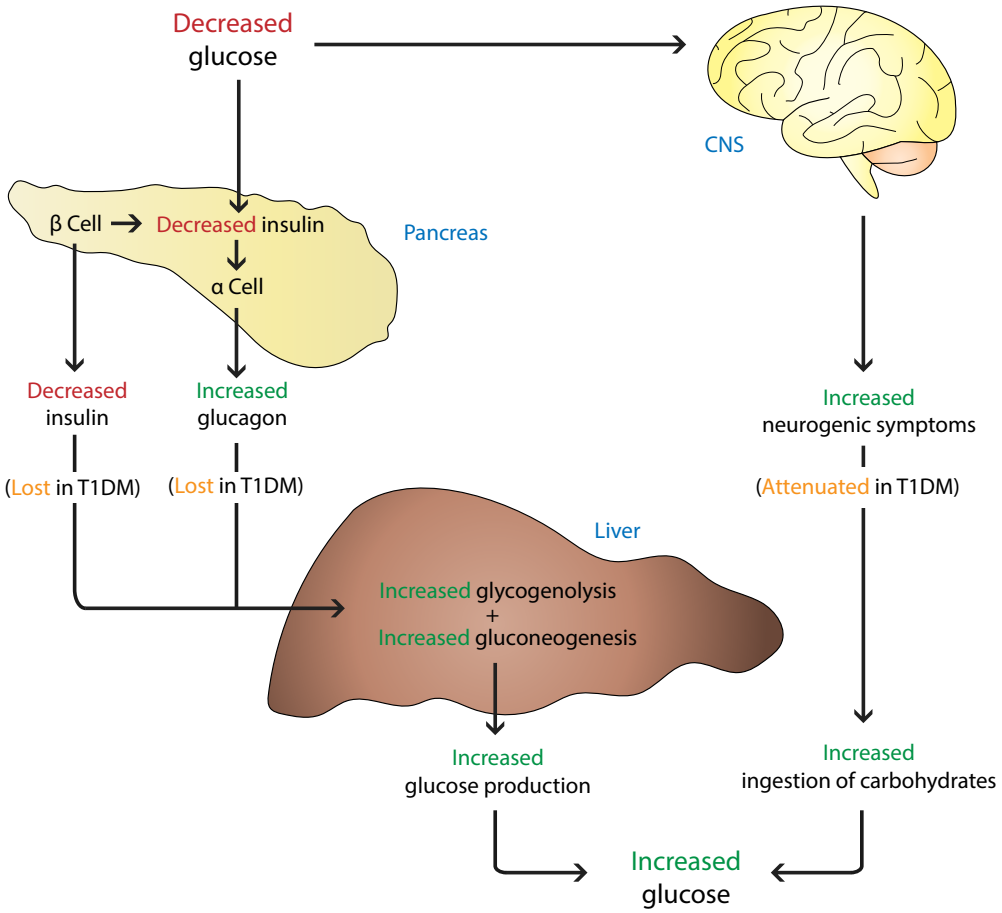


**Figure 11: Body protection systems against hypoglycemia and DM defects.** *The decrease of glucose in bloodstream activates a defense to alert the need of ingest food. These defenses are compromised in DM by pancreatic and CNS alterations. Adapted from Cryer, P (2006) Figure abbreviations: CNS, central nervous system; T1DM, type 1 diabetes mellitus.*

There is a concept associated to hypoglycemia named hypoglycemia-associated autonomic failure. This concept postulates that recent iatrogenic hypoglycemia causes both defective glucose counter-regulation, by reducing epinephrine responses, and hypoglycemia unawareness, by reducing sympathoadrenal stimulation and the consequent neurogenic responses and, thus, inducing a vicious cycle of recurrent hypoglycemia. [36]

## 4.3 Type 2 Diabetes Mellitus

T2DM is an endocrine and metabolic disorder characterized by insulin resistance and pancreatic β-cell malfunction. Insulin resistance is a pathological condition based on the lack of response from cells in front of a stimulus by insulin.

The most susceptible population to suffer this disease usually has overweight or obesity and is more than 30 years old; however, the incidence of T2DM is increasing in childhood due to the sedentary lifestyle. The influence of overweight and obesity to insulin resistance can be mediated by many pathways, such as deregulation of key hormones like glucagon or leptin, high concentrations of cytokines and other inflammatory signals. [31,37]

Although it is thought that hypoglycemia is only a T1DM complication, it is well known that some T2DM patients can also suffer this problem due to the treatment strategies employed and the longer life expectancy. It mainly occurs in elderly population with T2DM that have poor glycaemic control because they have been exposed to either exogenous insulin treatment or oral antidiabetic agents for a long time. [38] In these subjects, severe hypoglycemia can produce serious neuronal problems producing neuronal cell death and damaging essential regions of the brain. Furthermore, they frequently have nocturnal hypoglycemia, which is often associated with convulsions, coma, cardiac arrhythmias and sudden death.

# 5. Phosphatase and Tensin homolog (PTEN)

## 5.1 PTEN discovery

The Phosphatase and tension homolog deleted on chromosome 10 (PTEN) or Mutated in Multiple Advanced Cancers 1 (MMAC1) gene was discovered at the same time by two laboratories in 1997 who were studying chromosome 10q23 which is a chromosomal site prone to have loss of heterozygosity in advanced tumors identified in 1984. [39,40,41] In 1998, the protein was described due to the sequence homology with some well-known proteins such as the protein tyrosine phosphatase superfamily and the cytoskeletal protein tensin. Therefore, PTEN was distinguished as a dual lipid and protein phosphatase and as the mainly inhibitor of the PI3K/Akt pathway where acts as a lipid phosphatase which dephosphorylates $PIP_3$ to $PIP_2$, thereby inactivating Akt function. In the same year, the PTEN-KO mouse model was generated concluding that it had embryonic lethality [42,43]. Since then, it is established as one of the most important tumor suppressor genes and a cellular homeostasis regulator. [44,45,46]

## 5.2 PTEN structure

In humans, PTEN is located in the 10q23 region from the chromosome 10, while in mice, it is found in the qC1 region from the chromosome 19. It has a length of 105kb divided in 9 exons. [40,41] PTEN gene codifies for a 403 amino acids protein with a molecular weight of 47kDa. [47] Both human and murine proteins differ only in a single amino acid change from a serine to a threonine, located in the region of the carboxyl terminal tail, demonstrating that it is a much-conserved gene during the evolution. [48]

PTEN is divided into five functional domains, which were identified in 1999 by the resolution of its crystal structure. [49] $PIP_2$ binding domain (PBD), located in the N-terminal region between amino acid 7 and 13, regulates PTEN activity and its binding to the membrane. Phosphatase domain (from amino acid 15 to 185) has the catalytic activity from the protein and contains the HCxxGxxR active site from amino acid 123 to 130. C2 domain (from amino acid 190 to 350) orientates the catalytical activity trough regulating PTEN localization to the plasma membrane and to cytoplasmic vesicles. In

the C-terminal part, it has a tail between amino acid 351 and 400 that contains two proline-glutamic acid-serine-threonine (PEST) sequences, which control protein stability. The last functional domain is called PDZ-binding domain (PDZ-BD), from amino acid 401 to 403, and it is in charge of recognizing target proteins *(Figure 12)*.[50,51,52,53]

Recently, new isoforms of PTEN have been reported, even though, the 403 amino acid protein is the most abundant. All the isoforms are produced from the same canonical mRNA, but generated from alternative translation beginnings. Until now, four PTEN translational variants have been defined: PTEN-L, PTEN-M, PTEN-N and PTEN-O. All of them are being studied to define their structures, functions, physicochemical properties and their biological relevance. [45]

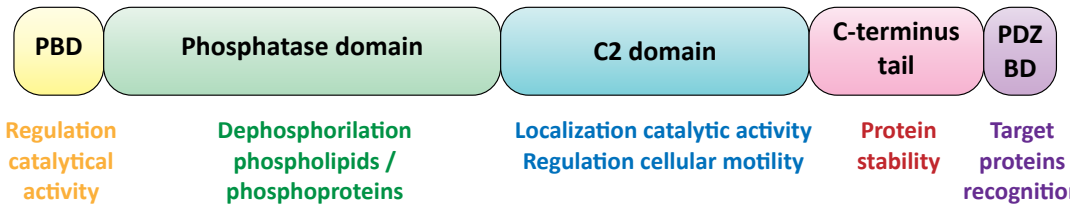


**Figure 12: PTEN structure.** *Representative image of the canonical PTEN isoform functional domains: PBD, Phosphatase domain, C2 domain, C-terminus tail and PDZ-BD. Adapted from Tesio, M et al. (2015). Figure abbreviations: PBD, phosphatidylinositol (4,5)-biphosphate binding domain; PDZ-BD, PDZ-binding domain.*

## 5.3 PTEN role in the PI3K/Akt signaling pathway

PTEN is a well-studied gene both at physiological or pathological level. Mainly it was investigated in the ontology of different tumors; however, the study of its role in normal cell function is not fully understood. PTEN can be located both in the cytosol and the nucleus, thus giving it plenty of different functions depending on its location. [53]

PTEN is a dual phosphatase not redundant that negatively regulates the PI3K/Akt pathway, regulating essential processes to maintain the cell homeostasis (growth and metabolism, cell polarity and migration, cell-cycle progression and stem cell renewal, and cell architecture and environment). [54]

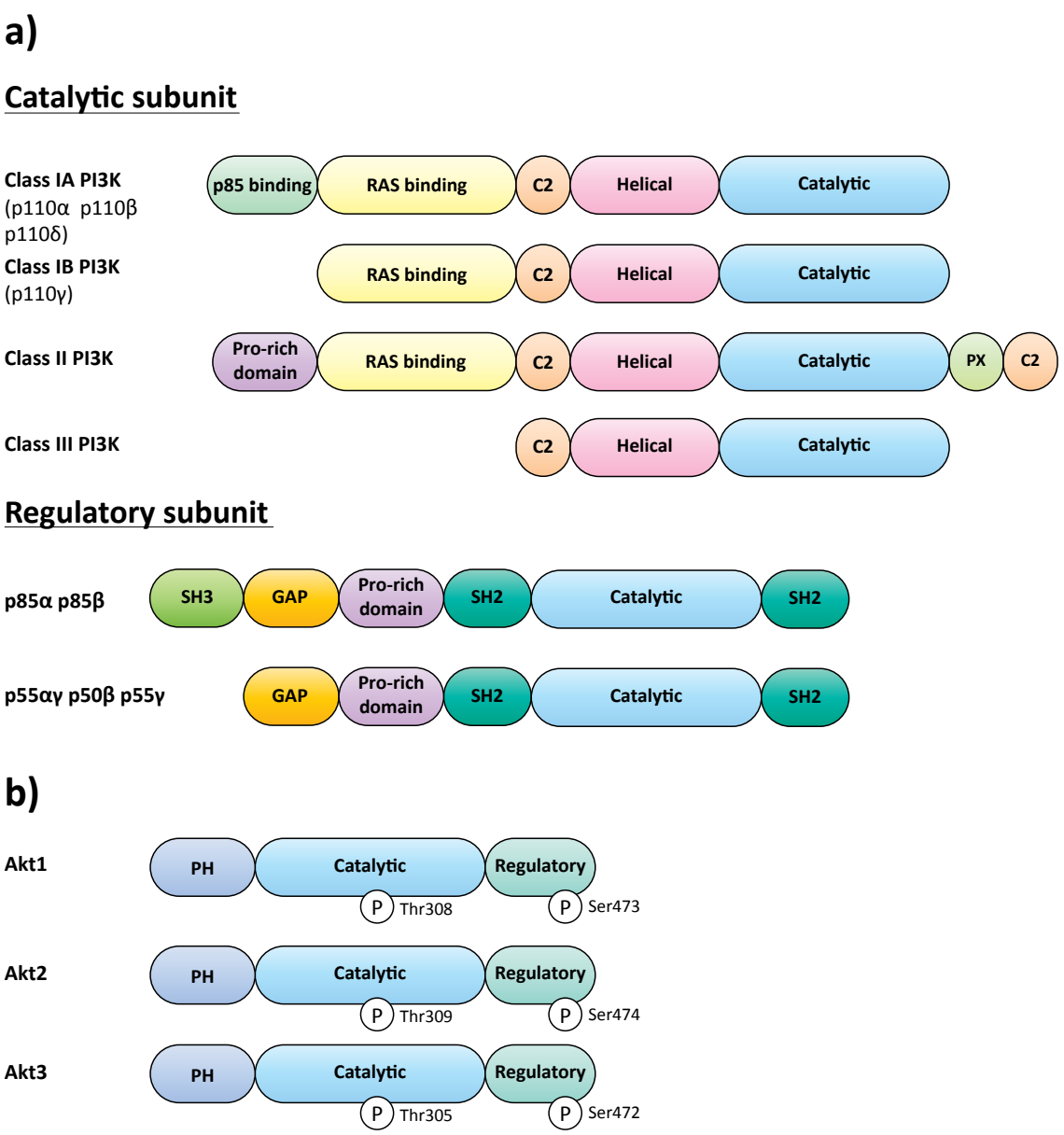


**Figure 13: Classification of PI3K and Akt family members.** ***(a)*** *PI3K is formed by catalytic and regulatory subunits. Catalytic subunit is divided in 3 classes and the regulatory subunit in 2 on the basis of their structural and biochemical features.* ***(b)*** *Akt is divided in 3 isoforms: 1, 2 and 3. Adapted from Sup Song, M et al. (2012) and Papadatos-Pastos (2015). Figure abbreviations: Akt, protein kinase B; GAP, GTPase-activating protein domain; PI3K, phosphatidylinositol 3-kinase; PH, pleckstrin homology domain; PX, phosphoinositide-binding structural domain; SH2, Src Homology 2; SH3, Src Homology 3.*

The PI3Ks constitute a lipid kinases family divided into 3 classes depend on their biochemical and structural characteristics (Class IA or IB PI3K, Class II PI3K and Class III PI3K). The three types contain a homology region formed by a catalytic domain, a helical domain and a C2 domain. All of them defined by the regulatory subunit, p85 (p85α, p85β, p55α, p50β and p55γ), and the catalytic subunit, p110 (p110α, p110β, p110δ and p110γ) *(Figure 13A)*. [55,56]

PI3K/Akt pathway classical activation starts with the binding of a growth factor (GF) to a tyrosine kinase receptor (RTK), like the insulin growth factor 1 receptor (IGFR1) or the human epidermal growth factor receptor (EGFR). This union will cause the dimerization and autophosphorylation of the RTK. The PI3K p85 subunit can be bound directly to the activated RTK through the physic interaction of its Src homology 2 (SH2) domain or indirectly, by intermediate phosphoproteins, such as IRS1 and IRS2. Thus, p85 has a key role into the activation of PI3K because it is not only the anchor to RTK, but also it will eliminate the inhibitory effect on p110. Then, the catalytic subunit p110 will be recruited to trigger the inositol ring lipids phosphorylation of the $PIP_2$ to obtain $PIP_3$. These lipids recruit and bind to membrane proteins with pleckstrin homology (PH) domains such as phosphoinositide dependent protein kinase 1/2 (PDK1/2) or Akt *(Figure 14)*. [54,57,58]

G protein-coupled receptors or the Ras GTPase can also alternatively activate PI3K/Akt pathway inducing conformational changes in the p110 subunit and activating it. [59,60]

Akt is a serine/threonine kinase protein that belongs to the PKA, PKG and PKC group of protein kinases with α (AKT1 or PKBα), β (AKT2 or PKB β) and γ (AKT3 or PKB γ) isoforms. They share approximately an 80% of the amino acid sequence, which have a pleckstrin homology (PH) domain in N-terminal, a central catalytic or kinase domain and a regulatory domain in C-terminal *(Figure 13B)*.[55] Akt is inactive in its basal state, however, when PI3K is activated, $PIP_3$ will interact with the Akt PH domain producing a conformational change in the protein. This, will allow its phosphorylation by different proteins like, PDK1 into the $Thr^{308}$ in the activation domain, [61] mammalian target of rapamycin complex 2 (mTORC2) [62] or deoxyribonucleic acid (DNA)-dependent protein kinase into the $Ser^{473}$ in the regulator domain [63,64]. All these phosphorylations will completely activate Akt allowing its dissociation from the membrane to start the phosphorylation of target genes involved in survival, glucose metabolism, cytoskeletal rearrangement, transformation, cell-cycle arrest, apoptosis, DNA repair, growth, translation, among others. [54]

It is known that PTEN has different functions depending on its location. The most studied function is its cytoplasmic phosphatase activity. Nevertheless, when locates in the nucleus its function is completely independent of its phosphatase-activity and not

mediated by Akt pathway. However, both the PI3K/Akt pathway and the cell cycle are regulating the localization of PTEN. When the cascade is active, PTEN will be in the cytoplasm, but it locates in the nucleus of resting cells. [65]

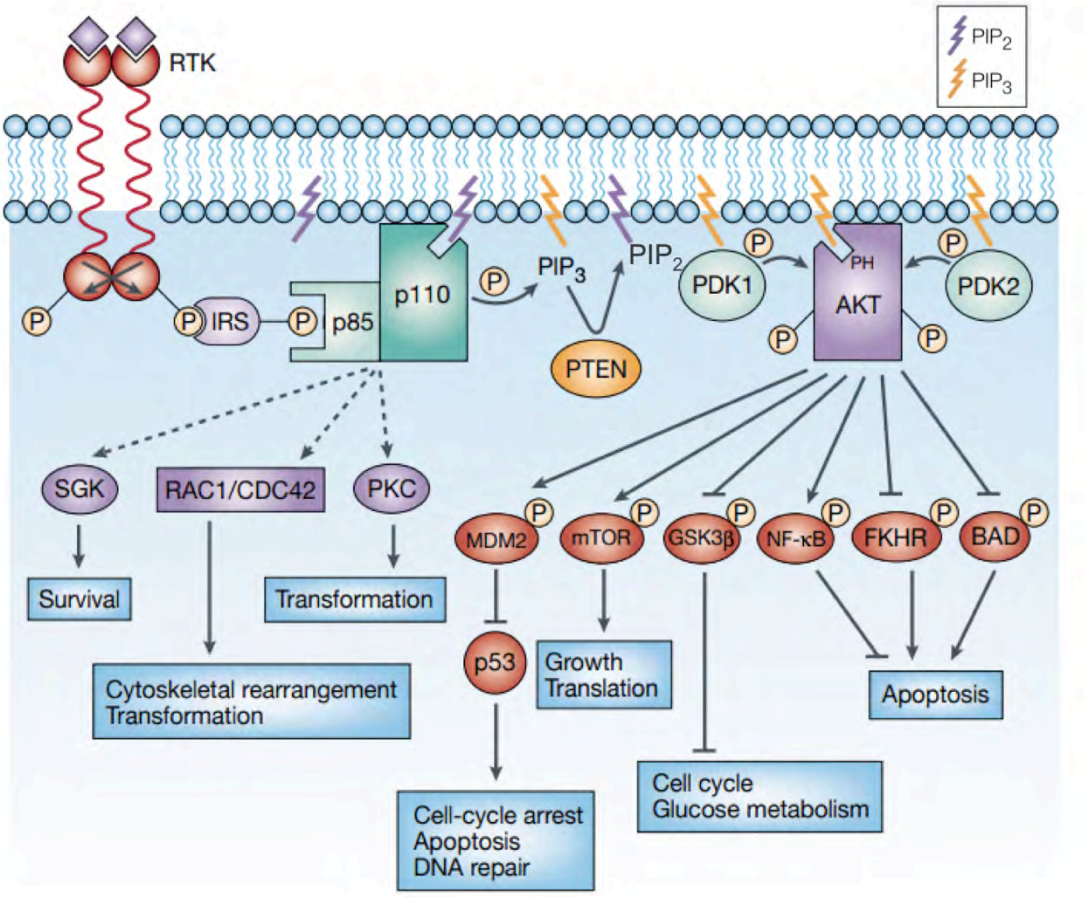


**Figure 14: PI3K/Akt signaling pathway.** *When there is RTK stimulation by a ligand, PI3K/Akt route is activated by a phosphorylation cascade, which will activate or inhibit a lot of targets resulting in survival and proliferation through many mechanisms. Extracted from Vivanco and Sawyers (2002). Figure abbreviations: Akt or PKB, protein kinase B; BAD, BCL2 Associated Agonist Of Cell Death; FKHR also known as FOXO1, Forkhead box O1; GSK3β, glycogen synthase kinasa 3β; IRS, insulin receptor substrate; MDM2, murine doble minute 2; mTOR, mammalian target of rapamycin; NF-kB, nuclear factor kappa-light-chain-enhancer of activated B cells; p85/p110 or PI3K, phosphatidylinositol 3-kinase; PDK1, phosphoinositide dependent protein kinase 1; PDK2, phosphoinositide dependent protein kinase 2; PIP2, phosphatidylinositol (4,5)-biphosphate; PIP3, phosphatidylinositol (3,4,5)-triphosphate; PKC, protein kinase C; RAC1/CDC42, Ras-related C3 botulinum toxin substrate 1/ Coiled-Coil Domain Containing 42; RTK, tyrosine kinase receptor; SGK, serum and glucocorticoid-regulated kinase 1.*

## 5.4 PTEN regulation

The expression and activity of PTEN are strictly regulated at multiple levels employing various molecular mechanisms, which include both transcriptional modulation and post-translational modifications. In addition, the cellular location of PTEN, cytoplasmic or nuclear, and interactions with other proteins also contribute to the regulation of

their function. Due to all these mechanisms it is possible to maintain a robust and appropriate activity of PTEN, regulate the cellular content of $PIP_3$ and thus restrict a possible excess of proliferation and aberrant cell survival. [53,66,55] Furthermore, PTEN may experience subtle or dramatic losses of function by post-translational modifications (phosphorylation, ubiquitinization, oxidation, acetylation and sumoylation), epigenetic silencing, transcriptional repression, microRNA regulation, disruption of competitive endogenous RNA networks or its aberrant localization. [53,55]

## 5.5 PTEN and cell metabolism

It is well known that PTEN is one of the most important tumor suppressor genes because it controls many key functions in the cell, such as cell metabolism. In a tumor cell, a metabolic reprogramming occurs characterized by the increase in glycolysis, the production of lactate or the synthesis of lipids to trigger rapid cell proliferation.

The PI3K/Akt pathway plays an important role in both glucose and lipid metabolism regulation as well as regulation of mitochondrial functions due to its activation under the IR signaling.

### *5.5.1 PTEN and glucose metabolism*

Insulin bound to the IR located in target cells, will lead to the activation of PI3K that is antagonized by PTEN. Akt stimulation inhibits GSK3 by phosphorylating its $Ser^{9}$ site and activates glycogen synthase to help storing the glucose as glycogen in hepatocytes, decreasing blood glucose levels. [67,68] GSK3 has an unconventional kinase characteristic which is to be constitutively active in the cell, and to be inhibited under the stimulation of a signaling pathway like the insulin signaling pathway. [69] Furthermore, when blood sugar is low, the body will increase GSK3 activity to increase glycemia through inhibiting glycogen synthase function by phosphorylation of $Tyr^{216}$ of GSK3.[70]

Some studies in DM mouse model demonstrate that a GSK3 overexpression decreases β-cell proliferation because in the physiological state, GSK3 triggers a negative feedback by PI3K/Akt cascade to regulate β-cells growth. [71] Moreover, it is known that

GSK3 plays a key role in the apoptosis of the β-cells that is related to insulin deficiency, which may lead to DM. DM patients also have an increase in oxidative stress that will activate some signaling pathways, like C-Jun-N terminal kinase (JNK) responsible for GSK3 phosphorylation stimuli, that will increase its anti-proliferative and pro-apoptotic properties.[72,73] β-cells apoptosis occurs because the phosphorylation of GSK3 inhibits the activity of cAMP-response element binding protein (CREB) and β-cell lymphoma 2 (Bcl-2), which leads to the activation of caspase-3 and caspase-9. [74] In addition, high glycemia induces the production of oxidative agents like superoxide in the mitochondria that will activate the uncoupling protein 2 (UCP2) and decrease the ATP/ADP ratio, deteriorating β-cells function and lowering insulin secretion. [75] Interestingly, a study points out that GSK3 activity inhibition in DM mice may prevent pathologies associated with this disease. [76,77]

Furthermore, Akt will initiate the GLUT4 translocation from the intracellular site to the plasma membrane in order to promote the glucose uptake into the muscle and fat cells through the inhibition of the RAB-GTPase-activating protein AS160. [78] The first evidences on this Akt function were observed initially in constitutively active mutants of Akt, which had overexpression of GLUT4. In addition, disruption of Akt in mice causes defects in glucose metabolism and insulin resistance. [79,80,81,82] Akt is involved in the inhibition of gluconeogenesis in the liver by phosphorylating and suppressing some gluconeogenesis-related proteins like FOXO1. Then, the phosphorylated FOXO1 will block the transcription of the two key gluconeogenesis enzymes, G6PC and PEPCK. In addition, it is known that Akt phosphorylates PGC1a at Ser***570*** that also mediates the transcriptional repression of G6PC and PEPCK. [83,84] This regulation is essential to control the response of metabolic organs like liver, muscle and adipose tissue to high insulin.

Akt dysfunction seems to be related to insulin resistance and DM, for example the Akt-β KO mice have less glucose absorption by diabetic muscle and adipose cells [85] or in humans, a negative dominant Akt-β mutation may cause diabetes and hyperinsulinemia. [86] It looks that Akt not only has an important role in the tissues where insulin acts, but also it accelerates proliferation of β-cells in pancreas.[87] Akt-α is the isoform considered to regulate lipid metabolism and stimulation of glycogen

synthesis in muscle and insulin function in adipocytes.[88,89,90] However, there is some debate about the role of Akt in insulin sensitivity. [91]

PI3K/Akt activation induced by PTEN loss also triggers the ectonucleoside triphosphate diphosphohydrolase 5 (ENTPD5) that promotes protein folding and glycosylation in the endoplasmic reticulum, increases ATP consumption and supports a typical phenomenon from tumorogenic cells called Warburg effect, which consists in converting most glucose to lactate through anaerobic glycolysis. [92,93]

Thus, on the one hand, PTEN inhibition enhances the phosphorylation of GSK3 and Akt through the insulin pathway. On the other, PTEN overexpression inhibits PI3K/Akt route hence glucose uptake by cells. This data suggest that people with elevated levels of PTEN might be more exposed to develop DM. [91,94,95]

### *5.5.2 PTEN and lipid metabolism*

Besides from glucose metabolism, PTEN is also involved in the regulation of lipid metabolism, however it is a quite unknown field yet. Some studies have linked insulin, PI3K/Akt pathway and lipogenesis in the liver.

PI3K/Akt activation via GSK3 inhibition will mediate the stimulation of the lipogenic transcription factor sterol-regulatory element-binding protein (SREBP), which is an important transcriptional factor for genes related to lipogenesis like acetyl-CoA carboxylase or fatty acid synthase (Fasn), as well as, genes involved in NADPH production, which is needed for the biosynthesis of lipids. [96] Therefore, PTEN deletion will induce the transcription of genes related to lipogenesis but also to β-oxidation by SREBP and PPARγ and fatty liver transformation. [97,98] Furthermore, Akt activates mTORC1 protein, which is involved in SREBP transcription showing that lipogenesis is mTORC1 activity dependent. [99] In addition, it has also been established that FOXO1 induction by Akt activates the synthesis of lipids. [100]

Recent studies pointed out a function of Maf1, which is a repressor of Fasn, in the suppression of intracellular lipid accumulation and its regulation by PTEN. [101] FOXO1 regulates posttranslational modifications to suppress Maf1 activity, while mTORC1

activates Maf1 expression. [102] For instance, Maf1-deficient mice were resistant to liver steatosis and obesity induced by high fat diet (HFD). [103]

### *5.5.3 PTEN and mitochondrial metabolism*

It is recently established that PI3K/Akt pathway has also a role in mitochondrial metabolism. Akt, which is localized in the inner membrane of the mitochondria, stimulates the union between the mitochondrial voltage dependent anion channel and the hexokinase II in the mitochondrial outer membrane. This binding allows the phosphorylation of available glucose molecules and to obtain a high throughput of energy in form of ATP from glycolysis.[104,105] Furthermore, it regulates mitochondrial respiration by means of GSK3β activation and the consequently pyruvate dehydrogenase phosphorylation and also controls the transcriptional regulation of mitochondrial DNA. [104]

PI3K/Akt cascade in the nucleus controls the transcription of some mitochondrial genes like the transcriptional factor FOXO3, which is a mitochondrial gene transcriptional regulator. For instance, a high number of mitochondrial genes are downregulated in some colon tumor cells with constitutively active FOXO3. [106]

As explained before, PGC1a is activated by CREB after suffering a phosphorylation by PKA, however Akt protein can also phosphorylate CREB and trigger PGC1a. PGC1a strongly increases the transcriptional activity of the estrogen-related receptor α (EERα) to improve the transcription of mitochondrial function genes. [107] In addition, the phenotype observed in livers without PTEN (lipid accumulation and injury) may be induced, among other factors, by EERα activation and mediated by the production of reactive oxygen species.

Furthermore, the Akt substrate consensus sequence has been found on another gene involved in mitochondrial gene transcription called nuclear respiratory factor 1 (NRF1). [108] Therefore, all these data point out an important implication of the PI3K/Akt pathway in mitochondrial gene transcription either directly through FOXO and NRF1 phosphorylation or indirectly induction through EERα expression.

## 5.6 PTEN mouse models

The development of genetically modified murine models has been crucial to study the molecular mechanisms of many diseases, as well as to identify new and better therapeutic and diagnostic strategies. In general terms, genetically modified mouse models used for the study of diseases include overexpressing transgenic mice, knock-in models for specific mutations, full KO mutations and conditional KOs using the Cre-LoxP system.

In 1998, the firsts PTEN-KO mouse models were generated by three independent laboratories evidencing the essential role of PTEN during development. The mice with a biallelic loss of PTEN ($PTEN^{-/-}$) had embryonic lethality, between E6.5 and E9.5 depending on the model, due to defects during embryonic development and malformations in the neural tube. In spite of this disadvantage, the study of heterozygous mice ($PTEN^{+/-}$) in three publications proved to be very useful and allowed to conclude that the loss of a single PTEN allele is sufficient to induce the development of different tumor types. For example, $PTEN^{+/-}$ mice developed lymphomas, gastrointestinal hyperplasia, endometrial, prostate and breast neoplasms and adrenal gland tumors. However, the tumor phenotype varied from one model to the other, since not all models developed the same lesions, neither with the same frequency nor at the same age. These differences could be, first of all, due to the strategy used to generate the PTEN-KO. Each model presented a different split between exons 3-6, although they coincided with the deletion of exon 5, which encoded the protein's phosphatase domain. [42,43,109,110]

However, it had been shown that variations in the tumor spectrum, in the frequencies described and at the time of the appearance of different histological alterations, depended, especially, on genetic background in which the colony was established.[111] These three studies as a whole, despite the differences reported, conclusively demonstrated that PTEN was important at the embryonic development level and that, in addition, played a key role in the origin of various neoplastic processes. [52]

In 2001, the first tissue-specific PTEN-KO mouse models were created, with a brain-specific PTEN ablation. [112,113] Later, series of mutant mice were generated expressing a hypomorphic allele of PTEN ($Pten^{hy/+}$ or $Pten^{hy/-}$), in which its expression decreased sequentially and progressively. These studies showed that the level of expression of PTEN was a key factor for tumor progression.[114,115]

Although these models were really useful for demonstrating the suppressive activity of tumors of PTEN, they presented a number of disadvantages, for instance, $PTEN^{+/-}$ mice developed multiple neoplasms in several locations which made it difficult to determine the influence of PTEN in a specific organ and to study those neoplasms that developed later in time.

The limitations had been overcome thanks to the generation of conditional KO animal models, in which the two PTEN alleles were flanked by LoxP sequences that eliminated the exon 5 of the gene ($PTEN^{fl/fl}$). [116]

To obtain PTEN's deletion, $PTEN^{fl/fl}$ animals can be crossed with mouse strains that express recombinase Cre, which recognizes and acts specifically on LoxP target sequences and is expressed under the control of specific promoters of tissues. In addition, using an inducible system the moment in which the deletion takes place can be controlled. Therefore, the combination of the two strategies (Cre-LoxP system) allowed to control the deletion of the target gene at the time needed and in the tissue selected. This system has been used to generate several animal models in which the PTEN biallelic ablation takes place in different organs or cell types selectively, [117,118] for instance, in the hepatocytes [97,98], adrenal glands [119], mammary glands [120] or astrocytes[121].

## 5.7 PI3K/Akt pathway, glucose homeostasis and hypoglycemia models

Besides from endless mouse models created to study the tumorogenic effect of the PI3K/Akt pathway, some animal or cell models can also be found in the literature focused on studying glucose metabolism and hypoglycemia. Moreover in the last years, there are also a few number of clinical cases related to it.

As mentioned before, PI3K/Akt pathway has an important role as an effector in the insulin actions like triggering glucose uptake and glycogen synthesis in the fat and muscle tissues, and blocking glucose release and glycogenolysis from the liver.

At the end of the last century, the homologue of the PTEN gene (DAF-18) was discovered in *Caenorhabditis elegans*. When DAF-18 was inhibited, DAF-2 (an insulin receptor-like molecule) was partially deleted what suggested that PTEN could have some critical role in insulin pathway. [122,123] These investigations opened the door to a new field of research: PTEN and its implications in glucose homeostasis. Later on, the Olefsky's laboratory overexpressed PTEN in 3T3-L1 adipocyte cells, which led to inhibition of GLUT4 translocation to the membrane, glucose transport and membrane ruffling, demonstrating that endogenous PTEN was a physiological GLUT4 and insulin action regulator. [95,124,125]

After the evidences of a relationship between PI3K/Akt pathway and glucose metabolism in worms and cells, different types of mouse models were generated.

The first studies were designed in diabetic mice (*db/db* mouse, a model of T2DM) in which antisense oligonucleotides were injected in order to inhibit PTEN. The results were that PTEN suppression in liver and fat improved glycemia and insulin sensitivity in T2DM mice, thus, protecting *db/db* mice from developing diabetes.[126] Furthermore, and supported by this first evidences, a Japanese group observed in Japanese T2DM population an association between a PTEN polymorphism and T2DM that provided a new insight into this pathology. [127]

PTEN is highly dependent on the tissue type and can have a specialized function for a specific tissue. In muscle, liver, pancreas and fat (the major insulin related organs) the lack of PTEN affects glucose homeostasis and results in resistance to diabetes.

Skeletal muscle is an insulin responsive key tissue. It has been reported that T2DM patients have insulin resistance in muscle in the early stages of the disease.[128] There are also evidences in mice with GLUT4 specifically deleted in muscle that developed diabetes and insulin resistance, whereas a muscle-specific insulin receptor KO did not seem to display a defect in glucose metabolism. [129,130] For a better understanding of the role of the skeletal muscle in glucose homeostasis, a selective PTEN deletion in

skeletal muscle was done with a Cre-LoxP system. It was concluded that PTEN ablation in muscle protected mice from the development of diabetes and insulin resistance without affecting the most lethal consequences of eliminating PTEN, the tumor formations. [131] Moreover, in diabetic obese Zucker rats a rise in PTEN expression was shown in the muscle. [132]

Liver-specific PTEN deletion studies in mice resulted in hepatomegaly due to liver steatosis, and raised glycogen synthesis. Furthermore, the deletion induced a drop in glucose levels in fasting accompanied by a decrease in insulinemia and ameliorated glucose tolerance. Thus, there was an increased insulin action in the liver and an improvement of the elimination of glucose. In addition, PTEN elimination resulted in activation of lipogenic enzymes and inhibition of gluconeogenesis in the liver.[97] Moreover, liver-specific PTEN KO mice with a supplementation of HFD for a short time significantly increased the liver injury and steatosis via downstream of Akt or lipid transport changes, and both *de novo* lipogenesis or dietary lipids played an important role in liver steatosis in those mice. [133] In Stiles's lab, the liver-specific PTEN KO mice was crossed with an $Akt2^{-/-}$ mouse and they observed a blocking in the liver fatty deposition that demonstrated a crucial role of Akt2 in the expression of lipogenic genes. They showed that this effect could be partially due to FOXO1, but not related to the atypical protein kinase C (PKC). [134]

In the literature there are some clinical cases that relate alterations in glucose and insulin homeostasis associated with PTEN and Akt2. For example, it has been reported that a family with DM and severe insulin resistance had a loss-of-function mutation in Akt2 [86]; in contrast, there are a couple of studies in which patients with a gain-of-function mutation in Akt2 showed a completely opposite phenotype: hypoglycemia, hypoketonemia, hypofattyacidemia and hyperinsulinemia. [135,136] In the same direction, two brothers were investigated because of persistent hypoglycemia since the neonatal period, among other pathologies like macrocephaly, developmental delay or short stature, which was attributed to a germline PTEN mutation. [137] Moreover, a Cowden syndrome patient (a disorder characterized by multiple noncancerous, tumor-like growths and high risk to suffer some tumors) with a germline mutation in PTEN had accelerated drop of glycemia after intravenous injection of glucose. [138]

Last year, Cadenas and Stiles' labs published a study of the brain of liver-specific PTEN KO mice demonstrating some metabolic and functional alterations attributed to the higher insulin sensitivity that those mice presented. Thus, a higher consumption of glucose was shown in most organs, and especially in the brain. After those observations, they proposed to treat brain insulin resistance in neurodegenerative diseases in order to slow the process of neuronal degeneration increased by the interruption of glucose uptake from brain. [139]

In a β-cell-specific PTEN deletion mouse an increased islet mass and a rescue of the STZ-induced β-cell damage were observed, stopping diabetes development. [140,141] Another study focused on a pancreas-specific deletion of PTEN mouse revealed a resistance to HFD-induced diabetes maybe due to the rise of Akt signalling in the liver. [142] Indeed, previous studies reported that Akt overexpression in the liver leads to reduce glycemia, [143] and PTEN suppression in liver could shift hyperglycemia in diabetic mice.[126] In addition, Zucker T2DM diabetic fatty rats treated with a pharmacological GSK3 inhibitor ameliorated hyperglycemia by liver glycogen synthesis induction. [144]

Adipose tissue is an endocrine organ that has a high metabolic activity because adipocytes produce and secrete adipokines, which act as hormones that regulate insulin sensitivity and energy intake and expenditure. For example, leptin has a key role in feeding behavior; adiponectin affects the energy balance by regulating AMP kinase; and resistin is associated with insulin resistance. There are some animal-models focused on this field, for instance, in the adipose tissue-specific PTEN-KO mouse it was observed that they had a decreased resistin production and did not increase body adiposity due to the high-energy metabolism. Therefore, PTEN has an important role in insulin sensitivity in the adipose tissue. [145] In addition, many in vitro studies related to PTEN and glucose or insulin homeostasis are performed in adipocytes. [78,90,95,124,125,146,147]

As previously explained, PTEN was only eliminated from specific tissues but not in the whole body, because of the problem of the early embryonic lethality of a $PTEN^{-/-}$, until Wong *et al*. in 2007 performed a PTEN haploinsufficiency ($PTEN^{+/-}$) mouse to study the global effect of the ablation of PTEN on glucose homeostasis. Their results showed that $PTEN^{+/-}$ had increased in both glucose uptake and insulin hypersensitivity. Thus,

suppressing only one allele of PTEN was enough to obtain an extended and strong insulin signal. Therefore, they suggested that inhibition of PTEN might be useful to treat the insulin resistance in T2DM. [148]

# 6. Vitamin D

The vitamin D (VD) is a steroid hormone that has an important role in $Ca^{+2}$ and phosphorus (P) homeostasis and metabolism, and also in bone mineralization. In the last decades, clinical and basic research has demonstrated the relevant function of VD in many physiological and pathological processes, other than mineral metabolism control.

## 6.1 Vitamin D history

VD was discovered at the beginning of the twentieth century as a result of the study of two diseases, rickets and its adult version, osteomalacia. Even though rickets had been known since Roman times, when a roman physician observed bone abnormalities in children, it was not until the first half of the seventeenth century (1645) when Whistler described in detail the physiopathology of rickets for the first time. However, it was not until the Industrial Revolution, when a lot of migration took place from the farms to the cities, that the disease began to be studied in depth in the United Kingdom, due to its increased prevalence especially in Scotland where sunlight was weak for most part of the year.

Some years later, other scientists started to relate rickets to a nutritional disorder caused by malnutrition. Moreover, Frunk started with the suggestion that a “vital amine” should be present in foods required for health and survival, preceding the name “vitamins”. After some studies with different diets and animal models, vitamin A, B and C were discovered. Afterward, Mellanby in Great Britain and McCollum in the United States of America investigated with rickets disease animal models demonstrating that the disease could be cured with cod liver oil. In 1789, McCollum warmed up cod liver oil to eliminate vitamin A content and surprisingly, that oil continued to be effective in curing rickets, and that was how VD was discovered.

Furthermore, Trousseau, some years later, in 1861, had noticed that patients with rickets that were exposed to sunlight or artificial UV radiation felt better, or even

healed. All these findings, from many scientists and years of research, culminated with the Nobel Prize in 1928 to Adolf Windows for the discovery of the chemical structure of VD. Therefore, little by little, all the pieces of the puzzle fitted and the relationship that we know nowadays between VD, diet and its production in the skin after UV radiation from light was established. [149,150,151]

## 6.2 Vitamin D structure and types

The different VD forms are, in terms of chemistry, secosteroids, thus, steroids in which one of the rings of its cyclopentanoperhydrophenanthrene ring structure is cleaved ($C_9$-$C_{10}$ bond of ring B). [152]

- Vitamin $D_1$: formed by a fifty-fifty combination of ergocalciferol and lumisterol.
- Vitamin $D_2$: ergocalciferol
- Vitamin $D_3$: cholecalciferol
- Vitamin $D_4$: dihydroergocalciferol
- Vitamin $D_5$: sitocalciferol

The two main types of VD present in humans are $VD_2$ and $VD_3$ *(Figure 15)*, which are obtained from vegetables and fish (ergocalciferol, $VD_2$), and from the synthesis that takes place in the skin after its irradiation with ultraviolet light (UV –λ=290-315nm) (cholecalciferol, $VD_3$). Humans can cover perfectly the VD vital requirements with the combination of an adequate diet and sunlight exposition.[153]

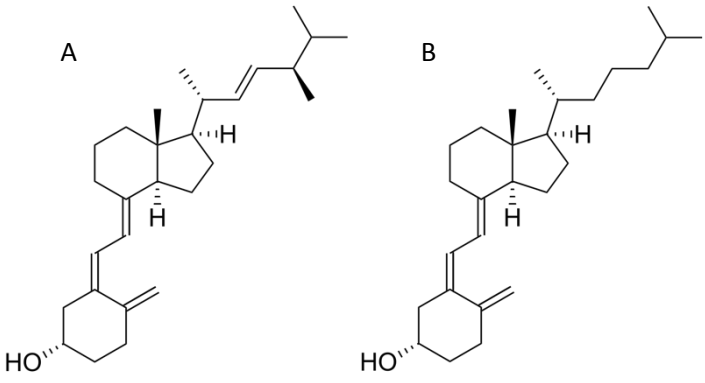


**Figure 15: Vitamin D chemical structure.** ***(A)*** *Vitamin D2* ***(B)*** *Vitamin D3*.

## 6.3 Vitamin D biosynthesis

The active VD form is the 1α,25-dihydroxyvitamin $D_3$ or calcitriol ($1,25(OH)_2D_3$) and derives from cholesterol. The main source of VD is the endogenously synthesized in the skin from its precursor molecule, 7-dehydrocholesterol after UV-B radiation. When pre-$VD_3$ is formed, a temperature-dependent isomerisation will take place to $VD_3$, which is then transported into the circulation, bound to the VD binding protein (DBP). At this point, VD does not have any biological activity. [154] However, some amounts can also be obtained from the diet from fatty fish like salmon or mackerel, in fish oils and in VD enriched food like milks, yogurts or cereals.

The first step in the $VD_3$ activation occurs mainly in the liver, however it can also take place in kidney, brain, intestine, lung, prostate gland, skin, blood vessels and macrophages. [154] It is based on the hydroxylation of the carbon-25 by the $VD_3$ 25-hydroxylase or P450 cytochrome (CYP27A1), to generate 25-hydroxyvitamin $D_3$ ($25(OH)D_3$). This first hydroxylation is not strictly regulated and, thus, $25(OH)D_3$ levels in serum are higher than $VD_3$ intake. These levels are used as VD state markers in the organism because $25(OH)D_3$ has a long half-life. The normal levels of $25(OH)D_3$ in serum range between 30 and 100 ng/ml. When they are below 15 ng/ml, VD deficiency is diagnosed. $25(OH)D_3$ levels in the bloodstream are low in many people who live at northern latitudes and lower altitude, especially during winter. [155]

Afterwards, the biological active hormone $1,25(OH)_2D_3$ is generated by the mitochondrial enzyme 25-hydroxyvitamin$D_3$-1-α-hydroxylase (CYP27B1 or 1-α-hydroxylase). This $25(OH)D_3$ hydroxylation at the carbon-1 mainly occurs in the kidney, however expression of 1-α-hydroxylase is found in other tissues but in low quantities. Likewise, $1,25(OH)_2D_3$ levels in the bloodstream are strictly regulated because it is implicated in many cellular processes either paracrine or autocrine, such as in $Ca^{+2}$ and P homeostasis, among others *(Figure 16)*. [156]

$1,25(OH)_2D_3$ represses directly 1-α-hydroxylase expression by a negative feedback as well as by suppressing synthesis and secretion of parathyroid hormone (PTH), which is the primary tropic hormone that stimulates 1-α-hydroxylase expression. [157]

$VD_3$ active metabolite levels are tightly regulated, both at synthesis and degradation levels. 24-hydroxylase enzyme is in charge of the degradation of $25(OH)D_3$ and $1,25(OH)_2D_3$ transforming them to $24,25(OH)_2D_3$ and $1,24,25(OH)_2D_3$, respectively. 24-hydroxylase is constitutively expressed in kidneys, but can be induced by $1,25(OH)_2D_3$ in all the tissues than respond to VD. Moreover, the 24-hydroxylase has more affinity to $1,25(OH)_2D_3$ than for $25(OH)D_3$, as its main role is to eliminate the excess of $1,25(OH)_2D_3$ in order to avoid its toxicity. [158]

Therefore, in terms of metabolism, $1,25(OH)_2D_3$ has a cyclic behaviour due to 24-hydroxylase and 1-α-hydroxylase enzymes. For instance, when $1,25(OH_{)2}D_3$ levels are low, 24-hydroxylase levels are also diminished, and in contrast, 1-α-hydroxylase levels are high, and vice versa.

## 6.4 Vitamin D Receptor

### *6.4.1 VDR structure*

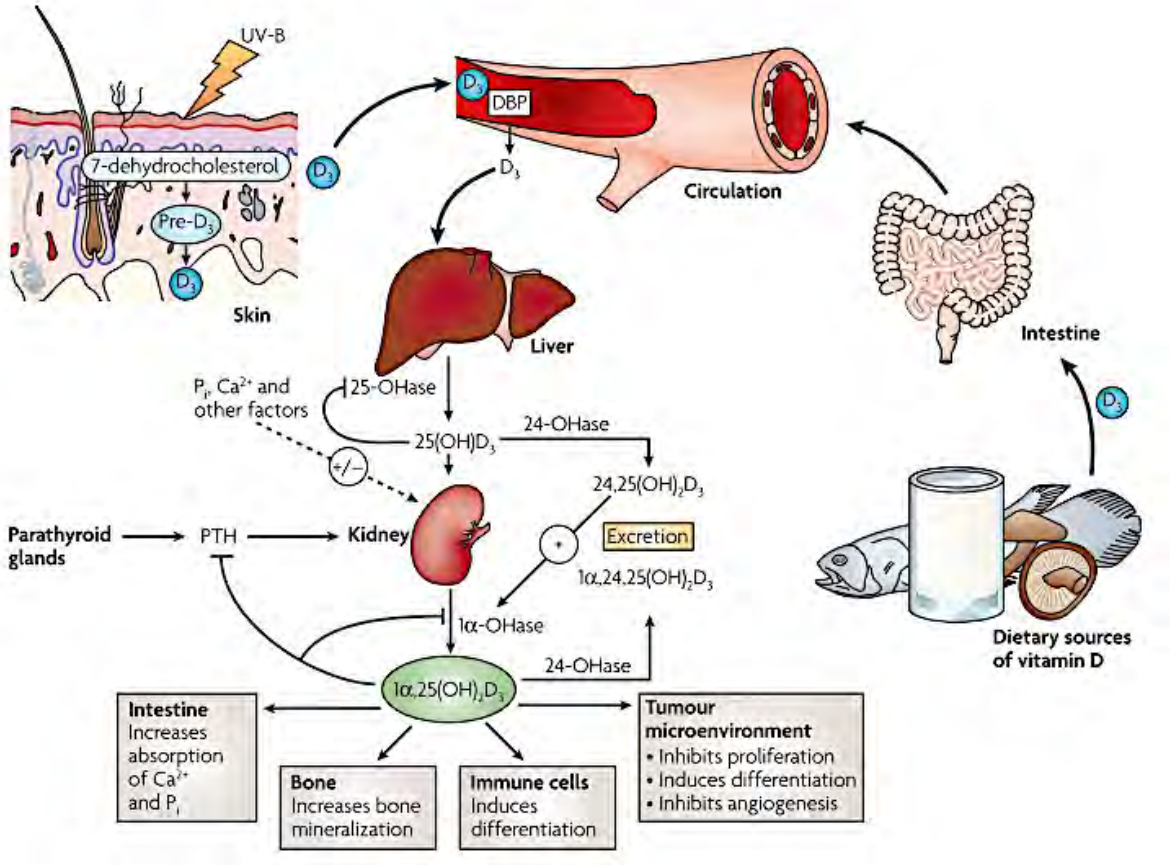

**Figure 16: VD metabolism.** *After UV radiation on the skin, 7-dehydrocholestoros is converted to pre-$VD_3$. Inactive $VD_3$ can also be obtained from dietary sources but in less quantity. $VD_3$ bound to DBP go through the circulation to the liver where the first hydroxylation takes place by 25-OHase and $25(OH)D_3$ is obtained. Then, $25(OH)D_3$ goes to the kidney, where the last metabolization occurs by 1α-OHase and it is converted to $1,25(OH)_2D_3$ (the active VD). The main effects of VD are related to mineral metabolism in intestines and bones, but VD also induces differentiation of immune cells or acts as a tumor suppressor. Extracted from K. Deeb et al. (2007). Figure abbreviations: 1α-OHase, 1α-hydroxylase; $1,25(OH)_2D_3$, 1α,25-dihydroxyvitamin $D_3$; 25-OHase, 25-hydroxylase; $25(OH)D_3$, 25 hydroxyvitamin $D_3$; $Ca^{+2}$, calcium; $D_3$, vitamin $D_3$; DBP, vitamin D binding protein; P, phosphorus; PTH, parathyroid hormone.*

The VD receptor (VDR) was discovered in 1974 by Brumbaugh *et al.* [159] and it is a 427 amino acid protein with a molecular weight of ~50kDa member of the superfamily of nuclear trans-acting hormone receptors or steroid nuclear receptors that regulate gene expression in the presence of ligand, in this case, the $1,25(OH)_2D_3$. It has an almost ubiquitous tissue distribution.

The human VDR is localized in the 12q chromosome comprised of promoter and regulatory regions and exons. Six exons (1A to 1F) occupy the 5'-noncoding region, and eight more exons (exons 2-9) encode the structural component of the VDR *(Figure 17)*. [160]

The protein is divided in different domains:

- *Ligand binding domain (LBD)*: located in the C-terminal where $1,25(OH)_2D_3$ ligand high affinity binding is carried out. In the same site, $25(OH)D_3$ can either be bound, but with approximately 200 times less affinity. [161]
- *Activation function 2 domain (AF-2)*: also located in C-terminal transmits the greatest conformational change of the three-dimensional structure of the VDR by joining the ligand that is necessary to recruit the proteins responsible for transactivation and transrepression in the transcription process.
- *DNA binding domain (DBD)*: located in the N-terminal part in zinc fingers-like domains. The zinc-fingers are a tetrahedral complex formed by four cysteines with a zinc molecule. They form a bond that stabilizes the union with DNA through contacts with phosphates of the DNA skeleton. On the one hand, the first zinc-finger (close to N-terminal) is responsible of the VDR binding to the promoters of VD-dependent genes, specifically in the sequences called VD response elements (VDRE) found in 5' site in the promoters of VD target genes. On the other hand, the second zinc finger is responsible for the necessary

heterodimerization with RXR. This is an indispensable process for the VDR to acquire the essential conformation to have high affinity to DNA and to perform its transactivating or transrepressing function; therefore, it needs to interact with co-regulating nuclear proteins that will give the positive or negative modulation of the transcription in which VDR intervenes. [162]

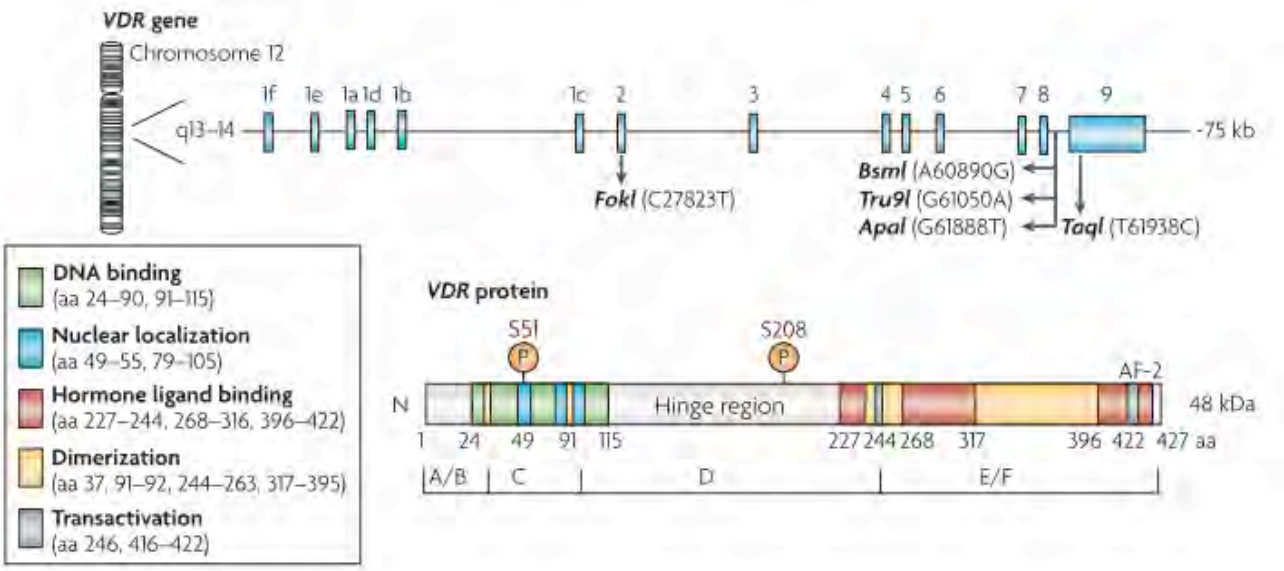


**Figure 17: VDR gene structure.** *VDR is located on chromosome 12q13-14 and composed of promoter and regulatory regions (1a-1f) and exons 2-9. VDR gene is translated to 6 domains (A-F) of the VDR protein that have different functions, DNA binding, nuclear localization, hormone ligand binding, dimerization and transactivation. Extracted from K. Deeb et al. (2007). Figure abbreviations: VDR, vitamin D receptor.*

### *6.4.2 VDR signalling pathway and regulation*

It is well known that VDR has an essential role in $Ca^{+2}$ and P homeostasis, but also has an important function in many systems in the organism, like cardiovascular, immune, nervous, cell proliferation, among others. Biochemical and *in situ* immunocytochemical localization experiments have demonstrated that VDR was mainly a nuclear protein, even in the inactivated state. [163] However, other studies showed that VDR is maintained in the cytoplasm when there are no VDR ligands, but when $1,25(OH)_2D_3$, or one of its analogues is bound, it is translocated from cytoplasm to the nucleus.[164] Furthermore, numerous studies have confirmed that the presence of functional VDR is necessary for both, the genomic and the non-genomic rapid responses to the

$1,25(OH)_2D_3$. [165] Therefore, two types of responses are described for VDR depending on the receptor localization:

- *VDR in the nucleus and its genomic response*: most of the effects of VD are mediated by the activation of a VDR located at the nuclear level, which is considered the classical action of the $1,25(OH)_2D_3$. VDR acts in association with other transcription factors, basically with RXR, forming heterodimers, which in turn bind to the elements of VDREs.

  On the one hand, transcriptional activation requires many co-activators like steroid receptor coactivators (SRCs) or histone acetyltransferases (HATs) to acetylate histones and unravel chromatin. In addition, when VDR-interacting protein 205 (DRIP205) is bound to the AF-2 domain, a set of proteins will come together to form a complex, which binds to RNA polymerase II (RNA Pol II) and activates the transcription of many genes. In the 24-hydroxylase two VDRE are reported. When $1,25(OH)_2D_3$ is not present, the VDR/RXR heterodimer binds to one or both VDRE to recruit a co-repressor. After ligand binding to VDR, a co-activator replaces the co-repressor. In contrast, when there are high amounts of $1,25(OH)_2D_3$, both VDREs are used synergistically to increase 24-hydroxylase levels, which in turn leads to efficient inactivation of the hormone. [156]

  On the other hand, transcriptional repression also needs the interaction between VDR-RXR and VDR-interacting repressor (VDIR) bound to E-box-type negative VDREs (nVDREs), dissociation of the HAT co-activator and recruitment of histone deacetylase (HDAC) co-repressor leading the suppression of different genes. [166]

  Therefore, VDR acts as a transcription factor that regulates the expression or repression of genes responsible for the maintenance of mineral homeostasis, immune activity and cell proliferation, as well as cardiovascular and renal function. This response mediated through the nuclear VDR is usually slow by manifesting itself several hours or days later, and can be blocked by transcription and translation inhibitors.
- *VDR in the membrane and its non-genomic rapid response*: VD, being a steroid hormone, is capable of producing very fast responses (seconds or minutes) on some

types of cells such as the opening of ion channels, the secretion of insulin in pancreatic β-cells or rapid migration of the endothelial cells.

This type of rapid response is not mediated by gene transcription but because of the activation of an extranuclear VDR, which has been postulated that it could be in the cytoplasm, in the membrane or in the caveolae of the plasma membrane (membrane invaginations rich in proteins and lipids that are in charge of the transmission of signals). The rapid response is thought to be involved in the activation of the mitogen-activated protein kinase (MAPK) / extracellular signal-regulated kinase (ERK) 1 and 2 (ERK-MAPK1/2) pathway through the phosphorylation and activation of Ras and Raf isoforms by PKC due to a $Ca^{+2}$ influx through store-operated $Ca^{+2}$ (SOC) channels. $1,25(OH)_2D_3$ triggers SOC $Ca^{+2}$ influx in muscle cells by the interaction of VDR to the plasma membrane, where VDR will contact with the SOC channels. $Ca^{+2}$ influx stimulates $Ca^{+2}$ messenger systems, such as PKC. In addition, when PKC is activated it can phosphorylate the VDR. $1,25(OH)_2D_3$ binding to G-protein coupled receptors (GPCRs) induces phospholipase Cγ (PLCγ), Ras, PI3K and PKA pathways, and promotes MAPK–ERK1/2 signalling. In addition, activated Raf/MAPK/ERK cascade may participate in a cross-talk with the classical VDR pathway to regulate gene expression *(Figure 18)*. [160]

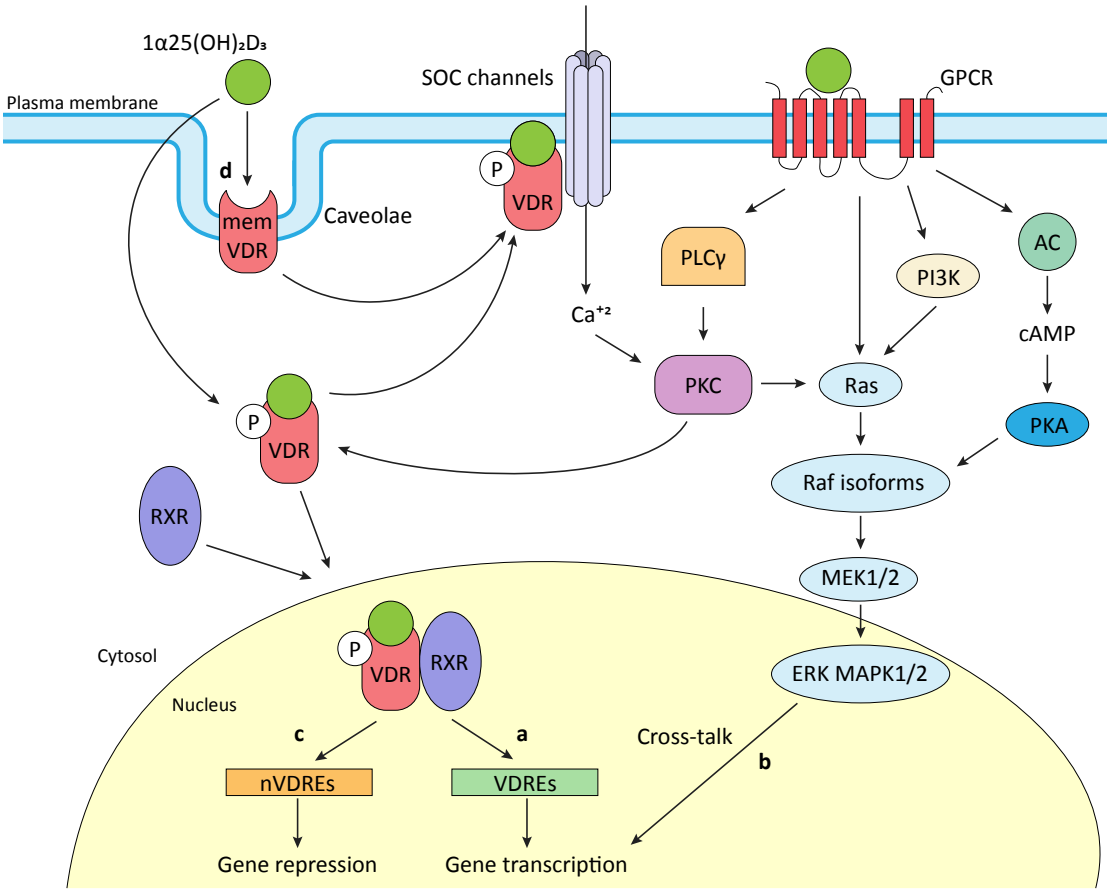


**Figure 18: $1,25(OH)_2D_3$ transcriptional regulation.** ***(a,b)*** *The complex formed by $1,25(OH)_2D_3$, VDR and RXR stimulates VDREs that activate gene transcription,* ***(c)*** *or gene repression.* ***(d)*** *There are non-genomic rapid actions of $1,25(OH)_2D_3$* that are associated with memVDR found in caveolae. *Adapted from K. Deeb et al. (2007). Figure abbreviations: $1,25(OH)_2D_3$, 1α,25-dihydroxyvitamin $D_3$; AC, adenylyl cyclase; $Ca^{+2}$, calcium; cAMP, cyclic adenosine monophosphate; ERK, extracellular signal–regulated kinases; GPCR, G protein-coupled receptor; MAPK1/2, mitogen-activated protein kinase 1/2; MEK1/2, mitogen-activated protein kinase kinase; memVDR, membrane VDR; nVDREs, negative vitamin D response elements; P, phosphorylation; PI3K, phosphoinositide 3-kinase; PLCγ, phosphoinositide phospholipase C; PKA, protein kinase A; PKC, protein kinase C; RXR, retinoid X receptor; SOC channels, store-operated $Ca^{+2}$ channels; VDR, vitamin D receptor; VDREs, vitamin D response elements.*

## 6.5 Vitamin D physiological functions

$1,25(OH)_2D_3$ is involved in many functions in the organism, some of them are known as the classical roles of VD that are involved in mineral homeostasis; but also, there are many non-classical functions in which VD is involved.

### *6.5.1 Classical VD functions*

The classical VD function is the regulation of mineral metabolism. Mineral metabolism refers to the biological processes that regulate homeostasis of $Ca^{+2}$, P and magnesium. $Ca^{+2}$ and P levels are involved in the regulation of other molecules and hormones, through bi-directional flows, at the level of different organs, such as the kidneys, the bones, the intestine and the parathyroid glands. The complex involvement of components and tissues can cause that a little alteration in any of the mechanisms involved can develop into big physiological imbalances. The maintenance of $Ca^{+2}$ and P levels in the body is done through the regulation of intestinal absorption, bone turnover and kidney excretion. In this way, a decrease in blood $Ca^{+2}$ levels would be detected by the membrane $Ca^{+2}$ sensor receptor (CaSR) of the parathyroid gland and would stimulate the secretion of PTH. This would act on the one hand, at the bone level by increasing bone remodelling and, thus, the blood $Ca^{+2}$ and P levels; and on the other hand, at the renal level by increasing $Ca^{+2}$ reabsorption and P excretion. Collaterally, $1,25(OH)_2D_3$ also increases intestinal P absorption, increasing the synthesis and secretion of PTH. Therefore a third actor is needed to stabilize the system, fibroblast growth factor 23 (FGF23), which is stimulated by $1,25(OH)_2D_3$, decreasing P by increasing kidney excretion and, at the same time, inhibits the formation of $1,25(OH)_2D_3$.[167,168]

The effects of $1,25(OH)_2D_3$ on $Ca^{+2}$ and P, after its union to VDR, are mainly in the intestines in order to increase the $Ca^{+2}$ and P absorption both at transcellular and paracellular level. The intestinal transcellular absorption of $Ca^{+2}$ occurs due to the entrance of the transient receptor potential cation channel subfamily V member 6 receptor (TRPV6) that is an epithelial protein involved in $Ca^{+2}$ transport, in the apical zone of the cell. $1,25(OH)_2D_3$ will increase the TRPV6 gene expression in the enterocytes. It will also raise the expression of calbindin, which transports the intracellular $Ca^{+2}$, and some proteins responsible for the basolateral excretion of $Ca^{+2}$. [169,170] Moreover, it has been suggested that $1,25(OH)_2D_3$ regulates the permeability of the tight junctions at paracellular level. [171]

VD also has an essential role in maintaining and developing the bones. As a regulator of the transcription of bone-related proteins, VD induces the expression of proteins like osteocalcin or RANKL and supresses the synthesis of type I collagen or osteoprogerin. It has been demonstrated *in vivo* and *in vitro* that VD stimulates the differentiation of osteoclasts, thus, $Ca^{+2}$ and P release. [172]

The endocrine system of VD is also a powerful modulator of parathyroid function. The deficiency of VD causes parathyroid gland hyperplasia and an increase in the synthesis and secretion of PTH, which recognizes the changes in $Ca^{+2}$ through the CaSR. When $Ca^{+2}$ is increased, PTH secretion will be inhibited. [173]

Finally, the main effect of $1,25(OH)_2D_3$ in the kidneys is to control its own synthesis and degradation due to inhibiting 1-α-hydroxylase or activating 24-hydroxylase. Moreover, it induces the expression of megalin (a protein that mediate the endocytosis of high-density lipoproteins) in the proximal tubule. [174] $1,25(OH)_2D_3$ it is also involved in $Ca^{+2}$ renal reabsorption by increasing some proteins, such TRPV5 and calbindin. [175]

### *6.5.2 Non-classical VD functions*

In the last years, it has been demonstrated that VD is involved in many other non-classical functions, such as, suppression of cell growth, regulation of apoptosis, modulation of immune responses, control of differentiation and function in the skin, control of the renin-angiotensin system, control of insulin secretion, control of muscle function or control of the nervous system. [162]

Cellular proliferation is affected by VD through modifications in cell cycle progression, differentiation and apoptosis. It has been demonstrated that VD mainly arrests the cell cycle between $G_0$-$G_1$ phases repressing the cell cycle progression by inducing cyclin dependent kinases inhibitors and other regulatory proteins of the cell cycle.[176,177,178,179] However, in some cell lines it is suggested that VD could also arrest the cell cycle in later stages like $G_1$ or $G_2$/M. [180,181] Moreover, VD controls the differentiation of many cell types, from malignant or benign cancer to normal cells. For instance, $1,25(OH)_2D_3$ stimulates the differentiation of mouse myeloid leukaemia cells to macrophages *in vitro* and also can activate the formation and maturation of an apical microvillus

membrane in human intestinal cells. [182,183] Finally, as mentioned before, VD can also modulate apoptosis in many tumor cell lines and normal cells by stimulating the pro-apoptotic proteins or inhibiting the anti-apoptotic ones. For example, regulating the mechanisms of the Bcl-2 family in leukaemia, colon cancer or retinoblastostoma cell lines. [184,185,186] It has also been shown that VD analogs could induce apoptosis by inhibiting insulin-like growth factor 1 (IGF1) pathway in breast cancer cell lines. [187] In addition, VD induces apoptosis by activating Forkhead box O3 (FOXO3) through downregulation of p-Akt and ERK. [188]

VD has an important immune-modulatory function due to the VDR presence in immune cells that are proliferating, and to the capacity of immune cells to metabolize VD. On the one hand, VD affects the innate immunity through its role in the synthesis induction of anti-microbial peptides and the inhibition of maturation, differentiation and survival of dendritic cells, which are the main antigen presenting cells. The global effect of VD treatment on dendritic cells is the decrease in T helper 1 cell response. [189,190] On the other hand, during the 80s and 90s it was established that VD played an important role in adaptive immunity because it was demonstrated VDR expression in T and B lymphocytes, specifically in an immunologically active state. [191,192] $1,25(OH)_2D_3$ inhibits T cells proliferation by reducing interleukin-2 (IL-2). [193] B cells have less VDR expression in normal conditions, but when they are activated its levels are upregulated. $1,25(OH)_2D_3$ supressed memory B cell generation and plasma cell formation. Moreover, it has been shown in *in vitro* studies that VD treatment inhibited the immunoglobulin (Ig) secretion, specifically IgG and IgM. [194]

It has been also demonstrated that VD has an important role in the insulin secretion in response to glucose, both *in vitro* and *in vivo* models. [195] And also, it has been shown that VDR is present in the β-cells and DBP in pancreatic tissue. [196,197,198]

In rats treated with low VD diet, glucose tolerance deterioration and low response to exogenous insulin was observed, producing insulin sensitivity alterations. [199,200] In addition, a deficiency of VD led to poor pancreatic insulin secretion, without modifying glucagon secretion. [201,202] Moreover, if the lack of VD is treated at early stages, an improvement in glucose tolerance and a better insulin secretion in response to glucose was shown. [203,204] In streptozotocin (STZ)-diabetes induced rats, VD, bone mass,

calcemia and DBP are decreased owing to altered VD metabolism because of an inhibitory effect of insulin deficiency on the function of the 1-α-hydroxylase. [205,206,207,208]

## 6.6 Vitamin D and non-classical related diseases

There are many diseases associated with VD beyond bone disorders, such as cancer, diabetes, hypertension and cardiovascular diseases, autoimmune diseases, dermatological diseases, among others.

### *6.6.1 Cancer*

VDR is considered a tumour suppressor gene because it exerts a beneficial effect on cancer by supressing proliferation, angiogenesis and metastasis of tumour cells and by triggering apoptosis and differentiation.

It is well demonstrated that VD inhibits proliferation in many experimental studies in cell lines like gastric tumour cells [209] or melanoma cells. [210] Moreover, VD has an anti-metastatic role mediated by degradation of proteases that degrade the extracellular matrix and by increasing the protease inhibitors that supress extracellular matrix degeneration. [211] VD also regulates angiogenesis due to the control of proangiogenic factors in a lot of malignancies such as hypoxia inducible factor 1α (HIF1α) and vascular endothelial growth factor (VEGF), [212,213] but also supressing the nuclear factor kappa-light-chain-enhancer of activated B cells (NF-κB) pathway that activates angiogenic factors in some cancers like prostate tumours. [214]

Furthermore, epidemiological studies also demonstrated a beneficial role of VD in cancer. For instance, 25(OH)$D_3$ levels in the bloodstream ≥40ng/mL are correlated to lower risk of develop invasive tumors; [215] VD in serum with values of ≥30ng/mL are associated with less risk to suffer a tobacco-related malignancy in smokers [216]; or high 25(OH)$D_3$ levels are positively correlated to lower incidence of breast cancer in postmenopausal women and better survival. [217] However, there are controverting results from the VD treatment in clinical trials on the cancer incidence. [218,219]

### *6.6.2 Diabetes*

In the last years, increasing animal and human studies have demonstrated a relationship between VD and DM (T1DM and T2DM). In DM patients the lack of VD is frequent and, in addition, supplementation with VD is associated with lower incidence of DM. [220,221]

#### 6.6.2.1 T1DM

It is suggested that VD might have beneficial effects in experimental T1DM. These effects have been associated to the immunomodulatory roles of VD. Furthermore, there are observational studies that report the association of low sunlight exposure and T1DM developing. [222]

Recently, it has been demonstrated that VD could improve hyperglycemia, hypoinsulinemia and IGF1 levels in T1DM rats in fasting state. [223] Moreover, in pancreatic β-cells treated with STZ, VD improves autophagy while suppressing apoptosis and increases insulin secretion and resistance to diabetes-induced cellular stress. [224] It has also been suggested that the beneficial effects of VD on T1DM could be due to up or down-regulation of anti-inflammatory molecules and, in addition, it was found that T1DM patients show lower levels of inflammatory-markers in urine after VD supplementation. [225,226]

Nowadays, observational studies in humans related to VD and T1DM further corroborated that VD could have a protective role against T1DM; although in some cases they show contradictory results. Some researches reveal that VD treatment in early life is correlated to lower incidence of T1DM; [227,228] some others, that patients who have suffered T1DM for more than fifty years present sufficient VD levels (above 30 ng/ml) [229] or even that VD intake could preserve β-cell role in these patients.[230] Moreover, it is suggested some genetic relationship between VD, T1DM and small nucleotide polymorphisms in VD metabolism related genes like VDR or 1-α-hydroxylase. [231,232] There are some randomized clinical trials with small sample size suggesting that the VD analogue, alphacalcidiol, could be the best option to test in big clinical trials. [233] In contrast, in other investigations, no effect of VD supplementation on β-cells in T1DM subjects was found. [234,235]

#### 6.6.2.2 T2DM

A large amount of studies support the link between the lack of VD and T2DM. This association is due to both direct and indirect effects of VD on insulin sensitivity, insulin secretion and inflammation.

It has been reported that VD has a crucial function in the maintenance of the proper β-cells function both *in vitro* or *in vivo,* as it was observed that $VDR^{-/-}$ mice had impaired insulin secretion and that cultured pancreatic islets increased insulin secretion after VD treatment. [236,237,238] Similar to T1DM, VD administration in T2DM rats diminished glycemia and insulin resistance by regulating inflammatory biomarkers and oxidative stress in the pancreas. [239] It is also shown that VD treatment in T2DM rats resulted in a reduction of the insulin-degrading enzyme and increased the phosphorylation of the IR, which ameliorated the insulin resistance and the glycaemic index. [240] In addition, VDRE has been described in the promoter of the IR gene, which is transcriptionally activated after VD administration. [241] Moreover, it is postulated that VD regulates $Ca^{+2}$ channel flux and, as $Ca^{+2}$ is essential for insulin secretion in pancreas, VD deficiency may cause insulin release impairment. [242,243]

VD has a function regulating $Ca^{+2}$ levels inside and outside the cell and, thus, it could dephosphorylate GLUT4 reducing the insulin-stimulated glucose transport. [243] However, there are no data showing the effect of VD treatment [244,245,246] or improvement [247,248] on insulin resistance in T2DM patients.

Inflammation is one of the responses associated with T2DM and it is demonstrated that VD reduces the levels of inflammatory cytokines, which are related to insulin resistance. VD has also the ability to reduce the aggregation of advanced glycation end products that are found in T2DM subjects, which are associated with insulin resistance. [249,250,251]

Furthermore, VD blood levels are negatively correlated to glucose status, insulin resistance, β-cell function and risk of suffering metabolic syndrome. [252,253,254] A few clinical trials concluded that low VD levels are associated with insulin resistance and hyperglycemia in diabetic and non-diabetic subjects [255,256,257] and high VD levels are related to better β-cell function and lower glycemia in patients with risk to develop

T2DM. [258] A similar beneficial effect of VD supplementation is found in gestational diabetic women. [259] Moreover, a recent meta-analysis of randomized controlled trials suggests that VD treatment ameliorates the chronic inflammation in T2DM patients. [260]

Nonetheless, last year Maddaloni *et al*. tried to summarize the results of published randomized clinical trials related to VD and T1DM or T2DM in order to see if there was a cause-effect relationship. The conclusions were that most of the investigations in T1DM could not prove a protective role of VD in β-cell function. However, it seemed to be a good preventive treatment if administrated from very early in life. In T2DM there are many *in vitro* and *in vivo* studies supporting a beneficial effects of VD in the disease, but clinical trials performed until then were not conclusive enough to support the effectiveness of the treatment with VD either in diabetes or insulin resistance. All these data together point out to VD as a good marker of healthy lifestyle but not specifically a causal factor of alterations in glucose metabolism. [221]

In conclusion, as it has been shown along this section, VD has an important role in many biological processes. Many basic and translational researches have demonstrated the VD effect on many diseases such as cancer, diabetes, hypertension, autoimmune disorders or cardiovascular diseases. Nonetheless, human clinical trials do not seem to be as consistent as molecular studies. This could be due to studies with not enough number of subjects, application of different VD analogues or doses or different ethnicities, among others. All these inconsistencies bring out the question of whether low VD levels are really a cause or a consequence of many human disorders. However, it seems unfair to classify VD deficiency only as an unhealthy life marker after so many studies showing that it has a lot to do with a large number of diseases. Nevertheless, stronger evidences are needed to hold the cause-effect relationship between VD and its non-classical disorders associated with. Therefore, the future should be better and large multi-centric clinical trials design in order to obtain more conclusive results and get to know what dose and analogues of the VD to use in all these diseases.

## 6.7 Vitamin D and lipid metabolism

In the latest years some investigations have pointed out the importance of VD in mitochondrial action and consequently in lipid metabolism because both the formation of precursors for lipid synthesis and the catabolic signal route occur in mitochondria. [261]

Recently it has been demonstrated that VDR is also localized in mitochondria of some cells [262,263] and it has been established that VD could inhibit mitochondrial respiration. Indeed, VDR is now considered as a protector of the ETC activity. [264,265]

It has been discovered that low $Ca^{+2}$ consumption could be related to more fat mass and that high $Ca^{+2}$ intake in the diet might activate fat oxidation. Thus, the VD-dependent $Ca^{+2}$ uptake in tissues improves the catabolism of lipids. [266] Bhat *et al.* have observed that the main part of changes seen in rats with VD deficiency reverted with $Ca^{+2}$ supplementation. [267] Moreover, obese subjects treated with VD associated with $Ca^{+2}$ are reported to diminish the fat mass, and VD-deficient and obese women show altered glucose metabolism and lipid levels. [268,269]

VDR supresses the mitochondrial respiratory chain activity and mitigate fatty acid β-oxidation. Therefore, VDR mitochondrial action inhibits lipid catabolism and triggers the route of acetyl-CoA to the lipid biosynthesis. In consequence, mice with VDR overexpressed have more adipose tissue and decreased energy metabolism. [270] Accordingly, mice without VDR present a raised respiratory activity that will activate the tricarboxylic acid cycle (TCA) and β-oxidation. Indeed, lipid catabolism in mitochondria is promoted, leading to a lean phenotype in VD deficient mice due to the oxidative metabolism overactivation and the muscle-protein expending in the TCA cycle *(Figure 19)*.

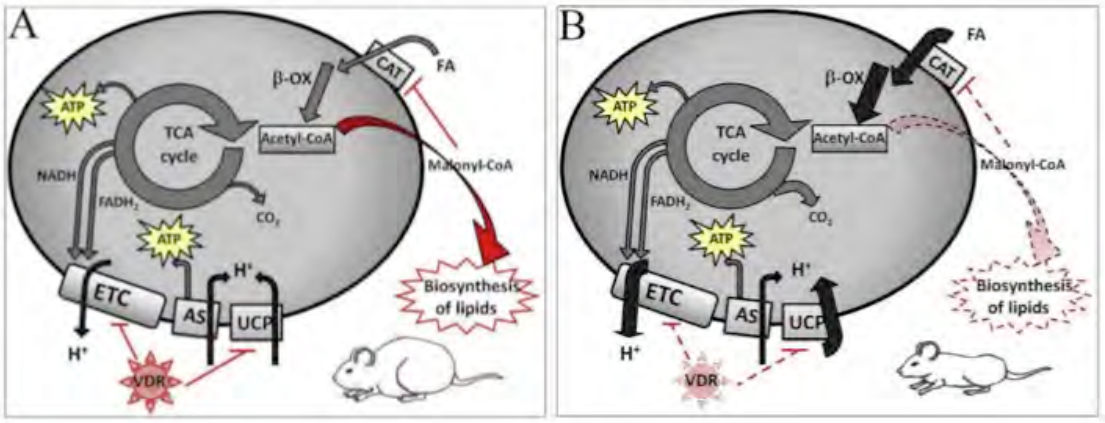


**Figure 19: Mitochondrial activity of VDR on lipid metabolism.** ***(A)*** *When VDR is overexpressed, ETC and UCP are inhibited, thus, there is a decreased utilization of NADH and $FADH_2$, which reduces β-oxidation. VDR inhibits lipid catabolism and activates channeling of acetyl-CoA to biosynthetic routes. Moreover, malonyl-CoA inhibits the entrance of FA, thus, reduces β-oxidation. (B) Loss of VDR increases ETC activity and UCP expression. TCA cycle and β-oxidation are triggered because of the ETC high activity, therefore, less free acetyl-CoA is found in cytosol to synthesize malonyl-CoA, which is the precursor of the lipid biosynthesis. Extracted from Silvagno et al. (2017) Figure abbreviations: AS, adenosine triphosphate synthase ATP, adenosine triphosphate; β-ox, β-oxidation; CAT, carnitine acyltransferase; ETC, electron transport chain; FA, fatty acids; $FADH_2$, flavin adenine dinucleotide reduced; $H^+$, hydrogen; NADH, nicotinamide adenine dinucleotide reduced; TCA cycle or Krebs cycle, tricarboxylic acid cycle; UCP, uncoupling protein; VDR, vitamin D receptor.*

Besides mitochondria, our laboratory reported a couple of years ago, a relationship between VDR and lipid metabolism in hepatocytes, specifically, in non-alcoholic fatty liver disease (NAFLD) subjects. [271] The VDR function in the liver is not well-established owing to its low expression in hepatocytes.[272] However, there are some studies that suggest a role of VDR in liver, for instance, it was seen that VDR was expressed in some hepatic cell lines [273] and that classic hepatocyte genes could respond to VDR. [274,275] Furthermore, a bile acid rate-limiting gene from liver called CYP7A1 is regulated in humans by VDR. [276,277] Our results pointed out that VDR was activated in NAFLD mice models and in fatty liver patients. In addition, the lack of VDR avoided HFD-induced liver steatosis in $apoE^{-/-}$ mice. In conclusion, it was suggested that VDR had a prosteatotic role as a result of activation of lipogenic routes and suppression of lipid β-oxidation in liver. [261]

## 6.8 VDR mouse models

Four different groups performed the full VDR KO mice around twenty years ago. They did not show phenotypical abnormalities at birth, however they had many disorders

associated with, such as: hypocalcemia, hypophosphatemia, rickets, develop growth retardation, secondary hyperparathyroidism, elevated alkaline phosphatase, alopecia, less bone density, bone growth retardation and flat face and short nose after weaning. In addition, active VD serum levels were ten times higher than in wild type (WT) mice, they had an impaired insulin secretory capacity and presented gonadal insufficiencies. Surprisingly, all these alterations, but alopecia, were normalized when the VDR KO mice were feeding with a $Ca^{+2}$, P and lactose enriched diet, which suggested that elevated $Ca^{+2}$ absorption is critical for VD action on bone and $Ca^{+2}$ homeostasis. [237,278,279,280]

The beginning of all these symptoms in mice starts at three weeks of age accordingly to weaning and to the beginning of intestinal $Ca^{+2}$ absorption dependent of VD. Before, in the neonatal stage, $Ca^{+2}$ homeostasis is regulated by milk from breast-feed. [281] Therefore, at the same time that $Ca^{+2}$ absorption is becoming VD-dependent, rickets, growth retardation, hypocalcaemia, etc. appear in VDR KO mice, as in VD resistant type II rickets subjects.

In order to deeply study the VD classical functions, tissue-specific conditional VDR KO mice were generated in intestine, bones, parathyroid glands and kidneys. All the investigations together, from full and conditional VDR KO mice concluded that VD is an important part of the tightly regulated $Ca^{+2}$ and P balance. [282]

The VD non-classical functions also have been well studied in the VDR KO mouse. In the 80s, Colston *et al.* [283] and Abe *et al.* [182] discovered the antineoplastic effect of VD. Since then, many studies supported that hypothesis in a wide variety of tumours, such as colon, skin, breast, prostate, lung or leukaemia.

In the early stages of colon tumour progression, VDR and 1-α-hydroxylase are increased, which could propose a key function of VD in growth inhibition of that malignancy. [284,285] In addition, it was seen that VD had antiproliferative and prodifferentiating roles on keratinocytes, and that VDR KO mice was hypersensitive to skin carcinogenesis in response to a tumor-causing agent. [286,287,288] Besides epithelial tumours (skin and colon), alterations on mammary gland morphology and

tumorigenesis were observed in female VDR KO mice, and additionally, VDR and 1-α-hydroxylase were enhanced in breast tumors. [289]

To sum up, VDR KO mice have many $Ca^{+2}$-related disorders, but also non- $Ca^{+2}$ related ones. The skin is the most evident non-calcemic target for VD because both VD-resistant rickets and VDR KO mouse present alopecia. The hair cycle is completely dependent on VDR but not on VD ligand, because it has not seen to be reproduced by VD deficiency.

In addition, VDR deficient mice in a physiological state do not present a major immune phenotype, although there are many slight molecular and cellular irregularities in their immune system. Nevertheless, VDR KO mice are more predisposed to suffer an autoimmune disease like T1DM. VDR KO mice are also prone to develop renal failure associated with DM and inflammation-induced multiorgan thrombosis.

Moreover, VDR null mice present signs of defective development of striated muscle. This could remember the effects of severe VD deficiency on muscle weakness, as in rickets subjects.

Even though VDR KO mice do not show neurological impairment, there are some behaviour abnormalities in them, such as abnormal grooming pattern and maternal behaviour. Additionally, VDR deficient mice have defective reproduction, however, most of VDR KO strains, with a high $Ca^{+2}$ rescue diet can correct this impairment.

Finally, there are many symptoms that VD-deficient humans and VDR-KO mice share like the calcemic ones: bone, growth plate or tooth phenotypes. Furthermore, there are also many overlapping characteristics between humans with lack of VD and VDR null mice in the VD-related non-classical disorders, such as immune, cardiovascular, antiproliferative effects or muscle phenotype.

However, more large-scale and long-term prospective clinical trials are needed to better understand the VD effect in non-calcemic VD-related disorders and to find the correct doses of VD treatment to have a beneficial effect. [238]

# Materials and Methods

# 1. *In vivo* experimental model

## 1.1 Legislation

All the experiments have been carried out in accordance with the laws regarding the use and welfare of animals in the laboratory:

- Directive of the EEC Council 86/609 / EEC, European Convention on the protection of vertebrate animals used in experimentation and other scientific purposes.
- Law 5/1995, of June 21, of the *Generalitat de Catalunya* for the protection of vertebrate animals used in experimentation and other scientific purposes.
- Decree 214/1997, July 30, which develops the previous law.
- Royal Decree 1201/2005, October 10, for the protection of animals used for experimentation and other scientific purposes.
- Directive of the European Parliament and the Council 2010/63 of September 22, 2010 on the protection of animals used for scientific purposes.
- Royal Decree 53/2013, February 1, which establishes the basic rules applicable for the protection of animals used in experimentation and other scientific purposes, including teaching.

The purpose is to ensure that the number of animals used is reduced to a minimum and that they are correctly treated to avoid pain, suffering and prolonged unnecessary injuries.

## 1.2 Animal house care

The mice were housed in the conventional rodent animal facility from the *Universitat de Lleida* following the sanitary controls and the bioethical animal care recommendations. They were constantly maintained at 22ºC and with cycles of 12 hours light/dark. Mice had *ad libitum* access to water and food.

### *1.2.1 Diets*

Mice have been treated with different diets depending on the experiment:

- Normal diet: (Teklad Global 14% Protein 4% Fat Rodent Maintenance Diet – Envigo)
- HFD (Paigen Diet 10MM S9358-E030 – 1.25 cholesterol, 0.5% cholic acid, 15% cocoa butter, 1% corn oil)
- $K^+$ Chelate (ResinCalcio-Rubió) diet: we used a homemade-pelleted diet. We grinded the $K^+$ Chelate powder, in a dose of 1g/kg/day, with the usual diet (Teklad-Envigo). Then, pellets were compacted with a bit of water and finally, lyophilized.

#### *1.2.2 Drinks*

In general terms, mice drank normal water but in some experiments it was mixed with some products to administer treatments:

- 10% D(+)-sucrose (PanReact Applichem A2211) in water. [290,291]
- 200mM sodium bicarbonate in water (Sigma S-5761). Dose: 16,8g/L. [292,293]

## 1.3 Experimental model generation

In the present study, we focused on the generation of an experimental model PTEN and VDR KO in order to find the interactions between these two genes. The model that has been created allows control of PTEN and VDR genes deletion in a given time and tissue specific.

The mice models that were performed for the experiment are:

- Inducible PTEN-VDR double knockout murine model (Cre-ER$^{TM\ +/-}$ PTEN $^{fl/fl}$ VDR $^{fl/fl}$ or DKO).
- Inducible PTEN-KO (Cre-ER$^{TM\ +/-}$ PTEN $^{fl/fl}$ VDR $^{+/+}$).
- Inducible VDR-KO (Cre-ER$^{TM\ +/-}$ PTEN $^{+/+}$ VDR $^{fl/fl}$).
- Control mouse (Cre-ER$^{TM\ -/-}$ PTEN $^{fl/fl}$ VDR $^{fl/fl}$ or CNT).

The colony was obtained by crossing an inducible PTEN-KO mouse (129S4/Swiss) with a VDR-KO mouse (C57BL6/129S1Sv/129X1SvJ/SJL). Both, PTEN and VDR alleles are flanked by LoxP sequences.

The PTEN-KO mouse is expressing the Cre recombinase (CAG-Cre-ER$^{TM}$) inducible by Tamoxifen (Sigma-Lifescience T564-1G) injection under the chicken β-actin promoter (CAG) coupled to the cytomegalovirus enhancer allowing a PTEN biallelic deletion. In this model, Tamoxifen caused PTEN deletion in the epithelial cells but not in stroma or hematopoietic cells and it was attributed to mice background effects. [294]

We obtained the Cre-ER$^{TM\ +/-}$PTEN$^{fl/fl}$ mouse from Dr. Xavier Dolcet. [294] They used a transgenic mouse Cre-ER$^{TM}$ (B6.Cg-Tg(CAG-cre/Esr1)5Amc/J) generated by Dr. Andrew P. McMahon and purchased in Jackson Laboratories (Bar Harbor, ME). To obtain the transgenic they used a pronuclear injection where the genetic material was injected in the pronucleus of a fecundated oocyte. The transgene included a fusion protein between Cre and a mutant form of the ligand-binding domain of the murine estrogen receptor (ER$^{TM}$). The fusion protein binds Tamoxifen, but not endogenous estrogens, staying in the cytoplasm waiting for the correct stimulus. In the absence of the inducing agent, Hsp90 kidnapped the Cre-ER$^{TM}$ in the cytosol, thus avoiding nuclear recombination. However, when Tamoxifen was present, the interaction with Hsp90 disappears, therefore allowing the translocation of the Cre-ER$^{TM}$ to the nucleus and the beginning of the recombination on target LoxP sequences. [295,296]. Cre-ER$^{TM}$ should be maintained in heterozygosis (Cre-ER$^{TM+/-}$) to obtain mice with a normal phenotype. The other mouse necessary to make Cre-ER$^{TM+/-}$PTEN$^{fl/fl}$ is the PTEN$^{fl/fl}$ (C:129S4-Pten$^{tm1Hwu}$/J) that was generated by Dr. Hong Wu and was purchased from Jackson Laboratories (Bar Harbor, ME). [116] It is characterized to have LoxP sequences flanking the exon 5 of PTEN gene, which codifies the phosphatase domain from the protein. It was generated by electroporation of embryonic stem cells and the following blastocyst injection. Their use allows the flanked-exon excision in different tissues or times depending on the recombinase used. PTEN$^{fl/fl}$ should be maintained in homozygosis to obtain fertile mice with a normal phenotype.

VDR-KO mouse (VDR$^{fl/fl}$) was generated by Dr. Geert Carmeliet in the Katholieke Universiteit Leuven. [280] They have two LoxP sequences flanking the exon 2 of VDR gene. Embryonic stem cells were electroporated and injected to a blastocyst.

The four experimental groups were obtained by crossing the F1 of the first pairing (P), which are heterozygous, and then, the genotypes of interest of the F2 are selected.

From the F1 we only needed 4 out of 18 resulting genotypes; thus, we wanted more productive crossings to make the colony. Finally, to achieve our objective, we performed two types of crossings: biallelic PTEN deletion in all animals that expressed Cre recombinase in which only varied the degree of ablation of VDR, and vice versa (CreER$^{TM+/-}$ PTEN$^{fl/fl}$ VDR$^{fl/+}$ with CreER$^{TM-/-}$ PTEN$^{fl/fl}$ VDR$^{fl/+}$ and CreER$^{TM+/-}$ PTEN$^{fl/+}$ VDR$^{fl/fl}$ with CreER$^{TM-/-}$ PTEN$^{fl/+}$ VDR$^{fl/fl}$ ) *(Figure 20)*.

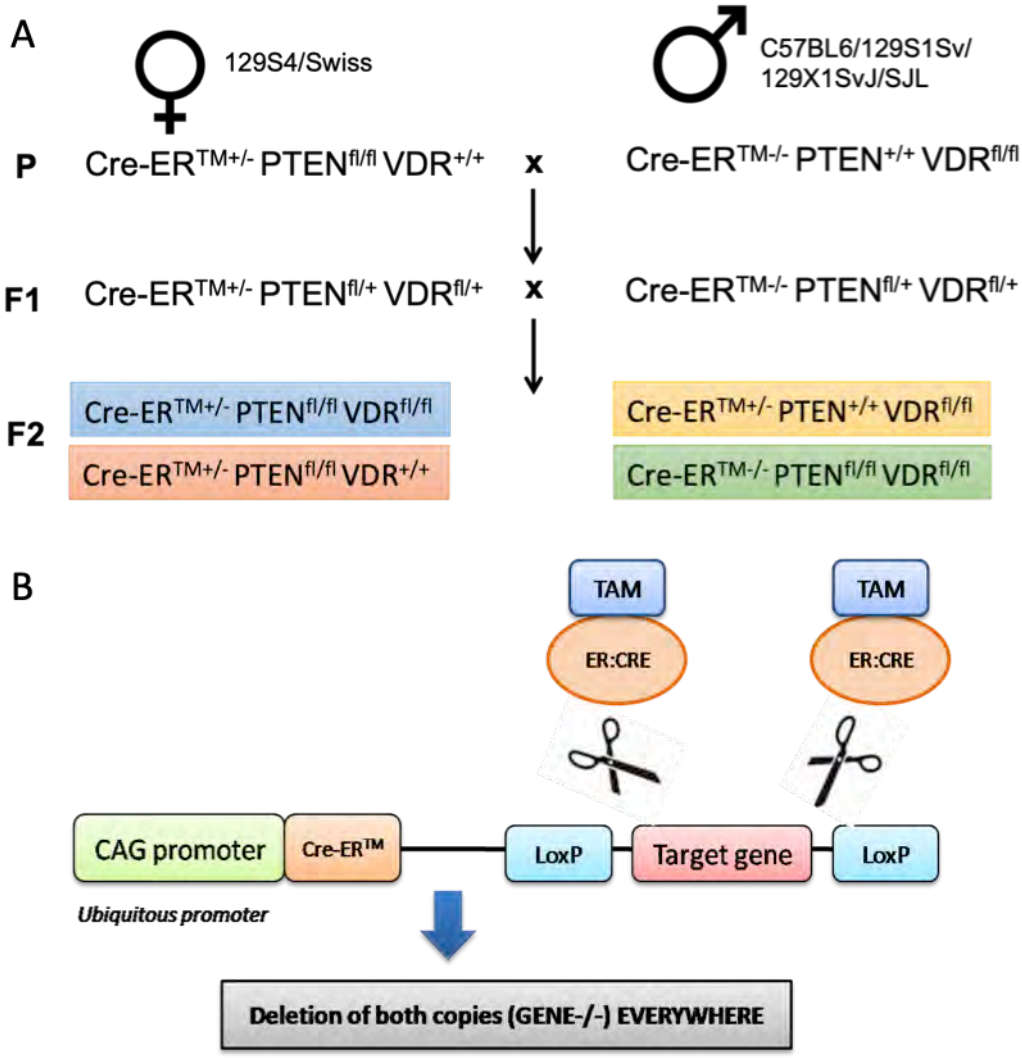


**Figure 20: Mouse model colony generation.** ***(A)*** *The parental generation (P) is formed by the crossing of an inducible CreER$^{TM+/-}$ PTEN$^{fl/fl}$ VDR$^{+/+}$ mouse (129S4/Swiss) with a CreER$^{TM-/-}$ PTEN$^{+/+}$ VDR$^{fl/fl}$ mouse (C57BL6/129S1Sv/129X1SvJ/SJL). The offspring of the P generation are called the first filial F1, which are heterozygotic mice. Finally, in the second filial generation F2 the four groups of study are obtained (CreER$^{TM-/-}$ PTEN$^{fl/fl}$ VDR$^{fl/fl}$, CreER$^{TM+/-}$ PTEN$^{fl/fl}$ VDR$^{+/+}$, CreER$^{TM+/-}$ PTEN$^{+/+}$ VDR$^{fl/fl}$, CreER$^{TM+/-}$ PTEN$^{fl/fl}$ VDR$^{fl/fl}$).* ***(B)*** *Gene construction of how tamoxifen and CRE recombinase act over LoxP sequences to remove the target genes. Figure abbreviations: CRE-ER$^{TM}$, Cre recombinase inducible by Tamoxifen; LoxP sequence, locus of X-over P1 sequence; TAM, tamoxifen.*

At this point, it is important to note that all the controls used in this work come from the same colony, in order to ensure that all animals analyzed present the same genetic background. Thus, it is possible to avoid errors when assessing the phenotype of animals and being certain that the observed effects are due to the genotype of study and not to different genetic backgrounds.

## 1.4 Tamoxifen administration

Tamoxifen was dissolved in ethanol 100º at 100 mg/ml and then the solution was emulsified in corn oil (Sigma-Aldrich C8267) at 10 mg/ml by vortexing. Then it was again dissolved in corn oil to obtain a final concentration of 5 mg/ml. Finally, the solution was completely homogenized 1-3 h in a bath at 37ºC mixing every hour. To induce PTEN and/or VDR ablation, a single intraperitoneal injection of 0,5 mg of tamoxifen solution per adult mice (4-5 weeks old in a weight between 12-20g) was administered (dose: 25mg/kg).

## 1.5 Experimental design

The experimental design that was carried out is shown in *Figure 21*. The animals were thoroughly monitored until they required euthanasia. The criterion of sickness was glucose levels <90 mg/dl after 2h of fasting in DKO mice. Usually these glycemia values were achieved around week 9-10 after tamoxifen injection. At this time point, all the *in vivo* studies performed with live mice, such as GTT or PTT were performed.

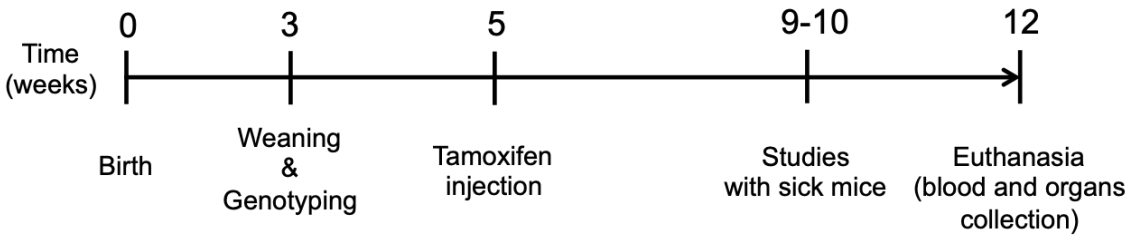

**Figure 21: Timeline experimental design.** *Mice are weaning and genotyping after 3 weeks of born and Tamoxifen is injected at 5 weeks. After 5 more weeks, when mice present signs of sickness, all studies are performed and they are monitored until they required euthanasia.*

## 1.6 Genotyping

Mice should be genotyped, sexed and selected before they were weaned, at 21 days of life.

### *1.6.1 DNA extraction*

Genomic DNA was obtained from the mouse-tail. Mice were asleep by inhaled anaesthesia (isoflurane, IsoFlo) to extract a biopsy of about 5mm from their tails and to mark them on the ears, to be identified later. Then, every sample was digested in 200µL of the mix prepared with 1ml of genotyping buffer (100mM Tris pH 8.5, 200mM Nacl, 5mM EDTA and 0.2% SDS) and 50µL of proteinase K at 20mg/mL (Sigma-Aldrich) overnight at 45°C. The day after, the samples were centrifuged at high speed for 10 minutes at 4°C and then the supernatant were removed trying not to catch the rest of the tail or hair that was not digested. Afterwards, DNA was precipitated with 500µL of cold ethanol 100º and then centrifuged at maximum speed for 10 min at 4°C to obtain the DNA pellet, which then was dried until the completely ethanol evaporation. Finally, to obtain the extracted DNA sample, the pellet was resuspended in 500µL of distilled water.

### *1.6.2 Polymerase Chain Reaction (PCR)*

PCR is used to make several copies of a specific DNA fragment. Every gene had its own protocol adapted from a general one. The mix components were (*Table 1*): *MilliQ* water, 10x Reaction buffer $MgC_2$l free (Biotools), 50mM $MgCl_2$ solution (Biotools), dNTPs mix (10mM each) (Biotools), *Taq* polymerase (Biotools) and specific forward and reverse primers from each gene (Sigma-Aldrich) (*Table 2*). Later on, the samples were introduced to the thermocycler (TC-412 Techne) where the protocol was set up (*Table 3*).

| Volume per sample (µl) | Cre-ER$^{TM}$ | PTEN wt/LoxP | VDR wt | VDR LoxP | PTEN Δ | VDR Δ |
|---|---|---|---|---|---|---|
| **Buffer 10x** | 2.5 | 2.5 | 2 | 2 | 2.5 | 2 |
| **MilliQ water** | 14.3 | 13 | 12.5 | 13 | 12.5 | 13 |
| **$MgCl_2$** | 1.25 | 1 | 0.6 | 0.6 | 1 | 0.6 |
| **dNTPs** | 0.5 | 0.5 | 0.4 | 0.4 | 1 | 0.4 |
| **Primer** *(Forward)* | 1 | 2.5 | 1 | 1 | 2 | 1 |
| **Primer** *(Reverse)* | 1 | 2.5 | 1 | 1 | 1 + 1 (both primers) | 1 |
| **DMSO** | 1,25 | - | 0.5 | - | - | - |
| **Taq Polymerase** | 1 | 1 | 1 | 1 | 1 | 1 |
| **DNA** | 2 | 2 | 1 | 1 | 2 | 1 |
| **Final volume** | **25** | **25** | **20** | **20** | **25** | **20** |

**Table 1: PCR mix components for each gene.** *Every column signifies a different gene analyzed by PCR: CreER$^{TM}$, PTEN wt/LoxP, VDR wt, VDR LoxP, PTEN Δ, VDR Δ. And every raw represents all PCR mix components needed for each gene. Table abbreviations: CRE-ER$^{TM}$, Cre recombinase inducible by Tamoxifen; DMSO, Dimethylsulfoxide; DNA, deoxyribonucleic acid; dNTPs, deoxynucleotide triphosphate; $MgCl_2$, magnesium chloride; PTEN Δ, Phosphatase and Tensin homolog Cre-excised band; PTEN wt/LoxP, Phosphatase and Tensin homolog wild type/ locus of X-over P1 sequence; VDR Δ, vitamin D receptor Cre-excised band; VDR LoxP, vitamin D receptor locus of X-over P1 sequence; VDR wt, vitamin D receptor wild type.*

| Gene | Primer sequence |
|---|---|
| **CreER$^{TM}$** | Forward: 5'-ACGAACCTGGTCGAAATCAGTGCG-3' |
| | Reverse: 5'-CGGTCGATGCAACGAGTGATGAG-3' |
| **PTEN wt/LoxP** | Forward: 5'-CAAGCACTCTGCGAACTGAG-3' |
| | Reverse: 5'-AAGTTTTTGAAGGCAAGATGC-3' |
| **VDR wt** | Forward: 5'-TTTGGCCTTTCTGCTTGCCTCTTC-3' |
| | Reverse: 5'-TCAGTTGATATCCCTGGGAGGC-3' |

| | |
|---|---|
| **VDR LoxP** | Forward: 5'-TTTGGCCTTTCTGCTTGCCTCTTC-3' |
| | Reverse: 5'-AGCGACACTCTTGGTCTGGTTCC-3' |
| **PTEN Δ** | Forward: 5'-ACTCAAGGCAGGGATGAGC-3' |
| | Reverse: 5'-AATCTAGGGCCTCTTGTGCC-3' |
| | Reverse: 5'-GCTTGATATCGAATTCCTGCAGC-3' |
| **VDR Δ** | Forward: 5'-CACAACAGTCAGAGGCAGTAAGCAAAGC-3' |
| | Reverse: 5'- AGCGACACTCTTGGTCTGGTTCC-3' |

**Table 2: Primer sequences.** *Forward and reverse primers, which are short nucleic acid sequences that provides a starting point for DNA synthesis for each analyzed gene. Table abbreviations: CRE-ER$^{TM}$, Cre recombinase inducible by Tamoxifen; PTEN Δ, Phosphatase and Tensin homolog Cre-excised band; PTEN wt/LoxP, Phosphatase and Tensin homolog wild type/ locus of X-over P1 sequence; VDR Δ, vitamin D receptor Cre-excised band; VDR LoxP, vitamin D receptor locus of X-over P1 sequence; VDR wt, vitamin D receptor wild type.*

| Temperature | Time | Cycles | Genotype | Band size |
|---|---|---|---|---|
| **94ºC** | 2' | 1 | CreER$^{TM-/-}$ | No band |
| **94ºC** | 45'' | 32 | | |
| **65ºC** | 45'' | | | |
| **72ºC** | 45'' | | CreER$^{TM+/-}$ | 350bp |
| **72ºC** | 5' | 1 | | |
| **4ºC** | ∞ | | | |

| Temperature | Time | Cycles | Genotype | Band size |
|---|---|---|---|---|
| **94ºC** | 3' | 1 | PTEN$^{+/+}$ | 156 bp |
| **94ºC** | 30'' | 35 | PTEN$^{fl/+}$ | 156 bp |
| **60ºC** | 1' | | | 328 bp |
| **72ºC** | 2' | | PTEN$^{fl/fl}$ | 328 bp |
| **72ºC** | 2' | 1 | | |
| **4ºC** | ∞ | | | |

| Temperature | Time | Cycles | Genotype | Band size |
|---|---|---|---|---|
| **95ºC** | 5' | 1 | VDR$^{+}$ | 368 bp |
| **95ºC** | 30'' | 40 | | |
| **65ºC** | 1' | | | |
| **72ºC** | 1' | | | |
| **72ºC** | 7' | 1 | | |
| **4ºC** | ∞ | | | |

| Temperature | Time | Cycles | Genotype | Band size |
|---|---|---|---|---|
| **94ºC** | 5' | 1 | VDR$^{fl}$ | 250 bp |
| **94ºC** | 30'' | 40 | | |
| **60ºC** | 1' | | | |
| **72ºC** | 1' | | | |
| **72ºC** | 7' | 1 | | |
| **4ºC** | ∞ | | | |

| Temperature | Time | Cycles | Genotype | Band size |
|---|---|---|---|---|
| **94ºC** | 3' | 1 | PTEN Δ | 300 bp |
| **94ºC** | 30'' | 35 | | |
| **60ºC** | 1' | | | |
| **72ºC** | 1' | | | |
| **72ºC** | 5' | 1 | | |
| **4ºC** | ∞ | | | |

| Temperature | Time | Cycles | Genotype | Band size |
|---|---|---|---|---|
| **95ºC** | 5' | 1 | VDR Δ | 300 bp |
| **95ºC** | 30'' | 40 | | |
| **65ºC** | 1' | | | |
| **72ºC** | 1' | | | |
| **72ºC** | 7' | 1 | | |
| **4ºC** | ∞ | | | |

**Table 3: PCR protocols.** *CreER$^{TM}$, PTEN, VDR, PTEN Δ and VDR Δ PCR thermocycler machine protocols. The first three columns indicate the temperature, time and cycles needed to perform the correct PCRs and obtain the PCR products with their properly size. Table abbreviations: bp, base pairs; CRE-ER$^{TM}$, Cre recombinase inducible by Tamoxifen; PTEN Δ, Phosphatase and Tensin homolog Cre-excised band; PTEN$^{+/fl}$, Phosphatase and Tensin homolog wild type/ locus of X-over P1 sequence; VDR Δ, vitamin D receptor Cre-excised band; VDR$^{+}$, vitamin D receptor wild type; VDR$^{fl}$, vitamin D receptor locus of X-over P1 sequence.*

### *1.6.3 Electrophoresis gel*

The PCR products were analyzed by an agarose electrophoresis gel. The gel was made by melting 1.5g of agarose in 100 mL of TAE 1X (pH 8.0, 40mM Tris, 20mM acetic acid, and 1mM EDTA), then, 8 µL of SyberSafe (Invitrogen) were added, which is an ultraviolet intercalating marker of DNA. DNA products, with the loading buffer Orange G, and 100 bp DNA ladder (Biotools) were loaded to the agarose gel.

## 1.7 Glucose analysis

### *1.7.1 Glucose detection*

To detect glucose from mice, a small incision was made in their tail to get a drop of blood. Afterwards, glycemia levels were measured introducing the little drop of blood into the test strip that was connected to the glucometer (Accu-Check Perfmorma – Roche).

In this study, the glycemia was analysed at different time points: without fasting (diet), after 2h of fasting and after 7h of fasting.

### *1.7.2 Glucose tolerance test*

Glucose tolerance test is an analysis used to determine the degree of insulin resistance. Insulin-resistant mice maintain high blood glucose levels after intraperitoneal glucose (Sigma-Aldrich C8270) administration, whereas normal mice show a recovery in blood glucose levels to normal values.

The mice were fasted during 2h before the glucose tolerance test. After these two hours, the initial glycemia detection was made (time 0). Then, an intraperitoneal single-injection of 4g/kg of glucose (20% glucose saline solution: 1g of glucose in 5ml of Phosphate-buffered saline 1x (PBS1x) well-homogenized) was administered. Finally, blood glucose measurements were taken at times 20, 40, 60 and 120 minutes.

### *1.7.3 Pyruvate tolerance test*

Pyruvate tolerance test is an analysis used to evaluate gluconeogenesis. Pyruvate tolerance test is a variant of the glucose tolerance test in which sodium pyruvate (100mM Gibco by Life Technologies - 11360-070) is administrated instead of glucose. The pyruvate injection will activate glucose synthesis, which will be a marker of hepatic gluconeogenesis.

The protocol performed in this test was exactly the same as for the glucose tolerance test; the only difference was the dose of pyruvate injected (2g/kg from a 20% pyruvate saline solution).

### *1.7.4 Glucose behavior test*

Glucose behaviour test is an analysis used to observe the glucose reaction in the bloodstream from the time when mice are fasted and, thus, to monitor their blood glucose for several hours (in this case during 6h). The response to fasting and the effects of insulin and glucagon during this period will be observed through glucose levels.

The protocol for this test was performed by removing food at time 0 and starting glycemia measurements at times 20, 40, 60, 120, 150, 180, 210, 240, 270, 300, 330 and 360 minutes.

## 1.8 Metabolic cages

Metabolic cages are a type of cage designed to make a metabolic control of mice in which urine and feces are collected from mice and their food and water intake are measured.

### *1.8.1 Food and water intake*

Food and water intake were quantified by weight and measuring food and water levels before and at the end of the experiment.

### *1.8.2 Urine collection*

Urine collection was carried out in tubes with 250µl of paraffin oil (Sigma-Aldrich 18512) and 25µl of 2% sodium azide (Sigma-Aldrich 76320) in order to preserve the urine in perfect conditions during the 24 hours of collection.

After one day of collection, the urine found in the collecting tube was centrifuged (Eppendorf 5415R Micro-Centrifuge) 5 minutes at 2800rpm in microcentrifuge tubes to split the different phases, oil, urine and solid precipitate. With a micropipette and a new microcentrifuge tube, the urine sample was obtained and its volume quantified.

## 1.9 Blood collection in mice

### *1.9.1 Heart blood*

The heart blood extraction is employed to obtain the whole blood of the organism and as a method of sacrifice approved by the ethics committee, called terminal exsanguination.

With the mouse asleep, an abdominal incision was made to open the intraperitoneal cavity without cutting the diaphragm to avoid a cardiorespiratory arrest, as the heartbeat was needed to obtain the maximum amount of blood. Then, a 1ml syringe (BD Plastipak 329654) with a 25G needle (BD Microlance 300600) was used to pierce the diaphragm and reach the heart directly and extract approximately 1ml of blood. Finally, the blood sample was injected into a serum extraction tube that contained a clot activating gel (S-Monovette 1.1ml Z-Gel 06.1667.001).

After clot formation, the blood tube was centrifuged (Hettich – Universal 32R) 10 minutes at 4ºC and 2500rpm. The supernatant (serum sample) was transferred to a new microcentrifuge tube.

### *1.9.2 Facial vein blood (cheek)*

There is a facial vein blood in mice that goes from the ocular plexus across the cheek, and a submandibular vein that goes through the lower mandible. Both vessels

converge into the jugular vein just below the mandible line, which is an accessible point to extract blood. [297]

With the mice asleep, a 25G needle was used to puncture the cheek with a depth of 3-4mm and to produce the bleeding. The blood was collected with 75mm capillary tubes without heparin (Deltalab 7311) to extract serum after clot formation and centrifugation (Hettich – Haematokrit 210 C2104) 10 minutes at 2500rpm.

#### *1.9.3 Caudal vein blood (tail)*

Caudal vein from tail is a good election to extract a small volume sample of blood (less than 200µl), quickly and minimally invasive.

Mice did not need to be asleep by anaesthesia, they only had to be immobilized and, with the help of a surgical blade, a small incision was made in their tail to obtain several drops of blood.

## 1.10 Renal function analysis

A proper renal function is considered when there is a good flow rate of filtered fluid through the kidneys, thus, an appropriate glomerular filtration rate (GFR). In clinical practice, the creatinine clearance is mainly used to estimate the GFR, however, in mice the blood urea nitrogen (BUN) test is preferred. BUN test measures the amount of urea nitrogen found in blood.

Urea can be measured with the QuantiChrom TM Urea Assay (DIUR-500 of BioAssay Systems) and from the uremia the levels of BUN can be calculated. If renal function is affected, the BUN will be elevated in serum.

## 1.11 Serum and urine biochemical analysis

Serum and urine were analyzed through two different colorimetric assays in the clinical analysis service of the Hospital Universitari Arnau de Vilanova de Lleida to evaluate $Ca^{+2}$ and P levels.

The $Ca^{+2}$ O-Cresolftalein complexona (Cromatest Lniear) kit allows the detection of $Ca^{+2}$ levels in fluids such as serum or urine. It is based on the detection of the specific

union of O-Cresolftalein complexona, a metallochromic indicator, to $Ca^{+2}$ at an alkaline pH, with the consequent displacement of the absorbance spectrum of the complex formed. The intensity of the chromophore is proportional to the total $Ca^{+2}$ concentration of the sample. The absorbance of the reaction is read at 570 nm and the concentration of the test sample is measured in reference to the values of the standard curve.

The phosphorus-C kit (Spinreact) allows the detection of P levels in fluids such as serum or urine. It is based on the reaction of inorganic P with the molybdic acid to form a phosphomolybdic complex. The subsequent reduction of the complex, in alkaline medium, results in molybdenum blue coloration. The intensity of the color formed is proportional to the concentration of inorganic P present in the sample. The absorbance of the reaction is read at 720 nm and the concentration of the test sample is measured in reference to the values of the standard curve.

Moreover, to analyze potassium ($K^+$) and sodium ($Na^+$) in serum and urine it was used the AU 5800 Series Clinical Chemistry Analyzers (Beckman Coulter) machine. The determination was made in the ISE module (for the determination of $Na^+$, $K^+$), using electrodes with a crown ether membrane for $Na^+$ and $K^+$. An electrical potential is developed according to the Nerst equation for a specific ion and then compared to an internal reference, converting that electric potential into voltage and then, into the sample ion concentration. Before carrying out the determinations of the samples, it is necessary to perform a calibration of the ions (where the equipment establishes a standard curve). The calibration patterns for the serum are ISE Low Serum Standard (nº 66317) and ISE High Serum Standard (nº 66316). And the calibration pattern for urine is ISE Low / High Urine Standard (nº 66315).

## 1.12 Urine glucose analysis

To detect glucose in urine, a glucose quantitative determination kit was used. (Spinreact. Glucose-TR 1001190).

A 100 mg/dl glucose calibrator was used to make serial dilutions as a standard curve. Then, 1.5µl of standards, blanks and urine samples were transferred in a 96-well-plate

together with 150µl of the commercial working reagent to be incubated 20 minutes at room temperature. Finally, the color obtained from the reaction was read within the next 30 minutes in a microplate spectrophotometer (Epoch. BioTek) at 505 nm.

The intensity of the color formed was proportional to the glucose concentration in the sample. To calculate the final concentration of the samples, a linear regression curve fitting was used. (Conversion factor used: mg/dl x 0.0555 = mmol/L).

## 1.13 pH measurement in urine

A pH meter (pHenomenal pH 1100L VWR) was used to measure the pH of urine samples.

First, the pH meter needed to be calibrated with 3 calibrators, the pH=9.21 (base), the pH=7 (neutral) and the pH=4.01 (acid). Then, the urine samples were placed in 15ml tubes to be detected by the machine.

## 1.14 Mouse perfusion

First, as explained before, the total blood volume was extracted from the heart. Then, organs were cleaned of the blood remnants with saline perfusion. The cleaning perfusion procedure was based on making two small cuts, the first one, to the posterior end of the left ventricle and, the second one, to the right atrium using surgical scissors. These two incisions allowed creating a large circuit to clean all the organs. Later, a 25G needle attached to a 10ml syringe with PBS1x was injected into the ventricle incision until the wall of the aorta, without arriving to the aortic arch, in order to flush the saline solution through all the circulatory system, cleaning the blood and exiting the circuit through the incision made in the auricle.

## 1.15 Organ samples extraction

When the experiments were finalized or the mice required euthanasia, the animals were sacrificed and organs collected.

The organ collection was done after the terminal exsanguination and perfusion. In this study, almost all the organs were extracted because of the interest on well characterize the model generated. Therefore, the organs collected were: thyroid gland, kidneys, uterus, prostate, liver, muscle, pancreas, lungs, heart, spleen and brain.

In general, organs were divided in two pieces, except in the case of the ones that are bilateral that were entire conserved, to preserve them in two different ways:

- Frozen immediately after the extraction in cryotubes in liquid nitrogen (-196ºC) and later stored at -80ºC in the freezer. They were used to extract DNA, mRNA and proteins.
- Fixated with paraformaldehyde 4% (PFA 4%) (Scharlau) and posterior inclusion in paraffin (PanReac AppliChem ITW Reagents 253211). They were used to obtain sections and perform histological studies.

## 1.16 Histological studies and immunohistochemistry

### *1.16.1 Organ fixation and inclusion*

Fixation was done by immersion with PFA 4% for 24 hours. After washing several times with PBS1x samples were left one hour with ethanol 60% (Casa Álvarez Histodry 99) at room temperature; then, they were placed with ethanol 95% for three hours and subsequently, with ethanol 100% for three extra hours. Then, samples were treated with xylene (Richard-Allan Scientific Clear-Rite 3 6901) 3 times for 45 minutes and included with paraffin at 60ºC in a heater for five hours. Finally, every sample was properly orientated in a plastic mold where hot paraffin was poured over a cold surface to make the paraffin block (Leica EG1150 H).

Then, 5µm slices were made with a microtome (Microm HM 340E) in silanized slides glass in order to perform different stains.

### *1.16.2 H&E staining*

First, a dewaxing of the paraffin sections was done leaving them at 60ºC for 30 minutes and then placed with xylene for 10 minutes to eliminate excesses of paraffin.

Then, they went through a series of alcohols in decreasing concentrations (100%, 95% and 70%) to gradually rehydrate the samples until they reached distilled water. They were immersed in hematoxylin (PanReac AppliChem ITW Reagents 251344), a basic substance that stains acidic structures with blue tones like the cell nucleus, for 10 minutes, next, they were washed with water and quickly passed through acidic alcohol to wash them again. Following, they were immersed in eosin (Master diagnostic MAD-109 1000), an acid substance that stains the basic structures with pink tones like the cell cytoplasm, for 30 seconds and alcohol baths were re-made, but that time with increasing order (70%, 95% and 100%) to dehydrate the sample. Posterior, slides were left in xylene for 10 minutes and finally, dried and mounted with Dibutylphthalate polystyrene xylene (DPX) mounting medium (Casa Álvarez 10-8500) and covered with coverslips.

#### *1.16.3 PAS-AB staining*

The combined staining with alcian blue (AB) (pH 2.5)/periodic acid Schiff (PAS) was performed to characterize different mucosubstances because it stains neutral and reactive periodic acid mucosubstances. PAS marks carbohydrates that contain one or two glycol groups: glycogen, glycolipids, neutral mucosubstances and some non-sulfated mucosubstances. AB marks acidic mucosubstances.

First, the same H&E staining protocol of dehydration and rehydration was followed. Then, the slides were incubated 5 minutes with AB and washed in distillated water for 2 minutes. Next, the periodic acid oxidation took place for 15 minutes and washed for 2 minutes in distillated water. Afterwards, they were incubated in the Schiff solution (4g basic fuchsin + 7,6g sodium metabisulfite + 400ml hydrochloric acid 0,25N) for 25 minutes and washed three times of 2 minutes in sodium metabisulfite. Finally, 5 minutes of washing with tap water was done and then, a 30-seconds-stain with hematoxylin (PanReac AppliChem ITW Reagents 251344) was performed at room temperature. Finally, the dehydration and mounting protocol followed was the same as for H&E staining.

### *1.16.4 Immunohistochemistry*

After dehydrating the samples, the epitope recovery or antigenic determinant was carried out by a treatment called antigen retrieval [10mM citrate buffer pH6 (1.92g citric acid (anhydrous) + 1l dH2O, pH6]. Samples were introduced into the microwave at 400W for 15 minutes and cool for 30 minutes at room temperature. Later, 3 washes with PBS1x for 5 minutes were done. Next, the blockage of endogenous peroxidase was performed with the blocking solution (200 ml PBS1x + 4 ml peroxide hydrogen) for 30 minutes and two washings with PBS1x of 5 minutes were done. Next, the antibody non-specific binding site was blocked (50µl of horse serum not immunized (Vector Laboratories, PK-6200) + 5ml PBS1x) for 30 minutes at room temperature. Afterwards, the primary antibody (anti-insulin: Polyclonal Guinea Pig Anti-Insulin A0564, Dako, Denmark. 1/100 dilution) was prepared at the adequate dilution with the same non-specific binding solution prepared for the blocking overnight at 4ºC in a humid incubation chamber.

Next day, two washings of 2 minutes were made with PBS1x and immediately afterwards, the samples were incubated for 30 minutes with the appropriate secondary antibody (VECTASTAIN Elite ABC HRP Kit (Peroxidase, Universal. 1/50 dilution)) in a blocking solution (1/50 horse serum/PBS1x). Then, the samples were incubated with the biotin-avidin kit, ABC (VECTASTAIN) for 30 minutes. The reagents were prepared in a 1/50 dilution (100µl reagent A + 5ml PBS 1x + 100µl reagent B) and the slides were incubated with it for 30 minutes at room temperature. 2 washings were made with PBS1x for 2 minutes and also two washes with distilled water for 2 minutes. Finally, the samples were placed with the DAB chromogen (DAB peroxidasesubstrate kit, vector laboratories) (1ml of distillated water + 20ml buffer solution at a pH of 7.5 + 40ml DAB + 20ml peroxide hydrogen) for 10 minutes at room temperature to react with the substrate and create a precipitate that allows the subsequent visualization.

Finally, slides were washed with tap water for 10 minutes and then a quick stain with hematoxylin (MHS1 Sigma-Aldrich) was performed for 30 seconds at room

temperature. Then, they were rinsed out with tap water for 15 minutes and finally dehydrated and mounted, as explained in H&E staining protocol.

## 1.17 Pancreatic islet isolation

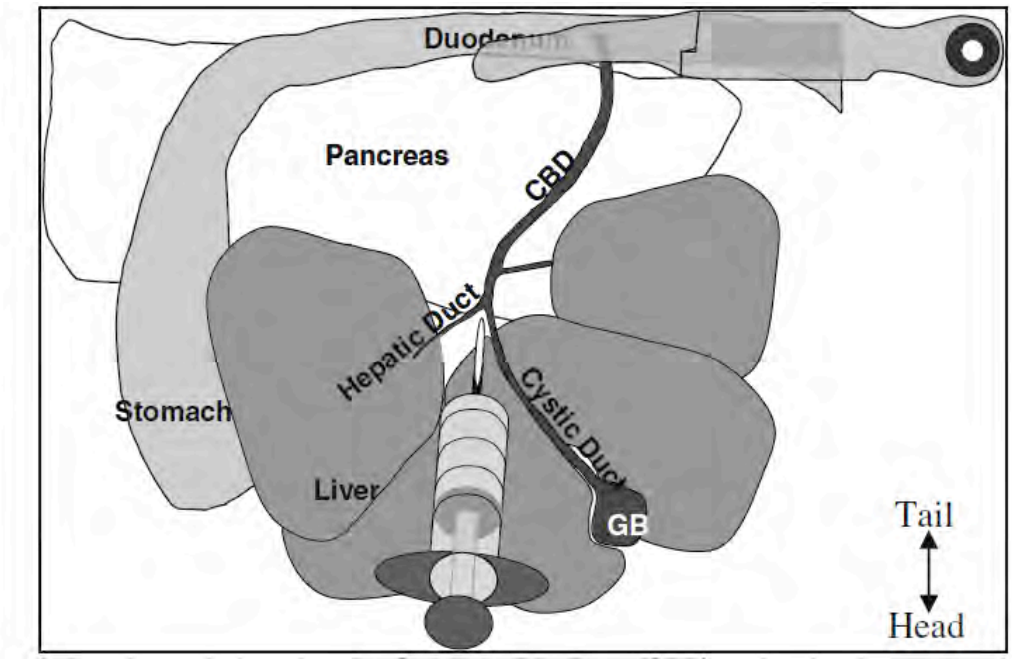


**Figure 22: Inoculation site to inflate pancreas.** *Position where collagenase has to be injected between hepatic duct and cystic duct. The common bile duct at the duodenum has to be clamped to inoculate all the liquid inside the pancreas and inflate it. Extracted from Carter et al. (2009). Figure abbreviations: CBD, common bile duct; GB, gallbladder.*

The main objective of isolating pancreatic islets is to acquire viable purified islets that can respond to stimuli *ex vivo*.

The mouse was in fasting during 2h before being sacrificed. Then, it was immobilized and an abdominal incision was made to expose the entire peritoneal cavity. The mouse's head was put as close to the surgeon as possible and the tail as far as possible. In that way, that position allowed the cannulation of the bile duct from the end of the liver, at the junction between the hepatic and cystic duct, leaving a large space to re-inject closer to the duodenum if there was any error. One clamp was placed stretching from the sternum and the other into the common bile duct where it joined with the small intestine to maintain the solution inside the tissue of interest. The pancreas

contains a system of ducts that allows the flow of pancreatic enzymes, and they were where the collagenase was diffused through the bile duct *(Figure 22)*.

4 ml of 0.8mg/ml collagenase (Collagenase from Clostridium histolyticum C6885-500mg - SIGMA) were suctioned in a 5 or 10ml syringe. The common bile duct was cannulated from the end of the liver to the point of connection between the hepatic and cystic duct with a 30G needle. Then, 2-3 ml of collagenase were injected.

It is important to properly cannulate the entire pancreas to get the most possible islets from the head to the tail. The distribution of the pancreatic islets is not uniform throughout the pancreas; most of them are in the tail, which is why the pancreas should be inflated completely. If the duct is destroyed after the cannulation, another possibility is still remaining, although it is less effective. The alternative method consists in directly injecting collagenase into each of the numerous lobes of the pancreas. In this method, it is important to inject small quantities of collagenase to as many lobes as possible.

The 1-2 ml of collagenase that was left over the syringe was placed in a conical tube of 15ml to collect the pancreas. It was extracted with the help of two fine clamps, carefully trying to not drill the intestines, as they are a source of bacterial contamination. The extraction started by the area of the pancreas that was attached to the intestines, stomach and finally to the spleen.

Every pancreas was introduced into a conical tube with 1-2 ml of collagenase and put on ice until the procedure was done in all the experimental animals. Then, the digestion of the entire pancreas started when all the tubes were incubated at 37ºC for 7 minutes (the incubation time varies between 7-11 minutes according to collagenase, therefore it is advisable to test it every time that a new batch of collagenase is acquired). A mechanical digestion up and down was made with a plastic Pasteur pipette. Next, each pancreas was placed in a 50 ml clean conical tube and covered up with 40 ml with the Hanks & Wallance saline solution. After 5-10 minutes on ice, the supernatant was eliminated (where there were remains of fat and pancreas exocrine) leaving about 10 ml of liquid with the pellet. After refilling up to 40 ml with Hanks & Wallance solution, the pellet was mixed by inverting the tube a few times. About 20ml

of the mixture were poured into a transparent petri dish and the rest were left on ice. Under a magnifying glass with light and a black base, the "Hand Picked" selection of pancreatic islets started. The selected ones were deposited in a new petri dish.

The pancreatic islets were distinguished under the magnifying glass of the rest of the impurities of the mixture obtained from the extraction because they had a well-defined round shape and were more compact. As a result, they looked more white and shining under lens than the rest of the degraded tissue. [298]

## 1.18 Pancreatic islets *Ex Vivo* incubation

*Ex Vivo* incubation was performed after the pancreatic islets isolation. It was essential to work under sterile conditions in a primary culture room with sterilized materials and solutions. First, islets were washed with glucose-free Dulbecco's Modified Eagle Medium (DMEM) (Gibco by life technologies 11966-025) 5 times at 200G for 45 seconds. Then, 100 islets/well in 24 well plates or 200 islets/well in 12 well plates were incubated in DMEM.

The amount of glucose in the medium was adjusted according to every experiment. The levels considered in the bibliography as not inducing a massive secretion of insulin were between 2-4mM of glucose.[299] The islets were incubated for 1 hour in a primary culture room incubator (37ºC, 5% $CO_2$ and 21% $O_2$).

After incubation, the medium was collected, centrifuged at 800G for 5 minutes and the supernatant was collected. The supernatant was stored at 4ºC or -20ºC depending on the time until the analysis of insulin secretion.

## 1.19 Glucose intraventricular delivery in the central nervous system and osmotic pumps implantation

### *1.19.1 Preparation of osmotic pumps*

Three days before the implantation surgery, the osmotic pumps (Alzet Mini-Osmotic pump model 2006. Duration 42 days with a 0.15µl/h pumping rate) *(Figure 23A)* were filled with the solution of interest and hydrated with saline serum 0.9% (Braun).

In this case, the solutions of interest were D-(+)-glucose (Sigma-Aldrich G8270) and D-mannitol (Sigma-Aldrich M4125), which were made as saturated solutions. The saturated concentration of each molecule is: 210mg/dl mannitol and 910mg/ml glucose; therefore, 1000mg/ml of glucose and 250mg/ml of mannitol were prepared as working solutions.

It was essential to work with sterile conditions under the hood and taking care to not directly touch anything in order to maintain sterility from the beginning. The osmotic pump, the flow moderator and the brain infusion kit (Alzet Brain infusion kit 3 0008851) had to be perfectly filled with the solution of interest and carefully assembled. Finally, they were incubated at 37ºC for 60 hours in saline serum 0.9% before the surgery.

### *1.19.2 Osmotic pump implantation*

The protocol of the direct intraventricular delivery of glucose or mannitol to the mouse central nervous system was strictly followed from DeVos and Miller's paper. [300]

As a summary of the protocol, after preparing the entire surgical place with sterile conditions and materials, the mouse were asleep and maintained during the intervention with inhaled anesthesia (isoflurane). First, the mouse was placed in a flat surface immobilized by the stereotax through two ear bars and one mouth bar. Then, the osmotic pump with the cannula and the brain catheter were settled in the stereotax. Next, a little incision was made in the cranium skin in order to localize the bregma, an anatomical point located at the intersection of the coronal and the sagittal

suture *(Figure 23B)*. Later, the osmotic pump was introduced in the right flank under the back skin. And following, the stereotax with the brain catheter went down in the correct position of the cranium, 0.5mm posterior and 1.1mm laterally to the right, and the catheter was placed through the skull *(Figure 23C)* to inoculate the lateral ventricle and the IV ventricle *(Figure 23D)*. The base of the catheter was previously smeared with glue to fix the catheter to the skull permanently. Finally, the head skin was sutured, analgesics administered and the mouse was placed in a warm blanket for post-operative recovery until awake. Mice were in intensive care some days after the operation and were injected with analgesia at least during the first week.

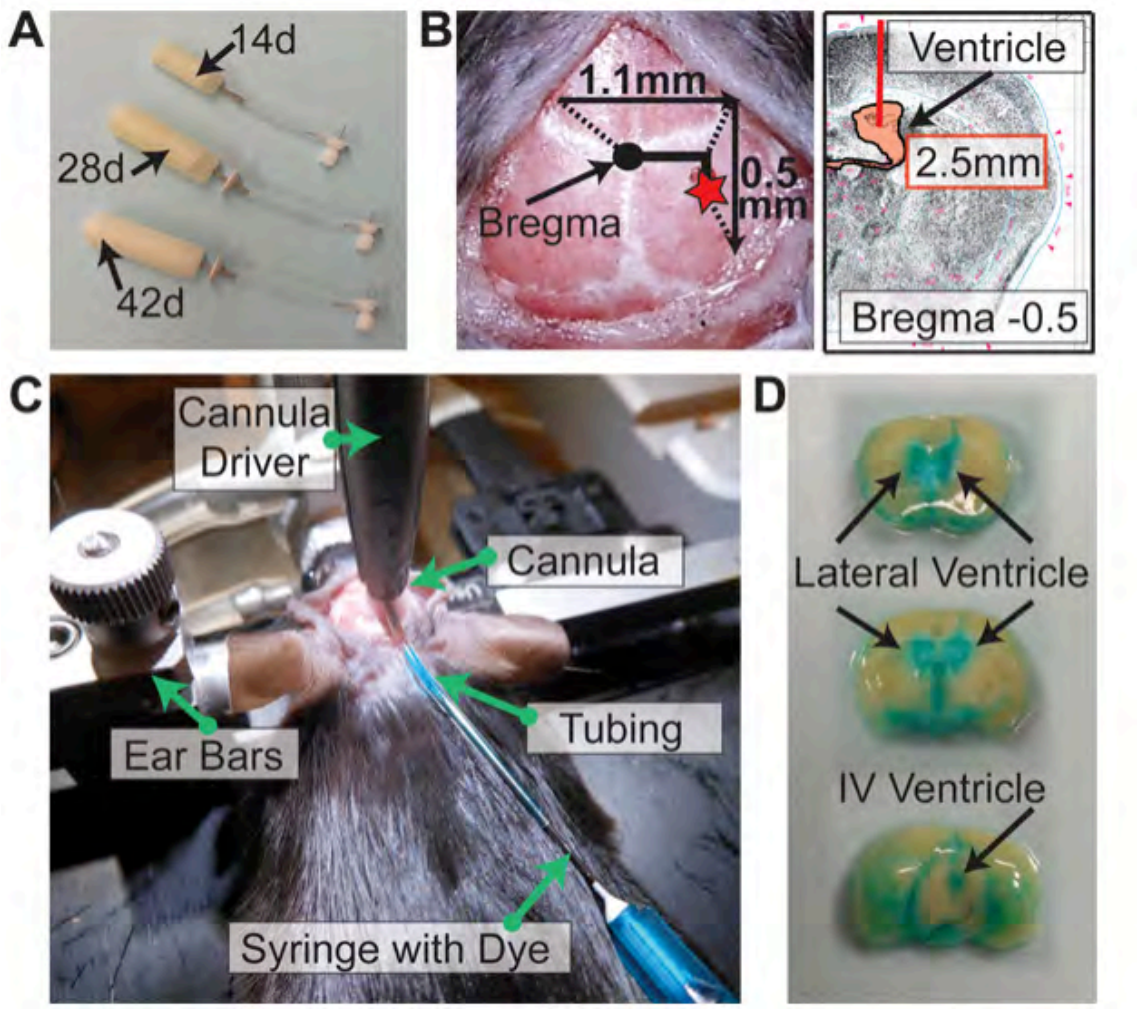


**Figure 23: Osmotic pump implantation.** ***(A)*** *Example of three different size osmotic pumps depending on their capacity of inoculation: 14 days, 28 days and 42 days. The 42 days osmotic pump, which is bind to a brain infusion kit, is the used in our experiment.* ***(B)*** *Bregma, which is an anatomical point located at the intersection of the coronal and the sagittal suture, has to be localized to move the stereotax with the brain catheter into the correct position of the cranium, 0.5mm posterior and 1.1mm laterally to the right.* ***(C)*** *Then, the catheter is placed through the skull.* ***(D)*** *Example of how lateral ventricle and the IV ventricle are inoculated with blue dye following all the previous steps accurately. Extracted from Devos et al. (2013).*

## 1.20 Ketone bodies detection

Ketone bodies are three types of molecules that are soluble in water: acetoacetate, β-hydroxybutyrate and acetone that contain a ketone group in their composition. They are produced from fatty acids in the liver in fasting periods in order to be converted into acetyl-CoA to be transformed in energy for all the body organs.

β-hydroxybutyrate assay kit was used (Sigma-Aldrich MAK041) to detect ketone bodies. β-hydroxybutyrate concentration was quantified by a coupled enzyme reaction (enzyme and substrate) that was converted to a colorimetric product, of 450nm, proportional to the amount of β-hydroxybutyrate. Therefore, after mixing the serum samples with assay buffer, enzyme and substrate, and waiting for 30 minutes at room temperature, the absorbance at 450nm was determined.

## 1.21 Hepatic glycogen detection

### *1.21.1 Liver extraction*

Glycogen detection was done in liver tissue homogenates. Thus, 100mg of liver sections were cut on dry ice and placed in 2ml tubes with stainless steel beads (Qiagen 69989) and 500µl of homogenization buffer (6g Tris (50mM)/HCl pH 7.5 + 1.86g EDTA (5mM) + 0.15g DTT (1mM)+10µl/ml PMSF + 5µl/ml PIC + 5µl/ml $Na_3VO_4$) and placed in the TissueLyser LT (Qiagen) machine 1 minute at 50Hz to effectively homogenize the samples. Following, the plastic tubes were centrifuged 10 minutes at maximum speed at 4ºC and the supernatant was collected in a new tube.

### *1.21.2 Glycogen obtainment from liver homogenates*

Hepatic glycogen detection was done from liver homogenates. 100µl of liver homogenate with 100µl of Tris 50mM buffer and 100µl of perchloric acid 0.2M were introduced in a tube and centrifuged at 10000rpm for 10 minutes. The supernatant was transferred to a new tube with 300µl of ethanol 90% at -20ºC overnight.

The day after, the tubes were centrifuged 5 minutes at 10000rpm and the ethanol was removed, keeping the glycogen pellet attached to the bottom of the tube. Then the samples were dried at room temperature.

#### *1.21.3 Hepatic glycogen quantification*

In the dried glycogen pellet, 1ml of HCl 2M was added; it was mechanically resuspended and transferred to a 15ml tube where 1ml of HCl 2M was added. Then, all samples remained 20 minutes at 100ºC in the thermoblock (Eppendorf). During the incubation, a glucose standard curve was prepared (0.4mg/ml, 0.3mg/ml, 0.2mg/ml. 0.1mg/ml. 0mg/ml) in HCl 2M. Next, 1ml of NaOH 4M and 1ml of 1% DNS (dissolved in NaOH 2M) were added to the experimental and standard curve samples. Finally, the tubes were boiled at 100ºC for 5 minutes. Once they were cold, their absorbance was read at 546nm to detect the hepatic glycogen quantity.

## 1.22 $^{3}$H glucose detection

In order to determine the glucose uptake by tissues during a glucose tolerance test and after four hours of fasting, a $^{3}$H glucose detection experiment was performed.

The same protocol used for the glucose tolerance test was performed, but in every time point a sample of blood was extracted from mice cheeks. Furthermore, normal glucose was mixed with radioactive glucose ($^{3}$H glucose - Perkin.Elmer #NET328001MC – concentration: 1µCi/µl). The mix was prepared for every mouse before being injected depending on its weight (dose: 20µCi/mouse at 3g/Kg of glucose).

When the glucose tolerance test was finished, the collection of 100mg of every tissue of interest (heart, brain, lung, thyroid gland, spleen, uterus, prostate, pancreas, muscle, kidney, liver and serum) was performed. The tissue was homogenized with 1ml of water in 2ml tubes with stainless steel beads (Qiagen 69989) and it was inserted into the TissueLyser LT (Qiagen) machine, from 1 to 3 cycles (depending on the tissue), 1 minute at 50Hz to homogenize the samples. Next, 800µl of the supernatant were transferred to a new tube with 800µl of 7% $HClO_4$ (Sigma-Aldrich 311421). The samples were then cleared by centrifugation at maximum speed for 5 minutes and 500µl of the supernatant was neutralized for 30 minutes with 2.2mol/l $KHCO_2$ (Sigma-Aldrich

37205) solution. The precipitate was removed by centrifugation at maximum speed for 5 minutes. 250µl of supernatant mixed with 10ml of scintillation liquid were used to determine total $^{3}H$ radioactivity. [301] The radioactivity amount was measured with the scintillation counter (Packard 1900 TR) machine.

# 2. *In vitro* experimental model

## 2.1 DNA amplification: plasmids and bacterial work

Plasmid to knockdown PTEN was designed in the laboratory (protocol explained in the following sections), while plasmid to knockdown VDR was purchased from Open Biosystems (clone ID: TRCN0000019507) and both cloned into the lentiviral vector, MISSION pLKO.1-puro Non-Mammalian shRNA Control Plasmid DNA (shC002) (Sigma-Aldrich).

### *2.1.1 Primer Annealing*

Primers of interest were ordered in a commercial company (Sigma-Aldrich) with a stock concentration of 100µM. The working concentration was 3µg/µl, so we used 1µl of initial primer, 1µl of forward primer and 48µl of annealing buffer (150mM NaCl and 50mM Tris pH=7.6) to perform the primer annealing and obtain the insert *(Table 4)*. The PTEN target sequence was GCAGTATAGAGCGTGCAGATA.

| Temperature | Time |
|---|---|
| 90ºC | 4 minutes |
| 70ºC | 10 minutes |
| 60ºC | 20 minutes |
| 50ºC | 30 minutes |
| 37ºC | 45 minutes |
| 10ºC | 60 minutes |

**Table 4: Primer annealing.** *Primer annealing protocol used in the thermocycler.*

### *2.1.2 Vector preparation*

The empty vector used for shPTEN was fsv-si (a modification of fsp-si). In order to open the vector and to introduce the insert, fsv-si was digested with BamHI (Takara) at

position 2891bp and AgeI (BioLabs) at position 2867bp after being incubated one hour at 37ºC.

5µl of GeneRuler 1kb DNA ladder (thermoscientific SM0311) were charged as a standard in the first well of a 0.8% agarose gel. 10µl of each vector with 2µl of 6x loading dye solution (thermoscientific R0611) were introduced into the other wells. The electrophoresis gel was run for 40 minutes at 120V. Finally, bands that represented the vector were selected under UV light, cut and placed in a new tube.

### *2.1.3 Extraction of the band*

The extraction of the band was performed with the QIAquick gel extraction kit (50) 28704. The vector band was placed in a tube with 300µl of solubilization buffer QG and incubated 10 minutes at 50ºC to dissolve agarose. After incubation, products of reaction should be the same color as QG Buffer (yellow). If not, 10µl of 3M sodium acetate pH=5 were incorporated. Later, 100µl of isopropanol were added and transferred to a column 1 minute and centrifuged at 10000rpm (liquid was obtained from the down part of the tube). 500µl of buffer QG were added into the column and a second centrifugation of 1 minute at 10000rpm was performed to obtain the remaining DNA from the column. 700µl of PE buffer were introduced and centrifuged 1 minute at 10000rpm (the liquid obtained in the tube was discarded). The digested DNA vector was eluted from the column with 30µl of elution buffer, which was placed in a clean tube and centrifuged 1 minute at 10000rpm. Finally, a sample of the digested vector was run 40 minutes at 100V into a 0.8% agarose gel with SYBR green (Invitrogen S7563). An estimation of the concentration was made by comparing the intensity of the vector band with standards.

### *2.1.4 Ligation protocol*

For ligation process, 5ng/µl of vector were mixed with 2µl of insert, 1µl ligation buffer (10x), 1µl of ligase and adjusted volume of distillated water, which was incubated overnight at 16ºC or 2 hours at room temperature.

### *2.1.5 Transfection of bacteria*

*Escherichia coli* (*E. Coli*) (DH5α strain - invitrogen) was the bacteria used for transfection. It was essential to work under sterile conditions with the Bunsen flame. 50µl of *E. Coli* and 4µl of DNA (obtained from the ligation process) were put in a tube and kept on ice for 30 minutes. After the incubation, a thermic shock was made putting the tube at 42ºC during 30 seconds to open the bacteria pores and then placed on ice for 2 more minutes. 950µl of Lysogeny Broth (LB) medium was add in every tube, incubated at 37ºC, 1 hour at 300rpm and centrifuged at 8000rpm during 3 minutes. The supernatant was leaving around 50µl of liquid in the tube with the bacterial pellet. The pellet was mixed gently with a pipet and the content transferred to a Petri dish with solid LB medium and the appropriate antibody for selection of each vector. The fsv-si vector was incubated with 100µg/ml of Ampicillin (Gibco 11593027) and the shC002 100µg/ml with Carbenicillin (Gibco 10177012). Plates were incubated overnight at 37ºC without agitation.

The next morning, individual colonies were taken with a pipette, diluted into a 15ml tube with 3ml of LB media supplemented with 3µl of Ampicillin or Carbenicillin and incubated 8 hours at 37ºC at 200rpm to prepare the preculture.

### *2.1.6 Positive colonies control by PCR*

The individual colony selected was diluted with 10µl of water and used as the DNA sample to do a positive colony screening by PCR *(Table 5) (Table 6)*. Electrophoresis of PCR products was performed in a 2% agarose gel with SYBR green. Positive colonies had heavier bands than the negative ones due to the insert of some base pairs.

| | Volume per sample (µl) |
|---|---|
| Buffer 10x | 2.5 |
| MilliQ water | 17 |
| $MgCl_2$ | 1 |
| dNTPs | 0.5 |
| Primer (Forward) | 1 |
| Primer (Reverse) | 1 |
| Taq Polymerase | 1 |
| DNA | 1 |
| **Final volume** | 25 |

**Table 5: PCR mix used to detect positive colonies.** *Every raw represents all PCR mix components needed for each gene. Table abbreviations: DNA, deoxyribonucleic acid; dNTPs, deoxynucleotide triphosphate; $MgCl_2$, magnesium chloride.*

| Temperature | Time | Cycles |
|---|---|---|
| 94ºC | 10 minutes | 1 |
| 94ºC | 30 seconds | 40 |
| 55ºC | 30 seconds | |
| 72ºC | 30 seconds | |
| 72ºC | 10 minutes | 1 |
| 4ºC | ∞ | |

**Table 6: Positive colony screening by PCR.** *Protocol set up into the thermocycler.*

### *2.1.7 Bacterial culture*

At the end of the day, the preculture of bacteria that had been growing over the day in a 10ml tube were transferred to a big flask (100µl of preculture, 100µl of antibiotic and 100ml of LB medium) to be incubated overnight at 37ºC at 200rpm.

The next morning, the content from the culture was transferred to 50ml tubes and centrifuged at 4000rpm for 30min. The supernatant was discarded and DNA was extracted from the pellet.

#### *2.1.8 Plasmid DNA isolation from E. coli culture*

The GenElute plasmid maxiprep kit (Sigma-Aldrich NA0300) was used to isolate plasmid DNA from recombinant *E. coli* culture. 12ml of solution were introduced per 150ml of overnight culture cell pellet and gently mixed. 12ml of lysis solution were added and gently inverted for 5 minutes. 12ml of neutralization solution were added to the lysed cells and gently mixed to prepare the lysate. Immediately after, the mix was added to the barrel of the filtered syringe and let for 5 minutes. The binding column was placed into a collection tube and 12ml of column preparation solution were added. Then, it was centrifuged at 3000rcf during 2 minutes and the flow-through was discarded. Following, half of the lysate was pushed out trough the filter syringe over the column and centrifuged at 3000rcf for 2 minutes. Then, the process was repeated with the other half of the lysate discarding the flow-through. The columns were washed twice to remove contaminants and finally, the purified plasmid DNA was eluted. DNA amount was quantified with the NanoDrop spectrophotometer and froze at -20ºC.

## 2.2 Cell culture

#### *2.2.1 HK-2 cell line and 293T cells*

Human kidney-2 (HK-2) cells are an immortalized cell line from proximal tubule cells of adult human kidney, used as a kidney model. They have a characteristic epithelial microscopic phenotype in culture, growing adhered to the substrate and between them, forming monolayer, which is an indication of the correct state of cells. [302]

293T cell line is a highly transfectable cell type that derives from HEK 293 cells commonly used in genetics engineering to product lentiviruses due to its easy-transfection characteristic.

### *2.2.2 Handling and procedure*

Cell lines handling was performed under sterile conditions in the hood placed in a mycoplasma-free culture room. Petri dishes (Falcon) were never opened out of the hood to maintain sterility. Growth culture medium *(Table 7)(Table 8)* was changed every three days and when cells were around 80% of confluence they were diluted 1/10 and transferred to a new plate. Culture medium was aspirated and a PBS1x wash was done to completely remove the serum.

Intercellular and cell-plate junctions were digested using 1ml of trypsin for 5 minutes in the incubator (37ºC, 5% $CO_2$). After five minutes, 2ml of culture medium was added directly into the plate to inactivate the trypsin. The cell suspension was collected and centrifuged 3 minutes at 1000rpm. The supernatant was aspirated and the pellet resuspended with the medium. Then, the Neubauer chamber was used to count the number of cells in suspension. Once cell density was known, the cells were seeded into an adequate culture plate.

| Components | Final concentration | Quantity for 500ml |
|---|---|---|
| DMEM (Gibco 11880-028) | 50% | 250ml |
| HAMF12 (Gibco 31765-027) | 50% | 250ml |
| HEPES (Gibco 15630-056) | 20mM | 10ml |
| L-Glutamine (Gibco 25030-081) | 2mM | 5ml |
| D-Glucose anhidre (Sigma-Aldrich G7021) | 56g/l | 1.12g |
| Transferrin (Sigma-Aldrich T8158) | 5µg/ml | 500µl |
| Insulin (Sigma-Aldrich I6634) | 5µg/ml | 250µl |
| Dexamethasone (Sigma-Aldrich D8893) | $5 \cdot 10^{-8}$M | 25µl |
| $T_3$ (Sigma-Aldrich T5516) | $10^{-9}$M | 5µl |
| EGF (Sigma-Aldrich E4127) | 5ng/ml | 25µl |
| Selenium (Sigma-Aldrich S9133) | 60nM | 100µl |
| FBS (Gibco) | 2% | 10ml |
| Streptomycin/Puromycin (Gibco) | 1% | 5ml |

**Table 7: HK-2 cells growth medium components.** *Final concentration and total amount of the HK-2 cells growth medium components to prepare 500ml of medium. Table abbreviations: DMEM, Dulbecco's modified eagle medium; EGF, epidermal growth factor; FBS, fetal bovine serum; HAMF12, F-12 nutrient medium; HEPES, 4-(2-hydroxyethyl)-1-piperazineethanesulfonic acid; $T_3$, 3,3',5-Triiodo-L-thyronine sodium salt.*

| Components | Quantity for 500ml |
|---|---|
| DMEM (Gibco 41965, 4.5g/l glucose 2mM glutamine) | 500ml |
| Fetal Bovine Serum (FBS) (Gibco) | 50ml |
| Sodium Piruvate (Gibco) | 5ml |
| NEAA (Gibco) | 5ml |
| Streptomycin/Puromycin (Gibco) | 5ml |

**Table 8: 293T cells growth medium.** *Total amount of 293T cells growth medium components to prepare 500ml of medium. Table abbreviations: DMEM, Dulbecco's modified eagle medium; FBS, fetal bovine serum; NEAA, non-essential amino acid.*

| Components | Quantity for 500ml |
|---|---|
| DMEM (Gibco 41965, 4.5g/l glucose 2mM glutamine) | 500ml |
| Sodium Piruvate (Gibco) | 5ml |
| NEAA (Gibco) | 5ml |

**Table 9: 293T cells deprivation medium.** *Total amount of 293T cells growth medium components to prepare 500ml of medium. Table abbreviations: DMEM, Dulbecco's modified eagle medium; NEAA, non-essential amino acid.*

### *2.2.3 Freezing and defrosting cells*

The medium was changed 24 hours before freezing the cells. Then, the culture medium was aspirated and washed with PBS1x. Cell trypsinization and centrifugation at 1500rpm for 3 minutes was performed. Next, the supernatant was aspirated, the pellet resuspended with freezing medium (90% FBS + 10% DMSO). Finally the cells were frozen 24h at -80ºC and then, for a long period at -196ºC in liquid nitrogen.

To defrost cells, the cell vial was directly thawed at 37ºC for 2 minutes. Once they were defrosted, the cells were transferred to a 15ml tube with 10ml of PBS1x and centrifuged 3 minutes at 1500rpm. Finally, they were resuspended with the appropriate growth medium, seeded in culture plates and incubated in cell incubators.

### *2.2.4 Production of lentiviruses in 293T cell line*

293T cells were used to produce lentiviruses. Plates were coated with 0.1% of gelatin for 20 minutes at 37ºC. Then, $2 \cdot 10^6$ 293T cells were seed the day before transfection in a safety cabinet class II Bio II.

On the day of transfection, when the cells were at 60% of confluence, the growth medium *(Table 8)* was carefully changed to 8ml of deprivation medium *(Table 9)* and incubated 2 hours.

In this study, the amount of plasmid DNA of interest was calculated following this protocol: 40µg of DNA were transfected (20µg of interest plasmid + 13µg of lentiviral packing plasmid + 7µg of envelope expressing plasmid) *(Table 10)* with 200µl of Polyethylenimine (PEI) (5µl PEI/µg DNA) and 800µl NaCl 150mM.

| Plasmid | Amount of plasmid DNA |
|---|---|
| fsv-si | 20µg |
| shPTEN<br>(Made in fsv-si plasmid) | 20µg |
| shC002<br>(Sigma-Aldrich SHC016-1EA) | 20µg |
| shVDR<br>(Made in shC002 plasmid) | 20µg |
| psPAX2 (Δ89.1)<br>(addgene #12260)<br>(Lentiviral packing plasmid) | 13µg |
| pMD2G (ENV)<br>(addgene #12259)<br>(Envelope expressing plasmid) | 7µg |

**Table 10: Amount of plasmid DNA.** First column represents each plasmid used, the four plasmids of interest, fsv-si, shPTEN, shC002, shVDR and the two plasmids needed to develop lentiviruses, psPAX2 (Δ89.1) and pMD2G (ENV). Second column represents the amount of plasmid DNA required.

The calculated amount of plasmid DNA of interest, lentiviral packing plasmid and envelope expressing plasmid were gently added into a 10ml sterile tube. An adequate amount (until 1ml/plate) of NaCl 150mM was added into the tube to dilute DNA. 200µl of PEI were diluted in 800µl of NaCl 150mM. PEI dilution was placed on to the DNA, mixed and let 10 minutes at room temperature in the hood. The mix was added dropwise to each plate until reaching 2ml/plate. After 3 hours at 37ºC, the transfection medium was aspirated and 10ml of complete growth medium for 293T cells was added. 72 hours later, 293T cells were transfected and, under magnification, big vacuoles were seen as a sign that the transfection worked correctly. Cell supernatant was collected from the plate to a 50ml tube and centrifuged at 3000rpm for 10 minutes to precipitate 293T cells. The supernatant was carefully collected because viruses are found in it.

Viruses could be used directly, only filtered in a 0.45µm filter (Sartorius); or they could be concentrated. Concentration of viruses was done by placing the filtered supernatant into the 50ml tube and centrifuged at 4000rpm for 1 hour at 4ºC. The liquid kept in a special small compartment of the filter was collected. Every 10ml of virus supernatant, after centrifugation in the filter compartment, should become 100µl of concentrated viruses. Both, non-concentrated and concentrated viruses were kept at -80ºC.

### *2.2.5 Infection of target cells with lentiviruses*

Four plasmids of interest were used to model in the HK-2 cells the four mice genotypes of this study: the two empty plasmids (fsv-si and shC002) and the two plasmids with the silencing sequence of interest (shPTEN made in the fsv-si plasmid and shVDR made in the shC002).

$3 \cdot 10^5$cells/well were seeded in two wells of a 24-well-plate. The next day, 500µl/ well of fresh growth medium was replaced and 7µl/well of the shC002 and shVDR concentrated viruses were added. The cells with viruses were incubated overnight at 37ºC. The next morning, the medium was aspirated and fresh growth medium was added for 48 hours.

shC002 and shVDR plasmids contained puromycin resistance, thus, 48 hours after infection, the selection with 1µg/ml puromycin (Gibco 10mg/ml A11138-03) was started. Cells were split upon reaching confluence. Wells or plates were re-fed every three days and kept under puromycin selection during 10 days. After selection, cells were maintained in their usual growth medium plus 0.5µg/ml puromycin.

After the puromycin selection, $3 \cdot 10^5$cells/well were seeded in four wells of a 24-well-plate (two wells with HK-2 maintenance cells, one well with shC002 and one well with shVDR). The next afternoon, 3µl/well of the fsv and shPTEN concentrated viruses (one well of HK-2 maintenance cells infected with fsv, one well of HK-2 maintenance cells infected with shPTEN, one well of shVDR cells infected with shPTEN and one well of shC002 cells infected with fsv) were added. The next morning, the medium was aspirated and fresh growth medium was added. After 48 hours, cells infected with fsv or shPTEN viruses were green because the plasmid contained the green fluorescence protein (GFP).

Finally, six groups of cells were obtained, 3 controls (fsv, shC002 and fsv-shC002), 2 single infected (shPTEN and shVDR) and 1 double infected (shPTEN-shVDR). In order to simplify work only one control was selected: fsv-shC002.

# 3. Biochemistry and molecular biology techniques

## *3.1 mRNA detection by quantitative reverse transcription PCR (qRT-PCR)*

The presence of mRNA in a tissue or a cell gives the information about the amount of gene expression of specific proteins, and thus their activity. Through the qRT-PCR the relative constitutive genes called as "housekeeping" genes, are used to quantify the gene expression of certain genes using specific primers. Quantification of gene expression is done through a process that includes three steps: RNA extraction, cDNA transcription and amplification.

### 3.1.1 RNA extraction with Trizol from cells

1ml of trizol was added in a p100 plate or 500µl in a 6-well-plate to extract RNA from cells. Cell monolayer was detached with a small spatula. A mucous substance of trizol and disrupted cells was obtained. The substance was transferred to a new microcentrifuge tube. Then, 200µl of chloroform were added, mixed, let stand for 3 minutes at room temperature and centrifuged 15 minutes at maximum speed. Approximately 400µl of supernatant was removed and transferred to a new tube. Finally, 500µl of isopropanol were added, left at room temperature for 10 minutes and centrifuged for 10 minutes at 4ºC at maximum speed. 1 ml of ethanol 75% was added and vortexed. Finally, samples were centrifuged for 5 minutes at 4ºC at 9400 rpm, dried for 15 minutes and 50µl of nuclease-free water (Sigma-Aldrich 3098) were added. When the pellet was completely dissolved, the mRNA amount was quantified by NanoDrop spectrophotometer and froze at -80ºC.

### 3.1.2 RNA extraction with Trizol from tissues

TissueLyser machine with stainless steel beads and 300µl of trizol (Sigma-Aldrich T9424) was used to disrupt the tissue (3 cycles of 30 seconds at 50 Hz) and removed mRNA from cellular components, especially the genetic material because it could interfere with the results. Then, 700µl of trizol were added per sample, transferred to a new tube and let at room temperature for 5 minutes.

Following steps of the protocol were exactly the same as explained before for cells (chloroform, isopropanol and 75% ethanol).

#### 3.1.3 Liver mRNA extraction with RNA isolation kit

Liver mRNA was extracted with a commercial RNA isolation kit (NucleoSpin RNA Macherey-Nagel 740955).

20mg of liver tissue and 350µl of Buffer RA1 with 1% Triton-X-100 and 3.5µl β-mercaptoethanol were homogenized using the TissueLyser disruptor (2 cycles of 60 seconds at 50 Hz). Then, the homogenized tissue was digested with 10µl of Proteinase K (Sigma-Aldrich) and 590µl of RNase-free water for 10 minutes at room temperature and 10 minutes at 55ºC. Then, the samples were centrifuged at 10000rcf for 3 minutes. Next, RNA binding conditions were adjusted by adding 0.5 volumes of 100% ethanol (around 475µl). 700µl of the mixture were added into the RNA column and centrifuged at 8000rcf for 30 seconds. Later, the silica membrane was desalted adding 350µl of membrane desalting buffer into the column and centrifuged 1 minute at 11000rcf. DNA was digested with 95µl of DNase reaction mixture for 15 minutes at room temperature. Afterwards, the silica membrane was washed and dried three times and RNA was eluted with 60µl of RNase-free water by centrifugation 1 minute at 11000rcf. Finally, mRNA sample was obtained.

#### 3.1.4 Reverse transcription

As mRNA is very unstable and easily degraded, it has to be retrotranscribed to convert it to complementary DNA (cDNA), which is much more stable and can be amplified by PCR.

Before starting with the reverse transcription, mRNA quantification was used to achieve similar concentrations (1µg/µl) between different samples, and to minimize the variation of values in the final qRT-PCR results.

PCR reaction was made by 9.5µl of 1µg/µl mRNA sample and 10.5µl of retrotranscription mixture (2µl Reaction Buffer 10x, 4µl MgCL2 25mM, 2µl dNTPs, 2µl Random Hexamers and 0.5µl AMV Reverse Transcriptase). Finally, the mRNA mixture

was ready to be retrotranscribed to cDNA in the thermocycler (TC-412® Techne) *(Table 11)*.

| Temperature | Time | Cycles |
|---|---|---|
| 25ºC | 10 minutes | 1 |
| 42ºC | 1 hour | |
| 99ºC | 5 minutes | |
| 4ºC | ∞ | |

**Table 11: Reverse transcription protocol.** *Protocol introduced into the thermocycler to perform the reverse transcription.*

### 3.1.5 Quantitative RT-PCR

qRT-PCR was a technique derived from the PCR and was used to amplify and quantify a DNA sequence at real time. In this study, the Taqman Real time PCR method for gene analysis was used. In the reaction 1µl of cDNA sample was added per 5µl of Master Mix (Applied Biosystem), 4.5µl of water miliQ and 0.5 µl of the forward and reverse primers *(Table 13)*. Before PCR reaction, the 96-well plate, where the PCR products were prepared, was centrifuged at 1000 rpm for 1 minute and placed in the specific qRT-PCR thermocycler (CFX96TM Touch Real-Time PCR, Bio rad) *(Table 12)*.

| Temperature | Time | Cycles |
|---|---|---|
| 50ºC | 2 minutes | 1 |
| 95ºC | 10 minutes | 1 |
| 95ºC | 15 seconds | 44 |
| 60ºC | 1 minute | |

**Table 12: qRT-PCR protocol.** *Protocol introduced into the thermocycler to amplify and quantify a DNA sequence at real time.*

The expression levels of the gene of interest are calculated relative to a housekeeping gene. This calculation is made from the expression cycle in which the device detects fluorescence signal, called cycle threshold (Ct). Ct is a value that reflects the amount of cDNA present in the sample and from which the expression level of the target gene can be calculated. The Ct, as all fluorescence values, can be affected by the characteristics of the detector equipment. Therefore, it is important to normalize the values to compare different plates within the same experiment.

The results were obtained through the software Bio-Rad CFX Manager in Ct. The relative amount of each gene was calculated from the formula:

$$\Delta Ct = Ct \text{ target gene} - Ct \text{ housekeeping gene}$$

$$\Delta(\Delta Ct) = \Delta Ct \text{ sample} - \Delta Ct \text{ control}$$

(Being the mRNA relative concentration compared to control: $2^{-\Delta(\Delta Ct)}$)

| Gene | Sequences | bp | ID |
|---|---|---|---|
| **Ppia** | FWD: AGACTGAATGGCTGGATGG | 128 | NM_008907.2 |
| | REV: GTCGGAAATGGTGATCTTCTTG | | |
| **Tbp** | FWD: AAA ATG GTG TGC ACA GGA GCC | 141 | NM_013684.3 |
| | REV: CAC ATC ACA GCT CCC CAC CAT | | |
| **mHMGCS2** | FWD: AGACTCCCGGAGACGCATGT | 239 | NM_008256.4 |
| | REV: GTTTGGGTAGCAGCTCGGCTCA | | |
| **mFoxa2** | FWD: AGTATGCTGGGAGCCGTGAAG | 218 | NM_001291065.1 |
| | REV: CCAGCGCCCACATAGGAT | | NM_010446.3 |
| **mPEPCK** | FWD: CCAGTGCCCCATTATTGAC | 249 | NM_011044.3 |
| | REV: CCGAAGTTGTAGCCGAAGAA | | |
| **mG6PC** | FWD: ACTTTCCCCACCAGGTCGT | 169 | NM_008061.4 |
| | REV: ACCCCTAGCCCTTTTAGTAGCA | | |
| **mPGC1a** | FWD: GATCACGTTCAAGATCGCCCTAC | 178 | NM_008904.2 |
| | REV: TAAATCACACGGCGCTCTTC | | |
| **mPPARa1** | FWD: ATTTGGGCGTATCTCACCG | 248 | NM_011144.6 |
| | REV: GGACTTTCCAGGTCATCTGC | | |
| **mCPT1** | FWD: ACATCGTGAGTGGCGTCCT | 171 | NM_013495.2 |
| | REV: GACCCGAGAAGACCTTGACCATA | | |
| **mAcox1** | FWD: TAACTTCCTCACTCGAAGCCA | 283 | NM_015729.3 |
| | REV: AGTTCCATGACCCATCTCTGTC | | |
| **mGLUT2** | FWD: TTGTCATCGCCCTCTGCT | 228 | NM_031197.2 |
| | REV: CACTCTCTGAAGACGCCAGGAA | | |
| **mANGPTL8** | FWD: GCCTGTCGGAGATTCAGGTG | 225 | NM_001080940.1 |
| | REV: GGCCAGTGAGAGCCCATAAG | | |
| **mFGF21** | FWD: TGAAGCCAGGGGTCATTCAA | 203 | NM_020013.4 |
| | REV: GTTTGGGGAGTCCTTCTGAGG | | |
| **mBAAT** | FWD: TGGCTTACTGGAACTATGATG | 188 | NM_007519.3 |
| | REV: GGCTCTTATTTGTTTTAGGTTA | | |
| **mCEBPa** | FWD: GTGGAGACGCAACAGAAGGT | 136 | NM_001287514.1 |
| | REV: CCTTGACCAAGGAGCTCTCA | | NM_007678.3 |
| **SGLT1** | Mm00451203_m1 (Applied Biosystems) | 109 | NM_019810.4 |
| | Hs01573790_m1 (Applied Biosystems) | 78 | NM_000343.3 |
| **SLGT2** | Mm00453831_m1 (Applied Biosystems) | 79 | NM_133254.3 |
| | Hs00894642_m1 (Applied Biosystems) | 75 | NM_003041.3 |
| **GLUT1** | Mm01192270_m1 (Applied Biosystems) | 75 | NM_011400.3 |
| | Hs00892681_m1 (Applied Biosystems) | 76 | NM_006516.2 |
| **GLUT2** | Mm00446229_m1 (Applied Biosystems) | 61 | NM_031197.2 |
| | Hs01096908_m1 (Applied Biosystems) | 65 | NM_000340.1 |

**Table 13: Primer sequences used for qRT-PCR.** *Genes and sequences of interest with their length and commercial identity reference. Table abbreviations: GLUT1, glucose transporter 1; GLUT2, glucose transporter 2; mAcox1, mouse acyl-CoA oxidase 1; mANGPTL8, mouse angiopoietin-like protein 8; mBAAT, mouse bile acid CoA:amino acid N-acyltransferase; mCEBPa, mouse CCAAT/enhancer-binding protein alpha; mCPT1, mouse carnitine palmitoyl transferase 1; mFGF21, mouse fibroblast growth factor 21; mFoxa2, mouse forkhead box A2; mG6PC, mouse glucose-6-phosphatase catalytic subunit; mGLUT2, mouse glucose transporter 2; mHMGCS2, mouse hydroxymethylglutaryl-CoA synthase 2; mPEPCK, mouse phosphoenolpyruvate carboxykinase; mPGC1a, mouse proliferator-activated receptor gamma coactivator 1 alpha; mPPARa1, peroxisome proliferator-activated receptor A1; Ppia, Peptidylprolyl Isomerase A; SGLT1, sodium-glucose transporter 1; SGLT2, sodium-glucose transporter 2; Tbp, TATA-box binding protein.*

## *3.2 Western Blot analysis: protein level detection*

Western Blot is an analytical technique that is widely used to identify a target protein in a mixture of complex proteins due to the specificity of antigen-antibody interaction. The method is based on the construction of an antibody-protein complex through the specific binding of antibodies to proteins immobilized on a membrane and in the detection of the bound antibody.

### 3.2.1 Protein extraction from cells

Cell medium was aspirated and cells were cleaned with PBS1x. 200µl/well of lysis buffer (Tris pH=7.5 20mM, 2% SDS) were needed to extract total protein from cells. Cell monolayer was detached with the help of a small spatula to scratch the bottom of the plate and a mucous substance was obtained. The pellet was transferred into microcentrifuge tubes, sonicated to completely disrupt the cell content and centrifuged 5 minutes at 10000rpm at 4ºC.

### 3.2.2 Protein extraction from tissues

The organs were cut into small portions with the help of a scalpel, introduced into 2ml tubes and placed to the TissueLyser with stainless steel beads and 300µl of lysis buffer (Tris pH=7.5 20mM, NaCl 120mM, Nonidet P-40 Igepal CA-630 0.5%, NaF 100mM, 10µl/ml PMSF 0.1M, 5µl/ml PIC; 5µl/ml Na3VO4 0.2M) during 1 minute at 50Hz to homogenize the tissues (depending on the hardness of the organ, the cycles and time might vary). Then, the tubes were kept on ice for 5 minutes and centrifuged at maximum speed for 15 minutes at 4ºC. The protein supernatant was collected in new tubes and stored at -20º.

### 3.2.3 Protein quantification

The amount of total protein present in each sample is quantified according to the Lowry Protein Assay protocol (Bio-Rad). This method is based on two complementary reactions that will cause changes in the absorbance of the reagents. A standard curve was obtained according to the absorbance obtained in the bovine serum albumin (BSA) (Sigma-Aldrich A2058) standard solution (0, 0.5, 1, 2, 4 and 8µg/µl). Protein

concentration was calculated using the BSA standard curve. This method is appropriate for protein concentrations between 0.01-1.0 mg/mL.

25µl/well of the mixture of reactive A and reactive S (1ml A + 20µl S), 5µl of each standard or protein sample and 200µl/well of reagent B were added in a 96-well-plate. After 15 minutes of incubation, the absorbance was read at 595nm in a plate spectrophotometer (Thermo LabsSystems Multisckan Ascent).

#### 3.2.4 Protein samples preparation

20µg of protein were prepared per condition according to the concentration of each sample previously calculated. Loading buffer 5x (LB 5x) was added to a 1:4 sample/buffer ratio respectively (10% SDS, 50% Glycerol, 25% β-mercaptoethanol, 0.015% blue Bromophenol and 62.5mM Tris-HCl pH=6.8). The final volume of all the samples was adjusted with lysis protein buffer to load the same volume of each sample. The protein preparations were boiled at 95ºC for 5 minutes to denaturalize the proteins.

#### 3.2.5 Polyacrylamide gel

The concentration of the polyacrylamide gel was chosen depending on the protein weight. Each gel was made of two parts, the separation gel in the lower part and the concentration gel in the upper part. The higher proportion of acrylamide, the smaller are the pores and, therefore, the smaller will be the proteins that can cross. Concentration gel was the part where the samples were loaded and was added when the separation gel was polymerized, remaining in the upper part. Before polymerizing, a 15-wells mini-protean comb (Bio-Rad) was added to the gel to make the wells.

#### 3.2.6 Monodimentional electrophoresis

The proteins of each sample were separated by molecular weight by electrophoresis through the Mini-Protean 3 (Bio-Rad) system with running buffer 1x made from running buffer 10x (TRIS 30.3 g/l, SDS 10 g/l, 144.1 g/l glycine) in 1l of water. The protein samples were loaded into the gel wells, and 5µl of the PageRuler ™ Prestained

Protein Ladder (Thermo-Fisher) molecular weight marker were loaded in the first well. The proteins were run for 2 hours at 100 V.

#### 3.2.7 Wet transference

Proteins were transferred from the gel to a polyinvinyldene diflororide (PVDF) membrane (Immobilon-P) of 0.45µm pores and a size of 8.5cm x 5.5cm. Previously, the membrane was activated by incubating it 1 minute in methanol, 1 minute in water and 1 minute in transfer buffer 1x (100ml of transfer buffer 10x (glycine, Tris and water), 100 ml of methanol and 800 ml of water). The gel was activated by incubating it in transfer buffer. The transference was done with the Mini-Protean 3 (Bio-Rad) system in an electrophoresis cuvette in which the transfer sandwich was prepared (sponge (Bio-Rad), 2 whatman papers (Bio-Rad), acrylamide gel, PVDF membrane, 2 whatman papers, sponge) and wet with transfer buffer 1x. An electric field of 80V for 1 hour was applied to transfer proteins to the membrane.

#### 3.2.8 Protein blocking

When the proteins were transferred to the membrane, they were blocked with milk at 5% in TBS-T 1x (50 ml TBS 20x (146.1g/l NaCl, 48.44g/l Tris pH=7.4), 1ml Tween-20 (Sigma-Aldrich) and 950 ml of distillated water) for 1 hour with shaking. Then, three washes of 10 minutes with TBS-T 1x were done to remove the excess of milk.

#### 3.2.9 Primary antibody

Proteins fixed and blocked in the membrane were incubated overnight with the specific antibody against the protein of interest at 4ºC in agitation. The antibody was prepared at the dilution indicated by the manufacturer in TBS-T 1x and 0.02% sodium azide *(Table 14)*. After incubation, the primary antibody was removed by three washes of 10 minutes to eliminate the excess of antibody and the nonspecific weakest unions.

#### 3.2.10 Secondary antibody

The secondary antibody will detect the primary antibody in case that the first one was attached to the protein in the membrane. The secondary antibody was an antibody

that reacts against the IgG of the primary antibody *(Table 14)*. The secondary antibody was prepared in 2.5% milk in TBS-T 1x and incubated on the membrane for 1 hour at room temperature in a shaker. Then, three washes of 10 minutes to eliminate the antibody excess were done.

| Protein | Company | Cat. Nº | Host | Reactivity | Dilution |
|---|---|---|---|---|---|
| **PTEN** | Cell Signaling | 9188 | Rabbit | H,M,R | 1/1000 |
| **VDR** | Santa Cruz | sc-1008 | Rabbit | H,M,R | 1/1000 |
| **pAkt** | Cell Signaling | 4060S | Rabbit | H,M,R | 1/1000 |
| **Akt** | Santa Cruz | sc-5298 | Mouse | H,M,R | 1/1000 |
| **FOXA-2** | Abcam | ab108422 | Rabbit | H,M,R | 1/1000 |
| **GAPDH** | BioLegent | 919501 | Mouse | H,M,R | 1/1000 |
| **anti-mouse IgG-HRP** | Jackson Immuno Research | 115-035-003 | Goat | Secondary antibody | 1/10.000 |
| **anti-rabbit IgG-HRP** | Cell Signaling | 7074 | Goat | Secondary antibody | 1/10.000 |

**Table 14: List of western blot primary and secondary antibodies.** *Every column is a characteristic of the proteins of interest, name, company, catalog number, antibody host, species reactivity and working dilution. Table abbreviations: Akt or PKB, protein kinase B; anti-mouse-IgG-HRP, anti-mouse immunoglobulin G horseradish peroxidase conjugated secondary antibody; anti-rabbit-IgG-HRP, anti-rabbit immunoglobulin G horseradish peroxidase conjugated secondary antibody; FOXA-2, forkhead box A2; GAPDH, glyceraldehyde-3-phosphate dehydrogenase; pAkt, phosphorylated protein kinase B; PTEN, phosphatase and tensin homolog; VDR, vitamin D receptor.*

#### 3.2.11 Chemiluminescence reaction

ECL SelectTM Western Blotting Detection Reagent developer (GE healthcare) was used to detect the secondary antibody by mixing the two reagents, 300µl of luminol solution and 300µl of peroxide-stabilizing buffer. The peroxidase, linked to the secondary

antibody in the presence of peroxides, catalyzed the oxidation reaction of the luminol that oxidized emitted chemiluminescence. The membrane was incubated for 3 minutes in the dark and was developed with the Chemi-DocTM (Bio-Rad) device. The software used to analyze the results was the Image Lab 4.0.1 (Bio-Rad).

#### 3.2.12 Stripping of the membrane

To incubate the membrane with another primary antibody, the stripping protocol was performed with the stripping buffer (0.2M glycine pH=2.5) that removed the antibody that was already in the membrane due to the low pH of this solution. Stripping was done for 30 min with the shaker at high speed at room temperature. Then the membrane was washed with TBS-T 1x 3 times of 10 minutes and blocked again with 1% milk solution with TBS-T 1x. Finally, 3 extra washes of 10 minutes were done and incubated again with the new primary antibody overnight.

### *3.3 Enzyme-linked immunosorbent assay (ELISA)*

#### 3.3.1 Insulin

The sandwich ELISA for insulin (EZRMI-13K - EMD Millipore) is a type of assay based on the capture of insulin molecules from serum samples. The wells of the microtiter 96-well-plate were coated by pre-titered amount of monoclonal mouse anti-rat insulin antibodies. Then, the biotinylated polyclonal antibodies were bound to the captured insulin (10µl of samples + 10µl of assay buffer + 80µl of detection antibody, incubation of 2 hours at room temperature in a plate shaker at 500rpm). Following, the strips were washed with the wash buffer 1x solution to eliminate the unbound materials from samples and incubated with 100µl of the horseradish peroxidase (enzyme solution) 30 minutes at room temperature at 500rpm, which was bound to the immobilized biotinylated antibodies. Finally, samples were washed again and 100µl of the substrate 3,3',5,5'-tetramethylbenzidine were added from 5 to 20 minutes to quantify the immobilized antibody-enzyme conjugates by monitoring horseradish peroxidase activities. 100µl of stop solution was added after the substrate incubation and the blue color turned into yellow after acidification.

The enzyme activity was measured in a 96-well-plate spectrophotometer at 450nm of absorbance, corrected from the absorbance at 590nm, after acidification of formed products. To perform the final quantification, with the standards of known concentrations of insulin, a directly proportional standard curve was made and thus, an extrapolation of the amount of insulin that each serum sample had.

#### 3.3.2 C-Peptide 2

To perform the sandwich ELISA for C-peptide 2 the same protocol as for insulin was followed. The only modification was the volumes used in the second biotinylated antibody to C-peptide 2 (20µl of samples + 30µl of assay buffer + 50µl of detection antibody).

## 4. Statistical analysis

The statistical analyses used along the experiments were mainly 1-way-ANOVA followed by Tukey method for pairwise comparison and 2-way-ANOVA, as well as, Kaplan-Meier survival curves. The results were analyzed with GraphPad Prim 7 software. In all the studies, the results were considered statistically significant when the statistical p value was under 0.05 (* $p<0.05$; ** $p<0.005$; *** $p<0.0005$)

The histology studies and the immunohistochemistry and western blot analysis were analyzed with ImageJ software.

# Objectives

PTEN is the main negative regulator of the PI3K/Akt pathway that controls many important cell functions like glucose and lipid metabolism after its activation under the insulin route. In addition, VDR has got as principal function to control the mineral metabolism, however it is also involved in other roles, such as insulin secretion and lipid accumulation.

Taking into consideration that the two genes are involved in similar processes, we wanted to study the relationship between PTEN, VDR and cellular metabolism.

Therefore, the main objectives of this doctoral thesis are:

1. Analysis of the global consequences of the loss of PTEN and VDR.

    1.1 Generation of an inducible PTEN and VDR double knock out mouse model to study their ablation.

    1.2 Evaluation of the general phenotype of the lack of PTEN and VDR in double knock out mouse.

2. Study of the implication of PTEN and VDR genes in glucose metabolism.

    2.1 Measurement of the levels of the two main actors of glucose metabolism, glucose and insulin.

    2.2 Analysis of glucose reabsorption in kidneys.

    2.3 Evaluation of the liver as principal regulator of gluconeogenesis and glycogen reservoir.

3. Investigation of the role of PTEN and VDR genes in lipid metabolism and ketone bodies formation.

# Results

## Objective 1:

Analysis of the global consequences of the loss of PTEN and VDR

# 1. DKO mouse model generation

We started the experiments by checking if our mice had lost the expression of both genes of interest, and whether the PI3K/Akt was activated in the mice in which PTEN was eliminated. We tested PTEN and VDR at DNA level by performing a PCR analysis to detect the DNA cleavage *(Figure 24A)* and also at protein level by western blot technique *(Figure 24B & 24C)*. We analyzed the expression of PTEN and VDR in different organs (thyroid gland, uterus, prostate, pancreas, kidney and liver) because the Cre recombinase system that we used was ubiquitous. The results show that PTEN was eliminated from PTEN-KOs and DKOs and VDR from VDR-KOs and DKOs. Moreover, the p-Akt/Akt ratio is increased in PTEN-KO and DKO mice compared to VDR-KO and CNT mice, demonstrating the PI3K/Akt pathway activation *(Figure 24B & 24C)*. Therefore, we generated a good mouse model to study the interaction between PTEN and VDR at a systemic level throughout the body.

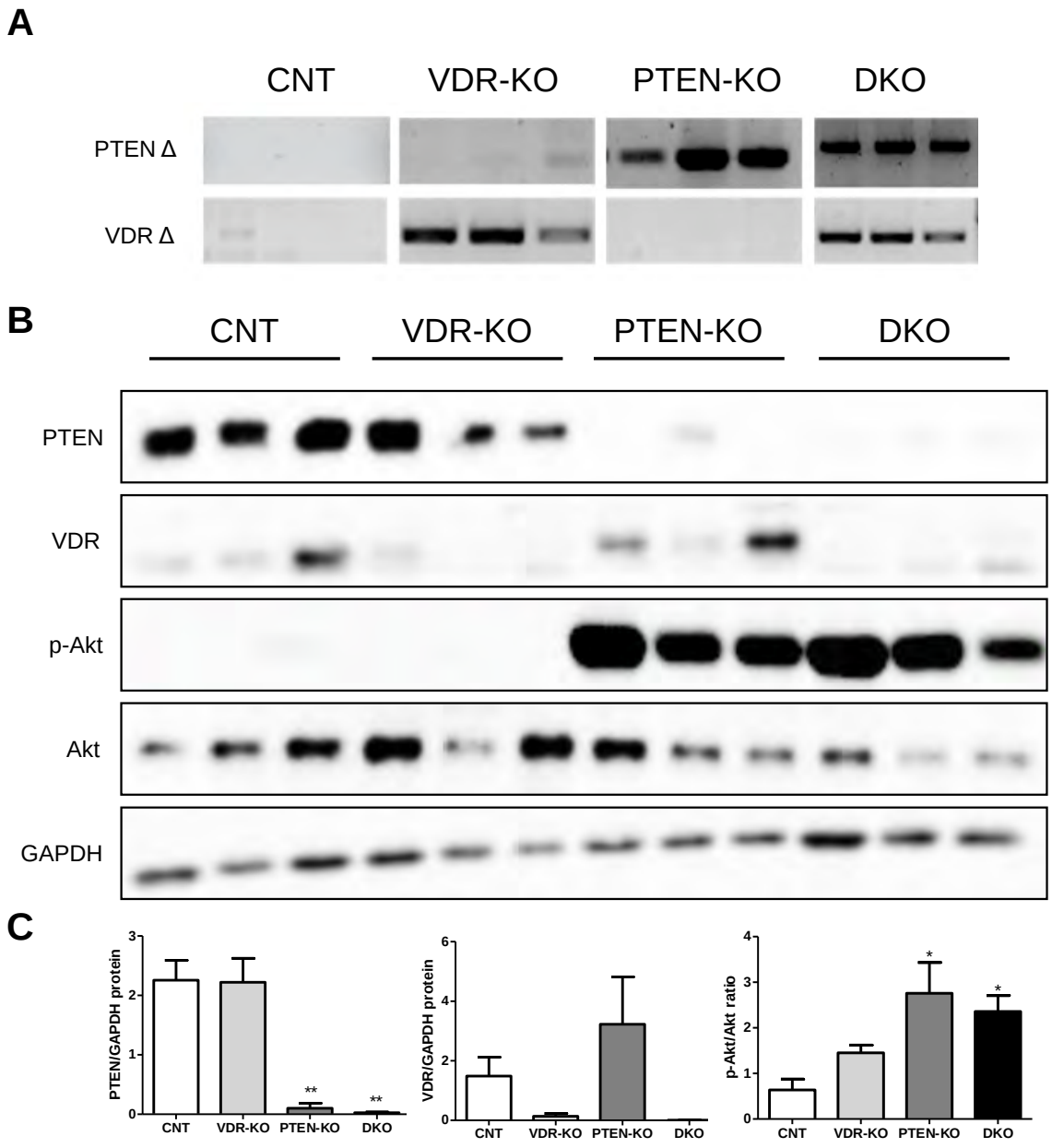


**Figure 24: Mice model generation.** ***(A)*** *Representative image after agarose gel electrophoresis demonstrates PTEN Δ* (300bp) and VDR *Δ* (300bp) *PCR products. They are obtained from the excision of PTEN Exon 5 and VDR Exon 2 after Cre recombination of their LoxP sequences. The samples are from thyroid gland, uterus or prostate and pancreas.* ***(B)*** *Representative Western blot shows the PTEN (54 kDa), VDR (50 kDa), p-Akt (60 kDa) and Akt (62 kDa) protein expression in triplicates in CNT, VDR-KO, PTEN-KO and DKO mice. The same samples are blotted with GAPDH (37 kDa) as loading control and quantification reference.* ***(C)*** *PTEN, VDR and p-Akt/Akt Western blot quantification. Data presents the mean ± SEM of 12 mice/group. *p<0.05; **p<0.01 vs. CNT mice.*

## 2. DKO mice present a deteriorated phenotype

After establishing the colony CreER$^{TM+/-}$PTEN$^{fl/fl}$VDR$^{fl/fl}$ and obtaining the four genotypes of interest, we proceeded to characterize the global effect of the absence of PTEN and VDR.

DKO mice had a deteriorated appearance compared to the PTEN-KOs, VDR-KOs and CNTs at the phenotypic level *(Figure 25)*.

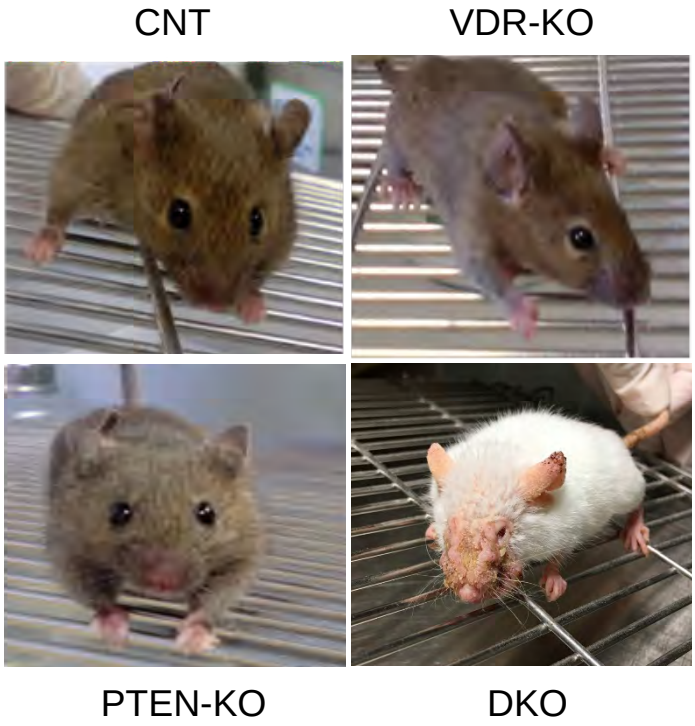


**Figure 25: Phenotype of mice**. *Representative images of every genotype show that DKO mice have a characteristic phenotype that allows to identify them easily in the cage: bristly hair, very long nails, scaly skin, thickened snout or slow movements, among other characteristics; CNT, VDR-KO and PTEN-KO mice have a normal phenotype.*

When the DKO mice were euthanatized, we could detect macroscopically the same types of tumors that were described in the literature for PTEN-KOs [294] (endometrial intraepithelial neoplasm, thyroid hyperplasia and prostate intraepithelial neoplasia) but with less frequency.

## 3. DKO mice show a lower survival rate

The first clear result that we obtained was that the DKO mice presented a lower survival rate after 65 days of the Tamoxifen injection compared with the other groups *(Figure 26A)*.

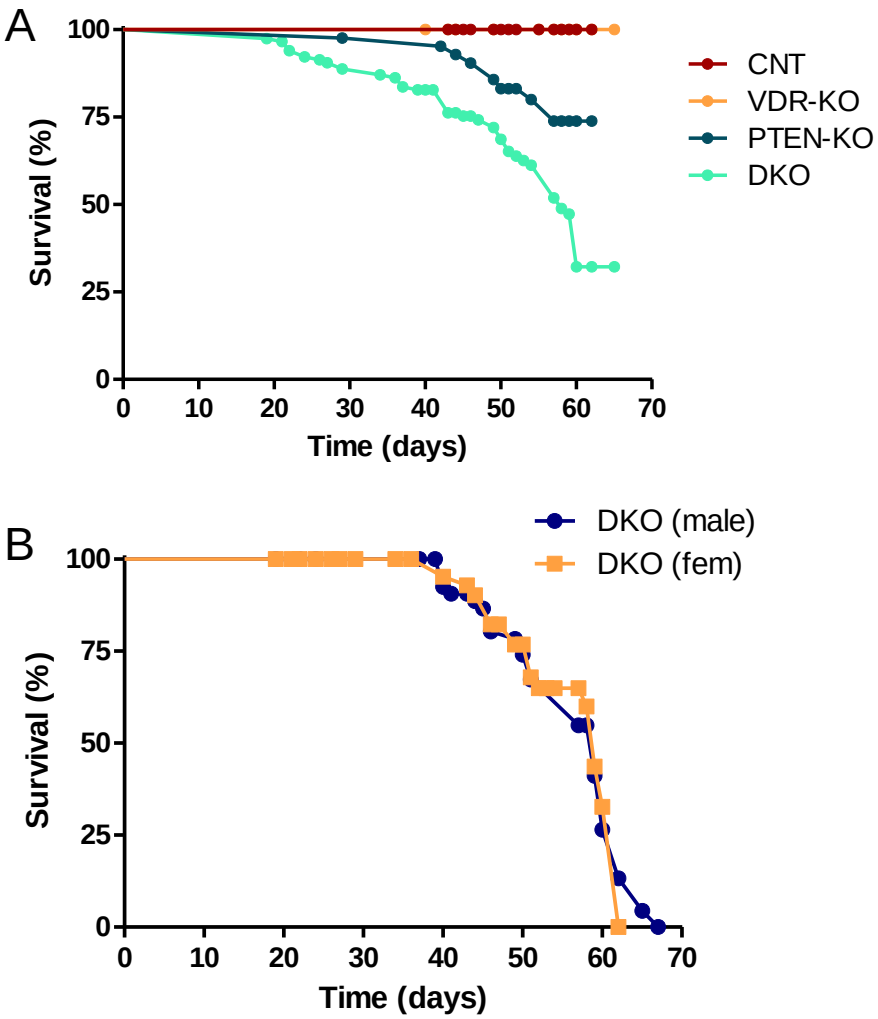


**Figure 26: Survival studies show premature death of DKO mice.** ***(A)*** *Kaplan-Meier survival curve measures the fraction of subjects living for a certain amount of time after treatment, in this case 65 days after Tamoxifen injection in CNT (N=57), VDR-KO (N=42), PTEN-KO (N=42) and DKO (N=115) mice.* ***(B)*** *Kaplan-Meier plot shows the survival percentage between males (N=62) and females (N=53) in DKO mice. Data is presented as a percentage of survival.*

We compared if there were survival differences between sexes in DKO mice, but we found that they had the same profile *(Figure 26B)*.

Then, we wondered what could be the cause of that premature death. Thus, we began to make general studies of these mice, such as blood and urine tests.

## 4. Ion disorders in PTEN-KO and DKO mice

We analyzed $Ca^{+2}$, P, $Na^{+}$ and $K^{+}$ in serum and urine trying to find more clues about the cause of the premature death in DKO mice.

### *4.1 High levels of serum $K^{+}$ in DKOs, high levels of serum $Ca^{+2}$ in PTEN-KOs and high levels of serum P in both mice*

We found higher levels of $K^{+}$ in serum in DKOs compared to the other groups *(Figure 27B)*, a fact that that could lead to death because of cardiac arrhythmias. Moreover, we found higher levels of P in serum in DKO and PTEN-KO mice, in comparison with the other mice *(Figure 27D)*, which are usually associated with renal failure. PTEN-KOs had higher levels of $Ca^{+2}$ than the rest of the groups *(Figure 27C)*. $Na^{+}$ levels did not show differences between groups *(Figure 27A)*.

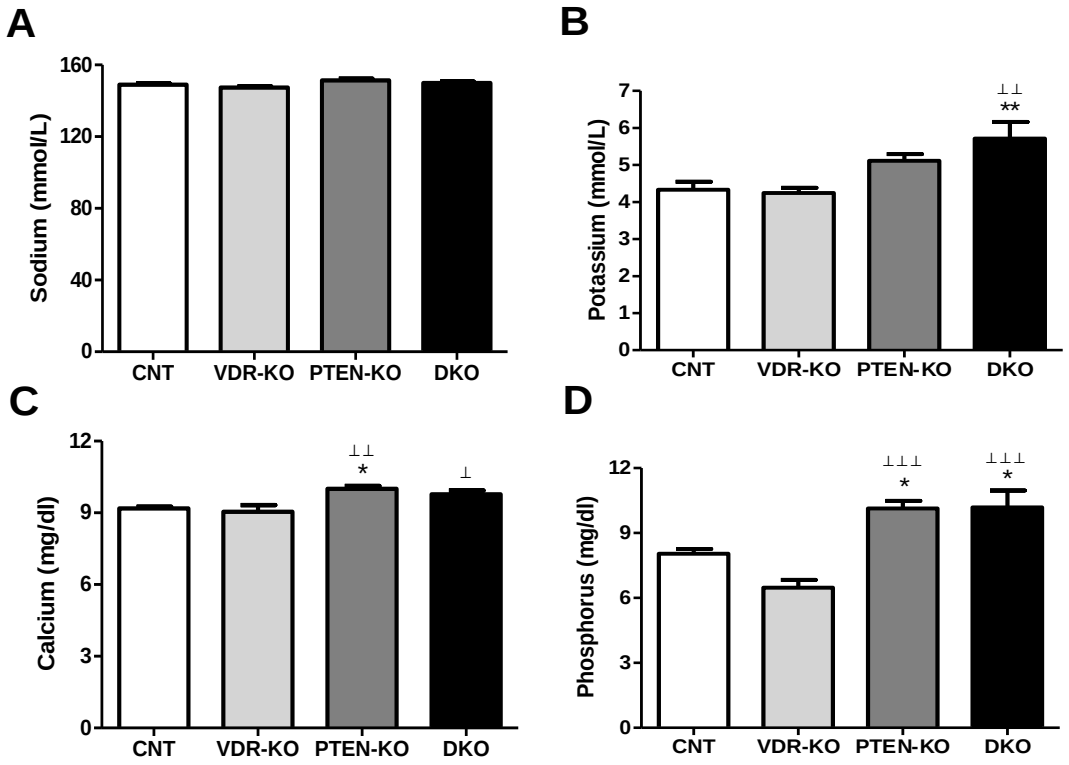

**Figure 27: Alterations in serum ions.** ***(A)*** *$Na^+$ serum concentrations (mmol/L) in CNT, VDR-KO, PTEN-KO and DKO mice.* ***(B)*** *$K^+$ levels in serum (mmol/L) in CNT, VDR-KO, PTEN-KO and DKO mice.* ***(C)*** *Serum $Ca^{+2}$ concentrations (mg/dl) in CNT, VDR-KO, PTEN-KO and DKO mice.* ***(D)*** *P levels in serum (mg/dl) in CNT, VDR-KO, PTEN-KO and DKO mice. Data presents the mean ± SEM of 9-10 mice/group. *p<0.05; **p<0.01 vs. CNT mice. ⊥p<0.05; ⊥⊥p<0.01; ⊥⊥⊥ p<0.001 vs. VDR-KO mice.*

### *4.2 Low levels of urinary $Ca^{+2}$ excretion and high levels of urinary P excretion in PTEN-KO mice*

In addition, we also measured the urinary excretion of those four ions. The analysis demonstrated that PTEN-KOs had lower urinary $Ca^{+2}$ excretion *(Figure 28C)* and higher urinary P excretion *(Figure 28D)* compared to the other groups of mice.

There were not statistically significant differences between groups in $Na^+$ *(Figure 28A)* and $K^+$ *(Figure 28B)* urinary excretion levels.

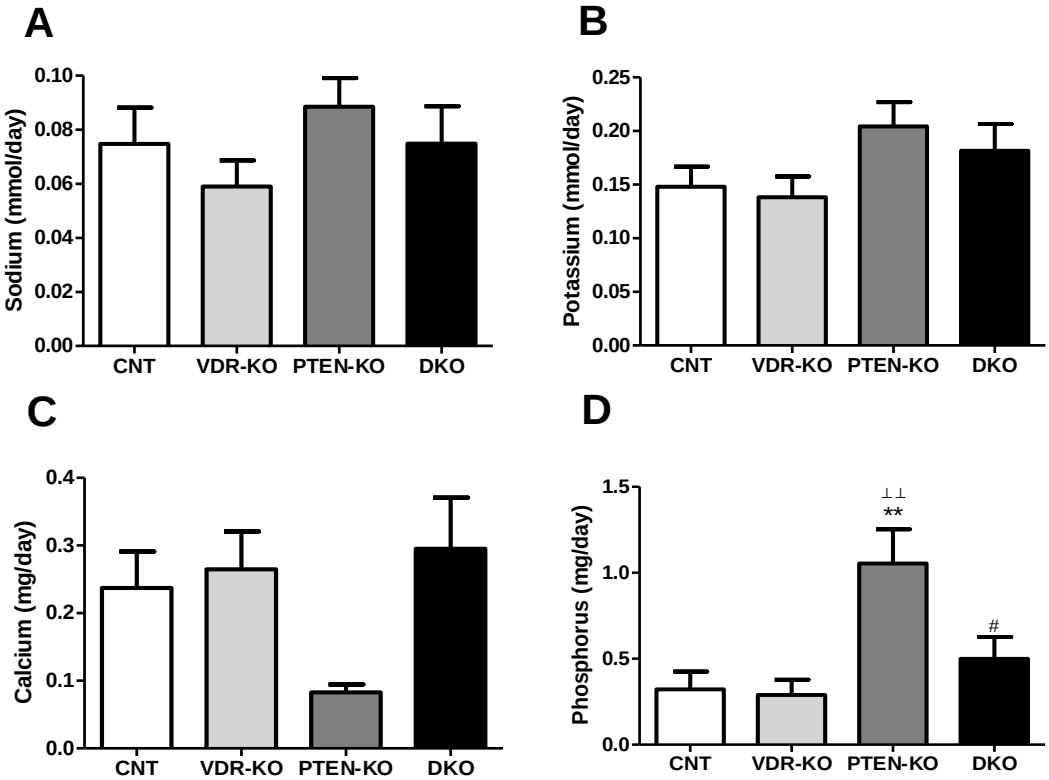


**Figure 28: Alterations in ions measured in urine.** ***(A)*** *$Na^+$ urine concentrations (mmol/day) in CNT, VDR-KO, PTEN-KO and DKO mice.* ***(B)*** *$K^+$ levels in urine (mmol/day) in CNT, VDR-KO, PTEN-KO and DKO mice.* ***(C)*** *$Ca^{+2}$ urine concentrations (mg/dl) in CNT, VDR-KO, PTEN-KO and DKO mice.* ***(D)*** *P levels in serum (mg/dl) in CNT, VDR-KO, PTEN-KO and DKO mice. Data presents the mean ± SEM of 12-17 mice/group. **p<0.01 vs. CNT mice. ⊥⊥p<0.01 vs. VDR-KO mice. # p<0.05 vs. PTEN-KO mice.*

### *4.3 $K^+$ chelate treatment in DKO mice do not extend their lifespan*

We found that DKO mice had higher $K^+$ levels than the rest of groups *(Figure 27B)*, thus, another possible reason for their premature death could be cardiac arrhythmias; therefore, we treated DKO mice with a $K^+$ chelate diet.

Survival of DKO mice was decreased after being treated with the $K^+$ chelate *(Figure 29A & 29B)*. Moreover, DKOs with $K^+$ chelate diet ate less than DKOs with normal diet *(Figure 29C)*, but there were no differences in drinking water *(Figure 29D)*.

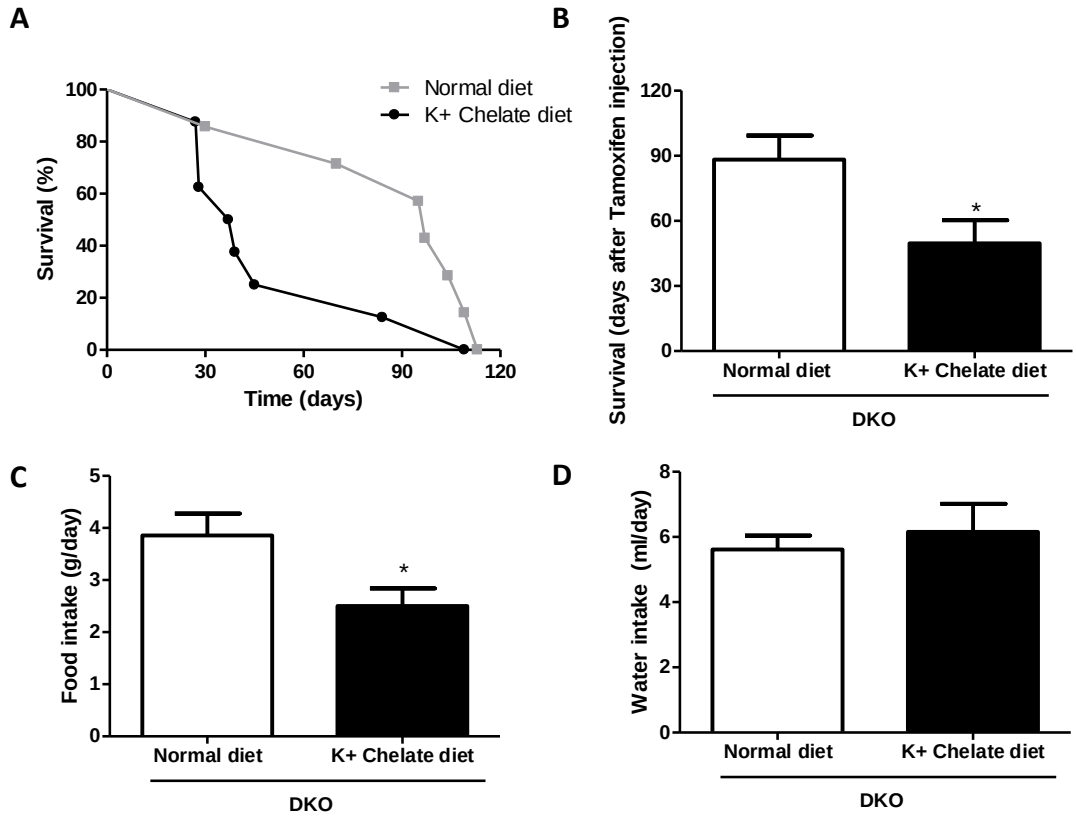


**Figure 29: $K^+$ chelate treatment does not extend DKO mice survival.** ***(A)*** *Kaplan-Meier curve shows the survival percentage between DKO mice treated with normal diet and DKO mice with $K^+$ chelate diet.* ***(B)*** *Survival graph (days after Tamoxifen injection).* ***(C)*** *Food intake (g/day).* ***(D)*** *Water intake (ml/day). Data is presented as a percentage of survival of 7 mice/group. Every dot corresponds to a mouse of study (A). Data presents the mean ± SEM of 7-8 mice/group (B,C,D). *p<0.05 vs. DKO mice treated with normal diet.*

## Objective 2:

Study of the implication of PTEN and VDR genes in glucose metabolism

# 1. Disrupted glucose behavior in PTEN-KO and DKO mice

## *1.1 Severe hypoglycemia*

The first thing that stood out in the general tests was the low blood glucose level that PTEN-KOs and DKOs had in basal terms, as well as in 2h and 7h fast state. Moreover, when we tried to let them fast overnight, most of DKO mice died. Thus, they did not have the capacity of maintain glucose levels without food intake.

CNT and VDR-KO mice had stable glucose blood levels, while PTEN-KO and DKO mice had severe hypoglycemia *(Figure 30)*.

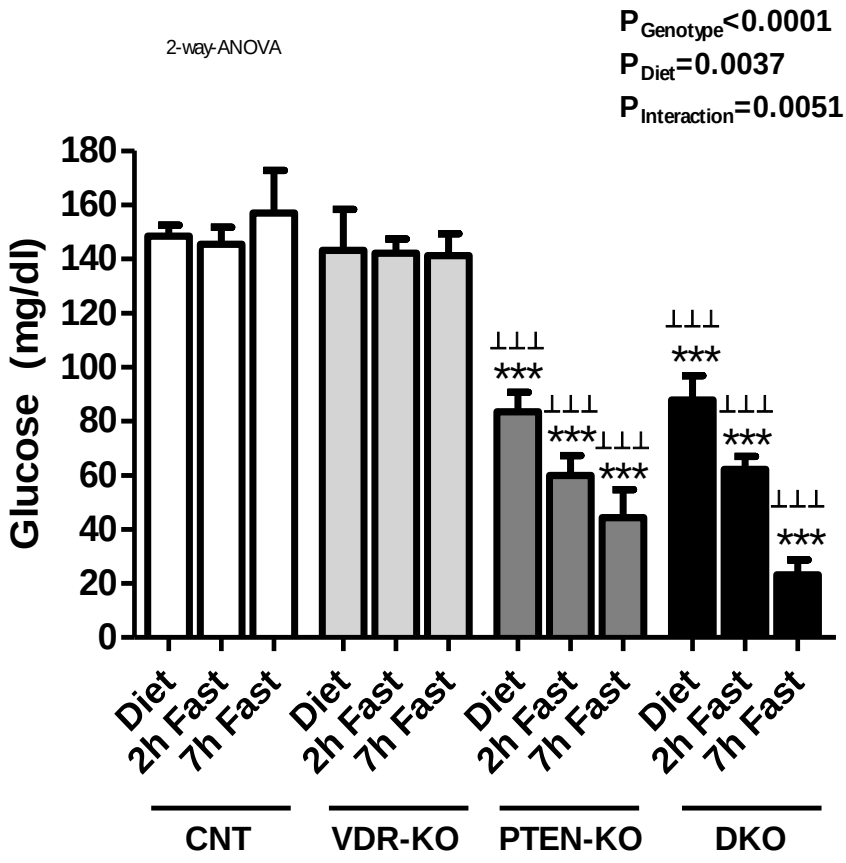


**Figure 30: Serum glucose levels behavior is altered in PTEN-KO and DKO mice.** *Glucose in serum measured in mice with diet, 2h fasting and 7h fasting (mg/dl). Data presents the mean ± SEM of 10-15 mice/group. *** p<0.001 vs. CNT mice. ⊥⊥⊥ p<0.001 vs. VDR-KO mice. 2-way-ANOVA gives the significance of the genotype, diet and its interaction.*

### *1.2 Impaired glucose absorption from bloodstream to cells*

A GTT was performed to study how fast glucose is cleared from the bloodstream after 2 hours of fasting and a 4g/kg glucose injection.

The results from the GTT followed the same pattern as in the *Figure 30*; both PTEN-KOs and DKOs had sustained-hypoglycemia. CNT and VDR-KO mice started the test with normal glucose levels in serum (around 150mg/dl), whereas PTEN-KO and DKO mice had a third of glycemia values *(Figure 31A)*. However, DKOs did not seem to respond to the glucose bolus, because they did not show a marked glucose peak 20 minutes after the injection related to other groups. *(Figure 31B)*.

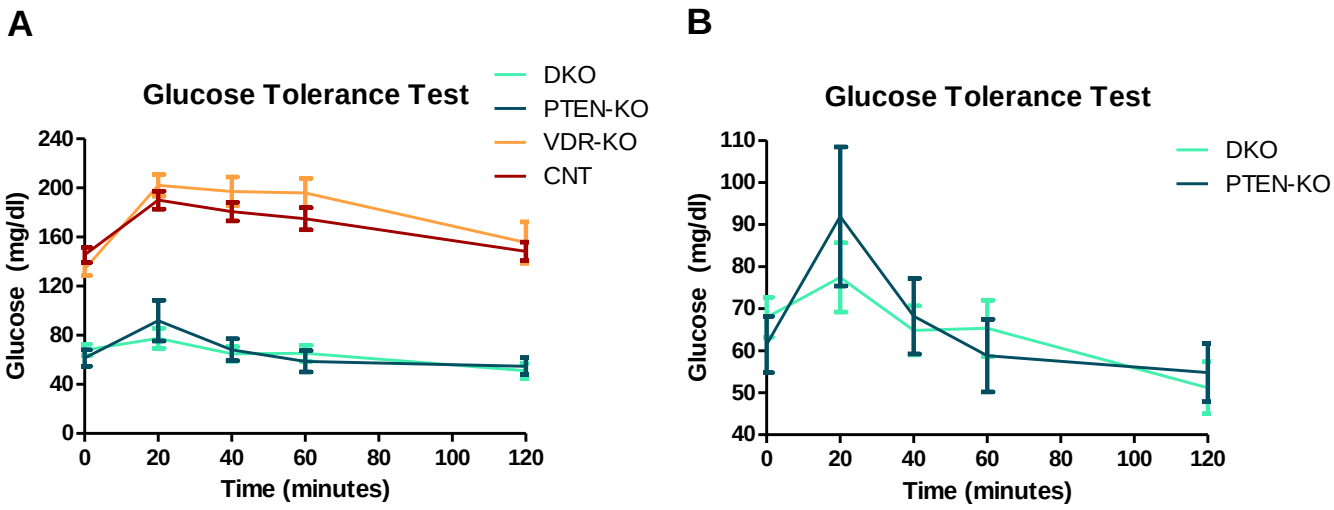


**Figure 31: Glucose tolerance test.** ***(A)*** *Glucose concentration (mg/dl) measured at time 0, 20, 40, 60 and 120 minutes in mice after 2h of fasting and a bolus of 4g/kg of glucose at time 0.* ***(B)*** *Magnification of the graph to observe in details the differences between PTEN-KO and DKO mice. Data presents the mean ± SEM of CNT (N=26), VDR-KO (N=20), PTEN-KO (N=15) and DKO (N=31) mice.*

### *1.3 PTT suggests a gluconeogenesis alteration*

Performing the PTT we checked if hepatic gluconeogenesis was altered after a bolus of pyruvate by measuring the blood glucose concentration.

PTT is considered a preliminary test to study gluconeogenesis, easy to perform; however, it has to be supplemented with extra substantive data from more specific tests.

A single 2g/kg pyruvate injection was done after 2h of fasting and, two hours later, the glycemia was monitored at different times (0, 20, 40, 60 and 120 minutes). CNT and VDR-KO mice started the test with regular glucose levels around 150mg/dl, which were 3-fold the PTEN-KO and DKO mice glucose concentration. Both, PTEN-KOs and DKOs, did not have a marked glucose peak 20 minutes after the injection in comparison with the other groups. PTT showed some alterations in the activation of gluconeogenesis in these two groups of mice *(Figure 32)*.

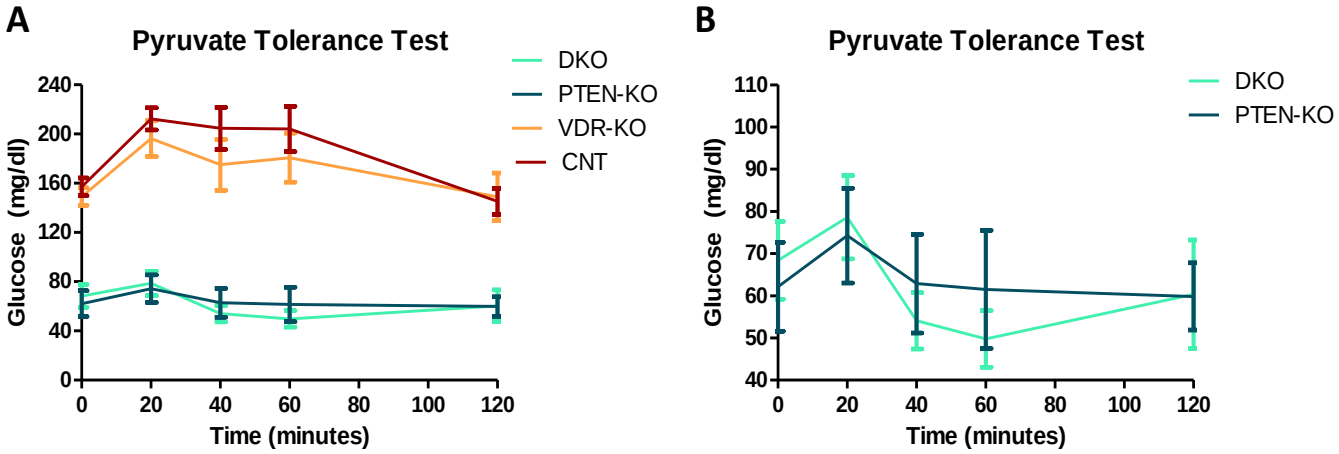


**Figure 32: Pyruvate tolerance test.** ***(A)*** *Glucose concentration (mg/dl) measured at time 0, 20, 40, 60 and 120 minutes in mice after 2h of fasting and a bolus of 2g/kg pyruvate.* ***(B)*** *Magnification of the graph to observe in details the differences between PTEN-KO and DKO mice. Data presents the mean ± SEM of CNT (N=11), VDR-KO (N=9), PTEN-KO (N=8) and DKO (N=13) mice.*

### *1.4 The insulin and glucagon effects on glucose are weak in DKO mice*

DKO mice did not stand overnight fasting; thus, we monitor the four groups of mice during 6 hours to study their glucose behavior.

We removed food from the cages at time 0 and we measured glucose at different time points. The glucose behavior plot showed that in DKOs the normal glucose peak within the first hour after removing the food did not appear, while in the other groups it did. Moreover, in CNT, VDR-KO and PTEN-KO mice, the effect of insulin and glucagon in the bloodstream can be observed by the peaks and falls of blood glucose levels along the 6 hours. In contrast, DKOs almost do not show this normal pattern, rather there is a

constant lowering of the glucose values until 120 min, and at this point they go up in a very mild way remaining in severe hypoglycemia *(Figure 33)*.

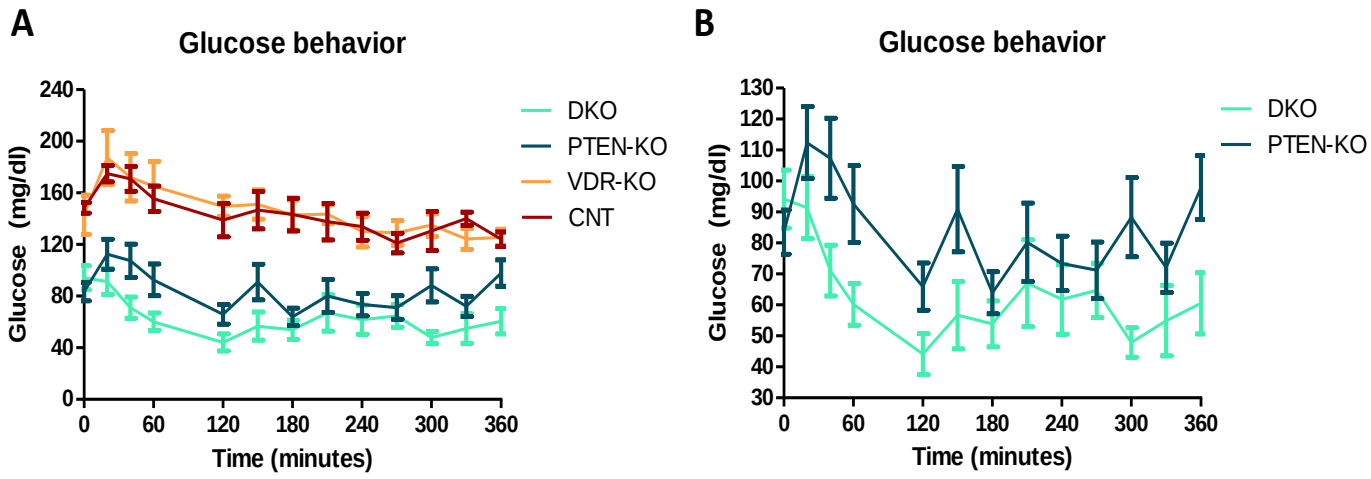


**Figure 33: Glucose behavior.** ***(A)*** *Glucose concentration (mg/dl) measured at time 0, 20, 40, 60, 120, 150, 180, 210, 240, 270, 300, 330 and 360 minutes after fast.* ***(B)*** *Magnification of the graph to observe in details the differences between PTEN-KO and DKO mice. Data presents the mean ± SEM of CNT (N=11), VDR-KO (N=7), PTEN-KO (N=10) and DKO (N=14) mice.*

Something that is also important to point out is that if we left DKO mice in fasting for more than 6 hours, they were not able to overcome the hypoglycemia. Their glucose levels were lower than 20 mg/dl, which induced coma and their subsequent death. On the other hand, if we left the PTEN-KO mice in longer fasts, 7 or 8 hours they also reached a similar hypoglycemia (<20mg/dl), but with a completely different behavior, they looked good, they run along the cage and if we gave them food again, they recovered and returned to their normal glucose levels (observational results, data not shown).

### *1.5 Tissue glucose absorption is increased in DKO mice*

PTEN and VDR are known as tumour suppressor genes; thus, even though macroscopically we did not observe more tumors in DKOs than in PTEN-KOs, we wanted to see if the DKO severe hypoglycemia was due to some tumour consuming a lot of glucose and therefore, blunting the glucose raise in serum levels after the injection.

We performed a GTT with CNT and DKO mice in with a mixture of normal glucose (3g/kg) and radioactive glucose ($^{3}$H glucose at 20µCi/mouse). We collected all their tissues (heart, lung, spleen, pancreas, muscle, kidney, brain, liver, thyroid gland and uterus or prostate) and we measured the radioactivity (counts per minute (CPM)) that they emit with a scintillation counter.

The results of the experiment did not show any statistically difference between CNTs and DKOs in any specific tissue. However, we could observe a clear tendency in all tissues to absorb more glucose *(Figure 34A)*.

We analyzed the prostates separately, since in the DKOs presented with prostate cancer and were bigger than in the CNTs *(Figure 35A)*. Therefore, to be able to compare the radiation that they emitted, we adjusted the values to their weight. The result was the same as all the other tissues studied, a tendency to absorb more glucose, but without being statistically different between groups *(Figure 35B)*.

Then, we put the radioactivity that all the organs emitted together, and we compared the CNTs with the DKOs and we observed a statistically significant difference between groups. Demonstrating that the DKO mice had increased global tissue absorption *(Figure 34B)*.

Therefore, we did not find any specific organ that absorbed much more glucose (which could have indicated a possible aggressive tumor that needed a lot of energy), but we found a clear increased absorption in all organs, which would support the results found of permanently low glycemia.

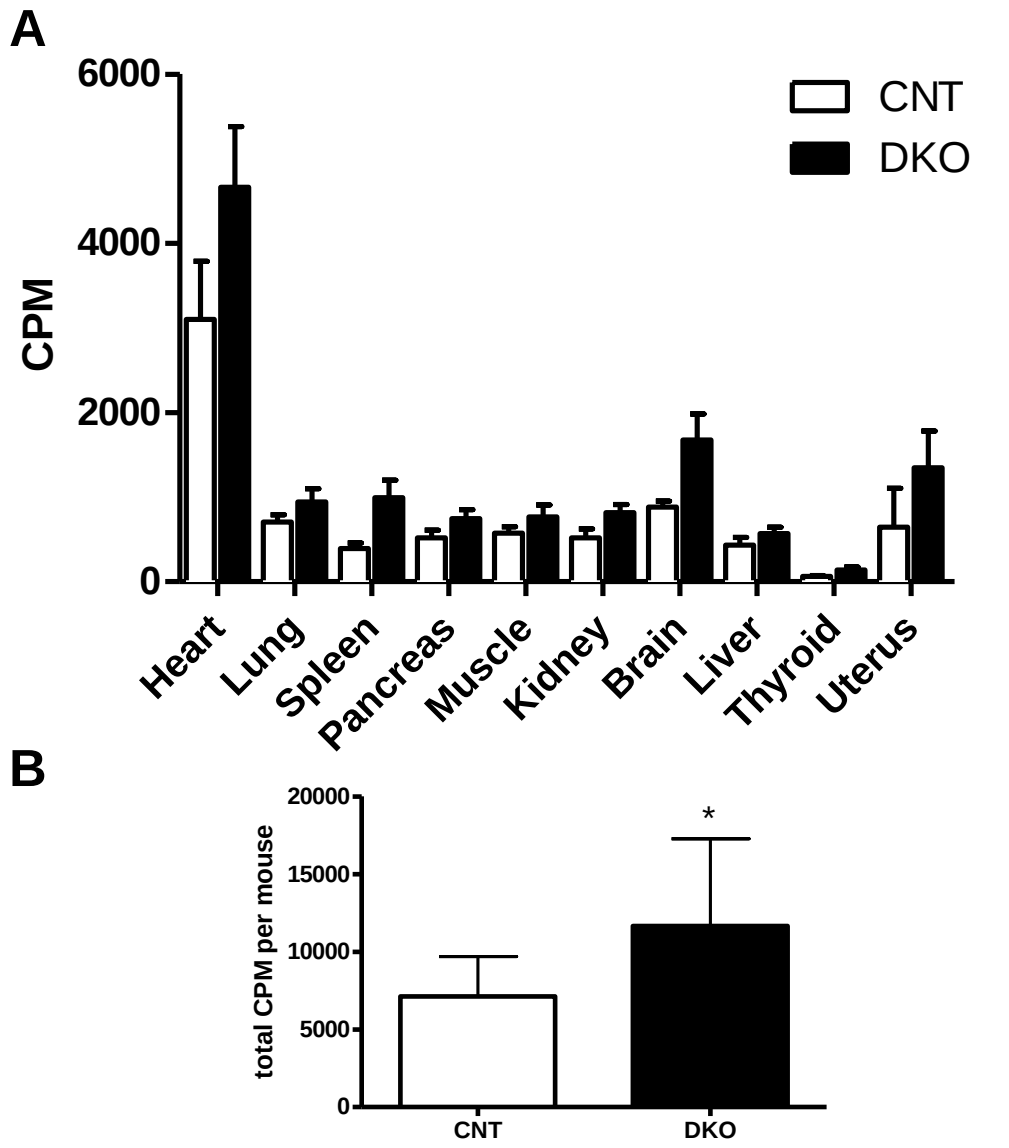


**Figure 34: $^{3}$H-glucose absorption in DKO mice organs is augmented.** ***(A)*** *$^{3}$H-glucose radioactivity (CPM) measured in heart, lung, spleen, pancreas, muscle, kidney, brain, liver, thyroid gland, prostate and uterus of CNT and DKO mice.* ***(B)*** *Sum of the $^{3}$H-glucose radioactivity (CPM) emitted by all organs in CNT and DKO mice. Data presents the mean ± SEM of 10-16 mice/group. *p<0.05 vs. CNT mice*

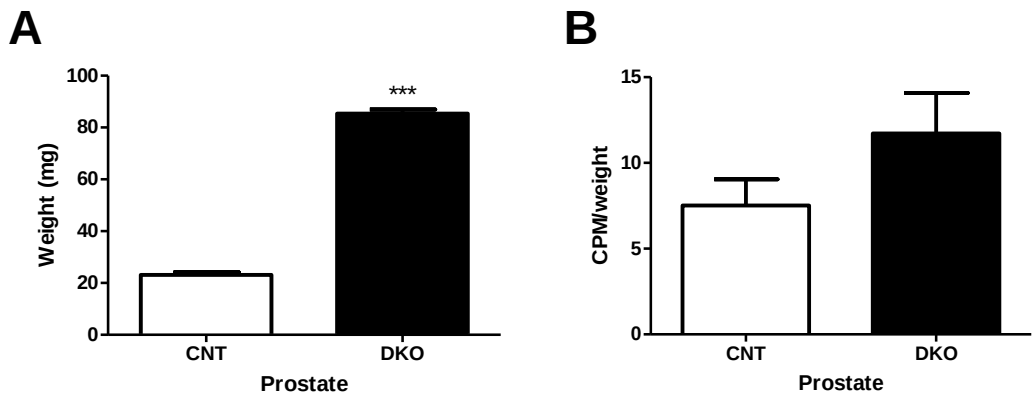


**Figure 35: $^{3}$H-glucose absorption in prostate corrected by weight.** ***(A)*** *Prostate gland weight (mg) in CNT and DKO mice.* ***(B)*** *$^{3}$H-glucose radioactivity (CPM) measured in prostate gland of CNT and DKO mice Data presents the mean ± SEM of 10-16 mice/group. *** p<0.001 vs. CNT mice*

### *1.6 Sucrose treatment in DKO mice does not increase their survival*

We treated DKO mice severe hypoglycemia with sucrose water to try to increase their survival. Nevertheless, no differences were found between survival of DKOs with normal water (79 days) and sucrose water (71 days) *(Figure 36A & 36B)*.

We also monitored water and food intake during a week of treatment and, as we expected, they statistically drank more (normal water: 5.29 ml/day, sucrose water: 24.68 ml/day) *(Figure 36C)* and ate less (normal water: 3.59 g/day, sucrose water: 2.1 g/day) *(Figure 36D)*, because they extracted calories from sucrose. Moreover, there were no differences in body weight *(Figure 36E)* and blood glucose concentrations *(Figure 36F)* between groups.

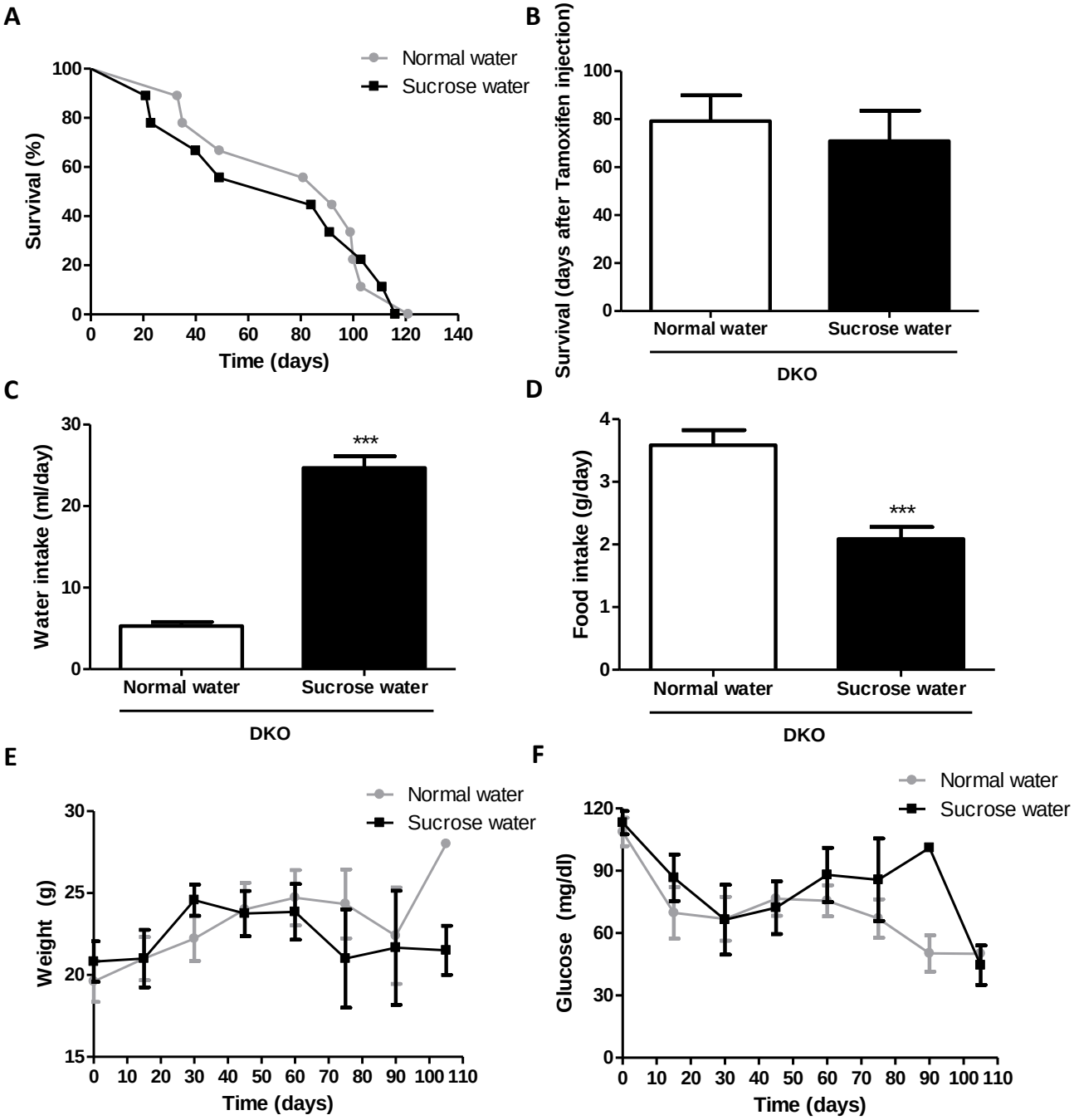


**Figure 36: Sucrose treatment does not extend DKO mice survival.** ***(A)*** *Kaplan-Meier curve shows the survival percentage between DKO mice treated with normal and sucrose water.* ***(B)*** *Survival graph (days after Tamoxifen injection).* ***(C)*** *Water intake (ml/day).* ***(D)*** *Food intake (g/day).* ***(E)*** *Mice weight (g) measured every 15 days during the experiment.* ***(F)*** *Glucose in serum (mg/dl) measured every 15 days during the experiment. Data is presented as a percentage of survival of 9 mice/group (A). Data presents the mean ± SEM of 9 mice/group (B,C,D,E,F). *** p<0.001 vs. DKO mice treated with normal water.*

### *1.7 Brain glucose administration with osmotic pumps does not prolong DKO mice survival*

After sucrose water treatment in DKO mice, we tried to go a step further and administrate glucose directly in the DKO mice brain ventricles. Therefore, we injected intraventricular glucose or mannitol with a brain infusion kit connected to an osmotic pump to produce a constant infusion of the drugs.

The results of the experiment did not show differences between DKO mice treated with glucose (52 days) and with mannitol (60 days) *(Figure 37A & 37B)*.

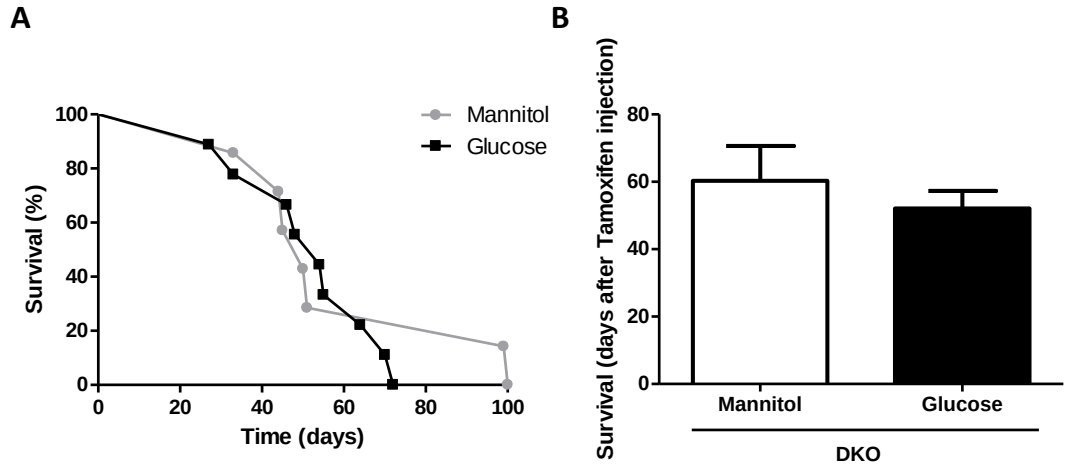


**Figure 37: Brain glucose administration with osmotic pumps does not extend DKO lifespan.** ***(A)*** *Kaplan-Meier curve shows the survival percentage between DKO mice treated with mannitol and glucose.* ***(B)*** *Survival graph (days after Tamoxifen injection). Data is presented as a percentage of survival of 7-9 mice/group (A). Data presents the mean ± SEM of 7-9 mice/group (B).*

## 2. DKO and PTEN-KO mice present hyperstimulation of the insulin receptor

First, to study glucose metabolism we focused on the pancreas because we thought that hypoglycemia could be due to the presence of an insulinoma, which is a pancreatic tumor of β−cells that is characterized by a high secretion of insulin. It leads patients suffering from it to have low blood glucose levels and hyperinsulinemia (excess levels of insulin relative to glucose in the bloodstream).

### *2.1 Insulin secretion inhibition in PTEN-KO and DKO mice*

We measured C-peptide serum levels and we observed that both PTEN-KO and DKO mice presented a statistically significant reduction of the amount of C-peptide compared with other groups of mice *(Figure 38A)*, which means low insulin levels into the bloodstream.

Moreover, we isolated pancreatic islets from the four groups of mice and we cultivated them *ex vivo*. Then, we treated the islets with 5mM of glucose [299] and we collected the culture supernatant to measure the amount of insulin secreted to the medium. The results were not statistically significant, but there was a clear tendency to secrete less insulin in the PTEN-KOs and even less in the DKOs compared to other groups *(Figure 38B)*.

Analyzing both experiments we saw that insulin was less secreted from pancreatic islets so, we dismissed the possibility that it was an insulinoma or hyperinsulinemia.

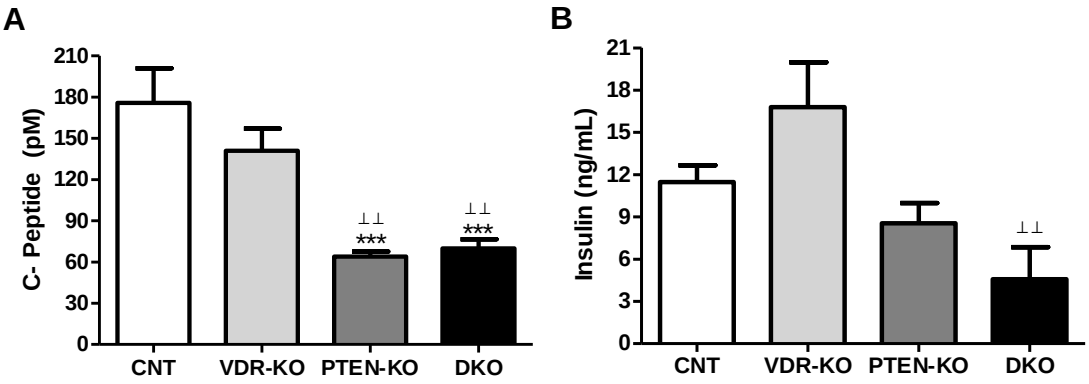


**Figure 38: Insulin secretion is reduced in PTEN-KO and DKO mice.** ***(A)*** *C-peptide serum concentration (pM) in CNT, VDR-KO, PTEN-KO and DKO mice.* ***(B)*** *Insulin secreted (ng/mL) from pancreatic islets from CNT, VDR-KO, PTEN-KO and DKO mice cultivated ex vivo and treated with 5mM of glucose. Data presents the mean ± SEM of 25-30 mice/group (A). Date shows the mean ± SEM of triplicates for each group of mice. *** p<0.001 vs. CNT mice. ⊥⊥ p<0.01 vs. VDR-KO mice.*

### *2.2 Enlarged Langerhans islets in DKO mice*

In order to complete the pancreas studies, we checked if there were morphological changes of the Langerhans islets between groups by performing an

immunohistochemistry against insulin *(Figure 39A)* to stain the pancreatic islets and to measure their total area.

First, we measured the Langerhans islets total area and we saw that DKO mice had islet hyperplasia accompanied by periductal inflammation. These symptoms can be related to nesidioblastosi, which is a pancreatic disorder that is associated with hypoglycemia. However, the hypoglycemia of this rare pancreatic condition is related to hyperinsulinemia, and as we had seen in the *Figure 38*, it was not the case of DKO mice. Therefore, we only could say from that measure that DKOs had islet hyperplasia compared with all the other groups *(Figure 39B)*.

We also evaluated the insulin stained area compared with the islet total area that we had previously measured, in order to observe if there was accumulated insulin-production cells inside the pancreatic islets. We only observe a decrease of insulin levels in VDR-KOs, but we did not observe more insulin per islet area in the other groups. Although we did not detect more insulin in islets *(Figure 39C)* in DKO mice, the increase of the total area of islets suggested augmented total insulin. Nevertheless, from the *ex vivo* incubation study of pancreatic islets, it was established that there was no more insulin secretion *(Figure 39B)*.

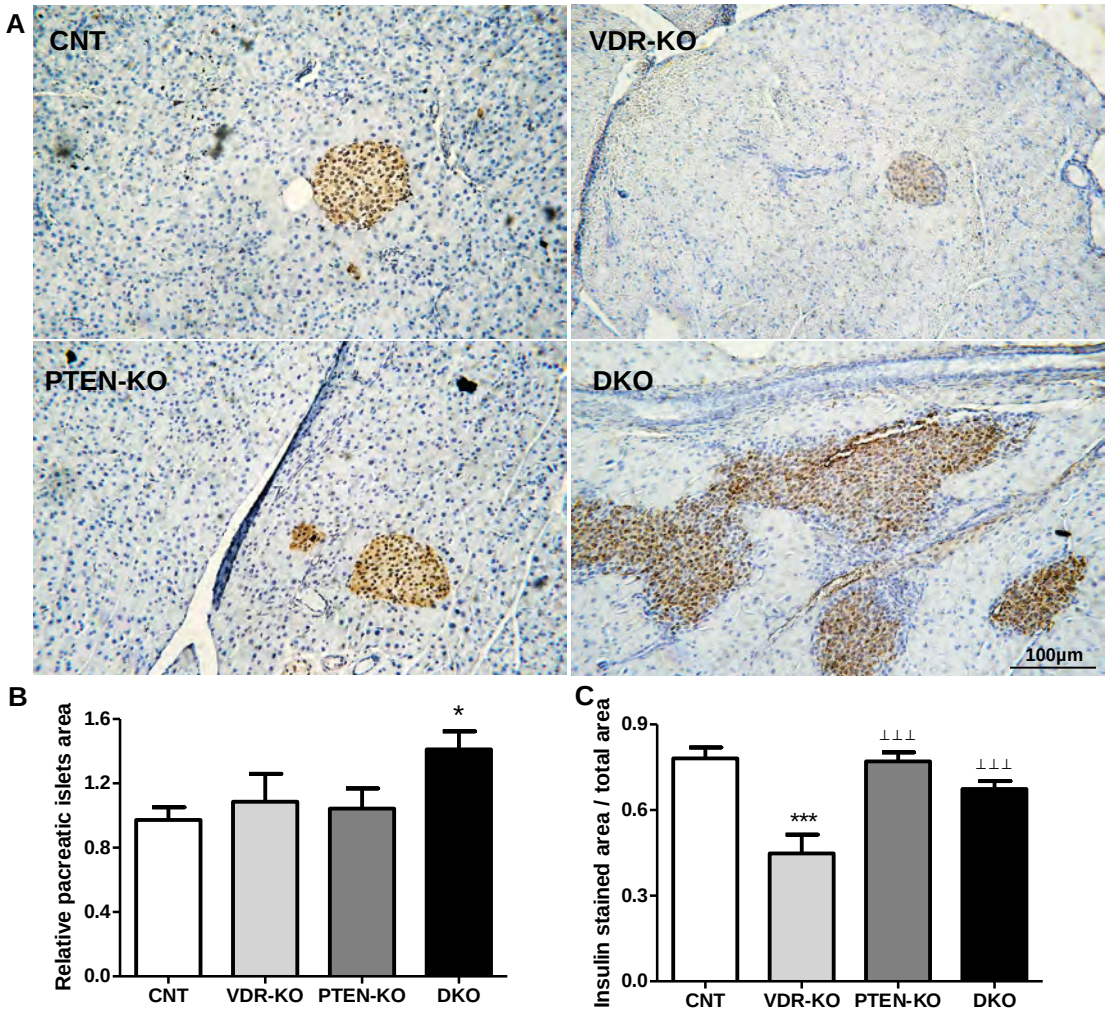


**Figure 39: Pancreatic islets hyperplasia in DKO mice.** ***(A)*** *Representative pancreatic islets images of insulin staining in CNT, VDR-KO, PTEN-KO and DKO mice.* ***(B)*** *Relative pancreatic islets area plot from CNT, VDR-KO, PTEN-KO and DKO mice* ***(C)*** *Insulin stained area compared to total area ratio in CNT, VDR-KO, PTEN-KO and DKO mice. Data presents the mean ± SEM of 5-7 mice/group (A,B). Original magnification x20. Scale bar, 100µm *p<0.05; *** p<0.001 vs. CNT mice. ⊥⊥⊥ p<0.001 vs. VDR-KO mice.*

## 3. Food intake is increased in PTEN-KO and DKO mice

We quantified the amount of food and water that they had ingested per day by monitoring mice in metabolic cages during 24 hours. As expected, both PTEN-KOs and DKOs had an increased food intake compared to the other two groups, due to their permanent hypoglycemia *(Figure 40A)*. Therefore, they were trying to compensate the lack of glucose in the bloodstream eating more quantity of food.

Furthermore, there was a slight tendency in DKOs to drink more water related to the other groups of mice *(Figure 40B)*; however, it was not statistically significant.

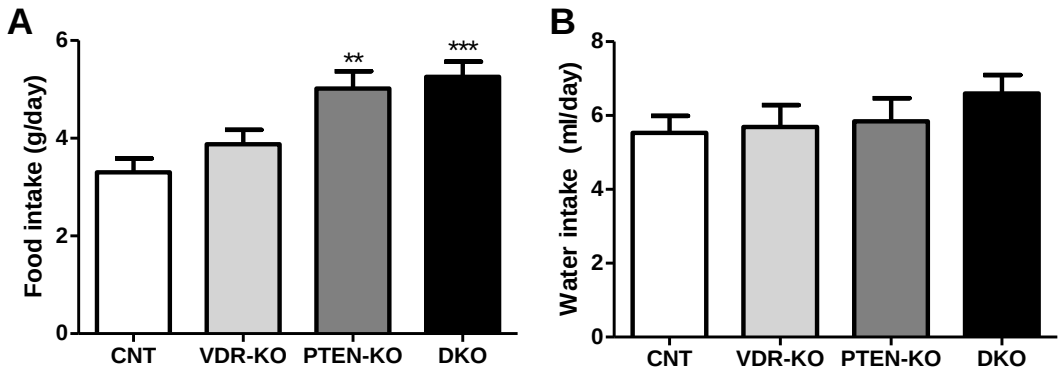


**Figure 40: Food and water usual consumption.** ***(A)*** *Food intake (g/day) in CNT, VDR-KO, PTEN-KO and DKO mice.* ***(B)*** *Water intake (ml/day) in CNT, VDR-KO, PTEN-KO and DKO mice. Data presents the mean ± SEM of 15-20 mice/group (A,B). **p<0.01; *** p<0.001 vs. CNT mice.*

# 4. Slight glycosuria and kidney glucose transporters deregulation in DKO mice but normal renal function

### *4.1 Urinary glucose presence in DKO mice*

When we monitored the mice in metabolic cages, we also collected urine from the four groups to check if there was glucose, because it could also be an escape route for it that would lead hypoglycemia.

DKOs excreted more glucose during 24h than the other three *(Figure 41A)*. Thus, and although glycosuria is light, DKOs excrete twice as much glucose as the others. Furthermore, DKO mice had a higher urine output than the other groups of mice *(Figure 41B)*.

Hence, we continue our research studying what might be the reason for this slight glycosuria by checking the glucose transporters located in the kidneys.

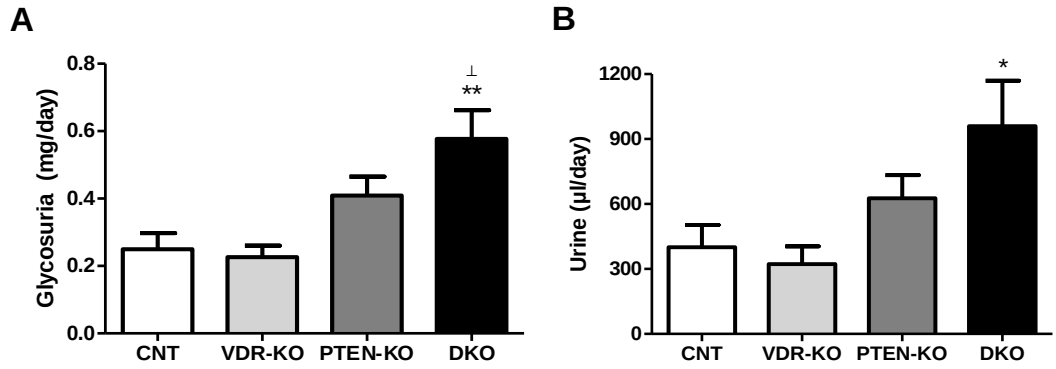


**Figure 41: Slight glycosuria in DKO mice.** ***(A)*** *Glucose in urine (mg/day) measurement in CNT (N=20), VDR-KO (N=9), PTEN-KO (N=20) and DKO (N=26) mice.* ***(B)*** *Urine excretion (µl/day) in CNT (N=17), VDR-KO (N=8), PTEN-KO (N=13) and DKO (N=21) mice. Data presents the mean ± SEM (A,B). *p<0.05; **p<0.01 vs. CNT mice. ⊥ p<0.05 vs. VDR-KO mice.*

### *4.2 Weak kidney glucose transporters malfunction*

We analyzed the mRNA expression of SGLT2/GLUT2 and SGLT1/GLUT1 glucose transporters pairs in the four groups of mice, but none of them had results statistically significant. Nonetheless, we observed a slight malfunction in the SGLT2/GLUT2 transporters pair.

SGLT2, which is located in the apical membrane, had a trend to be increased in DKOs and PTEN-KOs compared to VDR-KOs and CNTs *(Figure 42A)*. Whereas GLUT2, which is located in the basolateral membrane, had a trend to be decreased in DKOs and PTEN-KOs compared to the other two groups *(Figure 42B)*.

The second pair of glucose transporters (SGLT1/GLUT1) was less affected than the first pair. Although, SGLT1 showed a reduction of its expression in DKOs and PTEN-KOs compared to VDR-KOs and CNTs *(Figure 42C)*; GLUT1 had exactly the same mRNA expression in the four study groups *(Figure 42D)*.

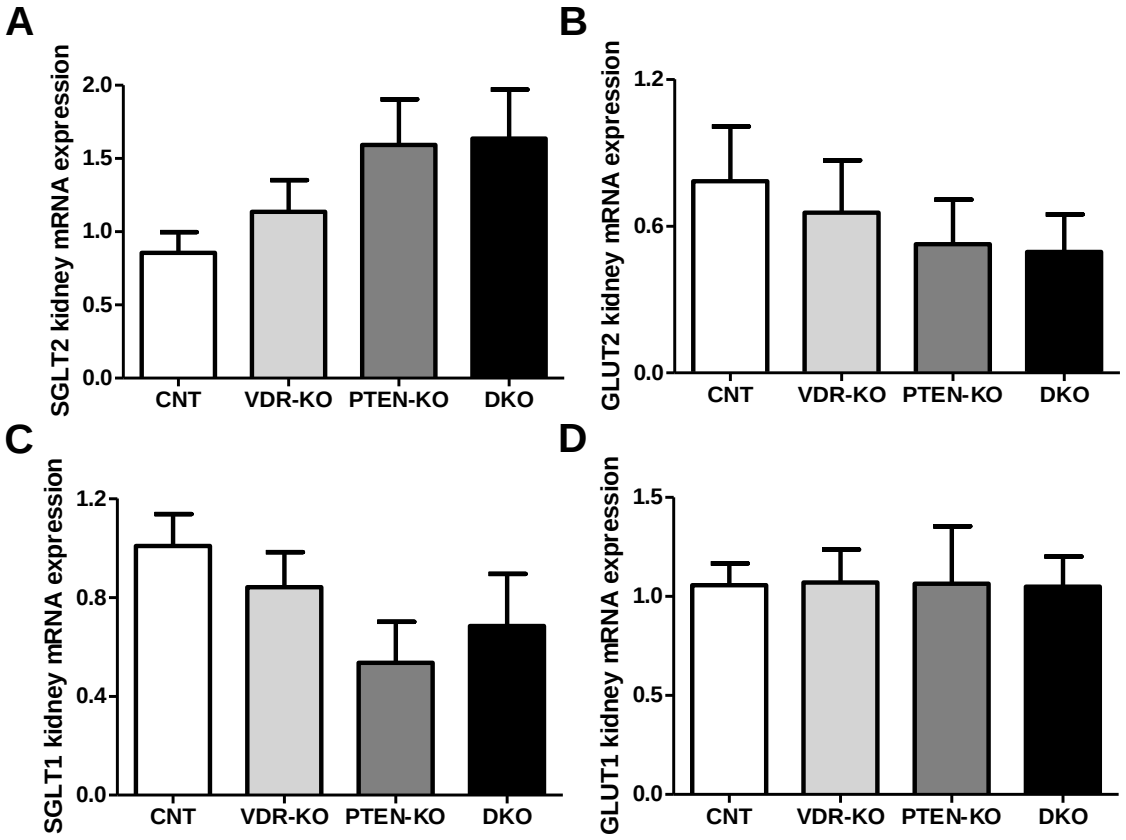


**Figure 42: Alterations in proximal tubule kidney glucose transporters.** ***(A)*** *SGLT2 mRNA expression,* ***(B)*** *GLUT2 mRNA expression,* ***(C)*** *SGLT1 mRNA expression and* ***(D)*** *GLUT1 mRNA expression were determined by real time qRT-PCR and normalized to TATA-Box Binding Protein (TBP) gene. Data presents the mean ± SEM of 6-9 mice/group.*

### *4.3 Glucose transporters altered in HK-2 cells*

In order to further analyze the glucose transporters, we performed some *in vitro* experiments with HK-2 cells from kidney proximal tubules. We used lentiviruses to downregulated PTEN, VDR or both and then, we studied SGLT2/GLUT2 and SLGT1/GLUT1 glucose transporters.

First, we checked if cells had downregulated PTEN and VDR proteins and also if the PI3K/Akt was activated in the cells lacking PTEN by measuring the protein ratio p-Akt/Akt. We corroborated by western blot that cells had lost PTEN protein in shPTEN and shPTEN-shVDR cells *(Figure 43A & 43C)* and VDR protein in shVDR and shPTEN-shVDR cells *(Figure 43A & 43D)*. Moreover, the ratio p-Akt/Akt showed that PI3K/Akt pathway was strongly activated in PTEN absence in shPTEN cells and even more, statistically significant, in shPTEN-shVDR cells compared to shVDR and cnt cells that had more total Akt than p-Akt *(Figure 43A & 43B)*. All together, it was demonstrated that we generated a good cellular model to perform kidney studies *in vitro*.

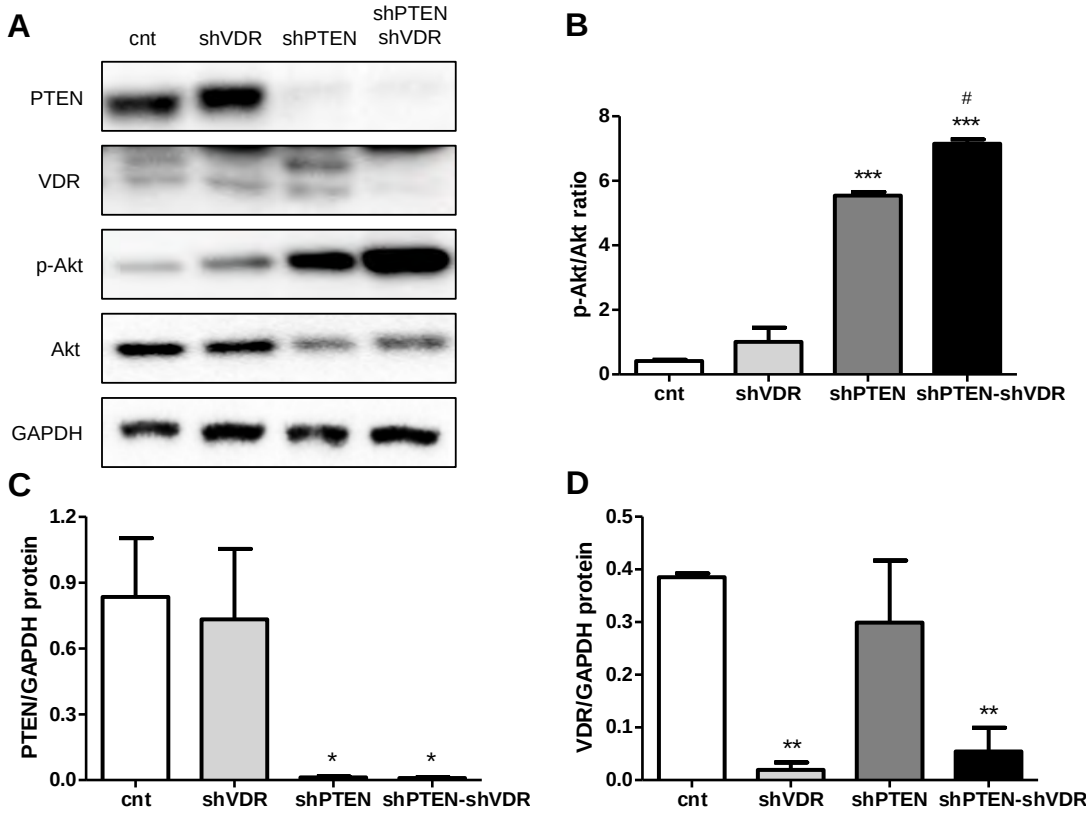


**Figure 43: Downregulation of PTEN and VDR in HK-2 cells.** ***(A)*** *Representative western blot analysis of PTEN, VDR, p-Akt and Akt from cnt, shVDR, shPTEN and shPTEN-shVDR cells extracts normalized to GAPDH gene.* ***(B)*** *p-Akt/Akt protein quantification.* ***(C)*** *PTEN protein quantification.* ***(D)*** *VDR protein quantification. Data presents the mean ± SEM from 3 independent experiments. *p<0.05; **p<0.01; *** p<0.001 vs. cnt cells. # p<0.05 vs. shPTEN.*

The results obtained *in vitro* from glucose transporters analysis were in agreement with those found in the *in vivo* studies.

The first pair of glucose transporters (SGLT2/GLUT2) was altered. SGLT2 was significantly increased in shPTEN-shVDR and shPTEN cells, in comparison to the other cells *(Figure 44A)*. While, GLUT2 showed a statistically significant decrease in shPTEN-shVDR and shPTEN cells, compared to the other groups of cells *(Figure 44B)*.

SGLT1 expression in shPTEN-shVDR and shPTEN cells showed a statistically significant decrease, compared to shVDR and cnt cells following the same trend that in the *in vivo* studies but in a more consistent way *(Figure 44C)*. Finally, GLUT1 was also not affected *(Figure 44D)*.

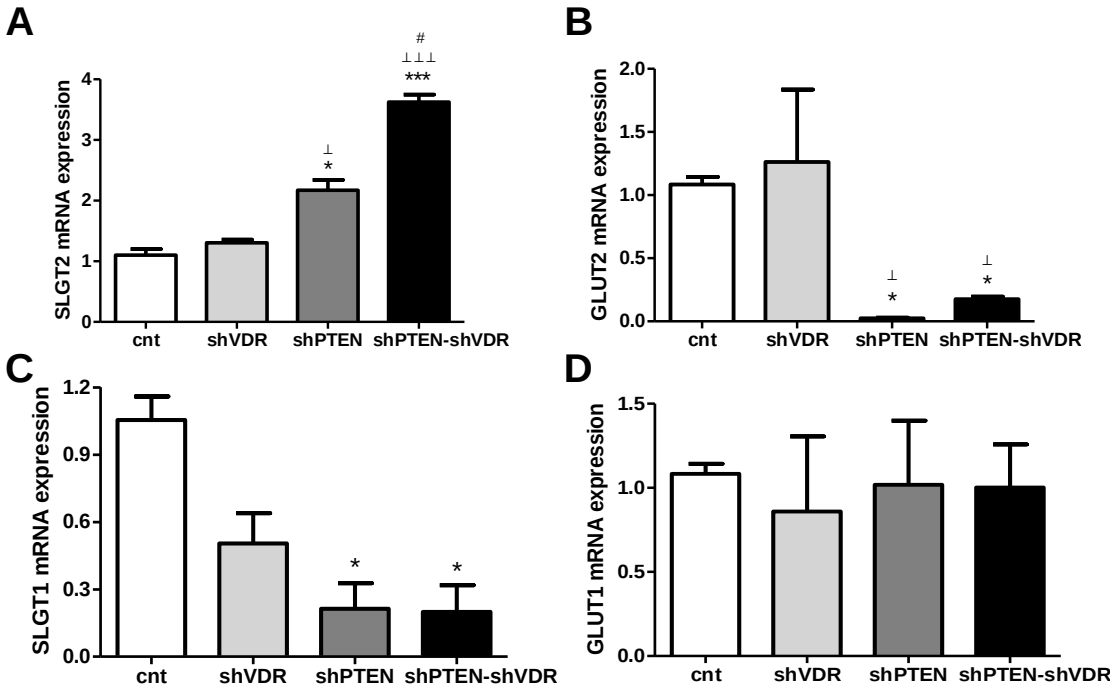


**Figure 44: Downregulation of PTEN and VDR in HK-2 cells leads to kidney glucose transporters alterations.** ***(A)*** *SGLT2 mRNA expression,* ***(B)*** *GLUT2 mRNA expression,* ***(C)*** *SGLT1 mRNA expression and* ***(D)*** *GLUT1 mRNA expression were determined by real time qRT-PCR and normalized to GAPDH gene. Data presents the mean ± SEM from 3 independent experiments. *p<0.05; *** p<0.001 vs. cnt cells. ⊥p<0.05; ⊥⊥⊥ p<0.001 vs. shVDR cells # p<0.05 vs. shPTEN cells.*

### *4.4 Normal renal function*

To finish the *in vivo* studies in kidneys, we checked if there were alterations in renal function by detecting BUN and urea in blood, both used to assess kidney function. Neither BUN *(Figure 45A)* nor urea *(Figure 45B)* tests showed any difference between groups, reporting that all mice had normal renal function.

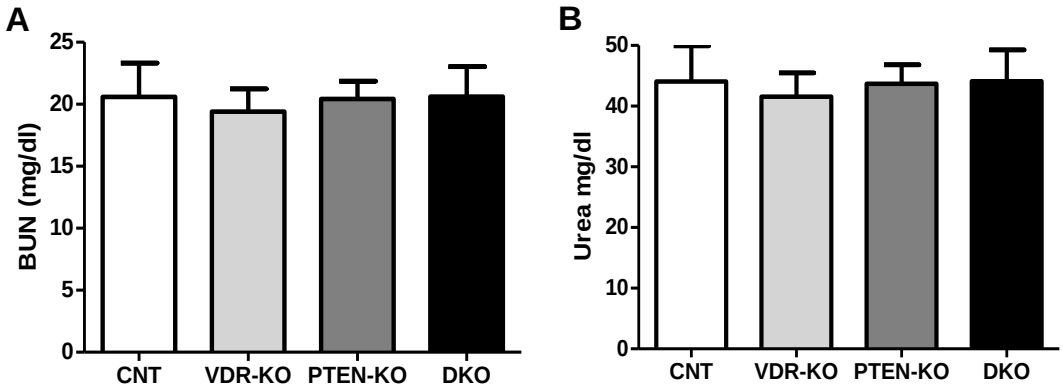


**Figure 45: Normal renal function.** ***(A)*** *BUN levels (mg/dl) in CNT, VDR-KO, PTEN-KO and DKO mice.* ***(B)*** *Urea concentration (mg/dl) in CNT, VDR-KO, PTEN-KO and DKO mice. Data presents the mean ± SEM of 7-11 mice/group.*

# 5. Liver histopathology disorder and reduced glycogen reservoir

### *5.1 Hepatocellular ballooning and inflammation but not steatosis in PTEN-KO and DKO mice*

We continued the investigations focusing into another key organ in glucose metabolism, the liver. We observed H&E stains from liver in which the morphology of the hepatocytes in PTEN-KOs (mainly) and DKOs was not normal compared with VDR-KOs and CNTs *(Figure 46A-D)*. They were enlarged (2x normal diameter); they presented a rare cytoplasmic shape; and they showed signs of inflammation. These set of morphological disorders are known as hepatocellular ballooning and it is a histological parameter used in the diagnosis of liver steatosis. It is considered a previous step to the accumulation of fat in the liver. We were not surprised because it is well described in the literature that PTEN-KO mice develop liver steatosis. [97] However, from our study, we observed that both PTEN-KOs and DKOs had hepatocellular ballooning but not hepatic steatosis at the moment in which we stopped the experiment demonstrating a hepatic alteration that could lead liver malfunction.

### *5.2 Reduced glycogen pool in fasting DKO mice*

Furthermore, we performed two different experiments to check glycogen storage in livers: a PAS staining and a biochemical glycogen-detection with liver lysates.

The PAS staining was done in livers without fasting and, although not clear enough to make a conclusion, we saw less glycogen in the PTEN-KOs and in the DKOs than in CNTs and VDR-KOs. In addition, this type of staining was difficult to use to quantify the glycogen amount *(Figure 46E-H)*.

Therefore, we decided to measure the levels of total hepatic glycogen from liver lysates in animals with and without fasting. We could not see differences between the four groups when mice were not fasted. However, we observed a clear tendency but not statistically significant, to contain less glycogen reservoir in the DKOs versus the rest of the groups both after 2 and 7 hours of fasting *(Figure 46I)*.

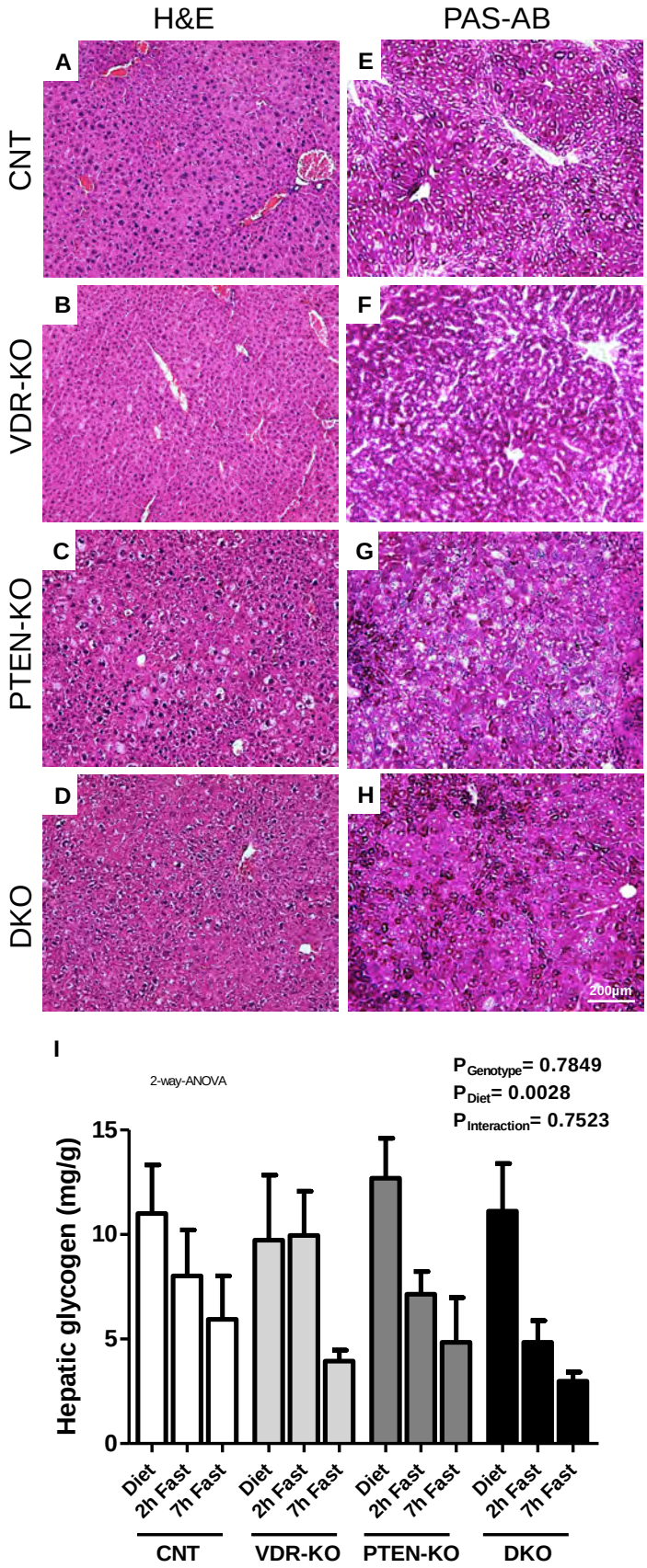


**Figure 46: Hepatocellular ballooning and reduced glycogen reservoir in PTEN-KO and DKO mice.** ***(A,B,C,D)*** *Representative H&E-staining of liver sections where hepatocellular ballooning can be observed in C and D.* ***(E, F, G, H)*** *Representative images of liver PAS-AB-staining.* ***(I)*** *Hepatic glycogen extraction and measurement. Data presents 3 mice/group (A-H) and the mean ± SEM of 10-11mice/group in diet condition, 11-13 mice/group in 2h fasting condition, 3 mice/group in 7h fasting condition (I). Original magnification x10. Scale bar, 200µm (A-H). 2-way-ANOVA gives the significance of the genotype, diet and its interaction (I).*

## 6. Delayed gluconeogenesis in PTEN-KO and DKO mice

We continued focusing our interest on the liver, but this time on gluconeogenesis to better understand the glucose behavior in these mice. The two main genes involved in gluconeogenesis process are PEPCK and G6PC. We observed that both PEPCK and G6PC genes behaved similarly in the four groups of study.

In CNT and VDR-KO mice, PEPCK *(Figure 47A)* and G6PC *(Figure 47B)* gene expression were increased after 2 hours of fasting and then, the levels were restored after 7 hours of fasting probably because the formation of new glucose in the liver had already been sufficient for the correct restoration of glycemia. However, in PTEN-KO and DKO mice, the gluconeogenesis was not activated until 7 hours of fasting.

Furthermore, we analyzed PGC1a and CEBPa, which are two genes involved in the transcriptional regulation of PEPCK and G6PC. On the one hand, PGC1a was highly activated at 2 and 7 hours of fasting in DKOs and at 7 hours of fasting in PTEN-KOs while in the other groups it was not *(Figure 47D)*. That result, perfectly correlated to PEPCK and G6PC expression. On the other hand, CEBPa was maintained at same levels in diet, 2h fast and 7h fast in CNTs and VDR-KOs whereas in PTEN-KOs and DKOs it was even diminished *(Figure 47E)*.

Finally, we also measured GLUT2, which is the hepatic glucose transporter in charge of transferring glucose between hepatocytes and the bloodstream, and we observed that in CNTs and VDR-KOs its expression was increased at 2 and 7 hours of fasting, while in PTEN-KOs and DKOs *(Figure 47C)*, as the gluconeogenesis activation was delayed, GLUT2 expression was not activated (just a slight increase at 7h of fasting that was when both groups activated the gluconeogenesis).

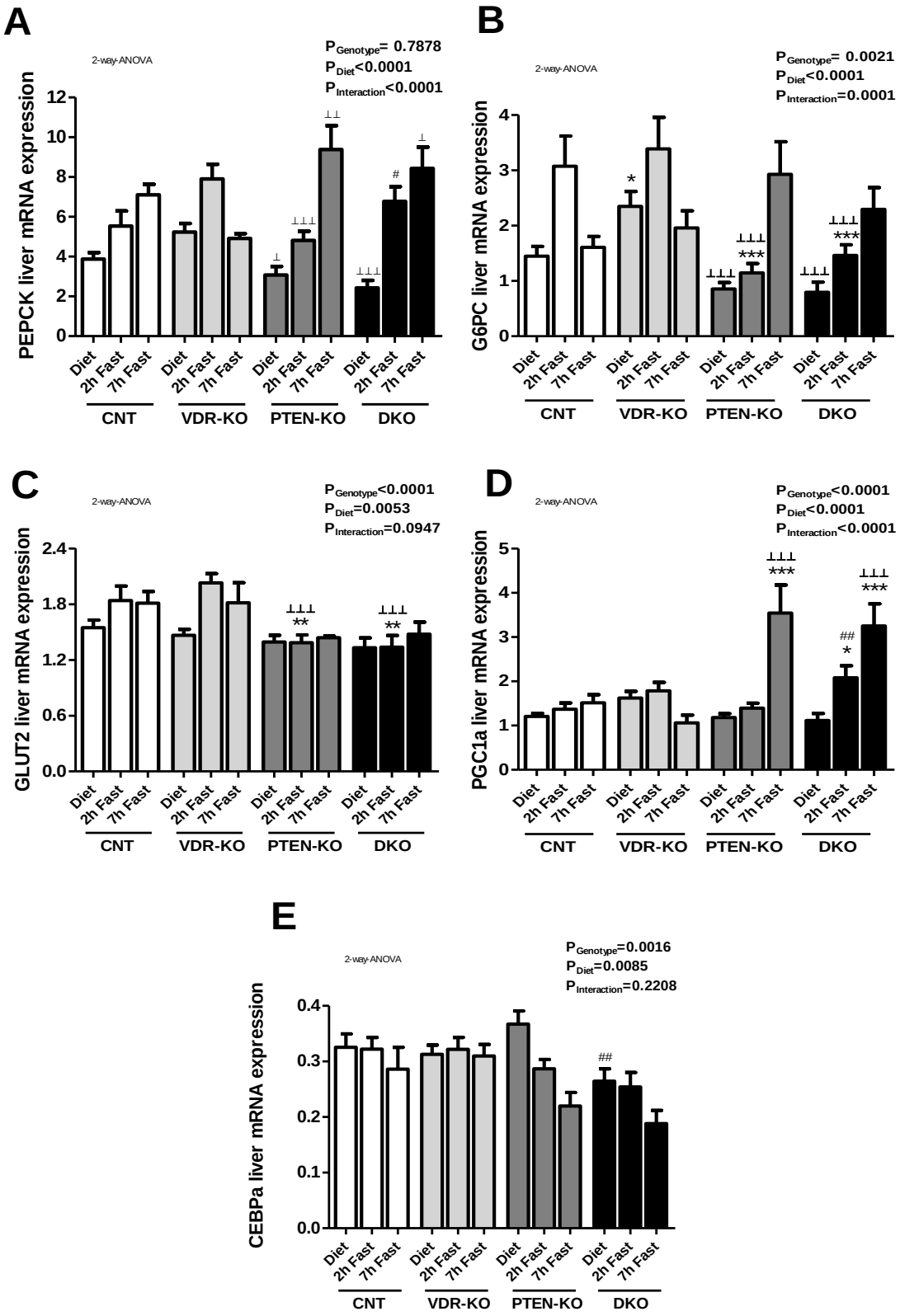


**Figure 47: Gluconeogenesis delayed in PTEN-KO and DKO mice.** *Liver **(A)** PEPCK, **(B)** G6PC, **(C)** GLUT2, **(D)** PGC1a and **(E)** CEBPa mRNA levels were determined by real time qRT-PCR and normalized to the mean of TBP and Ppia expression. Data presents the mean ± SEM of 15-20mice/group in diet condition, 15-20 mice/group in 2h fasting condition, 5-10 mice/group in 7h fasting condition *p<0.05; **p<0.01; *** p<0.001 vs. CNT mice with the same diet. ⊥p<0.05; ⊥⊥p<0.01; ⊥⊥⊥ p<0.001 vs. VDR-KO mice with the same diet . # p<0.05; ## p<0.01 vs. PTEN-KO with the same diet. 2-way-ANOVA gives the significance of the genotype, diet and its interaction.*

## Objective 3:

Investigation of the role of PTEN and VDR genes in lipid metabolism and ketone bodies formation

# 1. Ketone bodies presence in DKO mice without ketoacidosis

## *1.1 Increased ketone bodies in DKO mice without fasting*

DKO mice had severe hypoglycemia whether they were fasting or eating; thus, we checked their blood ketone bodies to see if they were extracting energy from fats. We analyzed β-hydroxybutyrate serum levels in animals with diet, 2h fast and 7h fast. We observed that DKO mice had statistically higher levels of β-hydroxybutyrate during meals compared to the other groups of mice. Moreover, PTEN-KO mice also showed a tendency to had increased ketone bodies in serum. However, when they were in prolonged fasting states, they had similar amounts of ketone bodies to the other groups that were also in starvation *(Figure 48A)*.

In addition, we measured their urine pH because high levels of ketone bodies lower the blood pH that activates an acid urine excretion by kidneys. Nonetheless, we did not find any differences between groups *(Figure 48B)*.

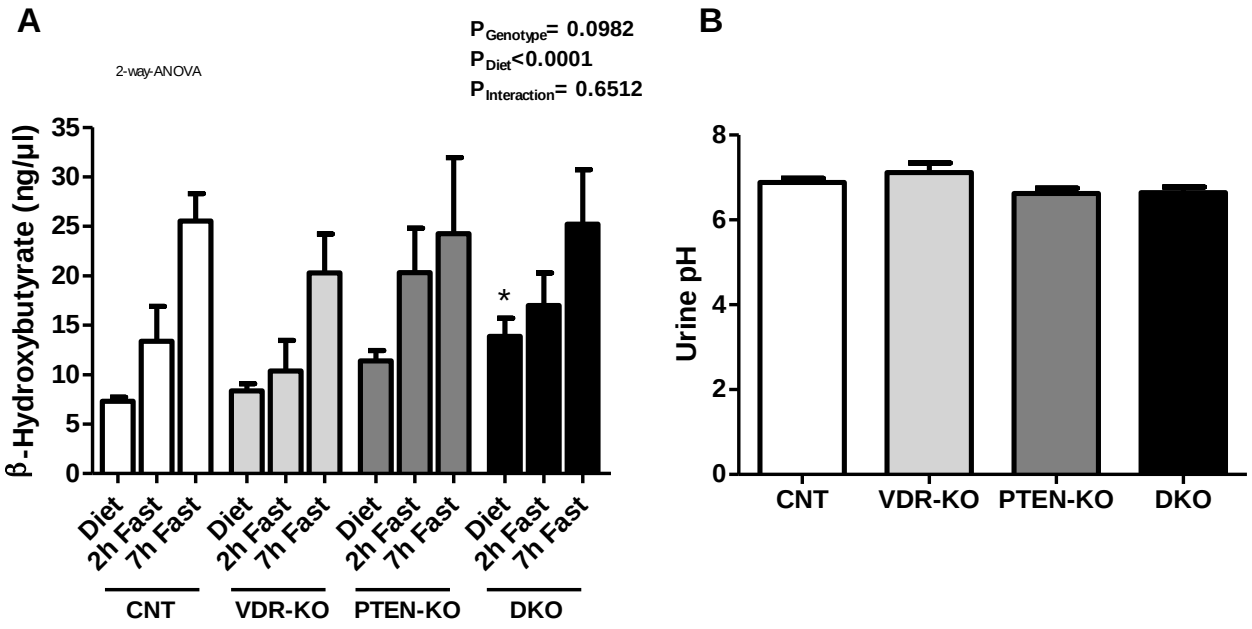


**Figure 48: Ketone bodies presence in DKO mice without ketoacidosis.** ***(A)*** *β-hydroxybutyrate serum levels (ng/µl)* ***(B)*** *Urine pH measurements in CNT (N=8), VDR-KO (N=5), PTEN-KO (N=12) and DKO (N=14) mice. Data presents the mean ± SEM of 15-20mice/group in diet condition, 15-20 mice/group in 2h fasting condition, 5-10 mice/group in 7h fasting condition (A) *p<0.05 vs. CNT mice with the same diet. 2-way-ANOVA gives the significance of the genotype, diet and its interaction (A).*

### *1.2 Bicarbonate water treatment does not extend DKO survival*

In order to double check if there was ketoacidosis, besides measuring the urine pH *(Figure 48B)*, we treated DKO mice with bicarbonate water, which is a basic substance to combat the possible blood acidification.

The bicarbonate water treatment did not increase DKOs survival compared to DKOs treated with normal water *(Figure 49A & 49B)*. Moreover we monitored their food *(Figure 49C)* and water intake and we observed that they did not eat more but they drank more bicarbonate water than normal water *(Figure 49D)*, even though they did not ameliorate their survival. They did not show differences in body weight *(Figure 49E)*.

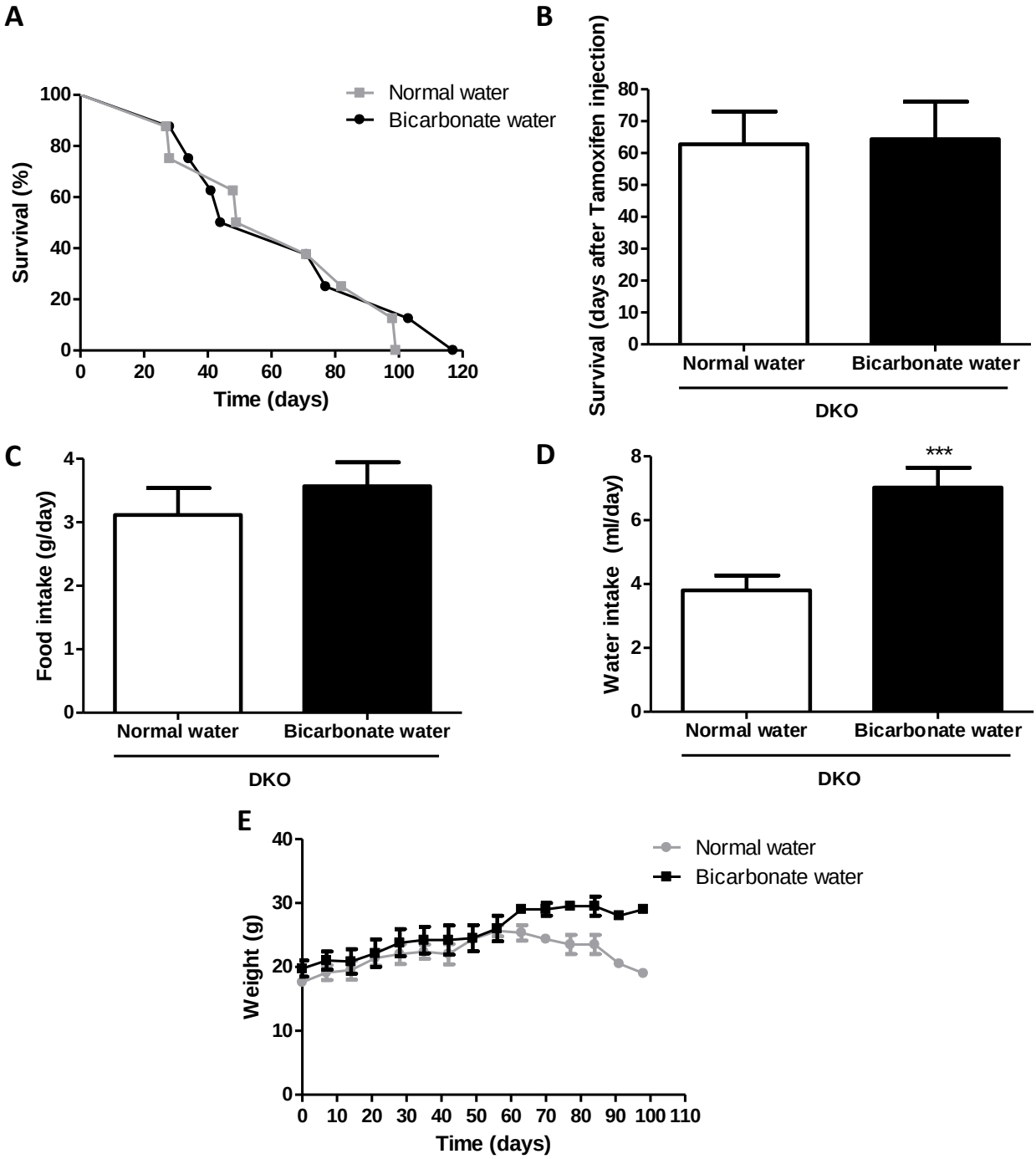


**Figure 49: Bicarbonate treatment does not extend DKO lifespan.** ***(A)*** *Kaplan-Meier curve shows the survival percentage between DKO mice treated with normal and bicarbonate water.* ***(B)*** *Survival graph (days after Tamoxifen injection).* ***(C)*** *Food intake (g/day).* ***(D)*** *Water intake (ml/day).* ***(E)*** *Mice weight (g) measured every week during the experiment. Data is presented as a percentage of survival of 8 mice/group. A). Data presents the mean ± SEM of 8 mice/group (B,C,D,E). *** p<0.001 vs. DKO mice treated with normal water.*

# 2. Lipid metabolism disorders in PTEN-KO and DKO mice

## *2.1 Absence of body fat in PTEN-KO and DKO mice*

Besides glucose metabolism, we focused on the study of lipid metabolism to better understand the interaction between PTEN and VDR and its lethal effect on DKO mice.

We measured fat mass and we observed that PTEN-KOs and DKOs did not have body fat compared to the other groups *(Figure 50)*.

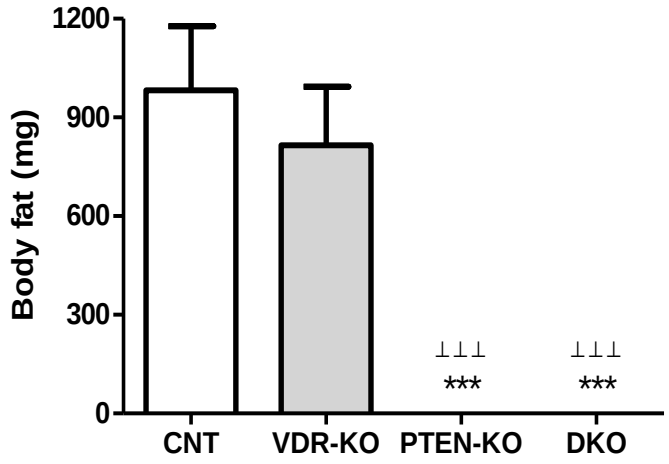


**Figure 50: Lack of body fat in PTEN-KO and DKO mice.** ***(A)*** *Body fat (mg) measured at the end point of the experiment. Data presents the mean ± SEM of 6-10 mice/group. *** p<0.001 vs. CNT mice. ⊥⊥⊥ p<0.001 vs. VDR-KO mice.*

## *2.2 High fat diet increases DKO mice survival*

From that point, we treated DKO mice with HFD trying to compensate for the lack of lipids in their body. And finally, we found a treatment that increased around one month DKO mice survival after tamoxifen injection statistically significant *(Figure 51A & 51B)*.

Furthermore, we monitored water and food intake and we observed that DKO mice treated with HFD ate significantly less *(Figure 51D)*. In contrast, they drank significantly more *(Figure 51C)*. Lastly, we also weighed the mice however we could not see differences in body weight between normal diet and HFD mice *(Figure 51E)*.

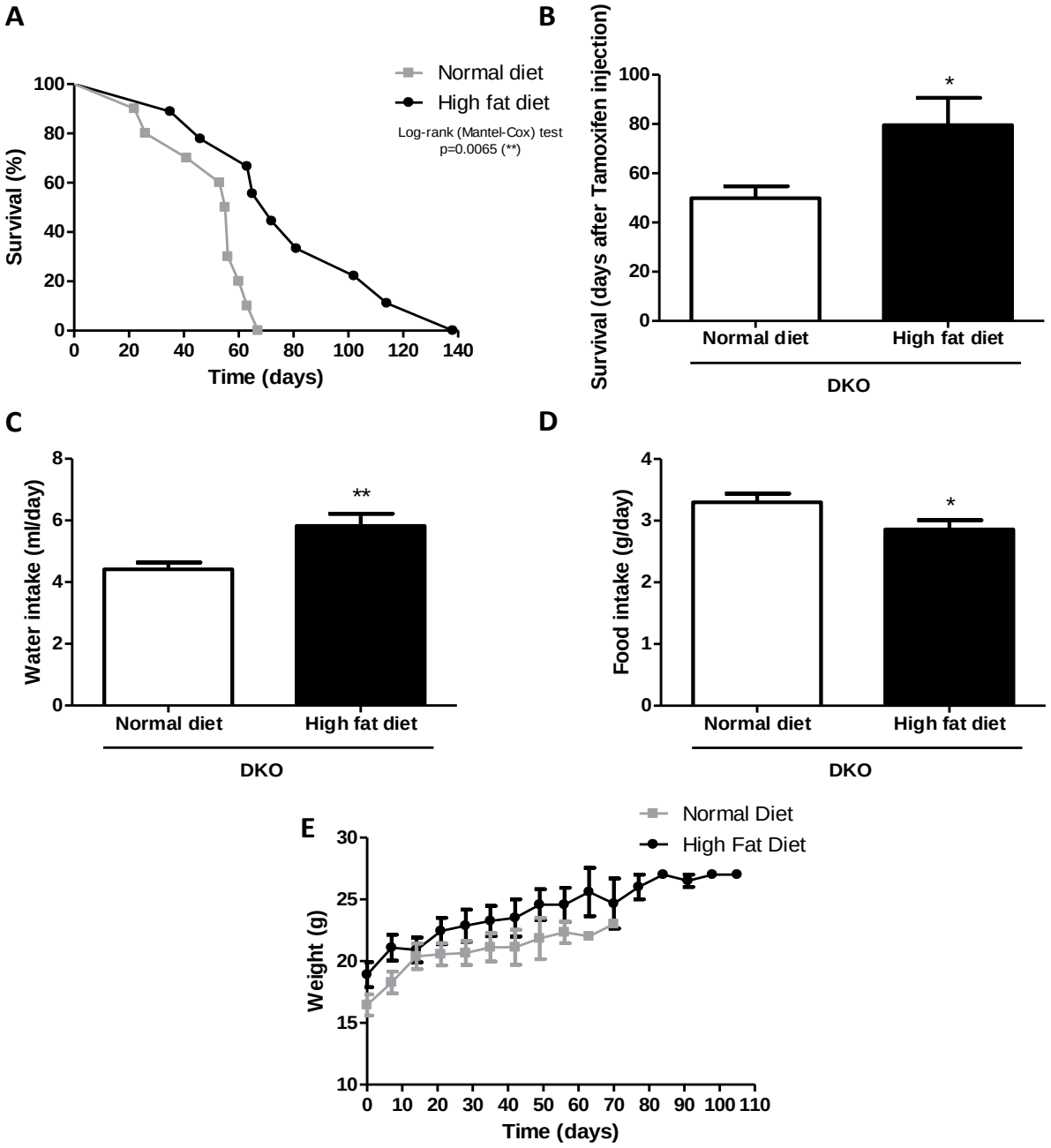


**Figure 51:** ***HFD prolongs DKO mice survival. (A)*** *Kaplan-Meier curve shows the survival percentage between DKO mice treated with normal diet and HFD.* ***(B)*** *Survival graph (days after Tamoxifen injection).* ***(C)*** *Water intake (ml/day).* ***(D)*** *Food intake (g/day).* ***(E)*** *Mice weight (g) measured every week during the experiment. Data is presented as a percentage of survival of 11 mice/group. (A). Data presents the mean ± SEM of 11 mice/group (B,C,D,E). A comparison of survival curves is done with the Log-rank (Mantel-Cox) test. *p<0.05; **p<0.01 vs. DKO mice treated with normal diet.*

### *2.3 Lipid metabolism genes modified in PTEN-KO and DKO mice*

We analyzed different genes involved in β-oxidation and ketogenesis. We saw that HMGCS2 gene, which catalyzes the first ketogenesis reaction, was not altered in mice without fasting. However, it was decreased after 2h of fasting in DKOs compared to VDR-KOs. Moreover, DKOs with 7h of fasting had statistically significant reduction of HMGCS2 in comparison with CNTs *(Figure 52A)*. Even though, we could not correlate those differences at 2h and 7h of fasting with total ketone bodies previously measured in serum *(Figure 48A)*.

BAAT, which is related to fatty acid absorption, was decreased in CNTs and VDR-KOs during fasting because it diminishes the amount of free fatty acids to absorb, while that reduction was smoothed or non-existent in PTEN-KOs and DKOs *(Figure 52B)*.

Another hepatic gene that was lowered after fasting was ANGPTL8, which increases serum triacylglycerol levels. In all the genotypes, the ANGPTL8 repression during fasting was similar. Even though, there was a slight reduction of its expression in VDR-KOs and PTEN-KOs in non-fasted animals compared with CNTs and DKOs *(Figure 52C)*.

In addition, FOXA2, which activates transcription of genes related to β-oxidation and ketogenesis, was altered in PTEN-KOs and DKOs both in mRNA *(Figure 52D)* and protein *(Figure 53)*. In CNTs and VDR-KOs, FOXA2 was deactivated after 7h of fasting, probably due to the decrease in fatty acids, while in PTEN-KOs and DKOs it was not activated neither during diet nor during 2h fasting and moreover, was progressively decreased until 7h of fasting.

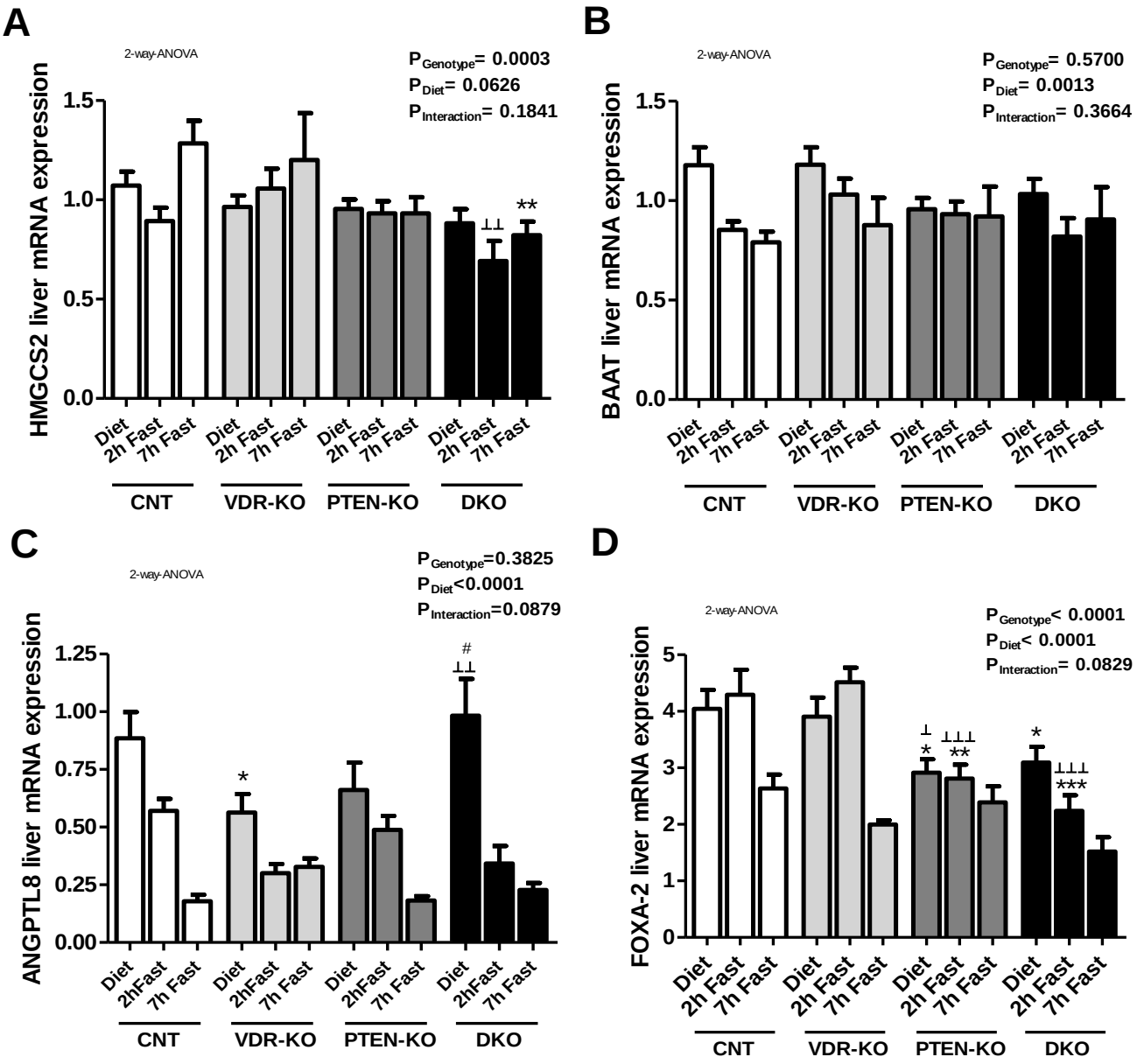


**Figure 52: Lipid metabolism disorders 1.** *Liver **(A)** HMGCS2, **(B)** BAAT, **(C)** ANGPTL8 and **(D)** FOXA-2 mRNA levels were determined by real time qRT-PCR and normalized to the mean of TBP and Ppia expression. Data presents the mean ± SEM of 15-20mice/group in diet condition, 15-20 mice/group in 2h fasting condition, 5-10 mice/group in 7h fasting condition *p<0.05; **p<0.001; *** p<0.001 vs. CNT mice with the same diet. ⊥p<0.05; ⊥⊥p<0.01; ⊥⊥⊥ p<0.001 vs. VDR-KO mice with the same diet. # p<0.05 vs. PTEN-KO with the same diet. 2-way-ANOVA gives the significance of the genotype, diet and its interaction.*

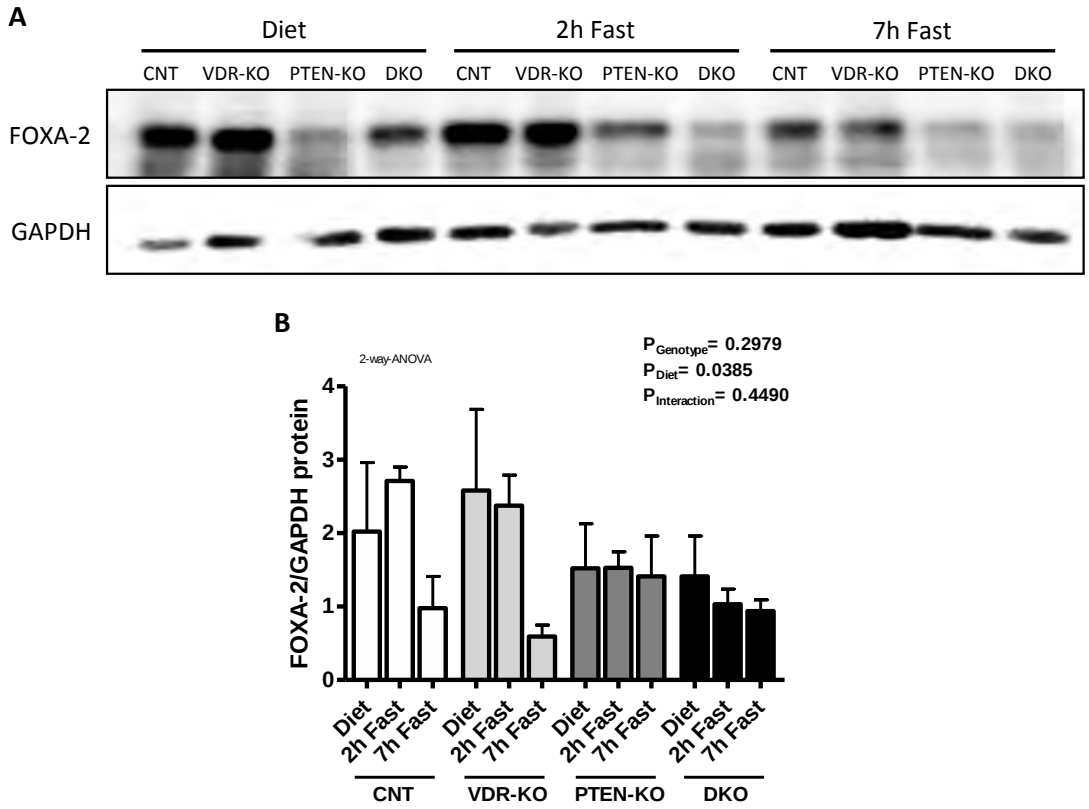


**Figure 53: Inactivation of FOXA-2 protein in PTEN-KO and DKO mice.** ***(A)*** *Representative western blot shows the FOXA-2 (52 kDa) protein expression in CNT, VDR-KO, PTEN-KO and DKO mice during diet, 2h of fasting and 7h of fasting. The same samples are blotted with GAPDH (37 kDa) as loading control and quantification reference.* ***(B)*** *FOXA-2 western blot quantification. Data presents the mean ± SEM of 3 mice/group. 2-way-ANOVA gives the significance of the genotype, diet and its interaction.*

We also studied PPARA that triggers the transcription of genes related to β-oxidation, fatty acid transport and ketogenesis, like ACOX1, CPT1 and FGF21.

PPARA gene was activated in fasting states in CNTs and VDR-KOs, whereas in PTEN-KOs there was a delayed induction and in DKOs the stimulation was really slight and only at 2h of fasting *(Figure 54A)*.

ACOX1 participates in peroxisomal β-oxidation and it responds to the early fasting states and then its levels are restored as could be observed in the CNTs and VDR-KOs. However, in PTEN-KOs the induction was delayed and in DKOs there was almost no response *(Figure 54B)*.

Levels of CPT1, which transports fatty acids, showed an induction by fasting in all groups except in DKOs, which started with lower levels and did not get induced by fasting *(Figure 54C)*.

Lastly, we measured FGF21, which is a crucial intermediate between hepatic lipid metabolism, diet and PPARA in ketonic state and we observed that FGF21 levels were increased in PTEN-KOs related to the other three groups of mice *(Figure 54D)*.

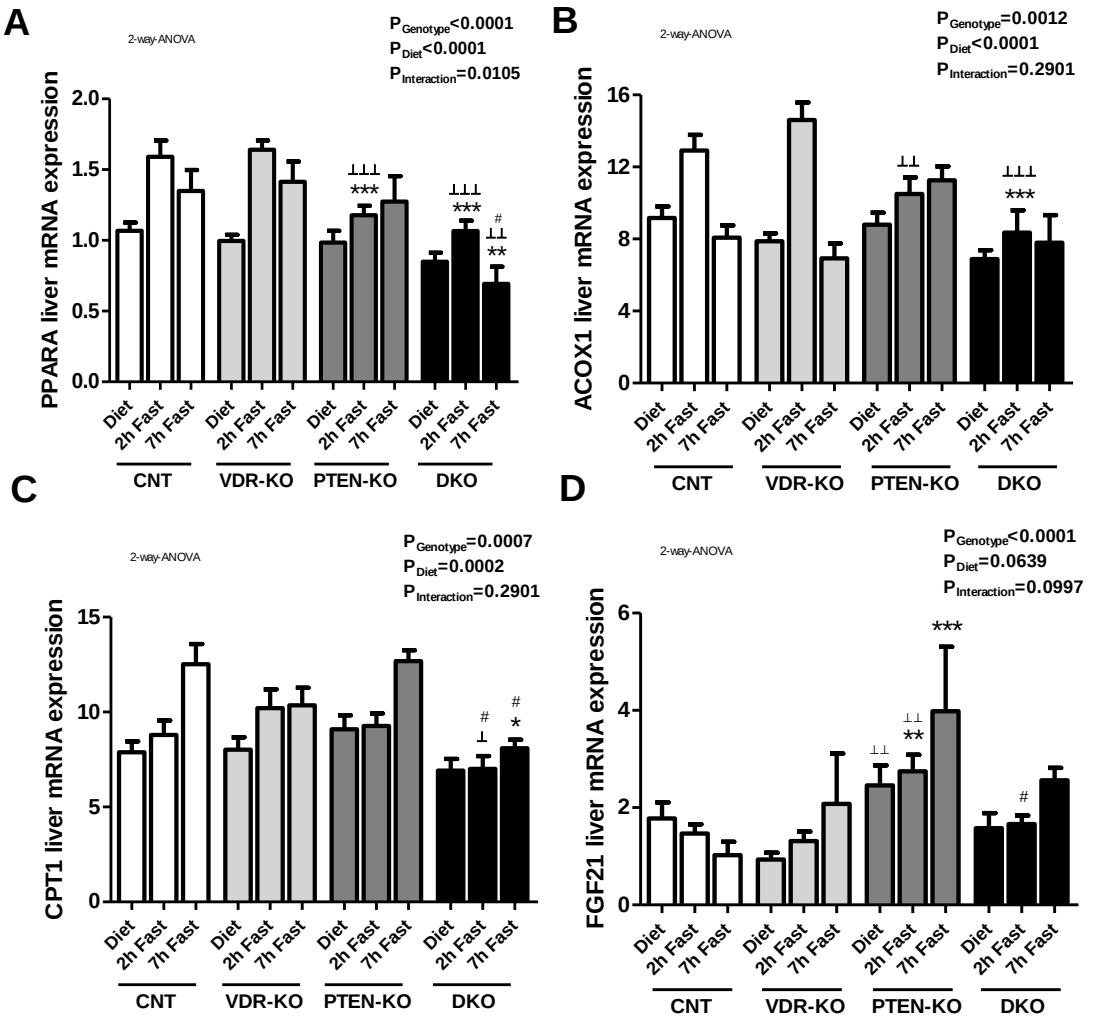


**Figure 54: Lipid metabolism disorders 2.** *Liver **(A)** PPARA, **(B)** ACOX1, **(C)** CPT1 and **(D)** FGF21 mRNA levels were determined by real time qRT-PCR and normalized to the mean of TBP and Ppia expression. Data presents the mean ± SEM of 15-20mice/group in diet condition, 15-20 mice/group in 2h fasting condition, 5-10 mice/group in 7h fasting condition *p<0.05; **p<0.001; *** p<0.001 vs. CNT mice with the same diet. ⊥p<0.05; ⊥⊥p<0.01; ⊥⊥⊥ p<0.001 vs. VDR-KO mice with the same diet. # p<0.05 vs. PTEN-KO mice with the same diet. 2-way-ANOVA gives the significance of the genotype, diet and its interaction.*

# Discussion

# 1. Analysis of the global consequences of the loss of PTEN and VDR

Conditional PTEN-KO is a highly studied mouse model in cancer. [294, 119, 303] In addition, VDR gene is also associated with malignancies as a tumor suppressor gene. [209-219] However, these two genes are also involved in some metabolic pathways like glucose and lipid metabolism, therefore, we were interested in the generation of a double KO PTEN-VDR to investigate synergies between them that promote alterations in metabolism.

PTEN-KO mouse that we used was generated in Dr. Dolcet's laboratory. They demonstrated that the loss of PTEN resulted in a high incidence of endometrial intraepithelial neoplasm, thyroid hyperplasia and prostate intraepithelial neoplasia, at 6-8 weeks after Tamoxifen injection.[294] Moreover, the injection of Tamoxifen also induced recombination in the epithelial tissue of kidney, liver, lung and colon. In any case, the loss of PTEN in those other organs did not lead to the development of neoplasms or other histological alterations.[294,304] Nevertheless, in this study, we changed the PTEN-KO mouse background due to the crossing with VDR-KO mouse.[280] Therefore, PTEN-KO and DKO mice rarely developed tumors two months after tamoxifen injection, only in some occasions in the thyroid gland and prostate. However, the first clear result that we obtained was a premature death of DKO mice compared with the two single KOs suggesting that tumors were not the cause of their death, because mice autopsies did not show tumor differences between PTEN-KO and DKO mice.

We also found severe glucose disorders and electrolytic alterations in serum and urine in both PTEN-KO and DKO mice from the beginning of the study. Ion disorders were stronger in single PTEN-KO mice than in DKO mice, thus, we focused these studies on the single PTEN-KO mice. We found low levels of $Ca^{+2}$ and high levels of P in urine indicating some mineral metabolism disorders, which are associated with chronic kidney disease and deregulation of FGF23, VD and PTH levels that tightly regulate $Ca^{+2}$ and P levels in the organism.[305–311] Although the results are not part of this doctoral thesis, we observed increased FGF23 in serum and bones and we found lower renal

levels of its receptor. Moreover, VD levels were low in serum of PTEN-KOs, in contrast to the increased 1α-hydroxylase expression in kidneys. However, serum PTH levels did not change. Therefore, loss of PTEN in mice induces a significant deregulation in mineral metabolism without changes in renal function, suggesting a key role of PTEN in the regulation of mineral metabolism. Consequently, we started a new parallel project to study the involvement of PTEN-KO mice in mineral metabolism. These investigations are not included in the present doctoral thesis because they are studies in very early stages and they had led to a new research area and a new project in our laboratory (Proyectos de Investigación en Salud del Instituto de Salud Carlos III: PI18/00610-Papel de la vía PI3K/Akt/mTOR en la regulación de las alteraciones del metabolismo mineral en la enfermedad renal crónica. Implicaciones en la regulación de la síntesis de FGF23. 212,052.52€)").

# 2. Study of the implication of PTEN and VDR genes in glucose metabolism

During the last years, insulin-signaling pathway has become a major focus of study by the scientific community to find new therapeutic targets as DM is caused by alterations in this route.

In our research, we were focused on the study of PI3K/Akt pathway and VD interactions, in glucose metabolism and in lipid metabolism. The mouse models used were tamoxifen inducible KOs for PTEN and/or VDR in the whole adult mice. On the one hand, PI3K/Akt pathway has an important role as an effector in insulin actions like activating glucose uptake and glycogen synthesis in fat and muscle tissues, [67,68] and inhibiting glucose release, gluconeogenesis and glycogenolysis in the liver.[83,84] In addition, PI3K/Akt pathway and lipogenesis are also related in the liver.[97,312] On the other hand, it has been shown that VD is involved in glucose metabolism. It has an important role in the secretion of insulin in response to glucose [195] and β-cells have VDR. [196,197,198] Furthermore, VD deficiency is common in DM patients and VD supplementation is related to lower prevalence of DM. [220,221] Full and tissue-specific conditional VDR-KO mice were generated to study their classical problems related to bone and $Ca^{+2}$ homeostasis. However, it was seen that VD was also involved in non-classical functions like cancer, diabetes, hypertension, autoimmune disorders or cardiovascular diseases. For example, it was established that VD had immunomodulatory functions that led to beneficial effects in T1DM like improving hyperglycemia; [224–226] or that VD can regulate lipid metabolism due to mitochondrial actions. [261]

The first result related to glucose metabolism obtained was that PTEN-KO and DKO mice had severe hypoglycemia. Therefore, we evaluated first if hypoglycemia was due to high insulin levels. However we detected hypoinsulinemia, in agreement to the low blood glucose levels, excluding the possibility that hypoglycemia was caused by an increase in insulin secretion. Accordingly, PTEN-KO mice showed normal pancreatic islet area, although this result does not agree with the one from Nguyen et al. who

observed increased pancreatic islet area in a β-cells-specific PTEN deficient mouse. [141] This difference could be explained by the fact that our animals had a deletion in most of the cells of the organism and different stimulus coming from fat, muscle, liver or kidney could be also modulating the size of the islets.[313] Furthermore, DKO mice showed an increase in pancreatic islets size, which could be explained due to the added effect of eliminating VDR, which is considered a tumor suppressor gene and for instance, it is published that VDR activation suppressed pancreatic tumor cells.[314] Moreover, pancreatic islets had a tendency to secrete less insulin in PTEN-KO mice, and again, this result did not correlate with Nguyen and Wang's investigations,[141,315] who observed an intact insulin secretion response to glucose administration when PTEN was absent in pancreatic cells. The reduction of insulin secretion in response to glucose is a typical β-cell alteration in T2DM.[316–318] Nonetheless, when PTEN was deleted in pancreas, mice were protected against HFD-induced DM and the insulin secretion was preserved.[315] The discrepancy of these results with our own could be justified again by the difference between full KO and tissue-specific KO. In addition, DKO mice had even less insulin secretion than PTEN-KO mice, which could be due to the fact that VD enhances insulin secretion stimulated by glucose.[319] Nevertheless, the total insulin levels inside pancreatic islets were not affected neither in PTEN-KO nor DKO mice. Therefore, we excluded the possibility that hypoglycemia was due to insulinoma or hyperinsulinemia, but as a result of a hyperstimulation of the IR, thus making mice more sensitive to insulin.

Moreover, another interesting result observed is that our DKO mice did not survive to fasting, they had signs of lethargy and nonresposiveness when food deprivation was for more than six hours. In contrast, PTEN-KO mice preserve a quite normal behavior, even though both had similar low blood glucose levels. This result in PTEN-KO mice was in contrast to what Kinross et al. [320] found in a mouse with a ubiquitous expression of a PI3K gain-of-function mutation that also presented hypoglycemia, but they could not survive four hours of fasting. This could be explained by the difference in the mutation, which means that probably, the effect of directly modifying PI3K protein is stronger than PTEN deletion, which is the negative regulator of the pathway. Even though, both models had robust increase in pAkt/Akt ratio.

Next, we focused on why DKO mice did not survive in short food starvations and also if that was the main reason of their premature death. Thus, we though that if they died in fasting, it could be due to two possibilities: they run out glucose quicker because they used it faster, or because they could not produce glucose to maintain the necessary glucose levels. Then, we performed some glucose and pyruvate tests to analyze their glucose behavior.

We studied how fast injected glucose was cleared from the bloodstream performing a GTT. The result was that DKO mice did not seem to respond to the glucose bolus, because they had a rapid return to baseline glucose levels within 20 minutes after glucose administration. This result could be elucidated by the fact that DKO mice had higher glucose uptake. Since they have hypoinsulinemia and insulin secretion defects, the increased glucose uptake has to be insulin-independent, like in the PI3K gain-of-function mutation mice,[320] or due to high insulin sensitivity. Another anomaly we found when we studied their glucose behavior in starvation was that DKO mice, in contrast with PTEN-KO mice, did not show the typical peaks and falls of blood glucose indicating again, insulin and glucagon defects.

Then, we hypothesized that DKO mouse premature death could be because of the detected sustained hypoglycemia, which in turn, could be caused by the increased glucose uptake that we observed in their whole body. Nevertheless, neither 10% sucrose treatment in drinking water nor brain glucose administration with osmotic pumps in DKO mice increased their survival. Similar results were obtained in the PI3K gain-of-function mutation mice, which was supplemented with 5% of glucose in water and it was not enough to increase its glycemia or survival.[320]

The hypoglycemia found in PTEN-KO mice is consistent with many investigations performed either with experimental models or in patients, which are related to alterations in PI3K/Akt pathway. For instance, as PTEN has a precise function for every particular tissue, there are several types of tissue specific PTEN-KO mice models, which were generated to study glucose metabolism. For example, in muscle,[131] liver,[97] pancreas[140] and fat[145] the loss of PTEN affects glucose homeostasis and consequently, they ameliorate diabetes by improving hyperglycemia. In addition, PTEN ablation in

hepatocytes and adipocytes improved blood glucose and insulin sensitivity in T2DM mice protecting them from DM.[126] For instance, the liver-specific PTEN deletion mouse had a downregulation of proteins involved in gluconeogenesis, as we also observed in our PTEN-KO mice; [97] or in adipose tissue, PTEN removal in STZ-induced diabetes resulted in elevated insulin resistance and sensitivity and increased localization of GLUT4 in the membrane of the adipocytes.[145] Moreover, an association between a PTEN polymorphism and T2DM patients had been described.[127]

After the organ-specific deletions of PTEN, a PTEN haploinsufficiency ($PTEN^{+/-}$) mouse was generated to analyze the global effect of PTEN deletion on glucose homeostasis and they observed that it was more sensitive to insulin, in agreement with our PTEN-KO mice.[148] Moreover, there are more clinical cases and experimental models that relate alterations in glucose and insulin homeostasis to PTEN deficiency. Thus, Akt overexpression in mouse liver led to hypoglycemia;[143] muscle and liver PTEN suppression turn hyperglycemia into euglycemia in diabetic mice;[126] constitutively activated PI3K mouse had sustained hypoglycemia, and hypoinsulinemia; [320] or patients with a gain-of-function mutation in Akt2 that had hypoglycemia, but contrary as we found in our PTEN-KO mice, they had hyperinsulinemia.[135,136] This could be due to a growth promoting effect of the Akt2 mutation affecting pancreas and increasing insulin release.

Furthermore, there are many published studies that have modified other PI3K/Akt pathway elements, which show alterations on glucose and insulin homeostasis. For instance, a p110α knock in (KI) mouse reveled that p110α is an important intermediate in insulin signaling. [321] In addition, elimination of p110α from the liver resulted in alterations of the insulin sensitivity and glucose homeostasis in the whole body, and in a decrease of insulin activity mediated by PI3K activity, as we observed in our PTEN-KO and DKO mice.[322] Additionally, in 2015, Kinross *et al*. developed a ubiquitous conditional p110α mutated mouse to study how the constitutively activated PI3K protein could affect to all the organs in the adulthood, which is similar to our inducible PTEN-KO mice, and they also found sustained hypoglycemia and hypoinsulinemia.[320] Furthermore, p110α inhibitors have been observed to block the phosphorylation of Akt triggered by insulin in 3T3-L1 adipocytes and L6 myotubes and to reduce insulin

sensitivity and glucose transport *in vivo*. [147] Recently, a patient with mutations in p110α had been reported, which presented persistent hypoglycemia. [323] Moreover, mice with alterations in p85α PI3K isoform also develop the same alterations that we found in our PTEN-KO and DKO mice, such as, increased insulin sensitivity and hypoglycemia due to a rise in glucose uptake in peripheral tissues in p85α deficient mice, [324] reduced activity of insulin induced by PI3K, accumulation of $PIP_3$ in the liver and defects in glucose and lipid homeostasis in p85α deleted liver-specific mice. [325,326]

Studies of VD on glucose metabolism found in the literature suggest a protector effect of VD in T1DM patients by decreasing their glycemia. Thus, VD ameliorated hyperglycemia, hypoinsulinemia and IGF1 levels in T1DM starving rats; [223] VD improved autophagy by activating insulin secretion and inhibiting apoptosis,[224] and VD treatment in T1DM subjects led to less inflammation.[225,226] In our single VDR-KO mice, we did not observe any increase in blood glucose levels. This result could be explained by the fact that the time that has passed for the loss of VDR in our mice is not enough to see effects on glucose metabolism. Additionally, another possible explanation could be that this beneficial effect of VD only occurs in DM.

According to these published investigations about PI3K/Akt and VD pathways together with the results that we obtained from our single KOs, we predicted a normal blood glucose levels in the DKO mice generated in our laboratory due to the overactivation of PI3K/Akt, which should decrease glycemia, and to the compensatory effect by the lack of VD, which should increase glycemia. However, we reported that DKO mice presented severe hypoglycemia, either in postprandial or starving state, suggesting that the hypoglycemic effect of over stimulate PI3K/Akt signaling pathway overcomes the fact of inhibiting the VD route.

Later on, we focused on studying glucose metabolism in more detail, analyzing different glucose-related tissues in PTEN and VDR single and double KOs. First, we examined whether mice had any glucose reabsorption issues in kidneys and we observed that DKO mice showed glucose in urine, whereas PTEN-KO mice only had a slight tendency. Thus, we focused on the role of PTEN and VDR deletion in glucose transporters in kidneys, which is a new insight of PTEN and VDR function.

Most of the investigations related to glucose transporters are focused on DM because it has been shown that SGLTs and GLUTs are therapeutic targets to treat hyperglycemia and its renal complications. Pharmacological blockers, like SGLT2 inhibitors,[327–329] led to glucose urine excretion in order to reduce hyperglycemia in diabetic patients, and inhibiting glucose tubular uptake protecting from renal and cardiovascular complications.[330] Their regulation is not highly understood yet, however there is some information in diabetic mice. For instance, GLUT2 was upregulated in diabetic mice related to HNF-1α and HNF-3β transcriptional acitivity.[331] Moreover, it is known that HNF-1α deficiency triggered PI3K/Akt pathway[332]. In our hypoglycemic PTEN-KO mice and in HK-2 proximal tubule cells with elimination of PTEN, we found downregulation of GLUT2 leading less reabsorption in the kidneys. In addition, SGLT2 expression was upregulated in DM and linked to activated ANG II AT1 receptors[333] and HNF-1α[334]. In our PTEN-KO, SGLT2 was also increased, which might be a compensatory mechanism to reabsorb more glucose, although it did not seem to be enough because GLUT2 was downregulated and, therefore, glucose would accumulate in the proximal tubular cells. It has also been reported that SGLT1 was increased in diabetic mice by the kinase SGK1, which transcription was stimulated by excessive glucose concentrations.[335] However, we detected decreased levels of SGLT1 *in vivo* and *in* vitro in PTEN ablated model, which could also mediate the reduction of glucose reabsorption in the proximal tubule. Hence, the global conclusion from *in vivo* and *in vitro* studies related to kidney glucose transporters was that PTEN-KO mice had a deregulation of glucose transporters expression that could be the reason of the small increase in glycosuria. Moreover, in our DKO mice all these facts were exacerbated. Although there are no data directly relating VD and kidney glucose transporters; we have found some evidences that associate VD with activation of some GLUTs in other tissues, such as, in pancreas[336] or in adipocytes[337]. Therefore, we hypothesized that the absence of VDR could increase the GLUT2 downregulation and, the subsequent glycosuria. Some studies considered glycosuria when glucose excretion was around 20-times compared to controls,[338] but we obtained a 3-fold increase. Therefore, we could not say that the loss of glucose through urine was the main reason of the hypoglycemia found in our mice, but it could contribute to it.

Following, we focused on liver because is another important regulator of glucose and lipid metabolism. Analyzing the morphology of the hepatocytes, we observed that PTEN-KO mice presented hepatocellular ballooning, which is a histological parameter used in the diagnosis of liver steatosis, and considered one of the previous steps to the accumulation of fat in the liver. It is well described in the literature that mice with liver-specific deletion of PTEN can develop liver steatosis accompanied by low body fat.[97] In addition, liver-specific PTEN KO had increased glycogen synthesis; however, we did not find it in our PTEN-KO mouse model. We detected a faster consumption of glycogen in PTEN-KO mice; hence, they had a reduced glycogen pool in fasting states to compensate their hypoglycemia. The same was happening in DKO mice, but in a more increased way. If we analyzed more precisely liver morphology, we realized that DKO mice had hepatocellular ballooning but in a lower stage than PTEN-KO mice. This result could be explained by a protective effect on liver steatosis when VDR was deleted, as demonstrated in previous studies in our laboratory where Dr. Bozic demonstrated that lack of VDR avoided HFD-induced fatty liver in apoE$^{-/-}$ mice on a HFD. Indicating that VDR could play a pro-steatotic role in non-alcoholic fatty liver disease due to stimulation of lipogenic pathways and inhibition of fat oxidation in hepatocytes. [271] Thus, an accurate study of lipid metabolism should be done in our DKO mice to confirm those preliminary findings.

Moreover, we found lower blood glucose levels (around 60 mg/dl) after 2 hours of fasting in PTEN-KO mice than Stiles et al. did in the PTEN liver-specific deletion (70 mg/dl) after 16 hours of fasting. [97] Thus, our results showed a more severe hypoglycemia model, which could be explained by the fact that our mice had PTEN ablation in all the tissues and different stimulus coming from other organs, which might modulate glucose levels. In addition, we observed gluconeogenesis impairments, reduced levels of G6PC and PEPCK in PTEN-KO mice with diet, that probably were a combination of a delayed effect of glucagon and a stronger effect of insulin that demonstrated an insulin inhibitory effect in gluconeogenesis. Accordingly, Stiles et al. also reported gluconeogenesis (PEPCK and G6PC) inhibition.[97] In addition, DKO mice also showed low glycemia after fasting and gluconeogenesis delayed activation, like PTEN-KO mice.

Furthermore, genes involved in the activation of PEPCK and G6PC or glucose transport, such as PGC1a, CEBPa and GLUT2, were activated very late, not activated or even diminished in PTEN-KO mice. Therefore, our results suggested that PTEN-KO mice presented delayed gluconeogenesis activation. Moreover, DKO mice also had retarded activation of gluconeogenesis. However, some genes (PEPCK and PGC1a) were activated before in DKO than in PTEN-KO mice. This difference could be explained by the fact that DKO mice had more acute hypoglycemia and lower survival than PTEN-KO mice; thus, they needed to generate new glucose earlier.

Regarding glucose metabolism, the results obtained from our mice and all the related literature, we assumed that almost all the alterations found in DKO mice were due to the lost of PTEN, not VDR. However, there was a clear difference in mortality between PTEN-KO and DKO mice. Therefore, we thought that the huge difference in survival between PTEN-KO mice and DKO mice should be due to another reason where VDR played a more crucial role. Hence, we focused on lipid metabolism, as it is essential to survive during starvation, as we observed in DKO mice a lean phenotype without deposition of adipose tissue.

# 3. Investigation of the role of PTEN and VDR genes in lipid metabolism and formation of ketone bodies

In the literature there are some studies associating PTEN and VDR with lipid metabolism, although it is a rather unknown field of study. On the one hand, there are investigations that linked insulin, PI3K/Akt pathway and lipogenesis in the liver.[97,312] On the other hand, it has been reported that VD is involved in mitochondrial actions and consequently in lipid metabolism because both the formation of precursors for lipid synthesis and the catabolic route occur in mitochondria. [261]

Liver PTEN deletion is also involved in the regulation of lipid metabolism stimulating the lipogenic transcription factor SREBP.[312] Moreover, Akt activates FOXO1 that regulates SREBP by repressing its transcription.[339] Thus, PTEN deletion will induce the transcription of lipogenesis and β-oxidation genes and the adipogenic-like transformation in hepatocytes.[97] Lipid metabolism is studied in liver-specific PTEN ablation but not in a full PTEN-KO or in a full PTEN-VDR KO, as we did.

Previous studies in our laboratory reported a relationship between VDR and lipid metabolism in the liver. We showed that VDR ablation protected HFD-induced liver steatosis in apoE$^{-/-}$ mice decreasing lipogenesis genes and increasing fat oxidation genes, suggesting that VDR deletion prevented fatty liver.[271] However, in the present thesis, we employed a different type of mouse model unlike the one used in the previous study. Instead of the full KO from birth, we used an inducible VDR-KO, which became adult-KO after Tamoxifen injection, mimicking a severe vitamin D deficiency.

First, we tested ketogenesis because it occurs when fatty acid oxidation produces an abundance of acetyl-CoA and the oxaloacetate is exhausted, like in a fasting state or in DM. The results indicated that PTEN-KO mice used ketone bodies even when they were not food-restricted because they could not obtain enough energy from meals, although they ate more. These alterations were found even further in DKO mice. Moreover, as we found high concentration of ketone bodies, we checked if ketoacidosis was present by measuring urine pH, finding a negative result.

Furthermore, we treated DKO mice with bicarbonate water in order to see whether we could decrease its mortality finding similar results.

We also found that PTEN-KO mice consumed all their fat storage as power source to survive, probably because they had sustained hypoglycemia. Consistently with the lack of adipose tissue deposition found in the p110α mutated mouse.[320] In consequence, we observed that they had more ketone bodies production and no body fat. Similar results were found in DKO mice.

From that point, we treated DKO mice with HFD trying to compensate the absence of lipids in their body. And finally, we found a treatment that increased DKO mice survival, which supported the theory that lipid metabolism played a very important role in the survival of DKO mice.

Next, we started with the study of the hepatic lipid metabolism genes implicated in ketogenesis and fatty acid β-oxidation and transport. First, we began with ketogenesis gene expression analysis. Although we had seen increased serum ketone bodies in mice in the postprandial period, we did not find more ketogenic gene expression. Even the opposite, the HMGCS2 gene was not activated in fasted PTEN-KO mice and were decreased in fasted DKO mice.

FOXA2 activity mediates fasting responses. Phosphorylated FOXA2 is retained in the cytoplasm by insulin signaling via PI3K/Akt pathway.[25,340] Nevertheless, when blood insulin levels drop in starvation, FOXA2 is dephosphorylated and translocated into the nucleus triggering the transcription of genes related to ketone body formation, β-oxidation, gluconeogenesis and augmented lipoprotein secretion.[26,341,342] In mice with hyperinsulinemia, FOXA2 is constantly inactive, thus, leading to the development of fatty liver and insulin resistance.[26] FOXA2 enhances ketogenesis in the liver through the activation of HMGCS2.[26] Consistent with this, we observed that FOXA2 was downregulated in postprandial state and after 2h of fasting in PTEN-KO and DKO mice. Nonetheless, this is not consistent with the increased ketone bodies concentration found in DKO mice with diet. However, we believe that the results obtained from the measurement of β-hydroxybutyrate in blood are more relevant than HMGCS2 and FOXA2 gene expression. Eventually, circulating ketone bodies are the end product of

the pathway and the energy source of DKO hypoglycemic mice. The fact that the studied ketogenic genes were not overexpressed, but ketone bodies increased, suggested that other genes involved in ketogenesis could be affected and need to be further analyzed.

Following, we checked BAAT, which is activated during meals and deactivated in starvation because it is related to fatty acid absorption. [19,343] We observed that BAAT expression was not induced in PTEN-KO mice with diet due to the lack of fatty acids. In DKO mice the same results were found.

Then, we measured ANGPTL8 that is decreased in postprandial state and raises serum triacylglycerol concentration by inhibiting LPL, which is responsible for degrade them into chylomicrons. In addition, ANGPTL8 increased levels are associated with T2DM, obesity and insulin resistance.[20,21] We found that during meals there were some differences in the total amount of ANGPTL8 between groups. However, the trend that ANGPTL8 expression followed was the same in all groups: it was reduced in fasting states; thus, AGPTL8 was not altered.

PPARA is a regulator of hepatic metabolism activated by fatty acids in response to fasting that activates the transcription of genes related to β-oxidation, fatty acid transport and ketogenesis, like ACOX1, CPT1 and FGF21. In addition, PPARA and PGC1a are acting together in fasting states to reduce lipogenesis and triacylglycerols secretion and increase fatty acid oxidation.[344]

In previous results in our laboratory, we found increased hepatic PGC1a in apoE$^{-/-}$ mice without VDR and thus, increased β-oxidation. This suggested that VDR deletion protected against fatty production and induces fatty consumption.[271] These prior findings correlated to our results regarding to PGC1a levels, which were high in PTEN-KO mice but only in a longer state of fasting, and also elevated in DKO mice but from the beginning of the starvation.

Nevertheless, the other genes that we analyzed involved in fatty acid oxidation, did not show activation, but on the contrary, they were inactivated or had a delayed response in starvation. PPARA, ACOX1 and CPT1 were delayed in PTEN-KO mice and almost inactivated during starvation in DKO mice. Therefore, the reported results in lipid

metabolism suggest that the lack of PTEN slowed down lipid metabolism and, when VDR is also deleted, the phenotype is aggravated.

CEBPa, apart from being involved in gluconeogenesis, activates genes involved in triacylglycerol synthesis and fatty acid uptake.[345,346] We observed that CEBPa was lowered in DKO mice during meals compared with PTEN-KO mice; thus, lipogenesis was reduced when both PTEN and VDR were deleted.

Furthermore, we measured FGF21 expression, which is a biomarker of hepatic lipid accumulation,[347,348] and we saw that PTEN-KO mice had activated lipogenesis during fasting states. That lipogenesis activation in PTEN-KO mice was in concordance with the state of pre-steatosis that the livers were found.[97] In contrast, DKO mice did not show increases in FGF21. Therefore, the reduced FGF21 expression in DKO mice could be explained by the anti-lipogenic effect of VDR that our laboratory described before.[271]

In summary, we have generated a PTEN-KO mouse that is a helpful model for studying insulin action in the whole body, as well as the complex interaction among insulin-sensitive organs and the complementary regulations of glucose and lipid metabolisms. In addition, we also created a PTEN-VDR KO to further study the effect of VD in lipid metabolism.

Altogether, our results demonstrate that severe hypoglycemia in PTEN-KO mice could be explained by insulin hypersensitivity, kidney glucose transporters impairment and delayed or reduced induction of key genes for gluconeogenesis. In addition, DKO mice presented similar glucose metabolism alterations, but with some differences, which aggravated their mortality, but was not enough to cause their premature death. For example, DKO mice did not survive a few hours food starvation, they suffered acutely disruptions on insulin and glucagon metabolism as the lack of peaks and falls of blood glucose, or they excreted more glucose through urine.

Moreover, comparing with PTEN-KO mice, DKO mice presented a huge increase in mortality, which might be because of the sum of all these little changes that took place in many important genes and proteins involved in glucose metabolism; but also the alterations associated with lipid metabolism.

Significantly, HFD partially reverted the premature death in DKO mice, which indicates more implication of lipid metabolism in mortality than glucose metabolism because when we treated DKO mice with sucrose in drinking water or we administrated glucose in brain with osmotic pumps they did not increase their survival. Regarding the exhaustive analysis of genes involved in lipid metabolism, we concluded that PTEN deletion delayed β-oxidation and decreased lipogenesis. Furthermore, the phenotype is aggravated when VDR is absent in DKO mice and fatty acid transport is also affected. Thus, lack of VDR enhanced severity in the phenotype acquired in PTEN deletion by altering glucose metabolism, but more acutely, lipid metabolism *(Figure 55)*.

The coincidences that our full PTEN-KO mouse model shares with tissue-specific PTEN deficient mice, highlight the significance of the PI3K/Akt pathway in insulin signaling and progress of DM and propose PTEN as a possible therapeutic target.

Consequently, if we extrapolate our DKO mice results to humans, we propose that VD levels should be clinically monitored in T1DM subjects that have lean phenotype and recurrent severe hypoglycemia. Furthermore, diet supplementation with VD and fats could reduce the risk of fatal consequences, like coma or death.

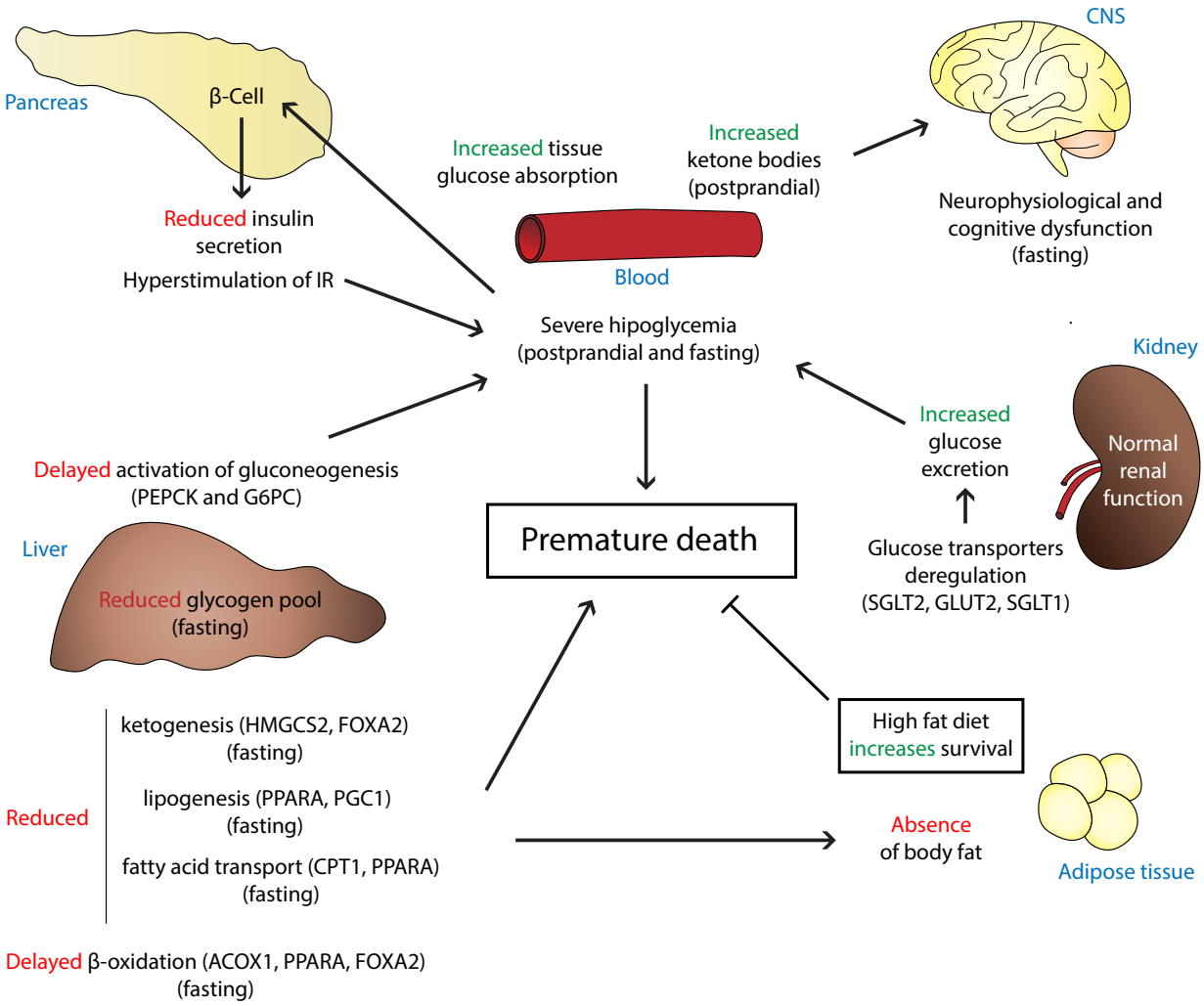


**Figure 55: Summary of *DKO premature death causes.*** *Scheme of the deregulation found in DKO mice organs, which are considered the causes of their premature death. There are alterations in pancreas (reduced insulin secretion and hyperstimulation of IR), in serum tests (severe hypoglycemia and increased ketone bodies), in kidneys (increased glycosuria due to glucose transporters deregulation), in liver (lipid metabolism and gluconeogenesis alterations and reduced glycogen reservoir) and in adipose tissue (absence of body fat). A HFD treatment increases survival in DKO mice. Figure abbreviations: β-cell, ; ACOX1, Acyl-CoA oxidase 1; CNS, central nervous system; CPT1, nitine palmitoyl transferase 1; FOXA2, Forkhead box A2; G6PC, Glucose-6-phosphatase catalytic subunit; GLUT2, Glucose transporter 2; HMGCS2, Hydroxymethylglutaryl-CoA synthase 2; IR, insulin receptor; PEPCK, Phosphoenolpyruvate carboxykinase; PGC1, Proliferator-activated receptor gamma coactivator 1 alpha; PPARA, Peroxisome proliferator-activated receptor A; SGLT1, Sodium-glucose cotransporter 1; SGLT2, Sodium-glucose cotransporter 2.*

# Conclusions

# Conclusions

1. Joined deletion of PTEN and VDR (DKO) leads to deteriorated phenotype and premature death without an increase in tumorigenesis with respect to single KO mice.

2. DKO mice do not survive short starvations showing rapid signs of lethargy and nonresposiveness, in contrast to single KO mice with similar levels of glycemia.

3. Deficiency of PTEN induces severe hypoglycemia, both in postprandial and starving state, and hypoinsulinemia due to hyperstimulation of the IR in both PTEN-KO and DKO mice.

4. PTEN ablation promotes defects on insulin secretion that are increased with the lack of VDR in DKO mice.

5. DKO mice have increased insulin-independent glucose uptake in all their tissues.

6. PTEN-KO mice and HK-2 cells with deletion of PTEN have a deregulation of renal glucose transporters expression that can explain the mild increase in glycosuria, which is exacerbated when VDR is deleted in DKO mice or in HK2 cells.

7. PTEN deletion induces a pre-steatotic state in the liver, which is attenuated by VDR ablation in DKO mice.

8. Lack of PTEN delays hepatic gluconeogenesis activation in PTEN-KO and DKO mice.

9. Sucrose or glucose supplementation does not prevent DKO mice accelerated mortality.

10. HFD treatment partially reverses the premature death in DKO mice indicating a key role of lipid metabolism on it. Moreover, PTEN-KO and DKO mice have a lean phenotype without deposition of lipids.

11. Although PTEN-KO and DKO mice eat more, they use ketone bodies even when they are not food-restricted.

12. PTEN deletion delays β-oxidation and decreases lipogenesis. This phenotype is aggravated when VDR is also absent, additionally affecting fatty acid transport in DKO mice.

# Conclusions

1. La deleció conjunta de PTEN i VDR (DKO) dóna lloc a un fenotip deteriorat i a la mort prematura, sense incrementar els tumors respecte els ratolins KO senzills.

2. Els ratolins DKO no sobreviuen a períodes curts de dejú que es manifesta amb signes ràpids de letargia i no resposta, a diferència dels ratolins KO senzills amb nivells similars de glucèmia.

3. La deficiència de PTEN indueix hipoglucèmia severa, tan en estat postprandial com en dejú, i hipoinsulinèmia deguda a la hiperestimulació del receptor de la insulina en els ratolins PTEN-KO i DKO.

4. L'ablació de PTEN promou defectes en la secreció d'insulina que encara es veuen més incrementats amb la pèrdua del VDR en els ratolins DKO.

5. Els ratolins DKO tenen incrementada la captació de glucosa en tots els teixits de manera independent a la insulina.

6. Els ratolins PTEN-KO i les cèl·lules HK-2 amb deleció de PTEN tenen una desregulació de l'expressió dels transportadors de glucosa que expliquen el lleuger increment de la glucosa en orina. Endemés, quan VDR s'elimina en els ratolins DKO, la glucosúria augmenta.

7. La deleció de PTEN en el fetge indueix un estat pre-esteatòtic, que s'atenua quan el VDR s'elimina en els ratolins DKO.

8. La manca de PTEN retarda l'activació de la gluconeogènesis en el fetge en els ratolins PTEN-KO i DKO.

9. La suplementació amb sucrosa o glucosa no impedeix la mortalitat accelerada dels ratolins DKO.

10. El tractament amb dieta alta en greix reverteix parcialment la mort prematura en els ratolins DKO, la qual cosa indica un paper important del metabolisme

lipídic. A més a més, els ratolins PTEN-KO i DKO tenen un fenotip magre sense deposicions de lípids i hipoglucèmies recurrents.

11. Tot i que els ratolins PTEN-KO i DKO mengen més, utilitzen cossos cetònics inclús quan no tenen restricció d'aliments.

12. La deleció de PTEN retarda la β-oxidació i disminueix la lipogènesis. Aquest fenotip s'agreuja quan s'elimina VDR, afectant també al transport d'àcids grassos en els ratolins DKO.

# Conclusiones

1. La depleción conjunta de PTEN y VDR (DKO) da lugar a un fenotipo deteriorado y a la muerte prematura, sin incrementar los tumores respeto a los ratones KO sencillos.

2. Los ratones DKO no sobreviven a periodos cortos de ayuno que se manifiesta con signos rápidos de letargia y no respuesta, a diferencia de los ratones KO sencillos con niveles similares de glucemia.

3. La deficiencia de PTEN induce hipoglucemia severa, tanto en estado postprandial como en ayuno e hipoinsulinemia debida a la hiperestimulación del receptor de insulina en los ratones PTEN-KO y DKO.

4. La ablación de PTEN promueve defectos en la secreción de insulina que aún están más aumentados con la pérdida de VDR en los ratones DKO.

5. Los ratones DKO tienen incrementada la captación de glucosa en los tejidos de manera independiente a la insulina.

6. Los ratones PTEN-KO y las células HK-2 con depleción de PTEN tienen una desregulación de la expresión de los transportadores de glucosa que explican el ligero incremento de la glucosa en orina. Además, cuando el VDR se elimina en los ratones DKO, la glucosuria aumenta.

7. La depleción de PTEN en el hígado induce un estado pre-esteatótico, que se atenúa cuando el VDR se elimina en los ratones DKO.

8. La falta de PTEN retarda la activación de la gluconeogénesis en el hígado en los ratones PTEN-KO y DKO.

9. La suplementación con sucrosa o glucosa no impide la mortalidad acelerada de los ratones DKO.

10. El tratamiento con dieta alta en grasa revierte parcialmente la muerte prematura en los ratones DKO, lo que indica un papel importante del metabolismo lipídico. Además, los ratones PTEN-KO y DKO tienen un fenotipo magro sin deposiciones de lípidos e hipoglucemias recurrentes.

11. Aunque los ratones PTEN-KO y DKO comen más, utilizan cuerpos cetónicos incluso cuando no tienen restricción de comida.

12. La depleción de PTEN retarda la β-oxidación y disminuye la lipogénesis. Este fenotipo empeora cuando se elimina VDR, afectando también al transporte de ácidos grasos en los ratones DKO.

# References

1. Svartberg, K., Tapper, I., Temrin, H., Radesater, T. & Thorman, S. Principles of Biochemistry. Lehninger. *Anim. Behav.* **69**, 283–291 (2005).

2. Jones & Bartlett. *Metabolism Chapter 7 THINK About It*.

3. Adeva-Andany, M. M., Pérez-Felpete, N., Fernández-Fernández, C., Donapetry-García, C. & Pazos-García, C. Liver glucose metabolism in humans. *Biosci. Rep.* **36**, 1–15 (2016).

4. Gautier-Stein, A., Mithieux, G. & Rajas, F. A Distal Region Involving Hepatocyte Nuclear Factor 4 and CAAT/Enhancer Binding Protein Markedly Potentiates the Protein Kinase A Stimulation of the Glucose-6-Phosphatase Promoter. *Mol. Endocrinol.* (2005). doi:10.1210/me.2004-0105

5. Liu, S. *et al.* Hypoglycemia and impaired hepatic glucose production in mice with a deletion of the C/EBPbeta gene. *J. Clin. Invest.* **103**, 207–13 (1999).

6. Adkins, A. *et al.* Higher insulin concentrations are required to suppress gluconeogenesis than glycogenolysis in nondiabetic humans. *Diabetes* **52**, 2213–20 (2003).

7. Adina-Zada, A., Zeczycki, T. N. & Attwood, P. V. Regulation of the structure and activity of pyruvate carboxylase by acetyl CoA. *Arch. Biochem. Biophys.* **519**, 118–30 (2012).

8. Fernandez-Marcos, P. J. & Auwerx, J. Regulation of PGC-1a, a nodal regulator of mitochondrial biogenesis 1-4. *Am J Clin Nutr* **93**, 884s-890s (2011).

9. Puigserver P1, Rhee J, Donovan J, Walkey CJ, Yoon JC, Oriente F, Kitamura Y, Altomonte J, Dong H, Accili D, S. B. Insulin-regulated hepatic gluconeogenesis through FOXO1-PGC-1alpha interaction. *Nature* **423**, 550–555 (2003).

10. Nakae, J., Silver, D. L. & Accili, D. The forkhead transcription factor Foxo1 (Fkhr) confers insulin sensitivity onto glucose-6-phosphatase expression. *J. Clin. Invest.* **108**, 1359–1367 (2001).

11. Herzig, S. *et al.* CREB regulates hepatic gluconeogenesis through the coactivator PGC-1. *Nature* **413**, 179–183 (2001).

12. Yoon, J. C. *et al.* Control of hepatic gluconeogenesis through the transcriptional coactivator PGC-1. *Nature* **413**, 131–138 (2001).

13. Brandt Poulsen, S., Fenton, R. A. & Rieg, T. Sodium-glucose cotransport. *Curr Opin Nephrol Hypertens* **24**, 463–469 (2015).

14. Pajor, A. M., Hirayama, B. A. & Wright, E. M. Molecular evidence for two renal Na+/glucose cotransporters. *Biochim. Biophys. Acta - Biomembr.* **1106**, 216–220 (1992).

15. Wilding, J. P. H. The role of the kidneys in glucose homeostasis in type 2 diabetes: Clinical implications and therapeutic significance through sodium glucose co-transporter 2 inhibitors. *Metabolism* **63**, 1228–1237 (2014).

16. Kanai, Y., Lee, W.-S., You, G., Brown, D. & Hediger, M. A. The Human Kidney Low Affinity Na+/glucose Cotransporter SGLT2 Delineation of the Major Renal Reabsorptive Mechanism for D-Glucose. *J. Clin. Invest.* **93**, 397–404 (1994).

17. Vallon, V. *et al.* SGLT2 mediates glucose reabsorption in the early proximal tubule. *J. Am. Soc. Nephrol.* **22**, 104–12 (2011).

18. Rieg, T. *et al.* Increase in SGLT1-mediated transport explains renal glucose reabsorption during genetic and pharmacological SGLT2 inhibition in euglycemia. *Am J Physiol Ren. Physiol* (2013).

19. Styles, N. *et al.* Carboxy-terminal mutations of bile acid CoA:N-acyltransferase alter activity and substrate specificity. *J. Lipid Res.* **57**, 1133–1143 (2016).

20. DiStefano, J. K. Angiopoietin-like 8 (ANGPTL8) expression is regulated by miR-143-3p in human hepatocytes. *Gene* **681**, 1–6 (2019).

21. Zhang, R. Lipasin, a novel nutritionally-regulated liver-enriched factor that regulates serum triglyceride levels. *Biochem. Biophys. Res. Commun.* **424**, 786–792 (2012).

22. Ros, E. Intestinal absorption of triglyceride and cholesterol. Dietary and pharmacological inhibition to reduce cardiovascular risk. *Atherosclerosis* **151**, 357–379 (2000).

23. Cahill, G. F. Fuel metabolism in starvation. *Annu. Rev. Nutr* **26**, 1–22 (2006).

24. Kumar Shukla, S. *et al.* HMGCS2 is a key ketogenic enzyme potentially involved in type 1 diabetes with high cardiovascular risk. *Sci. Rep.* **7**, 1–10 (2017).

25. Howell, J. J. & Stoffel, M. Nuclear Export-independent Inhibition of Foxa2 by Insulin. *J. Biol. Chem.* **284**, 24816–24824 (2009).

26. Wolfrum C1, Asilmaz E, Luca E, Friedman JM, S. M. Foxa2 regulates lipid metabolism and ketogenesis in the liver during fasting and in diabetes. *Nature* **432**, 1027–1032 (2004).

27. Mandard, S. & Kersten, S. Peroxisome proliferator-activated receptor a a target genes. *C. Cell. Mol. Life Sci* **61**, 393–416 (2004).

28. Michael K. Badman,1 Pavlos Pissios,1 Adam R. Kennedy,1 George Koukos,2 Jeffrey S. Flier, 1 & and Eleftheria Maratos-Flier1. “New” hepatic fat activates PPAR_ to maintain glucose, lipid, and cholesterol homeostasis. *Cell Press* (2007).

29. Badman, M. K. *et al.* Hepatic Fibroblast Growth Factor 21 Is Regulated by PPARa and Is a Key Mediator of Hepatic Lipid Metabolism in Ketotic States. *Cell Metab.* **5**, 426–437 (2007).

30. Inagaki, T. *et al.* Endocrine Regulation of the Fasting Response by PPARa-Mediated Induction of Fibroblast Growth Factor 21. *Cell Metab.* **5**, 415–425 (2007).

31. Siddiqui, A. A. *et al.* Diabetes: Mechanism, Pathophysiology and Management-A Review. *Int. J. Drug Dev. Res* **5**, 1–23 (2013).

32. Cho, N. H. *et al.* IDF Diabetes Atlas: Global estimates of diabetes prevalence for 2017 and projections for 2045. *Diabetes Res. Clin. Pract.* **138**, 271–281 (2018).

33. Kathleen M. Gillespie. Type 1 diabetes: pathogenesis and prevention. *CMAJ* **175**, 165–170 (2006).

34. Workgroup on Hypoglycemia, American Diabetes Association. Defining and reporting hypoglycemia in diabetes: a report from the American Diabetes Association Workgroup on Hypoglycemia. *Diabetes Care* **28**, 1245–9 (2005).

35. Cryer, P. E. Hypoglycemia in type 1 diabetes mellitus. *Endocrinol. Metab. Clin. North Am.* **39**, 641–654 (2010).

36. Cryer, P. E. Mechanisms of sympathoadrenal failure and hypoglycemia in diabetes. *Jounal Clin. Investig.* **116**, 1470–1473 (2006).

37. Gill-Carey, O. & Hattersley, A. T. Genetics and type 2 diabetes in youth. *Pediatr. Diabetes* **8**, 42–47 (2007).

38. Lingvay, I. Hypoglycemia in Type 2 Diabetes—Consequences and Risk Assessment. *US Endocrinol.* **7**, 95–102 (2011).

39. Bigner, S. H., Mark, J., Stephen Mahaley, M. & Bigner, D. D. Patterns of the early, gross chromosomal changes in malignant human gliomas. *Hereditas* **101**, 103–113 (1984).

40. Jing Li,* Clifford Yen,* Danny Liaw,* Katrina Podsypanina,* Shikha Bose, Steven I. Wang, Janusz Puc, Christa Miliaresis, Linda Rodgers, Richard McCombie, Sandra H. Bigner, Beppino C. Giovanella, Michael Ittmann, Ben Tycko, Hanina Hibshoosh, Michael H. Wig, R. P. PTEN, a Putative Protein Tyrosine Phosphatase Gene Mutated in Human Brain, Breast, and Prostate Cancer Jing. *Science (80-. ).* **270**, 1945–1954 (1995).

41. Steck, P. A. *et al.* Identification of a candidate tumour suppressor gene, MMAC1, at chromosome 10q23.3 that is mutated in multiple advanced cancers. *Nat. Genet.* **15**, 356–362 (1997).

42. Di Cristofano, A., Pesce, B., Cordon-Cardo, C. & Pandolfi, P. P. Pten is essential for embryonic development and tumour suppression. *Genet. - Nat.* **19**, 348–355 (1998).

43. Suzuki, A. *et al.* High cancer susceptibility and embryonic lethality associated with mutation of the PTEN tumor suppressor gene in mice. *Curr. Biol.* **8**, 1169–1178 (1998).

44. Ramaswamy, S. *et al. Regulation of G 1 progression by the PTEN tumor suppressor protein is linked to inhibition of the phosphatidylinositol 3-kinaseAkt pathway*. *Proc Natl Acad Sci U S A.* **96**, (1999).

45. Malaney, P., Uversky, V. N. & Davé, V. PTEN proteoforms in biology and disease. *Cell. Mol. Life Sci.* **74**, 2783–2794 (2017).

46. Pulido, R. PTEN: A yin-yang master regulator protein in health and disease. *Methods* **77–78**, 3–10 (2015).

47. Benjamin D. Hopkins, Barry Fine, Nicole Steinbach, Meaghan Dendy, Zachary Rapp, Jacquelyn Shaw, Kyrie Pappas, Jennifer S. Yu, Cindy Hodakoski, Sarah Mense, Joshua Klein, Sarah Pegno, Maria-Luisa Sulis, Hannah Goldstein, Benjamin Amendolara, Liang Lei, Mat, R. P. A Secreted PTEN Phosphatase That Enters Cells to Alter Signaling and Survival. *Science (80-. ).* **341**, (2013).

48. Leslie, N. R., Kriplani, N., Hermida, M. A., Alvarez-Garcia, V. & Wise, H. M. The PTEN protein: cellular localization and post-translational regulation. *Biochem. Soc. Trans.* **44**, 273–278 (2016).

49. Lee, J.-O. *et al.* Crystal Structure of the PTEN Tumor Suppressor: Implications for Its Phosphoinositide Phosphatase Activity and Membrane Association. *Cell* **99**, 323–334 (1999).

50. Tesio, M., Trinquand, A., Macintyre, E. & Asnafi, V. Oncogenic PTEN functions and models in T-cell malignancies. *Oncogene* **35**, 3887–3896 (2015).

51. Georgescu, M.-M. *et al. Stabilization and Productive Positioning Roles of the C2 Domain of PTEN Tumor Suppressor*. *CANCER RESEARCH* **60**, (2000).

52. Hollander, M. C., Blumenthal, G. M. & Dennis, P. A. PTEN loss in the continuum of common cancers, rare syndromes and mouse models. *Nature Reviews Cancer* **11**, 289–301 (2011).

53. Worby, C. A. & Dixon, J. E. PTEN. *Annu. Rev. Biochem* **83**, 641–669 (2014).

54. Vivanco I, S. C. The phosphatidylinositol 3-Kinase AKT pathway in human cancer. *Nat. Rev. Cancer* 489–501 (2002). doi:10.1038/nrc839

55. Sup Song, M., Salmena, L. & Paolo Pandolfi, P. The functions and regulation of the PTEN tumour suppressor. *Mol. cell Biol. - Nat. Rev.* **13**, (2012).

56. Papadatos-Pastos, D., Rabbie, R., Ross, P. & Sarker, D. The role of the PI3K pathway in colorectal cancer. *Crit. Rev. Oncol. Hematol.* **94**, 18–30 (2015).

57. Thorpe, L. M., Yuzugullu, H. & Zhao, J. J. PI3K in cancer: divergent roles of isoforms, modes of activation and therapeutic targeting. *Nat. Rev. Cancer* **15**, 7–24 (2015).

58. Courtney, K. D., Corcoran, R. B. & Engelman, J. A. The PI3K pathway as drug target in human cancer. *J. Clin. Oncol.* **28**, 1075–1083 (2010).

59. Michael E.Pacold, S. S. & Olga Perisic, Samuel Lara-Gonzalez, Colin T.Davis, Edward H.Walker, Phillip T.Hawkins, LenStephens, John F.Eccleston, R. L. W. Crystal Structure and Functional Analysis of Ras Binding to Its Effector Phosphoinositide 3-Kinase gamma. *Cell Press* (2000).

60. Rodriguez-Viciana, P. *et al.* Phosphatidylinositol-3-OH kinase as a direct target of Ras. *Nature* **370**, 527–532 (1994).

61. Alessi, D. R. *et al.* 3-Phosphoinositide-dependent protein kinase-1 (PDK1): structural and functional homology with the Drosophila DSTPK61 kinase. *Curr. Biol.* 776–789 (1997).

62. Sarbassov, D. D., Guertin, D. A., Ali, S. M. & Sabatini, D. M. Phosphorylation and Regulation of Akt/PKB by the Rictor-mTOR Complex. *Science (80-. ).* **307**, (2005).

63. Surucu, B., Bozulic, L., Hynx, D., Parcellier, A. & Hemmings, B. A. In Vivo Analysis of Protein Kinase B (PKB)/Akt Regulation in DNA-PKcs-null Mice Reveals a Role for PKB/Akt in DNA Damage Response and Tumorigenesis * □ S. *J. Biol. Chem.* **283**, 30025–30033 (2008).

64. Bozulic, L., Surucu, B., Hynx, D. & Hemmings, B. A. PKBa/Akt1 Acts Downstream of DNA-PK in the DNA Double-Strand Break Response and Promotes Survival. *Mol. Cell* **30**, 203–213 (2008).

65. Liu, J.-L. *et al.* Cell Cycle–Dependent Nuclear Export of Phosphatase and Tensin Homologue Tumor Suppressor Is Regulated by the Phosphoinositide-3-Kinase Signaling Cascade. *Cancer Res.* **67**, 11054–11063 (2007).

66. Tamgune, T. & Stokoe, D. New insights into PTEN. *J. Cell Sci.* **120**, 4071–4079 (2007).

67. Duan, C., Li, M. & Rui, L. SH2-B Promotes Insulin Receptor Substrate 1 (IRS1)-and IRS2-mediated Activation of the Phosphatidylinositol 3-Kinase Pathway in Response to Leptin* Downloaded from. *J. Biol. Chem.* **279**, 43684–43691 (2004).

68. Bijur, G. N. & Jope, R. S. Opposing actions of phosphatidylinositol 3-kinase and glycogen synthase kinase-3β in the regulation of HSF-1 activity. *J. Neurochem.* **75**, 2401–2408 (2000).

69. Beurel, E., Grieco, S. F. & Jope, R. S. Glycogen synthase kinase-3 (GSK3): regulation, actions, and diseases. *Pharmacol Ther* **0**, 114–131 (2015).

70. Bhat, R. V *et al.* Regulation and localization of tyrosine 216 phosphorylation of glycogen synthase kinase-3 in cellular and animal models of neuronal degeneration. *PNAS* **97**, 11074–11079 (2000).

71. Liu, Z., Tanabe, K., Bernal-Mizrachi, E. & Permutt, M. A. Mice with beta cell overexpression of glycogen synthase kinase-3β have reduced beta cell mass and proliferation. *Diabetologia* **51**, 623–631 (2008).

72. Kaneto, H. *et al.* Oxidative stress and the JNK pathway in diabetes. *Curr. Diabetes Rev.* **1**, 65–72 (2005).

73. Kaneto Taka-aki Matsuoka Yoshihisa Nakatani Dan Kawamori Takeshi Miyatsuka Munehide Matsuhisa Yoshimitsu Yamasaki, H. Oxidative stress, ER stress, and the JNK pathway in type 2 diabetes. *J Mol Med* **83**, 429–439 (2005).

74. Zou, Y. *et al.* DNA Hypermethylation of CREB3L1 and Bcl-2 Associated with the Mitochondrial-Mediated Apoptosis via PI3K/Akt Pathway in Human BEAS-2B Cells Exposure to Silica Nanoparticles. *PLoS One* (2016). doi:10.1371/journal.pone.0158475

75. Brownlee, M. A radical explanation for glucose-induced b b cell dysfunction. *J Clin Invest* **112**, 1788–1790 (2003).

76. Zhang, Y. *et al.* Diabetes mellitus and Alzheimer's disease: GSK-3β as a potential

link. *Behav. Brain Res.* **339**, 57–65 (2018).

77. Wang, Y. *et al.* Inactivation of GSK-3 by Metallothionein Prevents Diabetes-Related Changes in Cardiac Energy Metabolism, Inflammation, Nitrosative Damage, and Remodeling. *Diabetes* **58**, 1391–1402 (2009).

78. Eguez, L. *et al.* Full intracellular retention of GLUT4 requires AS160 Rab GTPase activating protein. *Cell Metab.* **2**, 263–272 (2005).

79. Hosseini Khorami, S. A., Movahedi, A., Huzwah, K., Mutalib, A. & Sokhini, M. PI3K/AKT pathway in modulating glucose homeostasis and its alteration in Diabetes. *Ann. Med. Biomed. Sci.* (2015).

80. Sale, E. M. & Sale, G. J. Review Protein kinase B: signalling roles and therapeutic targeting. *Cell. Mol. Life Sci.* 113–127 (2008). doi:10.1007/s00018-007-7274-9

81. Hajduch, E., Litherland, G. J. & Hundal, H. S. Protein kinase B (PKB/Akt) - A key regulator of glucose transport? *FEBS Lett.* **492**, 199–203 (2001).

82. Whiteman, E. L., Cho, H. & Birnbaum, M. J. Role of Akt/protein kinase B in metabolism. *Trends Endocrinol. Metab.* **13**, 444–451 (2002).

83. Logie, L. *et al.* Characterization of a Protein Kinase B Inhibitor In Vitro and in Insulin-Treated Liver Cells. *Diabetes* **56**, 2218–2227 (2007).

84. Li, X., Monks, B., Ge, Q. & Birnbaum, M. J. Akt/PKB regulates hepatic metabolism by directly inhibiting PGC-1a transcription coactivator. *Nature* **447**, 1012–1017 (2007).

85. Cho, H. *et al.* Insulin resistance and a diabetes mellitus-like syndrome in mice lacking the protein kinase Akt2 (PKB beta). *Science (80-. ).* **292**, 1728–31 (2001).

86. George, S. *et al.* A family with severe insulin resistance and diabetes due to a mutation in AKT2. *Science* **304**, 1325–8 (2004).

87. Elghazi, L., Rachdi, L., Weiss, A. J., Cras-Méneur, C. & Bernal-Mizrachi, E. Regulation of β-cell mass and function by the Akt/protein kinase B signalling pathway. *Diabetes, Obes. Metab.* **9**, 147–157 (2007).

88. Cleasby, M. E., Reinten, T. A., Cooney, G. J., James, D. E. & Kraegen, E. W. Functional Studies of Akt Isoform Specificity in Skeletal Muscle in Vivo; Maintained Insulin Sensitivity Despite Reduced Insulin Receptor Substrate-1 Expression. *Mol. Endocrinol.* **21**, 215–228 (2007).

89. Bouzakri, K. *et al.* siRNA-based gene silencing reveals specialized roles of IRS-1/Akt2 and IRS-2/Akt1 in glucose and lipid metabolism in human skeletal muscle. *Cell Metab.* 89–96 (2006). doi:10.1016/j.cmet.2006.04.008

90. Jiang, Z. Y. *et al.* Insulin signaling through Aktprotein kinase B analyzed by small interfering RNA-mediated gene silencing. *PNAS* **100**, 7569–7574 (2003).

91. Kim, Y.-B., Henry, R. R. & Kahn, B. B. Normal insulin-dependent activation of Akt/protein kinase B, with diminished activation of phosphoinositide 3-kinase, in muscle in type 2 diabetes-pdf. *J Clin Invest* **104**, (1999).

92. Weinhouse, S., Warburg, O., Burk, D. & Schade, A. L. On respiratory impariment in cancer cells. *Science (80-. ).* **124**, 267–272 (1956).

93. Fang, M. *et al.* The ER UDPase ENTPD5 Promotes Protein N-Glycosylation, the Warburg Effect, and Proliferation in the PTEN Pathway. *Cell* **143**, 711–724 (2010).

94. Fröjdö, S. *et al.* Phosphoinositide 3-kinase as a novel functional target for the regulation of the insulin signaling pathway by SIRT1. *Mol. Cell. Endocrinol.* **335**, 166–176 (2011).

95. Ono, H. *et al.* Regulation of Phosphoinositide Metabolism, Akt Phosphorylation, and Glucose Transport by PTEN (Phosphatase and Tensin Homolog Deleted on Chromosome 10) in 3T3-L1 Adipocytes. *Mol. Endocrinol.* **15**, 1411–1422 (2001).

96. Chen, C.-Y., Chen, J., He, L. & Stiles, B. L. PTEN: Tumor Suppressor and Metabolic Regulator. *Front. Endocrinol. (Lausanne).* **9**, 1–12 (2018).

97. Stiles, B. *et al.* Liver-specific deletion of negative regulator Pten results in fatty liver and insulin hypersensitivity. *PNAS* **101**, 2082–2087 (2004).

98. Horie, Y. *et al.* Hepatocyte-specific Pten deficiency results in steatohepatitis and hepatocellular carcinomas. *J. Clin. Invest.* **113**, 1774–1783 (2004).

99. Porstmann, T. *et al.* Cell Metabolism SREBP Activity Is Regulated by mTORC1 and Contributes to Akt-Dependent Cell Growth. *Cell Metab.* **8**, 224–236 (2008).

100. Matsumoto, M., Kitamura, T., Accili, D. & Han, S. Dual role of transcription factor FoxO1 in controlling hepatic insulin sensitivity and lipid metabolism. *J. Clin. Invest.* **116**, 2464–2472 (2006).

101. Palian, B. M. *et al.* Maf1 Is a Novel Target of PTEN and PI3K Signaling That Negatively Regulates Oncogenesis and Lipid Metabolism. *PLoS Genet.* **10**, e1004789 (2014).

102. Johnson, D. L. & Stiles, B. L. Maf1, A New PTEN Target Linking RNA and Lipid Metabolism. *Trends Endocrinol. Metab.* **27**, 742–750 (2016).

103. Bonhoure, N. *et al.* Loss of the RNA polymerase III repressor MAF1 confers obesity resistance. *Genes Dev.* **29**, 934–947 (2015).

104. Li, C. *et al.* PI3K/AKT signaling regulates bioenergetics in immortalized hepatocytes. *Free Radic. Biol. Med.* **60**, 29–40 (2013).

105. Arciuch, V. G., Galli, S., Franco, M. C., Lam, P. Y. & Cadenas, E. Akt1 Intramitochondrial Cycling Is a Crucial Step in the Redox Modulation of Cell Cycle Progression. *PLoS One* **4**, e7523 1-13 (2009).

106. Ferber, E. C. *et al.* FOXO3a regulates reactive oxygen metabolism by inhibiting mitochondrial gene expression. *Cell Death Differ.* **19**, 968–979 (2012).

107. Li, Y. *et al.* Phosphatase and Tensin Homolog Deleted on Chromosome 10 (PTEN) Signaling Regulates Mitochondrial Biogenesis and Respiration via Estrogen-related Receptor (ERR) *. *J. Biol. Chem.* **288**, 25007–25024 (2013).

108. Piantadosi, C. A. & Suliman, H. B. Mitochondrial Transcription Factor A Induction by Redox Activation of Nuclear Respiratory Factor 1 *. *J. Biol. Chem.* **281**, 324–333 (2006).

109. Podsypanina, K. *et al.* Mutation of PtenMmac1 in mice causes neoplasia in multiple organ systems. *PNAS* **96**, 1563–1568 (1999).

110. Stambolic, V. *et al.* High incidence of breast and endometrial neoplasia resembling human Cowden syndrome in pten(+/-) mice. *Cancer Res.* **60**, 3605–3611 (2000).

111. Freeman, D. *et al.* Genetic background controls tumor development in Pten-deficient mice. *Cancer Res.* **66**, 6492–6496 (2006).

112. Backman, S. A. *et al.* Deletion of Pten in mouse brain causes seizures, ataxia and defects in soma size resembling Lhermitte-Duclos disease. *Nat. Genet.* **29**, 396–403 (2001).

113. Kwon, C.-H. *et al.* Pten regulates neuronal soma size: a mouse model of Lhermitte-Duclos disease. *Nat. Genet.* **29**, 404–411 (2001).

114. Alimonti, A. *et al.* Subtle variations in Pten dose determine cancer susceptibility. *Nat. Genet.* **42**, 454–458 (2010).

115. Trotman, L. C. *et al.* Pten Dose Dictates Cancer Progression in the Prostate. *PloS Biol.* **1**, 385–396 (2003).

116. Lesche, R. *et al.* Cre/loxP-mediated inactivation of the murine Pten tumor suppressor gene. *Genesis* **32**, 148–9 (2002).

117. Knobbe, C. B., Lapin, V., Suzuki, A. & Mak, T. W. The roles of PTEN in development, physiology and tumorigenesis in mouse models: A tissue-by-tissue survey. *Oncogene* **27**, 5398–5415 (2008).

118. Suzuki, A., Nakano, T., Mak, T. W. & Sasaki, T. Portrait of PTEN: Messages from mutant mice. *Cancer Sci.* **99**, 209–213 (2008).

119. Korpershoek, E. *et al.* Conditional Pten knock-out mice: a model for metastatic phaeochromocytoma. *J. Pathol.* **217**, 597–604 (2009).

120. Li, G. *et al.* Conditional loss of PTEN leads to precocious development and neoplasia in the mammary gland. *Development* **129**, 4159–4170 (2002).

121. Kwon, C.-H. *et al.* Pten Loss Causes Hypertrophy and Increased Proliferation of Astrocytes In vivo . *Cancer Res.* **64**, 7773–7779 (2005).

122. Ogg, S. & Ruvkun, G. The C. elegans PTEN Homolog, DAF-18, Acts in the Insulin Receptor-like Metabolic Signaling Pathway. *Mol. Cell* **2**, 887–893 (1998).

123. Mihaylova, V. T., Borland, C. Z., Manjarrez, L., Stern, M. J. & Sun, H. The PTEN tumor suppressor homolog in Caenorhabditis elegans regulates longevity and dauer formation in an insulin receptor-like signaling pathway. *Proc. Natl. Acad. Sci. U. S. A.* **96**, 7427–32 (1999).

124. Vollenweider, P. *et al. An SH2 Domain-Containing 5 Inositolphosphatase Inhibits*

*Insulin-Induced GLUT4 Translocation and Growth Factor-Induced Actin Filament Rearrangement*. *MOLECULAR AND CELLULAR BIOLOGY* **19**, (1999).

125. Nakashima, N., Sharma, P. M., Imamura, T., Bookstein, R. & Olefsky, J. M. The tumor suppressor PTEN negatively regulates insulin signaling in 3T3-L1 adipocytes. *J. Biol. Chem.* **275**, 12889–95 (2000).

126. Butler, M. *et al.* Specific Inhibition of PTEN Expression Reverses Hyperglycemia in Diabetic Mice. *Diabetes* **51**, 1028–1034 (2002).

127. Ishihara, H. *et al.* Association of the polymorphisms in the 5'-untranslated region of PTEN gene with type 2 diabetes in a Japanese population. *FEBS Lett.* **554**, 450–454 (2003).

128. Vaag, A., Henriksen, J. E. & Beck-Nielsen, H. Decreased insulin activation of glycogen synthase in skeletal muscles in young nonobese Caucasian first-degree relatives of patients with non-insulin-dependent diabetes mellitus. *J. Clin. Invest.* **89**, 782–8 (1992).

129. Zisman, A. *et al.* Targeted disruption of the glucose transporter 4 selectively in muscle causes insulin resistance and glucose intolerance. *Nat. Med.* **6**, 924–928 (2000).

130. Brüning, J. C. *et al.* A Muscle-Specific Insulin Receptor Knockout Exhibits Features of the Metabolic Syndrome of NIDDM without Altering Glucose Tolerance. *Mol. Cell* **2**, 559–569 (1998).

131. Wijesekara, N. *et al.* Muscle-Specific Pten Deletion Protects against Insulin Resistance and Diabetes. *Mol. Cell. Biol.* **25**, 1135–1145 (2005).

132. Lo, Y. T., Tsao, C. J., Liu, I. M., Liou, S. S. & Cheng, J. T. Increase of PTEN Gene Expression in Insulin Resistance. *Horm. Metab. Res.* **36**, 662–666 (2004).

133. Shearn, C. T. *et al.* Short Term Feeding of a High Fat Diet Exerts an Additive Effect on Hepatocellular Damage and Steatosis in Liver-Specific PTEN Knockout Mice. *PLoS One* **9**, e96553 (2014).

134. He, L. *et al.* The Critical Role of AKT2 in Hepatic Steatosis Induced by PTEN Loss. *Am. J. Pathol.* **176**, 2302–2308 (2010).

135. Hussain, K. *et al.* An Activating Mutation of AKT2 and Human Hypoglycemia. *Science (80-. ).* **334**, 474 (2011).

136. Arya, V. B. *et al.* Activating AKT2 Mutation: Hypoinsulinemic Hypoketotic Hypoglycemia. *J. Clin. Endocrinol. Metab.* **99**, 391–394 (2014).

137. Granados, A., Eng, C. & Diaz, A. Brothers with germline PTEN mutations and persistent hypoglycemia, macrocephaly, developmental delay, short stature, and coagulopathy. *J. Pediatr. Endocrinol. Metab.* **26**, 137–141 (2013).

138. Iida, S. *et al.* Accelerated decline of blood glucose after intravenous glucose injection in a patient with Cowden disease having a heterozygous germline mutation of the PTEN/MMAC1 gene. *Anticancer Res.* **20**, 1901–1904 (2000).

139. Patil, I., Sancheti, H., Stiles, B. L. & Cadenasid, E. Brain metabolic and functional alterations in a liver-specific PTEN knockout mouse model. *PLoS One* **13**, (2018).

140. Stiles, B. L. *et al.* Selective deletion of Pten in pancreatic beta cells leads to increased islet mass and resistance to STZ-induced diabetes. *Mol. Cell. Biol.* **26**, 2772–81 (2006).

141. Nguyen, K.-T. T. *et al.* Essential role of Pten in body size determination and pancreatic beta-cell homeostasis in vivo. *Mol. Cell. Biol.* **26**, 4511–4518 (2006).

142. Tong, Z. *et al.* Pancreas-specific Pten deficiency causes partial resistance to diabetes and elevated hepatic AKT signaling. *Cell Res.* **19**, 710–719 (2009).

143. Ono, H. *et al.* Hepatic Akt activation induces marked hypoglycemia, hepatomegaly, and hypertriglyceridemia with sterol regulatory element binding protein involvement. *Diabetes* **52**, 2905–2913 (2003).

144. Cline, G. W. *et al.* Effects of a novel glycogen synthase kinase-3 inhibitor on insulin-stimulated glucose metabolism in Zucker diabetic fatty (fa/fa) rats. *Diabetes* **51**, 2903–2910 (2002).

145. Kurlawalla-Martinez, C. *et al.* Insulin Hypersensitivity and Resistance to Streptozotocin-Induced Diabetes in Mice Lacking PTEN in Adipose Tissue. *Mol. Cell. Biol.* **25**, 2498–2510 (2005).

146. Mosser, V. A., Li, Y. & Quon, M. J. PTEN Does Not Modulate GLUT4 Translocation in Rat Adipose Cells under Physiological Conditions. *Biochem. Biophys. Res. Commun.* **288**, 1011–1017 (2001).

147. Knight, Z. A. *et al.* A Pharmacological Map of the PI3-K Family Defines a Role for p110α in Insulin Signaling. *Cell* **125**, 733–747 (2006).

148. Wong, J. T. *et al.* Pten (phosphatase and tensin homologue gene) haploinsufficiency promotes insulin hypersensitivity. *Diabetologia* **50**, 395–403 (2007).

149. Wolf, G. The Discovery of Vitamin D: The Contribution of Adolf Windaus. *Am. Soc. Nutr. Sci. J. Nutr.* **134**, 1299–1302 (2004).

150. Deluca, H. F. History of the discovery of vitamin D and its active metabolites. *Bonekey Rep.* **3**, 1–8 (2014).

151. Bikle, D. Vitamin D : Production , Metabolism , and Mechanisms of Action. *Endotext* (2017).

152. Norman, A. W., Song, X., Zanello, L., Bula, C. & Okamura, W. H. Rapid and genomic biological responses are mediated by different shapes of the agonist steroid hormone, 1α,25(oh)2vitamin d3. *Steroids* **64**, 120–128 (1999).

153. Kulie, T., Groff, A., Redmer, J., Hounshell, J. & Schrager, S. Vitamin D: an evidence-based review. *J. Am. Board Fam. Med.* **22**, 698–706 (2009).

154. Bikle, D. D. Vitamin D regulated keratinocyte differentiation. *J. Cell. Biochem.* **92**, 436–44 (2004).

155. Valdivielso, J. M., Coll, B. & Fernandez, E. Vitamin D and the vasculature: can we teach an old drug new tricks? *Expert Opin. Ther. Targets* **13**, 29–38 (2009).

156. Omdahl, J. L., Morris, H. A. & May, B. K. Hydroxylase enzymes of the vitamin D pathway: expression, function, and regulation. *Annu. Rev. Nutr.* **22**, 139–66 (2002).

157. Haussler, M. R. *et al.* The Nuclear Vitamin D Receptor: Biological and Molecular Regulatory Properties Revealed. *J. Bone Miner. Res.* **13**, 325–349 (1998).

158. Boström, K. *et al.* Bone morphogenetic protein expression in human atherosclerotic lesions. *J. Clin. Invest.* **91**, 1800–9 (1993).

159. Brumbaugh, P. F. & Haussler, M. R. 1 Alpha,25-dihydroxycholecalciferol receptors in intestine. I. Association of 1 alpha,25-dihydroxycholecalciferol with intestinal mucosa chromatin. *J. Biol. Chem.* **249**, 1251–1257 (1974).

160. Deeb, K. K., Trump, D. L. & Johnson, C. S. Vitamin D signalling pathways in cancer: potential for anticancer therapeutics. *Nat. Rev. Cancer* **7**, 684–700 (2007).

161. Mellon, W. S. & DeLuca, H. F. An equilibrium and kinetic study of 1,25-dihydroxyvitamin D3 binding to chicken intestinal cytosol employing high specific activity 1,25-dihydroxy[3H-26, 27]vitamin D3. *Arch. Biochem. Biophys.* **197**, 90–95 (1979).

162. Dusso, A. S., Brown, A. J. & Slatopolsky, E. Vitamin D. *Am. J. Physiol. Physiol.* **289**, F8–F28 (2005).

163. Clemens, T. L. *et al.* Immunocytochemical Localization of the 1,25-Dihydroxyvitamin D 3 Receptor in Target Cells. *Endocrinology* **122**, 1224–1230 (1988).

164. Barsony, J., Pike, J. W., DeLuca, H. F. & Marx, S. J. Immunocytology with microwave-fixed fibroblasts shows 1 alpha,25-dihydroxyvitamin D3-dependent rapid and estrogen-dependent slow reorganization of vitamin D receptors. *J. Cell Biol.* **111**, 2385–2395 (1990).

165. Zanello, L. P. & Norman, A. W. Rapid modulation of osteoblast ion channel responses by 1,25(OH)2-vitamin D3 requires the presence of a functional vitamin D nuclear receptor. *PNAS* **101**, 1589–1594 (2004).

166. Falzon, M. DNA sequences in the rat parathyroid hormone-related peptide gene responsible for 1,25-dihydroxyvitamin D3-mediated transcriptional repression. *Mol. Endocrinol.* **10**, 672–681 (1996).

167. Maeda, A. *et al.* Critical role of parathyroid hormone (PTH) receptor-1 phosphorylation in regulating acute responses to PTH. *PNAS* **110**, 5864–5869 (2013).

168. Meng, K. *et al.* Calcium Sensing Receptor Modulates Extracellular Calcium Entry and Proliferation via TRPC3/6 Channels in Cultured Human Mesangial Cells. *PLoS One* **9**, 1–11 (2014).

169. Holick, M. F. Vitamin D: A millenium perspective. *J. Cell. Biochem.* **88**, 296–307 (2003).

170. Brown, A. J., Krits, I. & Armbrecht, H. J. Effect of age, vitamin D, and calcium on the regulation of rat intestinal epithelial calcium channels. *Arch. Biochem. Biophys.* **437**, 51–58 (2005).

171. Kopic, S. & Geibel, J. P. Gastric Acid, Calcium Absorption, and Their Impact on Bone Health. *Physiol. Rev.* **93**, 189–268 (2013).

172. Kondo, T., Kitazawa, R., Maeda, S. & Kitazawa, S. 1α,25 Dihydroxyvitamin D3 Rapidly Regulates the Mouse Osteoprotegerin Gene Through Dual Pathways. *J. Bone Miner. Res.* **19**, 1411–1419 (2004).

173. Dusso, A. S., Thadhani, R. & Slatopolsky, E. Vitamin D receptor and analogs. *Semin. Nephrol.* **24**, 10–16 (2004).

174. Nykjaer, A. *et al.* An Endocytic Pathway Essential for Renal Uptake and Activation of the Steroid 25-(OH) Vitamin D3. *Cell* **96**, 507–515 (1999).

175. Hoenderop, J. G. J., Nilius, B. & Bindels, R. J. M. Calcium Absorption Across Epithelia. *Physiol. Rev.* **85**, 373–422 (2005).

176. Wang, Q. M., Jones, J. B. & Studzinski, G. P. Cyclin-dependent kinase inhibitor p27 as a mediator of the G1-S phase block induced by 1,25-dihydroxyvitamin D3 in HL60 cells. *Cancer Res.* **56**, 264–7 (1996).

177. Moffatt, K. A., Johannes, W. U., Hedlund, T. E. & Miller, G. J. Growth Inhibitory Effects of 1,, 25-Dihydroxyvitamin D3 Are Mediated by Increased Levels of p21 in the Prostatic Carcinoma Cell Line ALVA-31. *Cancer Res.* **43**, 1809–1818 (2001).

178. Boyle, B. J., Zhao, X.-Y., Cohen, P. & Feldman, D. Insulin-like growth factor binding protein-3 mediates 1α,25-dihydroxyvitamin D3 growth inhibition in the LNCaP prostate cancer cell line through P21/WAF1. *J. Urol.* **165**, 1319–1324 (2001).

179. Freedman, L. P., Liu, M., Cohen, M., Bommakanti, M. & Lee, M. H. Transcriptional activation of the Cdk inhibitor p21 by vitamin D3 leads to the induced differentiation of the myelomonocytic cell line U937. *Genes Dev.* **10**, 142–153 (2007).

180. Pilon, C. *et al.* 1α,25-Dihydroxyvitamin D3 inhibits the human H295R cell proliferation by cell cycle arrest: A model for a protective role of vitamin D receptor against adrenocortical cancer. *J. Steroid Biochem. Mol. Biol.* **140**, 26–33 (2014).

181. Jiang, F., Li, P., Fornace, A. J., Nicosia, S. V & Bai, W. G2/M arrest by 1,25-dihydroxyvitamin D3 in ovarian cancer cells mediated through the induction of GADD45 via an exonic enhancer. *J. Biol. Chem.* **278**, 48030–40 (2003).

182. Abe, E. *et al.* Differentiation of mouse myeloid leukemia cells induced by 1 alpha,25-dihydroxyvitamin D3. *Proc. Natl. Acad. Sci. U. S. A.* **78**, 4990–4 (1981).

183. Halline, A. G. *et al.* Effects of 1,25-dihydroxyvitamin D3 on proliferation and

differentiation of Caco-2 cells. *Endocrinology* **134**, 1710–1717 (1994).

184. Kizildag, S., Ates, H. & Kizildag, S. Treatment of K562 cells with 1,25-dihydroxyvitamin D3 induces distinct alterations in the expression of apoptosis-related genes BCL2, BAX, BCLXL, and p21. *Ann. Hematol.* **89**, 1–7 (2010).

185. Krajewski, S., Krajewska, M., Reed, J. C., Binderup, L. & Hague, A. Immunohistochemical analysis of in vivo patterns of Bak expression, a proapoptotic member of the Bcl-2 protein family. *Cancer Res.* **56**, 2849–55 (1996).

186. Wagner, N. *et al.* 1,25-dihydroxyvitamin D3-induced apoptosis of retinoblastoma cells is associated with reciprocal changes of Bcl-2 and bax. *Exp. Eye Res.* **77**, 1–9 (2003).

187. Xie, S. ., Pirianov, G. & Colston, K. . Vitamin D analogues suppress IGF-I signalling and promote apoptosis in breast cancer cells. *Eur. J. Cancer* **35**, 1717–1723 (1999).

188. Lee, J. & Park, S.-H. Tumor-suppressive activity of 1,25-dihydroxyvitamin D3 against kidney cancer cells via up-regulation of FOXO3. *Biosci. Biotechnol. Biochem.* **80**, 1947–1953 (2016).

189. Piemonti, L. *et al.* Vitamin D3 Affects Differentiation, Maturation, and Function of Human Monocyte-Derived Dendritic Cells. *J. Immunol.* **164**, 4443–4451 (2000).

190. Griffin, M. D. *et al.* Potent Inhibition of Dendritic Cell Differentiation and Maturation by Vitamin D Analogs. *Biochem. Biophys. Res. Commun.* **270**, 701–708 (2000).

191. Veldman, C. M., Cantorna, M. T. & DeLuca, H. F. Expression of 1,25-Dihydroxyvitamin D3 Receptor in the Immune System. *Arch. Biochem. Biophys.* **374**, 334–338 (2000).

192. Yu, X.-P., Mocharla, H., Hustmyer, F. G. & Manolagas$, S. C. Vitamin D Receptor Expression in Human Lymphocytes. *J. Biol. Chem.* **266**, 7589–7595 (1991).

193. Alroy, I., Towers, T. L. & Freedman, L. P. Transcriptional repression of the interleukin-2 gene by vitamin D3: direct inhibition of NFATp/AP-1 complex formation by a nuclear hormone receptor. *Mol. Cell. Biol.* **15**, 5789–99 (1995).

194. Chen, S. *et al.* Modulatory effects of 1,25-dihydroxyvitamin D3 on human B cell differentiation. *J. Immunol.* **179**, 1634–47 (2007).

195. Palomer, X., González-Clemente, J. M., Blanco-Vaca, F. & Mauricio, D. Role of vitamin D in the pathogenesis of type 2 diabetes mellitus. *Diabetes, Obes. Metab.* **10**, 185–197 (2008).

196. Morrissey, R. L., Bucci, T. J., Richard, B., Empson, N. & Lufkin, E. G. Calcium-binding protein: its cellular localization in jejunum, kidney and pancreas. *Proc. Soc. Exp. Biol. Med.* **149**, 56–60 (1975).

197. Ishida, H. & Norman, A. W. Demonstration of a high affinity receptor for 1,25-

dihydroxyvitamin D3 in rat pancreas. *Mol. Cell. Endocrinol.* **60**, 109–17 (1988).

198. Johnson, J. A., Grande, J. P., Roche, P. C. & Kumar, R. Immunohistochemical localization of the 1,25(OH)2D3 receptor and calbindin D28k in human and rat pancreas. *Am. J. Physiol.* **267**, E356-60 (1994).

199. Inomata, S., Kadowaki, S., Yamatani, T., Fukase, M. & Fujita, T. Effect of 1 alpha (OH)-vitamin D3 on insulin secretion in diabetes mellitus. *Bone Miner.* **1**, 187–92 (1986).

200. Orwoll, E., Riddle, M. & Prince, M. Effects of vitamin D on insulin and glucagon secretion in non-insulin-dependent diabetes mellitus. *Am. J. Clin. Nutr.* **59**, 1083–1087 (1994).

201. Kadowaki, S. & Norman, A. W. Dietary vitamin D is essential for normal insulin secretion from the perfused rat pancreas. *J. Clin. Invest.* **73**, 759–66 (1984).

202. Gedik, O. & Akalin, S. Effects of vitamin D deficiency and repletion on insulin and glucagon secretion in man. *Diabetologia* **29**, 142–5 (1986).

203. Chertow, B. S. *et al.* Cellular Mechanisms of Insulin Release: The Effects of Vitamin D Deficiency and Repletion on Rat Insulin Secretion*. *Endocrinology* **113**, 1511–1518 (1983).

204. Boucher, B. J. Inadequate vitamin D status: does it contribute to the disorders comprising syndrome 'X'? *Br. J. Nutr.* **79**, 315 (1998).

205. Shires, R. *et al.* The effect of streptozotocin-induced chronic diabetes mellitus on bone and mineral homeostasis in the rat. *J. Lab. Clin. Med.* **97**, 231–40 (1981).

206. Ishida H *et al.* Effects of streptozotocin-induced diabetes on circulating levels of vitamin D metabolites. - PubMed - NCBI. *Acta Endocrinol* **104**, 96–102 (1983).

207. Nyomba, B. L., Bouillon, R., Lissens, W., Baelen, H. VAN & Moor, P. DE. 1,25-Dihydroxyvitamin D and Vitamin D-Binding Protein Are Both Decreased in Streptozotocin-Diabetic Rats*. *Endocrinology* **116**, 2483–2488 (1985).

208. Ishida, H. *et al.* Diabetic osteopenia and circulating levels of vitamin D metabolites in type 2 (noninsulin-dependent) diabetes. *Metabolism.* **34**, 797–801 (1985).

209. Li, M. *et al.* 1,25-Dihydroxyvitamin D3 suppresses gastric cancer cell growth through VDR- and mutant p53-mediated induction of p21. *Life Sci.* **179**, 88–97 (2017).

210. Spath, L. *et al.* Antiproliferative Effects of 1α-OH-vitD3 in Malignant Melanoma: Potential Therapeutic implications. *Sci. Rep.* **7**, 40370 (2017).

211. Meephansan, J., Komine, M., Tsuda, H. & Ohtsuki, M. Suppressive effect of calcipotriol on the induction of matrix metalloproteinase (MMP)-9 and MMP-13 in a human squamous cell carcinoma cell line. *Clin. Exp. Dermatol.* **37**, 889–896 (2012).

212. Ben-Shoshan, M. *et al.* 1 ,25-dihydroxyvitamin D3 (Calcitriol) inhibits hypoxia-

inducible factor-1/vascular endothelial growth factor pathway in human cancer cells. *Mol. Cancer Ther.* **6**, 1433–1439 (2007).

213. Mantell, D. J., Owens, P. E., Bundred, N. J., Mawer, E. B. & Canfield, A. E. 1α,25-Dihydroxyvitamin D $_3$ Inhibits Angiogenesis In Vitro and In Vivo. *Circ. Res.* **87**, 214–220 (2000).

214. Bao, B.-Y., Yao, J. & Lee, Y.-F. 1 , 25-dihydroxyvitamin D3 suppresses interleukin-8-mediated prostate cancer cell angiogenesis. *Carcinogenesis* **27**, 1883–1893 (2006).

215. McDonnell, S. L. *et al.* Serum 25-Hydroxyvitamin D Concentrations ≥40 ng/ml Are Associated with >65% Lower Cancer Risk: Pooled Analysis of Randomized Trial and Prospective Cohort Study. *PLoS One* **11**, e0152441 (2016).

216. Deschasaux, M. *et al.* Prospective associations between vitamin D status, vitamin D–related gene polymorphisms, and risk of tobacco-related cancers. *Am. J. Clin. Nutr.* **102**, 1207–1215 (2015).

217. Hu, K., Callen, D. F., Li, J. & Zheng, H. Circulating Vitamin D and Overall Survival in Breast Cancer Patients: A Dose-Response Meta-Analysis of Cohort Studies. *Integr. Cancer Ther.* **17**, 217–225 (2018).

218. Brunner, R. L. *et al.* The Effect of Calcium plus Vitamin D on Risk for Invasive Cancer: Results of the Women's Health Initiative (WHI) Calcium Plus Vitamin D Randomized Clinical Trial. *Nutr. Cancer* **63**, 827–841 (2011).

219. Bolland, M. J., Grey, A., Gamble, G. D. & Reid, I. R. Calcium and vitamin D supplements and health outcomes: a reanalysis of the Women's Health Initiative (WHI) limited-access data set. *Am. J. Clin. Nutr.* **94**, 1144–1149 (2011).

220. Umar, M., Sastry, K. S. & Chouchane, A. I. Role of Vitamin D Beyond the Skeletal Function: A Review of the Molecular and Clinical Studies. *Int. J. Mol. Sci.* **19**, (2018).

221. Maddaloni, E., Cavallari, I., Napoli, N. & Conte, C. Vitamin D and Diabetes Mellitus. *Front. Horm. Res.* **50**, 161–176 (2018).

222. Setty-Shah, N., Maranda, L. & Nwosu, B. U. Increased risk for vitamin d deficiency in obese children with both celiac disease and type 1 diabetes. *Gastroenterol. Res. Pract.* **2014**, 561351 (2014).

223. Derakhshanian, H., Javanbakht, M. H., Zarei, M., Djalali, E. & Djalali, M. Vitamin D increases IGF-I and insulin levels in experimental diabetic rats. *Growth Horm. IGF Res.* **36**, 57–59 (2017).

224. Wang, Y. *et al.* Vitamin D induces autophagy of pancreatic β-cells and enhances insulin secretion. *Mol. Med. Rep.* **14**, 2644–2650 (2016).

225. Ysmail-Dahlouk, L., Nouari, W. & Aribi, M. 1,25-dihydroxyvitamin D 3 down-modulates the production of proinflammatory cytokines and nitric oxide and enhances the phosphorylation of monocyte-expressed STAT6 at the recent-onset type 1 diabetes. *Immunol. Lett.* **179**, 122–130 (2016).

226. Mao, L., Ji, F., Liu, Y., Zhang, W. & Ma, X. Calcitriol plays a protective role in diabetic nephropathy through anti-inflammatory effects. *Int. J. Clin. Exp. Med.* **7**, 5437–44 (2014).

227. Hyppönen, E., Läärä, E., Reunanen, A., Järvelin, M. R. & Virtanen, S. M. Intake of vitamin D and risk of type 1 diabetes: a birth-cohort study. *Lancet (London, England)* **358**, 1500–3 (2001).

228. Dong, J.-Y. *et al.* Vitamin D Intake and Risk of Type 1 Diabetes: A Meta-Analysis of Observational Studies. *Nutrients* **5**, 3551–3562 (2013).

229. Maddaloni, E. *et al.* Bone health in subjects with type 1 diabetes for more than 50 years. *Acta Diabetol.* **54**, 479–488 (2017).

230. Gabbay, M. A. L., Sato, M. N., Finazzo, C., Duarte, A. J. S. & Dib, S. A. Effect of Cholecalciferol as Adjunctive Therapy With Insulin on Protective Immunologic Profile and Decline of Residual β-Cell Function in New-Onset Type 1 Diabetes Mellitus. *Arch. Pediatr. Adolesc. Med.* **166**, 601–607 (2012).

231. Cooper, J. D. *et al.* Inherited variation in vitamin D genes is associated with predisposition to autoimmune disease type 1 diabetes. *Diabetes* **60**, 1624–31 (2011).

232. Frederiksen, B. N. *et al.* Association between vitamin D metabolism gene polymorphisms and risk of islet autoimmunity and progression to type 1 diabetes: the diabetes autoimmunity study in the young (DAISY). *J. Clin. Endocrinol. Metab.* **98**, E1845-51 (2013).

233. Li, X. *et al.* Protective effects of 1-α-hydroxyvitamin D3 on residual β-cell function in patients with adult-onset latent autoimmune diabetes (LADA). *Diabetes. Metab. Res. Rev.* **25**, 411–416 (2009).

234. Bizzarri, C. *et al.* No protective effect of calcitriol on beta-cell function in recent-onset type 1 diabetes: the IMDIAB XIII trial. *Diabetes Care* **33**, 1962–3 (2010).

235. Walter, M. *et al.* No effect of the 1alpha,25-dihydroxyvitamin D3 on beta-cell residual function and insulin requirement in adults with new-onset type 1 diabetes. *Diabetes Care* **33**, 1443–8 (2010).

236. Cade, C. & Norman, A. W. Rapid Normalization/Stimulation by 1,25-Dihydroxyvitamin D 3 of Insulin Secretion and Glucose Tolerance in the Vitamin D-Deficient Rat*. *Endocrinology* **120**, 1490–1497 (1987).

237. Erben, R. G. *et al.* Deletion of deoxyribonucleic acid binding domain of the vitamin D receptor abrogates genomic and nongenomic functions of vitamin D. *Mol. Endocrinol.* **16**, 1524–37 (2002).

238. Bouillon, R. *et al.* Vitamin D and Human Health: Lessons from Vitamin D Receptor Null Mice. *Endocr. Rev.* **29**, 726–776 (2008).

239. Ali, T. M., El Esawy, B. & Elaskary, A. Effect of paricalcitol on pancreatic oxidative stress, inflammatory markers, and glycemic status in diabetic rats. *Irish J. Med. Sci. (1971 -)* **187**, 75–84 (2018).

240. Elseweidy, M. M., Amin, R. S., Atteia, H. H. & Ali, M. A. Vitamin D3 intake as regulator of insulin degrading enzyme and insulin receptor phosphorylation in diabetic rats. *Biomed. Pharmacother.* **85**, 155–159 (2017).

241. Maestro, B., Molero, S., Bajo, S., Dávila, N. & Calle, C. Transcriptional activation of the human insulin receptor gene by 1,25-dihydroxyvitamin D $_3$. *Cell Biochem. Funct.* **20**, 227–232 (2002).

242. Bland, R. *et al.* Expression of 25-hydroxyvitamin D3-1α-hydroxylase in pancreatic islets. *J. Steroid Biochem. Mol. Biol.* **89–90**, 121–125 (2004).

243. Reusch, J. E.-B., Begum, N., Sussman, K. E. & Draznin, B. Regulation of GLUT-4 Phosphorylation by Intracellular Calcium in Adipocytes*. *Endocrinology* **129**, 3269–3273 (1991).

244. Beilfuss, J., Berg, V., Sneve, M., Jorde, R. & Kamycheva, E. Effects of a 1-year supplementation with cholecalciferol on interleukin-6, tumor necrosis factor-alpha and insulin resistance in overweight and obese subjects. *Cytokine* **60**, 870–874 (2012).

245. Grimnes, G., Figenschau, Y., Almås, B. & Jorde, R. Vitamin D, insulin secretion, sensitivity, and lipids: results from a case-control study and a randomized controlled trial using hyperglycemic clamp technique. *Diabetes* **60**, 2748–57 (2011).

246. Muldowney, S. *et al.* Incremental Cholecalciferol Supplementation up to 15 µg/d Throughout Winter at 51–55° N Has No Effect on Biomarkers of Cardiovascular Risk in Healthy Young and Older Adults. *J. Nutr.* **142**, 1519–1525 (2012).

247. Borissova, A. M., Tankova, T., Kirilov, G., Dakovska, L. & Kovacheva, R. The effect of vitamin D3 on insulin secretion and peripheral insulin sensitivity in type 2 diabetic patients. *Int. J. Clin. Pract.* **57**, 258–61 (2003).

248. Nagpal, J., Pande, J. N. & Bhartia, A. A double-blind, randomized, placebo-controlled trial of the short-term effect of vitamin D $_3$ supplementation on insulin sensitivity in apparently healthy, middle-aged, centrally obese men. *Diabet. Med.* **26**, 19–27 (2009).

249. Christakos, S. & Liu, Y. Biological actions and mechanism of action of calbindin in the process of apoptosis. *J. Steroid Biochem. Mol. Biol.* **89–90**, 401–404 (2004).

250. Salum, E. *et al.* Vitamin D reduces deposition of advanced glycation end-products in the aortic wall and systemic oxidative stress in diabetic rats. *Diabetes Res. Clin. Pract.* **100**, 243–249 (2013).

251. Mark, A. B. *et al.* Consumption of a diet low in advanced glycation end products for 4 weeks improves insulin sensitivity in overweight women. *Diabetes Care* **37**, 88–95 (2014).

252. Forouhi, N. G., Luan, J., Cooper, A., Boucher, B. J. & Wareham, N. J. Baseline serum 25-hydroxy vitamin d is predictive of future glycemic status and insulin resistance: the Medical Research Council Ely Prospective Study 1990-2000. *Diabetes* **57**, 2619–25 (2008).

253. Kayaniyil, S. *et al.* Association of Vitamin D With Insulin Resistance and β-Cell Dysfunction in Subjects at Risk for Type 2 Diabetes. *Diabetes Care* **33**, 1379–1381 (2010).

254. Maki, K. C. *et al.* Vitamin D Intake and Status Are Associated with Lower Prevalence of Metabolic Syndrome in U.S. Adults: National Health and Nutrition Examination Surveys 2003–2006. *Metab. Syndr. Relat. Disord.* **10**, 363–372 (2012).

255. Chiu, K. C., Chu, A., Go, V. L. W. & Saad, M. F. Hypovitaminosis D is associated with insulin resistance and β cell dysfunction. *Am. J. Clin. Nutr.* **79**, 820–825 (2004).

256. Gannagé-Yared, M.-H. *et al.* Vitamin D in relation to metabolic risk factors, insulin sensitivity and adiponectin in a young Middle-Eastern population. *Eur. J. Endocrinol.* **160**, 965–971 (2009).

257. Scragg, R. *et al.* Serum 25-hydroxyvitamin D3 levels decreased in impaired glucose tolerance and diabetes mellitus. *Diabetes Res. Clin. Pract.* **27**, 181–8 (1995).

258. Kayaniyil, S. *et al.* Prospective associations of vitamin D with β-cell function and glycemia: the PROspective Metabolism and ISlet cell Evaluation (PROMISE) cohort study. *Diabetes* **60**, 2947–53 (2011).

259. Jamilian, M. *et al.* Vitamin D and Evening Primrose Oil Administration Improve Glycemia and Lipid Profiles in Women with Gestational Diabetes. *Lipids* **51**, 349–356 (2016).

260. Mousa, A., Naderpoor, N., Teede, H., Scragg, R. & de Courten, B. Vitamin D supplementation for improvement of chronic low-grade inflammation in patients with type 2 diabetes: a systematic review and meta-analysis of randomized controlled trials. *Nutr. Rev.* **76**, 380–394 (2018).

261. Silvagno, F. & Pescarmona, G. Spotlight on vitamin D receptor, lipid metabolism and mitochondria: Some preliminary emerging issues. *Mol. Cell. Endocrinol.* **450**, 24–31 (2017).

262. Silvagno, F. *et al.* Mitochondrial Localization of Vitamin D Receptor in Human Platelets and Differentiated Megakaryocytes. *PLoS One* **5**, e8670 (2010).

263. Silvagno, F., Consiglio, M., Foglizzo, V., Destefanis, M. & Pescarmona, G. Mitochondrial Translocation of Vitamin D Receptor Is Mediated by the Permeability Transition Pore in Human Keratinocyte Cell Line. *PLoS One* **8**, e54716 (2013).

264. Consiglio, M. *et al.* The Vitamin D Receptor Inhibits the Respiratory Chain, Contributing to the Metabolic Switch that Is Essential for Cancer Cell Proliferation. *PLoS One* **9**, e115816 (2014).

265. Consiglio, M. *et al.* Mitochondrial and lipogenic effects of vitamin D on differentiating and proliferating human keratinocytes. *Exp. Dermatol.* **24**, 748–753 (2015).

266. Pannu, P. K., Calton, E. K. & Soares, M. J. Calcium and Vitamin D in Obesity and Related Chronic Disease. *Adv. Food Nutr. Res.* **77**, 57–100 (2016).

267. Bhat, M., Noolu, B., Qadri, S. S. & Ismail, A. Vitamin D deficiency decreases adiposity in rats and causes altered expression of uncoupling proteins and steroid receptor coactivator3. *J. Steroid Biochem. Mol. Biol.* **144**, 304–312 (2014).

268. Zhu, W. *et al.* Calcium plus vitamin D3 supplementation facilitated fat loss in overweight and obese college students with very-low calcium consumption: a randomized controlled trial. *Nutr. J.* **12**, 8 (2013).

269. Asemi, Z. *et al.* Calcium plus vitamin D supplementation affects glucose metabolism and lipid concentrations in overweight and obese vitamin D deficient women with polycystic ovary syndrome. *Clin. Nutr.* **34**, 586–592 (2015).

270. Wong, K. E. *et al.* Targeted expression of human vitamin D receptor in adipocytes decreases energy expenditure and induces obesity in mice. *J. Biol. Chem.* **286**, 33804–10 (2011).

271. Bozic, M. *et al. Hepatocyte vitamin D receptor regulates lipid metabolism and mediates experimental diet-induced steatosis*. *Journal of Hepatology* **65**, (European Association for the Study of the Liver, 2016).

272. Bookout, A. L. *et al.* Anatomical profiling of nuclear receptor expression reveals a hierarchical transcriptional network. *Cell* **126**, 789–99 (2006).

273. Han, S. & Chiang, J. Y. L. Mechanism of Vitamin D Receptor Inhibition of Cholesterol 7α-Hydroxylase Gene Transcription in Human Hepatocytes. *Drug Metab. Dispos.* **37**, 469 (2009).

274. Drocourt, L., Ourlin, J.-C., Pascussi, J.-M., Maurel, P. & Vilarem, M.-J. Expression of CYP3A4, CYP2B6, and CYP2C9 is regulated by the vitamin D receptor pathway in primary human hepatocytes. *J. Biol. Chem.* **277**, 25125–32 (2002).

275. Echchgadda, I., Song, C. S., Roy, A. K. & Chatterjee, B. Molecular Pharmacology. *Mol. Pharmacol.* **41**, 865–872 (2004).

276. Han, S., Li, T., Ellis, E., Strom, S. & Chiang, J. Y. L. A Novel Bile Acid-Activated Vitamin D Receptor Signaling in Human Hepatocytes. *Mol. Endocrinol.* **24**, 1151–1164 (2010).

277. Chow, E. C. Y. *et al.* Vitamin D receptor activation down-regulates the small heterodimer partner and increases CYP7A1 to lower cholesterol. *Gastroenterology* **146**, 1048–59 (2014).

278. Yoshizawa, T. *et al.* Mice lacking the vitamin D receptor exhibit impaired bone formation, uterine hypoplasia and growth retardation after weaning. *Nat. Genet.* **16**, 391–396 (1997).

279. Li, Y. C. *et al.* Targeted ablation of the vitamin D receptor: an animal model of vitamin D-dependent rickets type II with alopecia. *Proc. Natl. Acad. Sci. U. S. A.*

**94**, 9831–5 (1997).

280. Van Cromphaut, S. J. *et al.* Duodenal calcium absorption in vitamin D receptor-knockout mice: Functional and molecular aspects. *PNAS* **98**, 13324–13329 (2001).

281. Dostal, L. A. & Toverud, S. U. Effect of vitamin D3 on duodenal calcium absorption in vivo during early development. *Am. J. Physiol.* **246**, G528-34 (1984).

282. Suda, T., Masuyama, R., Bouillon, R. & Carmeliet, G. Physiological functions of vitamin D: what we have learned from global and conditional VDR knockout mouse studies. *Curr. Opin. Pharmacol.* **22**, 87–99 (2015).

283. Colston, K., Colston, M. J. & Feldman, D. 1,25-dihydroxyvitamin D 3 and malignant melanoma: the presence of receptors and inhibition of cell growth in culture. *Endocrinology* **108**, 1083–1086 (1981).

284. Cross, H. S. *et al.* 25-Hydroxyvitamin D3-1α-hydroxylase and vitamin D receptor gene expression in human colonic mucosa is elevated during early cancerogenesis. *Steroids* **66**, 287–292 (2001).

285. Cross, H. S. *et al.* Vitamin D receptor and cytokeratin expression may be progression indicators in human colon cancer. *Anticancer Res.* **16**, 2333–2337 (1996).

286. Xie, Z. *et al.* Lack of the vitamin D receptor is associated with reduced epidermal differentiation and hair follicle growth. *J. Invest. Dermatol.* **118**, 11–6 (2002).

287. Hosomi, J., Hosoi, J., Abe, E., Suda, T. & Kuroki, T. Regulation of Terminal Differentiation of Cultured Mouse Epidermal Cells by l α ,25-Dihydroxyvitamin D 3 *. *Endocrinology* **113**, 1950–1957 (1983).

288. Zinser, G., Sundberg, J. & Welsh, J. Vitamin D(3) receptor ablation sensitizes skin to chemically induced tumorigenesis. - PubMed - NCBI. *Carcinogenesis* **12**, 2103–2109 (2002).

289. Zinser, G., Packman, K. & Welsh, J. Vitamin D3 receptor ablation alters mammary gland morphogenesis. *Development* **129**, 3067–3076 (2002).

290. Cao, D., Lu, H., Lewis, T. L. & Li, L. Intake of sucrose-sweetened water induces insulin resistance and exacerbates memory deficits and amyloidosis in a transgenic mouse model of Alzheimer disease. *J. Biol. Chem.* **282**, 36275–82 (2007).

291. Suez, J. *et al.* Artificial sweeteners induce glucose intolerance by altering the gut microbiota. *Nature* **514**, 181–186 (2014).

292. Robey, I. F. & Martin, N. K. Bicarbonate and dichloroacetate: evaluating pH altering therapies in a mouse model for metastatic breast cancer. *BMC Cancer* **11**, 235 (2011).

293. Robey, I. F. & Nesbit, L. A. Investigating mechanisms of alkalinization for reducing primary breast tumor invasion. *Biomed Res. Int.* **2013**, 485196 (2013).

294. Mirantes, C. *et al.* An inducible knockout mouse to model the cell-autonomous role of PTEN in initiating endometrial, prostate and thyroid neoplasias. *Dis. Model. Mech.* **6**, 710–720 (2013).

295. Feil, R. *et al. Ligand-activated site-specific recombination in mice*. *PNAS* **93**, (1996).

296. Metzger, D., Clifford, J., Chiba, H. & Chambon, P. Conditional site-specific recombination in mammalian cells using a ligand-dependent chimeric Cre recombinase. *PNAS* **92**, 6991–6995 (1995).

297. JoVE Science Education Database. Lab Animal Research. Blood withdrawal II. *JoVE, Cambridge, MA* (2019).

298. Carter, J. D., Dula, S. B., Corbin, K. L., Wu, R. & Nunemaker, C. S. A practical guide to rodent islet isolation and assessment. *Biol. Proced. Online* **11**, 3–31 (2009).

299. Nolan, A. L. & O'Dowd, J. F. The Measurement of Insulin Secretion from Isolated Rodent Islets of Langerhans. *Type 2 Diabetes, Methods Mol. Biol.* **560**, 43–51 (2009).

300. Devos, S. L. & Miller, T. M. Direct Intraventricular Delivery of Drugs to the Rodent Central Nervous System. *J. Vis. Exp* 50326 (2013). doi:10.3791/50326

301. Boini, K. M. *et al.* Serum-and Glucocorticoid-Inducible Kinase 1 Mediates Salt Sensitivity of Glucose Tolerance. *Diabetes* **55**, 2059–2066 (2006).

302. Ryan, M. J. *et al. HK-2: An immortalized proximal tubule epithelial cell line from normal adult human kidney*. *Kidney International* **45**, (1994).

303. Moselhy, J. *et al.* Withaferin A Inhibits Prostate Carcinogenesis in a PTEN-deficient Mouse Model of Prostate Cancer. *Neoplasia* **19**, 451–459 (2017).

304. Dosil, M. A. *et al.* Palbociclib has antitumour effects on Pten-deficient endometrial neoplasias. *J. Pathol.* **242**, 152–164 (2017).

305. Erben, R. G. & Andrukhova, O. FGF23-Klotho signaling axis in the kidney. *Bone* **100**, 62–68 (2017).

306. Liu, S. *et al.* Fibroblast Growth Factor 23 Is a Counter-Regulatory Phosphaturic Hormone for Vitamin D. *J. Am. Soc. Nephrol.* **17**, 1305–1315 (2006).

307. Quarles, L. D. Endocrine functions of bone in mineral metabolism regulation. *J. Clin. Invest.* **118**, 3820–8 (2008).

308. Shimada, T. *et al.* FGF-23 Is a Potent Regulator of Vitamin D Metabolism and Phosphate Homeostasis. *J. Bone Miner. Res.* **19**, 429–435 (2003).

309. Gattineni, J. *et al.* FGF23 decreases renal NaPi-2a and NaPi-2c expression and induces hypophosphatemia in vivo predominantly via FGF receptor 1. *Am. J. Physiol. Physiol.* **297**, F282–F291 (2009).

310. Haffner, D. & Leifheit-Nestler, M. Extrarenal effects of FGF23. *Pediatr. Nephrol.* **32**, 753–765 (2017).

311. Lunyera, J. & Scialla, J. J. Update on Chronic Kidney Disease Mineral and Bone Disorder in Cardiovascular Disease. *Semin. Nephrol.* **38**, 542–558 (2018).

312. Yecies, J. L. *et al.* Akt Stimulates Hepatic SREBP1c and Lipogenesis through Parallel mTORC1-Dependent and Independent Pathways. *Cell Metab.* **14**, 21–32 (2011).

313. Ackermann, A. M. & Gannon, M. Molecular regulation of pancreatic β-cell mass development, maintenance, and expansion. *J. Mol. Endocrinol.* **38**, 193.206 (2006).

314. Li, Z. *et al.* Activation of vitamin D receptor signaling downregulates the expression of nuclear FOXM1 protein and suppresses pancreatic cancer cell stemness. *Clin. Cancer Res.* **21**, 844–53 (2015).

315. Wang, L. *et al.* Deletion of Pten in Pancreatic-Cells Protects Against Deficient-Cell Mass and Function in Mouse Models of Type 2 Diabetes. *Diabetes* **59**, 3117–3126 (2010).

316. Robinson, K. A. & Buse, M. G. Mechanisms of high-glucose/insulin-mediated desensitization of acute insulin-stimulated glucose transport and Akt activation. *Am. J. Physiol. Endocrinol. Metab.* **294**, E870 (2008).

317. Marchetti, P. *et al.* Pancreatic Islets from Type 2 Diabetic Patients Have Functional Defects and Increased Apoptosis That Are Ameliorated by Metformin. *J. Clin. Endocrinol. Metab.* **89**, 5535–5541 (2004).

318. Mitrakou, A. *et al.* Role of Reduced Suppression of Glucose Production and Diminished Early Insulin Release in Impaired Glucose Tolerance. *N. Engl. J. Med.* **326**, 22–29 (1992).

319. Kjalarsdottir, L. *et al.* 1,25-Dihydroxyvitamin D3 enhances glucose-stimulated insulin secretion in mouse and human islets: a role for transcriptional regulation of voltage-gated calcium channels by the vitamin D receptor. *J. Steroid Biochem. Mol. Biol.* **185**, 17–26 (2019).

320. Kinross, K. M. *et al.* Ubiquitous expression of the Pik3ca H1047R mutation promotes hypoglycemia, hypoinsulinemia, and organomegaly. *FASEB J.* **29**, 1426–1434 (2015).

321. Foukas, L. C. *et al.* Critical role for the p110α phosphoinositide-3-OH kinase in growth and metabolic regulation. *Nature* **441**, 366–370 (2006).

322. Sopasakis, V. R. *et al.* Specific Roles of the p110α Isoform of Phosphatidylinsositol 3-Kinase in Hepatic Insulin Signaling and Metabolic Regulation. *Cell Metab.* **11**, 220–230 (2010).

323. Stutterd, C. *et al.* Polymicrogyria in association with hypoglycemia points to mutation in the mTOR pathway. *Eur. J. Med. Genet.* **61**, 738–740 (2018).

324. Terauchi, Y. *et al.* Increased insulin sensitivity and hypoglycaemia in mice lacking the p85α subunit of phosphoinositide 3–kinase. *Nat. Genet.* **21**, 230–235 (1999).

325. Taniguchi, C. M. *et al.* Divergent regulation of hepatic glucose and lipid

metabolism by phosphoinositide 3-kinase via Akt and PKCλ/ζ. *Cell Metab.* **3**, 343–353 (2006).

326. Aoki, K. *et al.* Role of the liver in glucose homeostasis in PI 3-kinase p85 α-deficient mice. *Am. J. Physiol. Metab.* **296**, E842–E853 (2009).

327. Thomson, S. C. *et al.* Acute and chronic effects of SGLT2 blockade on glomerular and tubular function in the early diabetic rat. *Am J Physiol Regul Integr Comp Physiol* (2011).

328. Vallon, V. *et al.* SGLT2 inhibitor empagliflozin reduces renal growth and albuminuria in proportion to hyperglycemia and prevents glomerular hyperfiltration in diabetic Akita mice. *Am J Physiol Ren. Physiol* **306**, 194–204 (2014).

329. Vallon, V. *et al.* Knockout of Na-glucose transporter SGLT2 attenuates hyperglycemia and glomerular hyperfiltration but not kidney growth or injury in diabetes mellitus. *Am J Physiol Ren. Physiol* (2012).

330. Sarafidis, P. *et al.* SGLT-2 inhibitors and GLP-1 receptor agonists for nephroprotection and cardioprotection in patients with diabetes mellitus and chronic kidney disease. A consensus statement by the EURECA-m and the DIABESITY working groups of the ERA-EDTA. *Nephrol. Dial. Transplant.* **34**, 208–230 (2019).

331. Freitas, H. S. *et al.* SLC2A2 gene expression in kidney of diabetic rats is regulated by HNF-1α and HNF-3β. *Mol. Cell. Endocrinol.* **305**, 63–70 (2009).

332. Luo, Z. *et al.* Hepatocyte nuclear factor 1A (HNF1A) as a possible tumor suppressor in pancreatic cancer. *PLoS One* **10**, e0121082 (2015).

333. Osorio, H. *et al.* Effect of treatment with losartan on salt sensitivity and SGLT2 expression in hypertensive diabetic rats. *Diabetes Res. Clin. Pract.* **86**, e46–e49 (2009).

334. Freitas, H. S. *et al.* Na+-Glucose Transporter-2 Messenger Ribonucleic Acid Expression in Kidney of Diabetic Rats Correlates with Glycemic Levels: Involvement of Hepatocyte Nuclear Factor-1α Expression and Activity. *Endocrinology* **149**, 717–724 (2008).

335. Ackermann, T. F. *et al.* SGK1-sensitive renal tubular glucose reabsorption in diabetes. *Am. J. Physiol. Physiol.* **296**, F859–F866 (2009).

336. Lahbib, A. *et al.* Effects of vitamin D on insulin secretion and glucose transporter GLUT2 under static magnetic field in rat. *Environ. Sci. Pollut. Res.* **22**, 18011–18016 (2015).

337. Manna, P. & Jain, S. K. Vitamin D up-regulates glucose transporter 4 (GLUT4) translocation and glucose utilization mediated by cystathionine-γ-lyase (CSE) activation and H2S formation in 3T3L1 adipocytes. *J. Biol. Chem.* **287**, 42324–32 (2012).

338. Chhabra, K. H. *et al.* Reduced renal sympathetic nerve activity contributes to

elevated glycosuria and improved glucose tolerance in hypothalamus-specific Pomc knockout mice. *Mol. Metab.* **6**, 1274–1285 (2017).

339. Haeusler, R. A. *et al.* Integrated control of hepatic lipogenesis versus glucose production requires FoxO transcription factors. *Nat. Commun.* **5**, (2014).

340. Wolfrum, C., Besser, D., Luca, E. & Stoffel, M. Insulin regulates the activity of forkhead transcription factor Hnf-3beta/Foxa-2 by Akt-mediated phosphorylation and nuclear/cytosolic localization. *Proc. Natl. Acad. Sci. U. S. A.* **100**, 11624–9 (2003).

341. Zhang, L., Rubins, N. E., Ahima, R. S., Greenbaum, L. E. & Kaestner, K. H. Foxa2 integrates the transcriptional response of the hepatocyte to fasting. *Cell Metab.* **2**, 141–148 (2005).

342. Wolfrum, C. & Stoffel, M. Coactivation of Foxa2 through Pgc-1beta promotes liver fatty acid oxidation and triglyceride/VLDL secretion. *Cell Metab.* **3**, 99–110 (2006).

343. Sfakianos, M. K., Wilson, L., Sakalian, M., Falany, C. N. & Barnes, S. Conserved residues in the putative catalytic triad of human bile acid Coenzyme A:amino acid N-acyltransferase. *J. Biol. Chem.* **277**, 47270–5 (2002).

344. Finck, B. N. *et al.* Lipin 1 is an inducible amplifier of the hepatic PGC-1a/PPARa regulatory pathway. *Cell Metab.* **4**, 199–210 (2006).

345. Leone, T. C. *et al.* PGC-1alpha deficiency causes multi-system energy metabolic derangements: muscle dysfunction, abnormal weight control and hepatic steatosis. *PLoS Biol.* **3**, e101 (2005).

346. Aharoni-Simon, M., Hann-Obercyger, M., Pen, S., Madar, Z. & Tirosh, O. Fatty liver is associated with impaired activity of PPARγ-coactivator 1α (PGC1α) and mitochondrial biogenesis in mice. *Lab. Investig.* **91**, 1018–1028 (2011).

347. Dushay, J. *et al.* Increased fibroblast growth factor 21 in obesity and nonalcoholic fatty liver disease. *Gastroenterology* **139**, 456–63 (2010).

348. Dasarathy, S. *et al.* Elevated hepatic fatty acid oxidation, high plasma fibroblast growth factor 21, and fasting bile acids in nonalcoholic steatohepatitis. *Eur. J. Gastroenterol. Hepatol.* **23**, 382–8 (2011).

# Annex

# 1. Publications

- ***Effect of renal tubule-specific knockdown of the Na+/H+ exchanger NHE3 in Akita diabetic mice*.**
  Onishi A, Fu Y, Darshi M, **Crespo-Masip M**, Huang W, Song P, Patel R, Kim YC, Nespoux J, Freeman B, Soleimani M, Thomson S, Sharma K, Vallon V. Am J Physiol Renal Physiol. 2019 Aug 1;317(2):F419-F434. doi: 10.1152/ajprenal.00497.2018. Epub 2019 Jun 5. PMID: 31166707

- ***Peritoneal dialysis is an independent factor associated to lower intima media thickness in dialysis patients free from previous cardiovascular disease.***
  Borràs M, Cambray S, **Crespo-Masip M**, Pérez-Fontán M, Bozic M, Bermudez-López M, Fernández E, Betriu À, Valdivielso JM. Front Physiol. 2018 Dec 4;9:1743. doi: 10.3389/fphys.2018.01743. eCollection 2018. PMID: 30564145

- ***Full PTEN deletion induces severe hypoglycemia associated with kidney glucose transporters, gluconeogenesis and lipid metabolism disorders.***
  **Crespo-Masip M**, Pérez A, Guzmán C, Rayego S, Doladé N, Garcia A, Jover R, Valdivielso JM. (Written manuscript ready to be published)

# 2. Congresses and conferences

- ***Overactivation of the PI3K/Akt pathway leads to mineral metabolism alterations*.**
  **Crespo-Masip M**; Pérez A; Garcia A; Muñoz-Castañeda JR; Rodriguez M; Fernández E; Valdivielso JM. 56th ERA-EDTA Congress, June 2019. European congress. Budapest, Hungary (Poster).

- ***PTEN en la regulación del metabolism mineral.***
  **Crespo-Masip M**; Pérez A; Garcia A; Muñoz-Castañeda JR; Díaz-Tocados JM; Fernández E; Valdivielso JM. XLVIII congreso nacional de la S.E.N. y IX congreso iberoamericano de nefrología, November 2018. Madrid, Spain (Oral communication).

- ***PTEN inducible KO mice show altered mineral metabolism.***
  **Crespo-Masip M**; Pérez A; Garcia A; Muñoz-Castañeda JR; Rodriguez M; Fernández E; Valdivielso JM. 55th ERA-EDTA Congress, May 2018. European congress. Copenhaguen, Denmark (Poster, awarded by ERA-EDTA).

- ***Tubular NHE3 is a determinant of the acute natriuretic and chronic blood pressure lowering affect of the SGLT2 inhibitor empagliflozin.***
  Huang W; Patel R; Onishi A; **Crespo-Masip M**; Soleimani M; Freeman B; Vallon V. Experimental Biology 2018, April 2018. San Diego, California (Poster, awarded by EB).

- ***PTEN inducible KO mice show altered mineral metabolism.***
  **Crespo-Masip M**; Pérez A; Garcia A; Muñoz-Castañeda JR; Rodriguez M; Fernández E; Valdivielso JM. 55th ERA-EDTA Congress, May 2018. European congress. Copenhaguen, Denmark (Poster, awarded by ERA-EDTA).

- ***El ratón knockout inducible PTEN presenta alteraciones en el metabolism mineral.***
  **Crespo-Masip M**; Pérez A; Garcia A; Muñoz-Castañeda JR; Rodriguez M; Fernández E; Valdivielso JM. XLVII congreso nacional de la S.E.N., October 2017. Burgos, Spain (Poster).

- ***Caracterització d'un model murí doble knockout PTEN-VDR.***
  **Crespo-Masip M**; Fernández E; Valdivielso JM. XXIII Jornada de Biologia Molecular. June 2016. Barcelona, Spain (Poster).

- ***Characterization of an inducible PTEN-VDR double knock out murine model.***
  **Crespo-Masip M**; Valdivielso JM. Retreat of Nefrology. June 2016. Torrelameu, Spain (Oral comunication).

- ***Caracterització d'un model murí doble knockout PTEN-VDR.***
  **Crespo-Masip M**; Fernández E; Valdivielso JM. I Jornada d'investigació en la UdL. May 2016. Lleida, Spain (Poster).

# 3. Short-stays

- **University of California San Diego (UCSD) in United States of America.** Stay in the *Division of Nephrology-Hypertension* under the supervision of **Dr. Volker Vallon.** (March - July 2017).
- **Institut d'Investigació Sanitària La Fe – Universitat de València.** Stay in *Unidad Mixta en Hepatología Experimental* under the supervision of **Dr. Ramiro Jover** (one week in January 2019).

UNIVERSITY *of* CALIFORNIA, SAN DIEGO

Volker Vallon, M.D.
Professor of Medicine and Pharmacology
Departments of Medicine and Pharmacology
School of Medicine
Division of Nephrology-Hypertension
University of California, San Diego

VA San Diego Healthcare System
3350 La Jolla Village Drive (9151)
San Diego, CA 92161
Tel: (858) 552-8585 ext: 5945
Fax: (858) 642-1438
vvallon@ucsd.edu

**RE: visiting scholar Maria Crespo Masip**

| Name: **Crespo Masip, Maria** | NIF/NIE: **47691060P** |
|---|---|
| Host Research Center: University of California, San Diego | |
| Department: Division of Nephrology-Hypertension | |
| Country: United States of America | |

The undersigned certifies that the scholar has remained in this centre from 28th March 2017 until 26th July 2017.

Host Research Director Name: **Volker Vallon**

Date: 25/07/2017

Volker Vallon, MD